Ventricular arrhythmias in the remodeled heart: focus on risk prediction and monitoring

David Sprenkeler

ISBN: 9789463233767
Cover design: Jens Weidenaar
Layout: David Sprenkeler
Printed by: Gildeprint

Ventricular arrhythmias in the remodeled heart: focus on risk prediction and monitoring

Ventriculaire ritmestoornissen in het geremodelleerde hart: focus op risicopredictie en monitoring

(met een samenvatting in het Nederlands)

Proefschrift

ter verkrijging van de graad van doctor aan de Universiteit Utrecht op gezag van de rector magnificus, prof. dr. H.R.B.M. Kummeling, ingevolge het besluit van het college voor promoties in het openbaar te verdedigen op donderdag 13 december 2018 des middags te 2.30 uur

door

David Jaap Sprenkeler

geboren op 2 mei 1990 te Amsterdam

Promotor: Prof. dr. M.A. Vos
Copromotor: Dr. A.E. Tuinenburg

The research described in this thesis was performed as part of the EU-CERT-ICD project and was supported with funding from the European Community's Seventh Framework Programme FP7/2007-2013 under grant agreement no. 602299.

לאמא שלי

Contents

Chapter 1

Introduction

David J. Sprenkeler

Introduction

Heart disease is the leading cause of mortality and morbidity worldwide and sudden cardiac death (SCD) accounts for up to 50% of all cardiovascular deaths.[1] In the Netherlands, 15.000 people each year are resuscitated on the street because of a sudden cardiac arrest.[2] SCD is most often caused by a fast ventricular arrhythmia such as ventricular tachycardia (VT) or ventricular fibrillation (VF). Despite the widespread availability of Automatic External Defibrillators (AEDs) and increased knowledge of basic life support in the public, the prognosis after resuscitation remains poor. Since appropriate treatment often comes too late, focus has shifted towards risk prediction and prevention of SCD.

The Implantable Cardioverter-Defibrillator (ICD) is an internal device that can detect the occurrence of life-threatening ventricular arrhythmias and terminate them by delivery of a high energy electric shock. In the early years of ICD therapy, implantation of an ICD was only indicated for patients with a history of sudden cardiac arrest (i.e. secondary prevention). Later studies evaluated the use of ICD therapy in patients who did not yet experience life-threating arrhythmias, but were at high risk (i.e. primary prevention). Two major landmark trials, the MADIT-II and SCD-HeFT trial, showed that the ICD could significantly reduce mortality in patients with an ischemic or non-ischemic cardiomyopathy and a reduced left ventricular ejection fraction (LVEF).[3,4] The results of these trials were implemented in both American and European guidelines[5,6], which led to an immense increase in the number of ICDs implanted worldwide and in the Netherlands.[7]

The importance of risk prediction

Recently, it has become clear that the main criterion for ICD implantation, LVEF, lacks sensitivity and specificity in identifying the patient at highest risk of SCD. On the one hand, nationwide registries have shown that the majority of victims of SCD have an ejection fraction above the cut-off value of 35%.[8,9] On the other hand, in patients who do fulfil the criteria for ICD implantation, the number of appropriate shocks have decreased significantly compared to the original landmark trials, probably due to better pharmacological or device-based (e.g. Cardiac Resynchronization Therapy, CRT) treatment of heart failure.[10] Furthermore, the recent DANISH trial, a nationwide RCT that randomized patients with non-ischemic cardiomyopathy and reduced LVEF to ICD therapy or conventional medical therapy, could not demonstrate a survival benefit of ICD implantation due to a low event rate.[11] The results of this trial further question the benefit of ICD implantation in these patients. One must not forget that ICD implantation by itself is not without risks. Major adverse effects can occur, ranging from infections

and procedural complications, to lead failures and the occurrence of inappropriate shocks, which has been associated with severe psychological distress and reduced quality of life.[12]

In general, two types of patients can be discerned who will not benefit from ICD therapy:

1. Patients who are too healthy: they will have the ICD their whole life, but will never experience a life-saving shock.
2. Patients who are too sick: these patients will die from other causes, for example progressive heart failure, before they could have benefited from the ICD.

Hence, two competing risks of mortality, i.e. the risk of sudden arrhythmic death and the risk of non-sudden death, should be taken into account when selecting those patients who will benefit the most from ICD implantation.

Monitoring of imminent arrhythmias

While the ICD is highly effective in the prevention of SCD by defibrillation of lethal arrhythmias, it does not prevent the arrhythmia itself from occurring. In most cases, patients require additional therapy, such as antiarrhythmic medications or radiofrequency ablation of the arrhythmic substrate, to reduce the number of ICD shocks. However, both these treatment modalities are associated with significant adverse effects or peri-procedural complications. Ideally, the ICD would not only terminate the arrhythmia when present, but would also predict upcoming arrhythmias in order to initiate preventive therapy. A possible preventive measure could be to temporarily alter the pacing rate, which has shown to reduce the number of ICD shocks.[13] However, in order to do so, the device requires a simple parameter that reflects an increased risk of upcoming arrhythmias.

To find new parameters of arrhythmic risk that could help in both risk prediction and monitoring, we must go from the 'bedside' back to the 'bench' of cardiac physiology to study the mechanisms by which arrhythmias arise.

Normal physiology: electro-mechanical coupling of the heart

During each heartbeat, a coordinated sequence of electrical excitation and contraction of all cardiomyocytes ensures that blood is efficiently pumped throughout the body. Electrical excitation arises from a sudden change in voltage of the cardiomyocyte, known as the action potential, which consists of a highly orchestrated interplay of ionic currents across the cell membrane (see Figure 1A). In rest, cardiomyocytes are negatively charged. When a cell is excited, Na^+ channels at

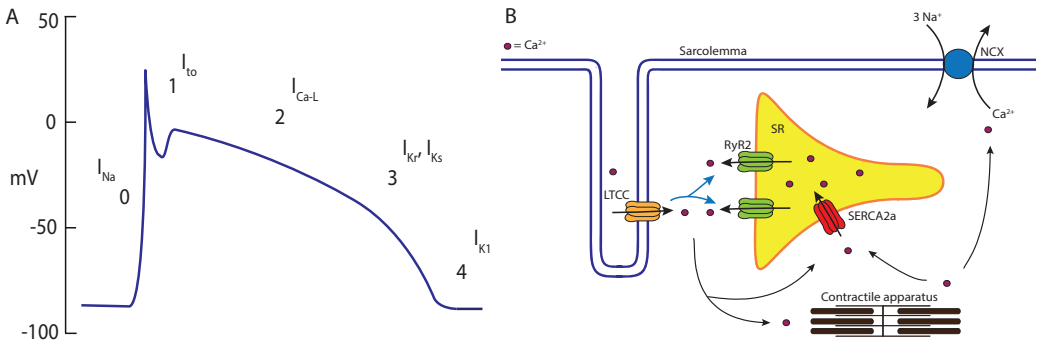

Figure 1. A) Normal action potential. During phase 0, there is a rapid influx of Na^+. Phase 1 consists of early repolarization due to a transient outward K^+ current. Phase 2 or plateau phase represents Ca^{2+} entry through L-type Ca^{2+} channels. Repolarization occurs during phase 3 caused by delayed rectifier currents (I_{Kr}, I_{Ks}). I_{K1} stabilizes the cell at the resting membrane potential during phase 4. B) Excitation-contraction coupling. Ca^{2+} entry through L-type Ca^{2+} channels (LTCC) activates ryanodine receptors (RyR2), causing release of Ca^{2+} from the sarcoplasmic reticulum (SR). Relaxation occurs by active sequestration of Ca^{2+} back into the SR by SR Ca^{2+} ATPase (SERCA2a) and by extruding Ca^{2+} out of the cell in exchange for Na^+ in a 1:3 ratio by the Na^+-Ca^{2+} exchanger (NCX).

the sarcolemma open, causing a rapid influx of Na^+ ions (I_{Na}; phase 0), depolarizing the cell. This change in membrane potential initiates early repolarization via the transient outward K^+ current (I_{to}; phase 1). In the meantime, L-type Ca^{2+} channels (LTCC) have also opened, generating in an inward Ca^{2+} current that remains present during the plateau phase (I_{Ca-L}; phase 2). In a process called excitation-contraction coupling (ECC), the resulting rise in local subsarcolemmal [Ca^{2+}] activates neighbouring Ca^{2+} release channels, the ryanodine receptors (RyR2), to release more Ca^{2+} out of the sarcoplasmic reticulum (SR) (see Figure 1B). The elevated cytosolic [Ca^{2+}] will then interact with the contractile apparatus, causing the cardiomyocyte to contract.

During diastole, Ca^{2+} is removed from the cytosol by actively pumping Ca^{2+} back into the SR by the SR Ca^{2+} ATPase (SERCA2a) or by extruding 1 Ca^{2+} out of the cell in exchange for 3 Na^+ ions by the Na^+-Ca^{2+} exchanger (NCX). Meanwhile, efflux of K^+ ions out of the cell through multiple types of K^+ channels (I_{Kr}, I_{Ks}, I_{K1}; phase 3 & 4) is responsible for repolarization, returning the membrane potential back to its resting state.

Finally, cell-to-cell coupling via gap junctions ensures that electrical excitation is conducted quickly throughout the heart. In addition, coupling of cardiomyocytes also maintains synchronization of repolarization via electrotonic interactions. Disturbances anywhere in this highly coordinated system of depolarization, conduction, contraction and repolarization can result in inefficient pump function and arrhythmias.

Ventricular remodeling

Ventricular remodeling describes the plasticity of the heart to adapt to certain pathological insults. In patients with structural heart disease, e.g. due to myocardial infarction, hypertension or valvular heart disease, cardiac function is impaired, resulting in reduced cardiac output, elevated end-diastolic pressures and increased left ventricular wall stress. In response, the sympathetic nervous system and renin-angiotensin-aldosterone system (RAAS) are activated, stimulating intracellular signalling pathways that contribute to cardiomyocyte hypertrophy and apoptosis, local inflammation and interstitial fibrosis.[14] As a result, structural, contractile and electrical alterations of the myocardium occur. Initially, ventricular remodeling is considered an adaptive process in order to maintain normal cardiac output. However, after chronic exposure to neurohumoral signalling, remodeling becomes maladaptive, resulting in progressive loss of cardiac function, electrical instability and ventricular arrhythmias.[15] Therefore, markers of these remodeling processes may be suitable for risk prediction and monitoring of arrhythmic events.

Contractile remodeling

Contractile remodeling comprises the alterations in contractility caused by disturbances in cardiac Ca^{2+} handling. Early on in the remodeling process, increased contractility helps to maintain normal cardiac output. On a cellular level, an increased amplitude and duration of the Ca^{2+} transient and higher Ca^{2+} content of the SR is found.[16] However, during progression of the disease towards heart failure, SR Ca^{2+} load and Ca^{2+} transients will become more and more reduced, resulting in a decline in contractile performance of the heart.

An important hallmark of contractile remodeling is Ca^{2+} overload of the cardiomyocyte, caused by altered expression and function of different Ca^{2+} handling proteins. In patients with ventricular remodeling the expression and function of SERCA2a is reduced, causing slower reuptake of Ca^{2+} into the SR and accumulation of Ca^{2+} in the cytosol.[17] NCX, on the other hand, appears to be upregulated.[18] Together with increased intracellular [Na^+] (possibly due to increased influx of Na^+ via the Na^+-H^+ exchanger)[19], NCX will switch into reverse mode (Na^+ out, Ca^{2+} in), leading to further Ca^{2+} loading of the cardiomyocyte. These disturbances in Ca^{2+} handling can cause alterations in contractility, impairment of relaxation and diastolic dysfunction. More importantly, increased intracellular [Ca^{2+}] has also been associated with ventricular arrhythmias. High cytosolic [Ca^{2+}] will drive NCX to extrude Ca^{2+} in exchange for Na^+. Since NCX exchanges Ca^{2+} for Na^+ in a 1:3 ratio, a net inward current is generated. When large enough, this inward current can depolarize the cardiomyocyte, initiating early- or delayed afterdepolarizations (EAD/DAD), as a trigger of ventricular arrhythmias.[20]

Therefore, markers of contractile remodeling could be used to determine the risk of EAD/DAD-triggered arrhythmias. The force-frequency relationship (FFR), mechanical restitution (MR) and post-extrasystolic potentiation (PESP) are macroscopic parameters of Ca^{2+} handling and can reflect changes in Ca^{2+} homeostasis *in vivo*. The FFR describes the potentiation of contractility when heart rate increases.[21] MR and PESP describe the changes in contractility of the extrasystolic and post-extrasystolic beat, respectively, when the coupling interval of the extraystole is varied. Changes in these parameters have been described in patients with hypertrophy and heart failure.[22,23] However, the relation of these parameters with arrhythmogenesis has not yet been demonstrated.

Electrical remodeling

Alterations in the electrophysiological properties of the heart, referred to as electrical remodeling, have been associated with the development of ventricular arrhythmias in patients with structural heart disease. A distinct feature of electrical remodeling is prolongation of the action potential duration (APD), due to altered expression and function of ion-channels and pumps. In the healthy cardiomyocyte there is a redundancy of repolarizing K^+ currents, commonly referred to as 'repolarization reserve', in order to withstand arrhythmogenic challenges on repolarization.[24] Therefore, blockade of one K^+ current will not lead to failure of repolarization. However, electrical remodeling causes downregulation of K^+ channels, thereby reducing repolarization reserve to that extend that repolarization becomes instable. A final 'hit' on repolarization (certain drugs, hypokalaemia or excessive β-adrenergic stimulation) will then result in early afterdepolarizations (EADs), ectopic beats and potentially life-threatening triggered arrhythmias.

Beat-to-beat variability of repolarization, quantified as short-term variability (STV), is a new electrophysiological marker of reduced repolarization reserve that measures repolarization instability of 30 consecutive beats.[25] Small retrospective studies have demonstrated a significantly higher baseline STV of the QT interval compared to controls in patients with congenital[26] or drug-induced[27] long QT syndrome and in patients with non-ischemic heart failure and a history of ventricular arrhythmias.[28] However, large prospective studies on the use of STV as risk marker of SCD have not yet been conducted. Furthermore, methodological questions on how and at what time during the day to measure STV have to be answered before this parameter can be implemented into clinical practice. Interestingly, STV does not only predict arrhythmic risk in the long term, but also rises abruptly a couple of minutes prior to the occurrence of ventricular arrhythmias.[29] Therefore, STV could be an ideal parameter for 24/7 monitoring of imminent arrhythmic risk that can be incorporated into a device.

Neural remodeling

Changes in the autonomic nervous system (ANS) play an important role in ventricular remodeling and the development of cardiac arrhythmias.[30] The ANS consists of two branches, the sympathetic and parasympathetic nervous system, which both have opposing effects on the heart. Sympathetic innervation of the heart originates in the right and left stellate ganglion; the parasympathetic effects are carried to heart by the vagal nerve. An imbalance of these two branches contributes to arrhythmogenesis: increased sympathetic activity triggers the occurrence of ventricular arrhythmias, while high vagal tone appears to be protective. This explains (partially) the beneficial effects of β-blockade and stellectomy (removal of sympathetic innervation by transsection of the stellate ganglion) in the prevention of arrhythmias in patients with heart failure or long QT syndrome.[31] During ventricular remodeling, chronic exposure to sympathetic stimulation results in dysfunction of β-adrenergic signalling with downregulation of receptors and uncoupling of the associated G-proteins.[32] Furthermore, in response to any form of myocardial injury, neurotrophic factors are released, triggering nerve sprouting, partial re-innervation and regional hyperinnervation.[33] Consequently, this neural remodeling results in increased heterogeneity of sympathetic innervation, with some regions being more densely innervated than others. In combination with reduced repolarization reserve due to electrical remodeling, sympathetic bursts will cause paradoxical lengthening of APD in hyperinnervated regions, leading to increased spatial dispersion of repolarization.[34] In addition, β-adrenergic stimulation augments Ca^{2+} overload, triggering EADs/DADs.[35,36]

The neurons of the sympathetic nervous system fire in low frequency bursts of around 0.1 Hz.[37] Recently, low frequency oscillations have been discovered in activation recovery interval of intracardiac electrograms in heart failure patients[38] and as changes in T wave vector on the electrocardiogram, which have been attributed to bursts of sympathetic firing on the myocardium.[39] Therefore it has been hypothesized that low frequency variations of APD can function as non-invasive marker of sympathetic overactivity on the ventricles and might reflect arrhythmic potential.

The chronic complete AV-block dog model

The chronic complete AV-block dog is an animal model to study the mechanisms of ventricular remodeling and arrhythmogenesis.[40] In this model, third degree AV-block is created by radiofrequency ablation of the proximal His bundle. As a result, heart rate drops from a sinus rate of 110 beats/min to a slow idioventricular rhythm (IVR) of 40 to 50 beats/min. To compensate for the drop in cardiac output, neurohumoral signalling pathways are activated resulting in ventricular remodeling (see Figure 2). The time course varies for the different remodeling processes. For instance, electrical and contractile

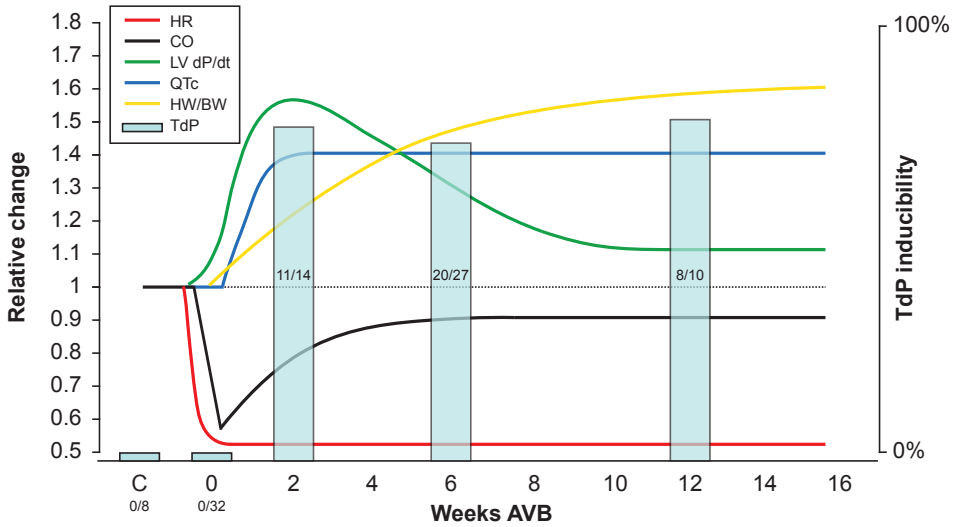

Figure 2. time course of ventricular remodeling in the chronic AV-block dog model.

After creation of complete AV-block, heart rate drops to around 50 beats/min (red line) and cardiac output decreases (black line). As a response, there is augmentation of contractility as measured by LV dP/dt_{max} within 2 weeks, which slowly decreases thereafter (green line). In addition, QTc increases and remains stable after 2 weeks of CAVB (blue line). Finally, biventricular hypertrophy starts to develop, as seen by an increase in ratio heartweight to bodyweight (HW/BW, yellow line), which is fully present after 16 weeks of remodeling. As a consequence, the dogs become reproducibly inducible to Torsades de Pointes (TdP) arrhythmias after 2 weeks (blue bars). Adapted from Bourgonje et al., with permission of the authors.

remodeling occur relatively fast: within two weeks after AV-block, APD is prolonged and contractility, as measured by left ventricular dP/dt_{max}, has increased.[41,42] In contrast, structural remodeling (i.e. biventricular hypertrophy) follows a much slower path and is fully present after 16 weeks of remodeling.[43] These remodeling processes reduce repolarization reserve and increase the vulnerability to ventricular arrhythmias.[44] Bradycardia, in combination with certain anesthesia[45] and a pro-arrhythmic drug (e.g. the I_{Kr}-blocker dofetilide), will act together as the final 'hit' on repolarization, resulting in single- and multiple ectopic beats and episodes of polymorphic ventricular arrhythmias, particularly Torsades de Pointes (TdP) arrhythmias.

The CAVB dog model has been used extensively for evaluation of new antiarrhythmic agents as well as for drug safety testing. Moreover, the chronic AV-block dog is a model of ventricular remodeling that represents the 'vulnerable patient' at increased risk of ventricular arrhythmias. Therefore, this model is ideal for evaluation of new markers of arrhythmic risk.

Thesis outline

In this thesis, the relation between parameters of ventricular remodeling and arrhythmia susceptibility is investigated, both in the CAVB dog model as well as in patient cohorts. We have used the CAVB model to search for new markers that may be related to arrhythmogenesis. In a large patient cohort, we have prospectively studied risk markers as predictors of arrhythmic episodes. We hypothesize that markers of ventricular remodeling are suitable candidates for risk prediction and may eventually improve patient selection for ICD therapy. Furthermore, we hypothesize that markers of electrical remodeling, mainly STV, can be used for continuous monitoring of imminent ventricular arrhythmias. Initiating preventive treatment when an upcoming arrhythmia is sensed, would significantly improve the functionality of implantable devices.

Part I focuses on the relation between contractile remodeling and arrhythmogenesis. **Chapter 2** reviews the current literature on alterations in contractile parameters in heart failure and hypertrophy. In **Chapter 3** three contractile parameters (FFR, MR and PESP) are studied in the CAVB dog and related to dofetilide-induced Torsades de Pointes arrhythmias.

In Part II, the use of electrical markers for risk prediction and monitoring is discussed. In **Chapter 4** the results of the EU-TrigTreat study are presented. This study focuses on the use of electrophysiological parameters for separate stratification of appropriate shock risk and all-cause mortality risk. **Chapter 5** contains an editorial on the differences in repolarization reserve between men and women. In **Chapter 6** we evaluate the circadian pattern of STV_{QT} in high and low arrhythmic patients in a substudy of the EU-CERT-ICD study. The use of STV_{ARI} of the right ventricular electrogram of implanted ICD leads for continuous monitoring is described in **Chapter 7**. A fully automatic method for measurement of STV_{ARI} that can be incorporated in implantable devices, is introduced in **Chapter 8**.

Finally, in part III, neural remodeling is discussed. **Chapter 9** describes the effects of ventricular remodeling on both respiratory and low frequency oscillations of APD in the CAVB dog. The latter is related to bursts of sympathetic activity and could reflect neural remodeling. In the final chapter, **Chapter 10**, a general discussion is provided.

References

1. Adabag AS, Luepker R V, Roger VL, et al. Sudden cardiac death: epidemiology and risk factors. *Nat Rev Cardiol* 2010;7:216–25.

2. Zijlstra J, Radstok A, Pijls R, et al. Overleven na een reanimatie buiten het ziekenhuis: vergelijking van de resultaten van 6 verschillende Nederlandse regio's. In: Reanimatie in

Nederland., 2016. Hartstichting; 2016.

3. Moss AJ, Zareba W, Hall WJ, et al. Prophylactic implantation of a defibrillator in patients with myocardial infarction and reduced ejection fraction. *N Engl J Med* 2002;346:877–83.
4. Bardy GH, Lee KL, Mark DB, et al. Amiodarone or an implantable cardioverter-defibrillator for congestive heart failure. *N Engl J Med* 2005;352:225–37.
5. Al-Khatib SM, Stevenson WG, Ackerman MJ, et al. 2017 AHA/ACC/HRS Guideline for Management of Patients With Ventricular Arrhythmias and the Prevention of Sudden Cardiac Death. *Heart Rhythm* 2017;
6. Priori SG, Blomström-Lundqvist C, Mazzanti A, et al. 2015 ESC Guidelines for the management of patients with ventricular arrhythmias and the prevention of sudden cardiac death: The Task Force for the Management of Patients with Ventricular Arrhythmias and the Prevention of Sudden Cardiac Death of the Europe. *Eur Heart J* 2015;36:2793–867.
7. Wijers SC, van der Kolk BYM, Tuinenburg AE, et al. Implementation of guidelines for implantable cardioverter-defibrillator therapy in clinical practice: Which patients do benefit? *Neth Heart J* 2013;21:274–83.
8. Adabag S, Rector TS, Anand IS, et al. A prediction model for sudden cardiac death in patients with heart failure and preserved ejection fraction. *Eur J Heart Fail* 2014;16:1175–82.
9. Stecker EC, Vickers C, Waltz J, et al. Population-based analysis of sudden cardiac death with and without left ventricular systolic dysfunction: two-year findings from the Oregon Sudden Unexpected Death Study. *J Am Coll Cardiol* 2006;47:1161–6.
10. Verhagen MP, van Boven N, Ruiter JH, et al. Follow-up of implantable cardioverter-defibrillator therapy: comparison of coronary artery disease and dilated cardiomyopathy. *Netherlands Hear J* 2014;22:431–7.
11. Køber L, Thune JJ, Nielsen JC, et al. Defibrillator Implantation in Patients with Nonischemic Systolic Heart Failure. *N Engl J Med* 2016;375:1221–30.
12. Sola CL, Bostwick JM. Implantable Cardioverter-Defibrillators, Induced Anxiety, and Quality of Life. Mayo Clin Proc 2005;80:232–7.
13. Wietholt D, Kuehlkamp V, Meisel E, et al. Prevention of sustained ventricular tachyarrhythmias in patients with implantable cardioverter-defibrillators-the PREVENT study. *J Interv Card Electrophysiol* 2003;9:383–9.
14. Schirone L, Forte M, Palmerio S, et al. A Review of the Molecular Mechanisms Underlying the Development and Progression of Cardiac Remodeling. *Oxid Med Cell Longev* 2017;2017:3920195.
15. Konstam MA, Kramer DG. Left ventricular remodeling in heart failure: current concepts in clinical significance and assessment. *JACC Cardiovasc Imaging* 2011;4:98–108.
16. Balke CW, Shorofsky SR. Alterations in calcium handling in cardiac hypertrophy and heart failure. *Cardiovasc Res* 1998;37:290–9.

17. Alpert NR, Leavitt BJ, Ittleman FP, et al. A mechanistic analysis of the force-frequency relation in non-failing and progressively failing human myocardium. *Basic Res Cardiol* 1998;93 Suppl 1:23–32.

18. Zaugg CE, Buser PT. When calcium turns arrhythmogenic: intracellular calcium handling during the development of hypertrophy and heart failure. *Croat Med J* 2001;42:24–32.

19. van Borren MMGJ, Vos MA, Houtman MJC, et al. Increased sarcolemmal Na^+/H+ exchange activity in hypertrophied myocytes from dogs with chronic atrioventricular block. *Front Physiol* 2013;4:322.

20. Volders PG, Vos MA, Szabo B, et al. Progress in the understanding of cardiac early afterdepolarizations and torsades de pointes: time to revise current concepts. *Cardiovasc Res* 2000;46:376–92.

21. Endoh M. Force–frequency relationship in intact mammalian ventricular myocardium: physiological and pathophysiological relevance. *Eur J Pharmacol* 2004;500:73–86.

22. Prabhu SD, Freeman GL. Effect of tachycardia heart failure on the restitution of left ventricular function in closed-chest dogs. *Circulation* 1995;91:176–85.

23. Seed WA, Noble MI, Walker JM, et al. Relationships between beat-to-beat interval and the strength of contraction in the healthy and diseased human heart. Circulation 1984;70:799–805.

24. Roden DM. Taking the "idio" out of "idiosyncratic": predicting torsades de pointes. *Pacing Clin Electrophysiol* 1998;21:1029–34.

25. Varkevisser R, Wijers SC, van der Heyden MAG, et al. Beat-to-beat variability of repolarization as a new biomarker for proarrhythmia *in vivo*. *Heart Rhythm* 2012;9:1718–26.

26. Hinterseer M, Beckmann B-M, Thomsen MB, et al. Relation of increased short-term variability of QT interval to congenital long-QT syndrome. *Am J Cardiol* 2009;103:1244–8.

27. Hinterseer M, Thomsen MB, Beckmann B-M, et al. Beat-to-beat variability of QT intervals is increased in patients with drug-induced long-QT syndrome: a case control pilot study. *Eur Heart J* 2008;29:185–90.

28. Hinterseer M, Beckmann B-M, Thomsen MB, et al. Usefulness of short-term variability of QT intervals as a predictor for electrical remodeling and proarrhythmia in patients with nonischemic heart failure. *Am J Cardiol* 2010;106:216–20.

29. Thomsen M, Oros A, Schoenmakers M, et al. Proarrhythmic electrical remodelling is associated with increased beat-to-beat variability of repolarisation. Cardiovasc Res 2007;73:521–30.

30. Kalla M, Herring N, Paterson DJ. Cardiac sympatho-vagal balance and ventricular arrhythmia. *Auton Neurosci* 2016;199:29–37.

31. Schwartz PJ. Cardiac sympathetic denervation to prevent life-threatening arrhythmias. *Nat Rev Cardiol* 2014;11:346–53.

32. Florea VG, Cohn JN. The Autonomic Nervous System and Heart Failure. Circ Res 2014;114:1815–26.

33. Chen P-S, Choi E-K, Zhou S, et al. Cardiac neural remodeling and its role in arrhythmogenesis. *Heart Rhythm* 2010;7:1512–3.

34. Kang C, Badiceanu A, Brennan JA, et al. β-adrenergic stimulation augments transmural dispersion of repolarization via modulation of delayed rectifier currents IKs and IKr in the human ventricle. *Sci Rep* 2017;7:15922.

35. Johnson DM, Heijman J, Pollard CE, et al. IKs restricts excessive beat-to-beat variability of repolarization during beta-adrenergic receptor stimulation. *J Mol Cell Cardiol 2010*;48:122–30.

36. Johnson DM, Heijman J, Bode EF, et al. Diastolic spontaneous calcium release from the sarcoplasmic reticulum increases beat-to-beat variability of repolarization in canine ventricular myocytes after β-adrenergic stimulation. *Circ Res* 2013;112:246–56.

37. Malpas SC. Neural influences on cardiovascular variability: possibilities and pitfalls. *Am J Physiol Heart Circ Physio*l 2002;282:H6-20.

38. Hanson B, Child N, Van Duijvenboden S, et al. Oscillatory behavior of ventricular action potential duration in heart failure patients at respiratory rate and low frequency. *Front Physiol* 2014;5:414.

39. Rizas KD, Nieminen T, Barthel P, et al. Sympathetic activity–associated periodic repolarization dynamics predict mortality following myocardial infarction. J Clin Invest 2014;124:1770–80.

40. Oros A, Beekman JDM, Vos MA. The canine model with chronic, complete atrio-ventricular block. *Pharmacol Ther* 2008;119:168–78.

41. Donker DW, Volders PGA, Arts T, et al. End-diastolic myofiber stress and ejection strain increase with ventricular volume overload--Serial in-vivo analyses in dogs with complete atrioventricular block. *Basic Res Cardiol* 2005;100:372–82.

42. Vos MA, de Groot SH, Verduyn SC, et al. Enhanced susceptibility for acquired Torsades de pointes arrhythmias in the dog with chronic, complete AV block is related to cardiac hypertrophy and electrical remodeling. *Circulation* 1998;98:1125–35.

43. Schoenmakers M, Ramakers C, van Opstal JM, et al. Asynchronous development of electrical remodeling and cardiac hypertrophy in the complete AV block dog. *Cardiovasc Res* 2003;59:351–9.

44. Dunnink A, van Opstal JM, Oosterhoff P, et al. Ventricular remodelling is a prerequisite for the induction of dofetilide-induced Torsades de pointes arrhythmias in the anaesthetized, complete atrio-ventricular-block dog. *Europace* 2012;14:431–6.

45. Dunnink A, Sharif S, Oosterhoff P, et al. Anesthesia and Arrhythmogenesis in the Chronic Atrioventricular Block Dog Model. *J Cardiovasc Pharmacol* 2010;55:601–8.

1

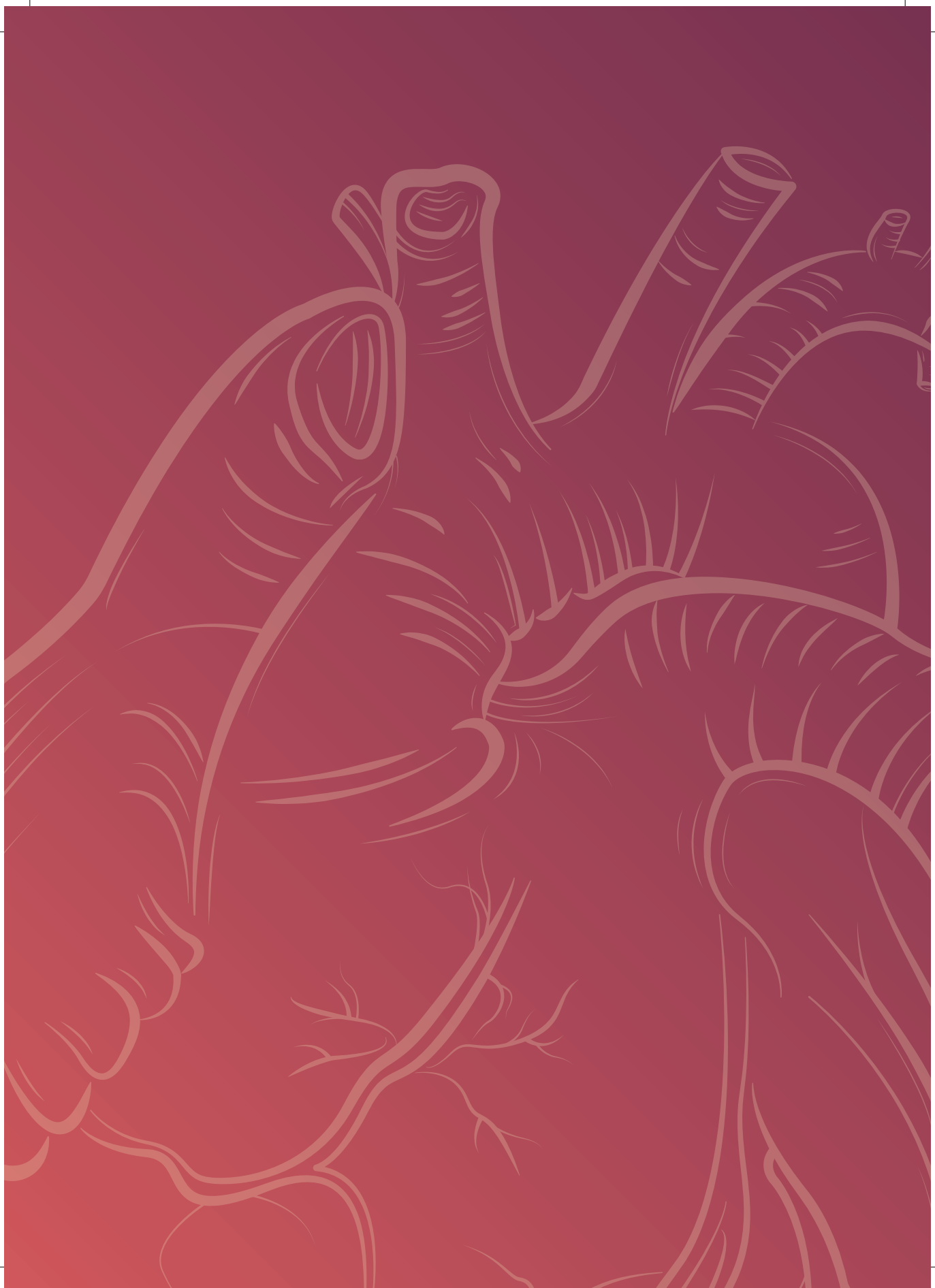

PART I

PARAMETERS OF CONTRACTILE REMODELING FOR RISK PREDICTION

Chapter 2

Post-extrasystolic potentiation: Link between Ca^{2+} homeostasis and heart failure?

David J. Sprenkeler, Marc A. Vos

Department of Medical Physiology, University Medical Center Utrecht, Utrecht, the Netherlands

Arrhythm Electrophysiol Rev. 2016 May;5(1):20-6

Abstract

Post-extrasystolic potentiation (PESP) describes the phenomenon of increased contractility of the beat following an extrasystole and has been attributed to changes in Ca^{2+} homeostasis. While this effect has long been regarded a normal physiological phenomenon, a number of reports describe an enhanced potentiation of the post-extrasystolic beat in heart failure patients. The exact mechanism of this increased PESP is unknown, but disruption of normal Ca^{2+} handling in heart failure may be the underlying cause. The use of PESP as a prognostic marker or therapeutic intervention has recently regained new attention, however, the value of the application of PESP in the clinic is still under debate. In this review, the mechanism of PESP with regard to Ca^{2+} in the normal and failing heart is discussed and the possible diagnostic and therapeutic roles of this phenomenon are explored.

Introduction

The concept of post-extrasystolic potentiation (PESP), which describes the phenomenon of increased contractility of the beat following an extrasystole, has intrigued physiologists and clinicians for more than 120 years. Since its first description in 1885 by Oskar Langendorff[1], PESP has become a widely debated concept, not only for its fundamental basis, but also because of the potential diagnostic and therapeutic properties. Existence of PESP has been demonstrated in isolated papillary muscles[2], perfused isolated hearts[3,4] and *in vivo* models, including humans.[5] PESP has formerly been attributed to alterations in preload and/or afterload during the compensatory pause following an extrasystolic beat. However, numerous studies in which preload and/or afterload were controlled[6–9], have demonstrated that PESP is independent of these loading conditions and that its mechanism is the consequence of changes in intracellular Ca^{2+} handling.

A number of reports describe differences in the magnitude of PESP in patients with heart failure and state that PESP could be used as a marker of myocardial dysfunction.[10–13] In addition, recent studies by Sinnecker et al. have shown that the presence of PESP of blood pressure could predict mortality in post-MI patients with sinus rhythm or atrial fibrillation.[14,15] These results have revived the possible diagnostic or prognostic role of PESP. In this review, the mechanism of PESP with regard to Ca^{2+} homeostasis will be discussed in normal and in heart failure individuals and the diagnostic and therapeutic consequences will be explored.

Normal Ca^{2+} homeostasis

Excitation-contraction coupling (ECC) is the process by which electrical stimulation results in contraction of cardiac myofilaments, which involves sarcolemmal ion currents and various intracellular pathways.[16] Ca^{2+} is an important element for both electrical and contractile function of the cardiomyocyte. In resting state, the cardiomyocyte has a low cytosolic concentration of Ca^{2+} ($[Ca^{2+}]_i$) of less than 200 nmol/l.[17] When the cardiomyocyte is depolarized, voltage-dependent L-type Ca^{2+} channels (LTCC) at the sarcolemma open, causing an influx of Ca^{2+} along its electrochemical gradient into the dyadic cleft. This small inflow of Ca^{2+} results in release of Ca^{2+} from the adjacent sarcoplasmic reticulum (SR) through the SR Ca^{2+} release channels, also known as type 2 ryanodine receptors (RyR2), a process called Ca^{2+}-induced Ca^{2+} release (CICR). Synchronized opening of RyR2 will generate a global Ca^{2+} transient[18,19], which increases $[Ca^{2+}]_i$ a tenfold. Free Ca^{2+} binds to troponin C, causing a conformational change, which allows the myosinhead to bind to actin and move along the actin filament, shortening the cardiomyocyte. For relaxation to occur, Ca^{2+} needs to be dissociated from troponin

C and be removed from the cytosol. In human cardiac cells approximately 70% of cytosolic Ca^{2+} is sequestered back into the SR by SR Ca^{2+} ATPase 2a (SERCA2a) and 30% is extruded out of the cell by the sarcolemmal Na^{+}-Ca^{2+} exchanger (NCX), which expels one Ca^{2+} ion in exchange for three Na^{+} ions.[20]

Calcium handling in heart failure

Disruption of Ca^{2+} homeostasis is an important contributor to depressed ventricular function in heart failure. Alterations in Ca^{2+} reuptake, storage and release result in a reduced Ca^{2+} transient and consequently a diminished contraction.[21–23]

First, multiple studies suggest that Ca^{2+} uptake in the SR is diminished due to downregulation or a decreased activity of SERCA2a.[24–27] A reduced reuptake results not only in decreased SR Ca^{2+} content, but also in higher cytosolic Ca^{2+} concentration, which inhibits normal relaxation. Therefore, decreased SERCA2a expression contributes to both systolic and diastolic ventricular dysfunction. On the other hand, expression of NCX appears to be increased in patients with heart failure.[28] When functioning in forward mode (Ca^{2+} efflux and Na^{+} influx), upregulation of NCX results in increased extrusion of Ca^{2+} and a decrease of $[Ca^{2+}]_i$. While this may counter the diastolic dysfunction caused by decreased Ca^{2+} reuptake, there is further reduction in systolic function, due to a decrease in intracellular Ca^{2+} available for excitation-contraction coupling.[29]

Next, hyperphosphorylation of RyR2 by proteinkinases such as CaMKII or PKA is suggested to cause diastolic Ca^{2+} leak from the SR.[30,31] This Ca^{2+} leak results in partial depletion of SR Ca^{2+} stores and contributes further to high diastolic $[Ca^{2+}]_i$. In addition, diastolic Ca^{2+} leak may induce Ca^{2+} release by activating other RyR2, resulting in Ca^{2+} waves. When Ca^{2+} is exchanged for 3 Na^{+} by the upregulated NCX, a transient inward current (I_{ti}) is generated, which may result in early or delayed afterdepolarizations (EAD/DADs), that could trigger lethal ventricular arrhythmias.

Finally, sensitivity of RyR2 for luminal Ca^{2+}appears to be enhanced; the set point for Ca^{2+} release is decreased, therefore RyR2 are activated at lower SR Ca^{2+} levels in heart failure compared to normal hearts.[32] This sensitization of RyR2 may be an adaption to the decreased Ca^{2+} concentration in order to maintain normal Ca^{2+} transients.[33] All of these alterations of Ca^{2+} homeostasis influence both long-term force-frequency and short-term force-interval relationships.

Force-frequency and force-interval relationships

Force-frequency and force-interval relationships describe contractility changes when stimulation rate is varied. While the force-frequency relationship (FFR) describes contractility changes when heart rate increases or decreases, force-interval relationship

(FIR) accounts for alterations in contractility by abrupt variations in stimulation pattern, i.e. by introducing extrasystolic beats.

Force-frequency relationship (FFR)

In most mammalian species, including humans, a positive FFR exists by which contractility is enhanced, when stimulation frequency is increased.[34] This positive staircase phenomenon or 'treppe' was first described by Bowditch in 1871[35] and is an important mechanism for increased inotropy during exercise.[36,37] The rise of contractility appears to be related to an increased amplitude of the Ca^{2+} transient at higher frequencies.[38,39] This increase in Ca^{2+} transient is the product of different mechanisms. First, an increased number of depolarizations leads to more Ca^{2+} influx per unit of time which results in increased Ca^{2+} release and uptake in the SR. Next, when increasing the frequency of stimulation, the influx of Na^{+} during depolarization is increased. To maintain a low cytosolic concentration of Na^{+}, NCX will switch to its reverse mode to extrude Na^{+} in exchange for Ca^{2+}.[40] This influx of Ca^{2+} will further increase SR Ca^{2+} content. Finally, reuptake of Ca^{2+} by SERCA2a relative to extrusion of Ca^{2+} by NCX is increased.[41] This increased SERCA2a activity might be caused by phosphorylation of phospholambam, the main regulatory protein of SERCA2a. In dephosphorylated state, phospholambam decreases the affinity of SERCA2a for Ca^{2+}. When phospholambam is phosphorylated, this inhibitory effect is removed and reuptake of Ca^{2+} is enhanced.

In failing myocardium, FFR is blunted or even inversed, resulting in a decrease of contractility with increasing heart rate.[34,42–44] This negative force-frequency relation is attributed to decreased Ca^{2+} reuptake due to downregulation of SERCA2a and upregulation of NCX in failing hearts.[45,46] When stimulation rate increases, time per cycle for Ca^{2+} reuptake is reduced, which, in case of less Ca^{2+} pumps, results in insufficient Ca^{2+} reuptake.

Force-interval relationship (FIR)

The change in contractility when premature beats occur, is described in the short-term force-interval relationship. FIR is divided into two concepts: mechanical restitution (MR) and post-extrasystolic potentiation (PESP).[2] These phenomena are both related to the coupling interval between the regular beat and the premature beat, the extrasystolic interval (ESI), and the interval between the extrasystolic beat and the following post-extrasystolic beat, the post-extrasystolic interval (PESI). MR accounts for recovery of contractile strength of the extrasystolic beat when ESI is lengthened. PESP displays the opposite behavior; with decreasing ESI, there is an increase in contractility of the post-extrasystolic beat. In other words, the earlier the extrasystolic beat occurs, the weaker the extrasystolic beat and the stronger the post-extrasystolic beat. (see Figure 1A)

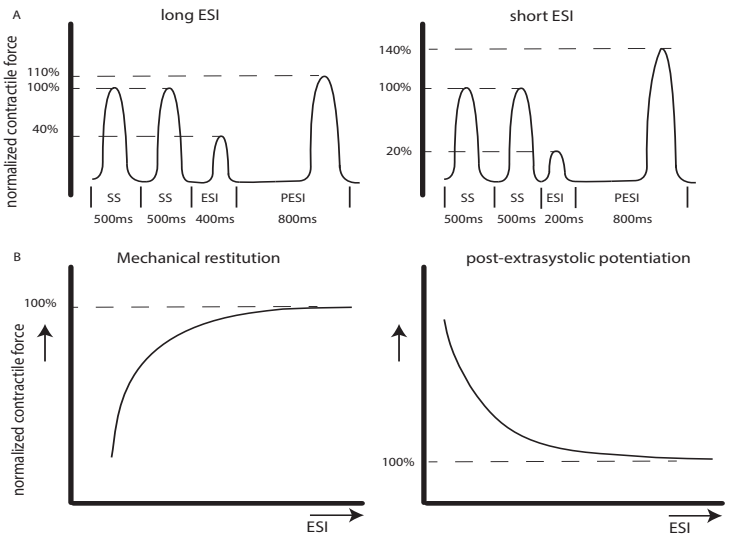

Figure 1. mechanical restitution and post-extrasystolic potentiation

A) SS = steady state, ESI = extrasystolic interval, PESI = post-extrasystolic interval. Contractile force normalized to last steady state beat. When ESI is shortened, contractility of the extrasystolic beat decreases but contractility of the post-extrasystolic beat increases.

B) MR (left) and PESP (right) curves are mono-exponential curves with similar time constants. When ESI is sufficiently lengthened, contractility of both the extrasystolic and post-extrasystolic beat approaches contractility of steady state beat.

Wier and Yue performed pacing experiments with isolated papillary muscles from ferret hearts to demonstrate the concepts of MR and PESP and the relation with the extrasystolic interval.[2] After a steady state pacing series, an extrasystolic stimulus was introduced with varying ESI. The post-extrasystolic interval was held constant. As expected, contractility of the extrasystolic beat increased and contractility of the post-extrasystolic beat decreased, when ESI was prolonged. When the contractile strength of the extrasystolic beat and the post-extrasystolic beat were plotted as a function of ESI, monoexponential functions were found with similar time constants (see Figure 1B), indicating a common underlying mechanism for both phenomena. Nowadays, the mechanism of these effects is attributed to changes in Ca^{2+} handling.

Mechanism of mechanical restitution and post-extrasystolic potentiation

A fundamental concept for the mechanism of MR and PESP is a time-dependent recovery period of Ca^{2+} release. The mechanism was formerly explained by a model of

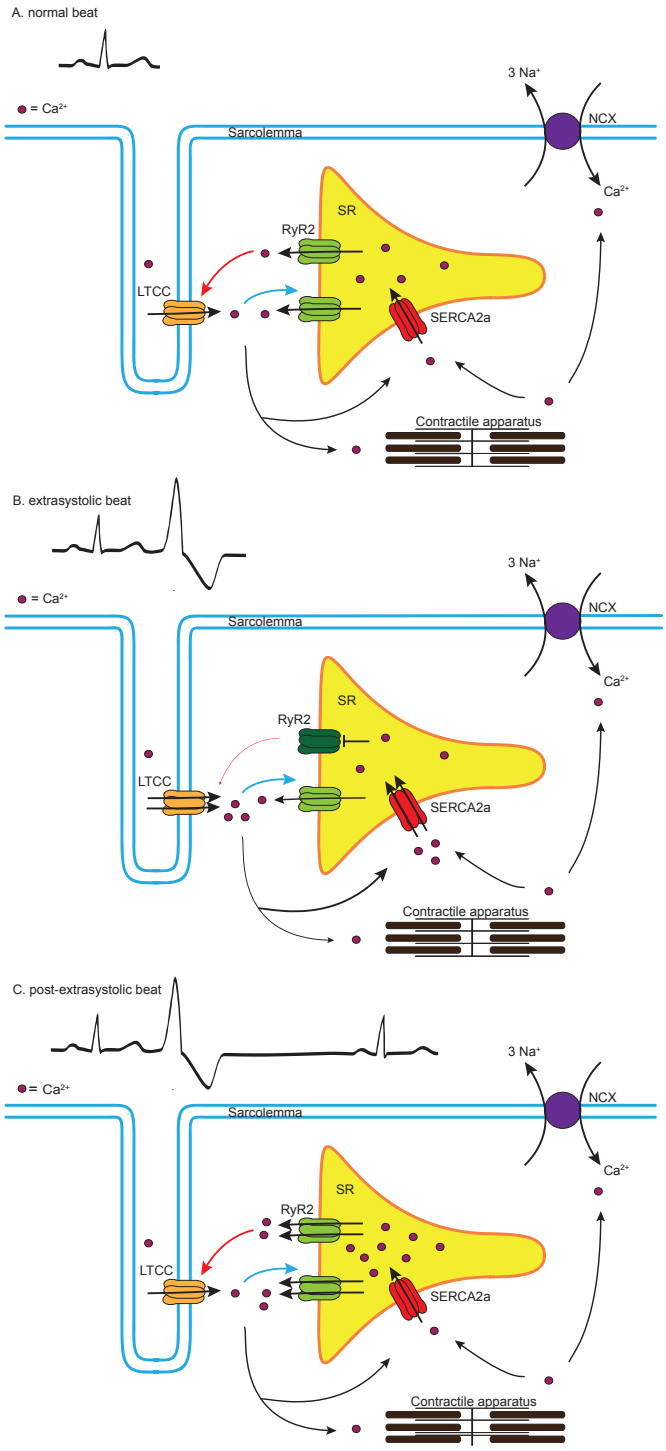

Figure 2. mechanism of mechanical restitution and post-extrasystolic potentiation

A) ECC during normal beat. Ca^{2+} influx through LTCC activates RyR2 to release Ca^{2+} from SR, which inhibits further sarcolemmal Ca^{2+} influx. After contraction, Ca^{2+} is sequestered back into the SR by SERCA2a or is extruded out of the cell by NCX in exchange for 3 Na^{+}.

B) ECC during extrasystolic beat. Some RyR2 are refractory (darkgreen), thus less Ca^{2+} is released from the SR. This smaller Ca^{2+} transient opposes less negative feedback to sarcolemmal Ca^{2+} influx. This increased cytosolic Ca^{2+} is taken up by SERCA2a, further loading the SR.

C) ECC during post-extrasystolic beat. The SR contains more Ca^{2+} because less Ca^{2+} was released during extrasystole and uptake of Ca^{2+} was enhanced. After the compensatory pause all RyR2 are recovered from inactivation and Ca^{2+} sequestered during the two previous beats is released.

SR: sarcoplasmic reticulum; LTCC: L-type Ca^{2+} channel; RyR2: ryanodine receptor; SERCA2a: SR Ca^{2+} ATPase; NCX: Na^{+}-Ca^{2+}-exchanger;

different Ca^{2+} compartments within the SR, in which diffusion of Ca^{2+} from an uptake department to a release department was time dependent.[2,3] However, this model lacks experimental evidence, since no anatomic compartment structures have been found in the SR and transfer by diffusion of Ca^{2+} within the SR would occur rapidly.[47,48]

Refractoriness of Ca^{2+} release channels has been postulated as an alternative explanation for the process of MR and PESP (see Figure 2). In a study by Fabiato[49], recovery from inactivation of ryanodine receptors had a time constant, which was similar to the kinetics of MR and PESP by Wier and Yue. According to this model, when a premature beat occurs, most of the ryanodine receptors are refractory to activation, causing a diminished Ca^{2+} transient and thus a less forceful contraction. After the premature beat, SR Ca^{2+} load is increased in a number of ways. First, while less Ca^{2+} is released, Ca^{2+} loading of the SR continues. Next, the low Ca^{2+} transient during the premature beat opposes less negative feedback to sarcolemmal Ca^{2+} influx and this extra Ca^{2+} further increases SR Ca^{2+} content. During the compensatory pause there is full mechanical restitution, thus all release channels have recovered from inactivation. At the post-extrasystolic beat, the total of Ca^{2+} sequestered during the previous two beats will be released, resulting in increased force of the post-extrasystolic beat.

PESP in heart failure

A number of studies have found differences in PESP of LV dP/dt_{max} between heart failure patients and controls. In 1971, Beck et al. observed that patients with obstructed or failing ventricles had an increased potentiation of the post-extrasystolic contraction compared to controls.[10] This paradoxical observation was confirmed in other studies.[11–13] However, only the study by Seed et al. controlled all coupling intervals (ESI, PESI), which, as we have seen, influence the extent of potentiation.[13] Despite the methodological flaws of these clinical studies, a small number of experimental and modeling studies are supportive of this observation.

The increase in PESP is attributed to abnormal Ca^{2+} homeostasis in heart failure. First, abnormal Ca^{2+} sequestration could result in a higher PESP. In the study of Seed et al. an inverse linear relation was seen between post-extrasystolic potentiation and the so called 'recirculation fraction', the ratio of contractility of the second post-extrasystolic beat compared to the first post-extrasystolic beat. The recirculation fraction has been suggested to account for the fraction of released Ca^{2+} sequestered back into the SR. Patients with heart failure appeared to have a lower recirculation fraction, which could be related to decreased Ca^{2+}-reuptake seen in these patients.

Studies by Hoit et al.[50,51] confirmed these results. They evaluated MR and PESP in mice with overexpression of phospholambam, in which Ca^{2+} reuptake was diminished and recirculation fraction was decreased. They found slower MR and increased PESP in

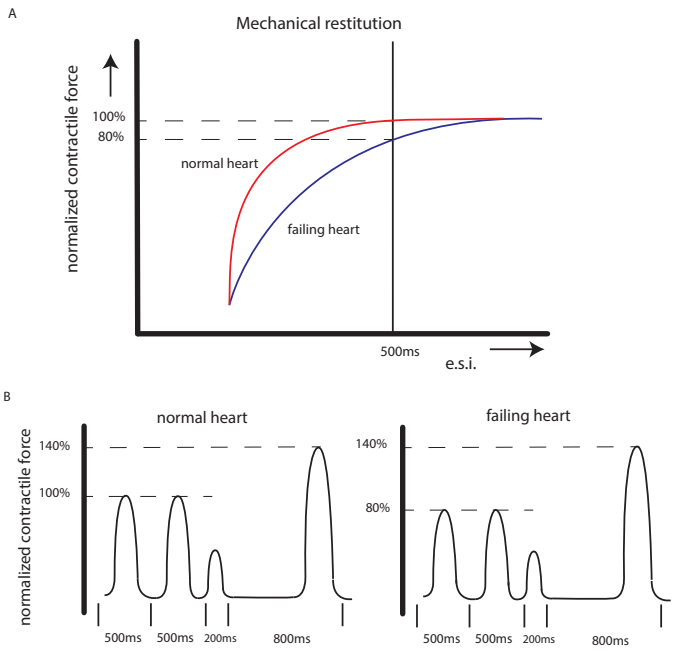

Figure 3. Influence of slower MR on PESP

A) Mechanical restitution is slowed in failing hearts. At a certain cycle length (i.e. 500ms) the failing heart operates at a lower level of contractile performance due to incomplete MR. B) Pacing at a steady state cycle length of 500ms with ESI of 200ms and PESI of 800 ms. When PESP is normalized to the incomplete restituted steady state beats, an increased relative PESP is seen.

these mice compared to isogenic controls, which indicates a role for SR Ca^{2+} reuptake in these force-interval relationships. The authors hypothesized that lower SR Ca^{2+} content slows down recovery of RyR2. When more ryanodine receptors are refractory during the premature beat, even more Ca^{2+} remains in the SR. During the post-extrasystolic beat the build-up of Ca^{2+} is released, which results in a higher PESP. Another explanation for the augmented potentiation in heart failure could be found in an increased sensitivity of RyR2 for Ca^{2+}. In case of more sensitive ryanodine receptors, a larger fraction of the SR content will be released during the post-extrasystolic beat, resulting in an even higher relative PESP in the failing heart.

Both of these hypotheses are supported by a study of Rice et al., in which the experiments of Wier and Yue were simulated using a computational model to address different aspects of the short-term force-interval relationship.[52] The model computed the changes in MR and PESP when certain parameters of excitation-contraction coupling were altered. In this model, PESP increased, when the releasable fraction (i.e. the fraction of total Ca^{2+} in the SR that is released) was increased. This is in accordance with increased sensitivity of RyR2 as an explanation for higher PESP. Furthermore, a

decrease in recirculation fraction (the fraction of Ca^{2+} sequestered back in SR) was also associated with a higher PESP. While this may sound counterintuitive, a lower recirculation fraction results in higher beat-to-beat variability of SR Ca^{2+} load, that is essential for MR and PESP. In contrast, a theoretical maximal recirculation fraction (all released Ca^{2+} is recirculated back in the SR) will cause the same SR load of every beat, which makes potentiation impossible to occur.

Finally, overall slower recovery of RyR2 may contribute to the increase in PESP. Prabhu et al. investigated alterations of both MR and PESP in dogs with tachycardia induced heart failure.[48,53] They found slower MR kinetics, which they attributed to slower recovery of RyR2. Thus, at faster heart rates, the failing heart does not operate at optimal performance, because most of the ryanodine receptors are refractory, resulting in incomplete mechanical restitution. When the cycle length is increased, there is full restitution and contractility will return to normal. This observation is consistent with the negative force-frequency relationship seen in heart failure. These altered MR kinetics will consequently have implications on PESP. When the failing heart is stimulated at a steady state cycle length below that at which full restitution is achieved, the contractile response of these steady state beats will be suboptimal. During the compensatory pause, the heart is fully restituted and a normal PESP is seen. However, if the magnitude of the post-extrasystolic beat is normalized to the (suboptimal) steady state beats, a higher relative PESP will be found in the failing heart compared to controls (see Figure 3).

PESP as a diagnostic instrument or therapeutic intervention

Diagnostics

PESP has been studied formerly as a diagnostic instrument to differentiate viable from non-viable myocardium during revascularization procedures.[54–56] However, this diagnostic approach has not demonstrated consistent results and has largely been replaced by more accurate techniques such as nuclear imaging or magnetic resonance imaging (MRI). Recently, PESP has gained new attention as a possible prognostic marker in myocardial infarction patients.[14] Sinnecker et al. measured post-extrasystolic potentiation of arterial blood pressure using a non-invasive photoplethysmographic device in 941 patients who survived the acute phase of MI and correlated the presence of post-extrasystolic potentiation to all cause 5-year mortality. Post-extrasystolic potentiation was defined as an increase in post-extrasystolic pulse pressure of 3% or more, compared to the mean of the subsequent beats. The authors found a significant higher mortality risk in patients in whom PESP was present compared to patients in whom PESP was absent. PESP remained a significant risk predictor after adjusting for LVEF, the amount of ventricular premature beats and GRACE score. Addition of PESP

to LVEF as risk predictor increased the area under the ROC-curve from 0.61 to 0.75 ($p < 0.001$), indicating that the combination of PESP and LVEF could better stratify patients with high or low mortality risk.

The mechanism on how PESP is correlated to a worse prognosis was not made clear. The end point all-cause mortality was not further stratified in death of mechanical or arrhythmic origin. As one can assume, changes in PESP display alterations in Ca^{2+} handling, which could, in addition to myocardial dysfunction, also lead to early and delayed afterdepolarizations. Thus, altered PESP might indicate an early stage of heart failure, but may also be a marker of increased risk of lethal ventricular arrhythmias.

However, some methodological remarks have to be made. First, the rise in blood pressure of the post-extrasystolic beat was compared to the subsequent beats. However, PESP usually decays in a number of beats, therefore for correct analysis of the percentage of PESP, using the beats preceding the PVC would have been more accurate. Second, in this study PESP was defined as difference in blood pressure, measured with a noninvasive device at the finger, while most studies used invasive measurements of contractility, like the maximal rise in left ventricular pressure (dP/dt_{max}). When measuring PESP more distally, vascular influences may alter the blood pressure measurements of PESP. In other words, the phenomenon measured in this study might not be comparable to PESP seen during earlier invasive experiments. More importantly, as seen in other studies of PESP in heart failure, the intervals were not held constant. Therefore, when basic rhythm, extrasystolic interval or post-extrasystolic interval differ, the magnitude of potentiation will change.[57,58] Therefore, from a physiological point of view, no strong conclusions can be made on the relation between high PESP and heart failure, when the intervals are not controlled. Nonetheless, since PESP appears to be a strong predictor of mortality, it could still have prognostic value, even if the underlying mechanism is not completely understood. Further validation of the use of PESP as a prognostic marker will be needed before it could be implemented as a clinical tool.

Therapeutics

The therapeutic use of PESP has been extensively investigated in the 1960's and 1970's, but has long been abandoned due to conflicting evidence of its effectiveness.[59–62] Inducing PESP and therefore increasing the force of contraction, might be beneficial in heart failure patients. By using coupled or paired pacing, in which a premature beat is introduced after every other intrinsic or paced beat, respectively, the effect of PESP is extended, which improves contractility and cardiac output. This technique has been studied in patients with cardiogenic shock, by which cardiac function significantly improved. However, reports of increased myocardial oxygen consumption and risk of arrhythmias have waned the interest in this mode of pacing.[63]

More recently, a number of studies have reevaluated the safety and efficacy of

coupled pacing. In 2008 a study by Lieberman et al.[64] studied dual chamber coupled pacing (DCCP) in 16 heart failure patients. DCCP increased LV dP/dt_{max} and arterial pulse pressure, however other hemodynamic parameters such as mean arterial pressure, cardiac output and mixed venous O_2 saturation did not differ. In the same year, Freudenberg investigated the use of atrioventricular coupled pacing in ten heart failure patients and concluded that this mode of pacing is safe and well tolerated.[65] In this study, coupled pacing was applied during 15 to 20 minutes. A significant increase in ejection fraction and stroke volume and a reduced end-systolic volume were seen, accompanied by a decrease in cardiac output due to a decreased heart rate. Two studies evaluated the use of coupled pacing in addition to cardiac resynchronization therapy in heart failure patients with mechanical dyssynchrony.[66,67] A further increase in contractility and ejection fraction was seen along with a decrease in heart rate without disrupting the synchronization properties of CRT. While Steegeman et al. concluded that this drop in heart rate reduced the hemodynamic benefit of paired pacing, Bemont et al. suggested that the heart rate reduction could have an additional beneficial effect, because of increased time for ventricular filling and reduced myocardial work.

These recent trials indicate that there still may be a role for coupled pacing in heart failure patients, however, the long-term effects remain unknown. Furthermore, because of introduction of stimuli during the vulnerable period of repolarization, the risk of inducing ventricular arrhythmias remains present. Another device-based therapy, cardiac contractility modulation (CCM), is increasingly being investigated and has already shown to be a safe and effective alternative to coupled pacing. CCM uses high-intensity, non-excitatory electrical stimulation applied during the absolute refractory period, which, in contrast to PESP, does not result in an action potential nor contraction.[68–70] Studies in isolated papillary muscles[71], isolated hearts[72], *in vivo* animal models[73] and patients[74] have shown a positive effect on cardiac contractility. This treatment might be a good option for patients with advancing heart failure despite optimal medical treatment, who are not a candidate for CRT. The exact mechanism of action is unknown, but the effect has been attributed to an increase in Ca^{2+} transient by a number of possible mechanisms, including an increase in phosphorylation of phospholambam, increased SERCA2a expression[75], normalization of NCX activity[76], but also an increased influx of Ca^{2+} through the L-type Ca^{2+} channels[69]. A number of randomized clinical trials[77–79] have been executed to investigate the safety and efficacy of CCM in heart failure patients and showed an improved exercise tolerance and quality of life, without increased myocardial oxygen consumption or arrhythmia risk. However, no difference in mortality nor morbidity has yet been found, thus the long-term consequences need to be further elucidated before these techniques can be implemented in clinical practice.

Conclusion

Since it was last reviewed extensively in 1993 by Cooper, much has been discovered about the phenomenon of post-extrasystolic potentiation.[80] The fundamental physiology of an altered calcium homeostasis has been more elucidated; the SR compartment model of Wier and Yue has been replaced by the central role of the ryanodine receptor and its refractory period in the mechanism of PESP.

The diagnostic and therapeutic properties of PESP have recently been rediscovered. However, the relationship between PESP and heart failure remains a complex interplay of both short-term force-interval and force-frequency relationships. Therefore, experimental studies of control versus failing hearts, in which all intervals are controlled, will be needed to confirm the assumption of an augmented post-extrasystolic potentiation in failing hearts. In addition, the prognostic value of PESP of blood pressure needs to be further evaluated and validated, since this non-invasive test might be of great value for selecting therapeutic interventions, e.g. ICD therapy, in certain patient groups. The *EUropean Comparative Effectiveness Research to assess the use of primary prophylacTic Implantable Cardioverter Defibrillators (EU-CERT-ICD)* study, which investigates new parameters for identification of high arrhythmia risk in ICD patients, is currently ongoing and will incorporate the use of PESP for stratification of mortality and ICD shock risk. Finally, the therapeutic use of coupled pacing in conjunct to CRT therapy has gained new attention. However, CCM might take its place as a new device-based therapy for heart failure, because of a better safety profile. Further evaluation of the long-term effects of this new therapeutic option will be needed to confirm these promising results.

Acknowledgement

EU-CERT-ICD is a Collaboration Project funded by the European Union under the 7th Framework Programme under grant agreement n° 602299.

References

1. Langendorff O. Uentersuchungen am Uberlebenden Saugethierherzen. III. Abhandlung, Vorubergehende Unregelmassigkeiten des Herzschlages und ihre Ausgleichung. *Pfluger Arch Physiol* 1898;70:473–86.
2. Wier WG, Yue DT. Intracellular calcium transients underlying the short-term force-interval relationship in ferret ventricular myocardium. *J Physiol* 1986;376:507–30.
3. Yue DT, Burkhoff D, Franz MR, et al. Postextrasystolic potentiation of the isolated canine left

ventricle. Relationship to mechanical restitution. *Circ Res* 1985;56:340–50.

4. Burkhoff D, Yue DT, Franz MR, et al. Mechanical restitution of isolated perfused canine left ventricles. *Am J Physiol* 1984;246:H8-16.
5. Anderson PA, Manring A, Serwer GA, et al. The force-interval relationship of the left ventricle. *Circulation* 1979;60:334–48.
6. Kuijer PJ, van der Werf T, Meijler FL. Post-extrasystolic potentiation without a compensatory pause in normal and diseased hearts. *Br Heart J* 1990;63:284–6.
7. Wisenbaugh T, Nissen S, DeMaria A. Mechanics of postextrasystolic potentiation in normal subjects and patients with valvular heart disease. *Circulation* 1986;74:10–20.
8. Sung CS, Mathur VS, Garcia E, et al. Is postextrasystolic potentiation dependent on Starling's law? Biplane angiographic studies in normal subjects. *Circulation* 1980;62:1032–5.
9. Yellin EL, Kennish A, Yoran C, et al. The influence of left ventricular filling on postextrasystolic potentiation in the dog heart. *Circ Res* 1979;44:712–22.
10. Beck W, Chesler E, Schrire V. Postextrasystolic ventricular pressure responses. *Circulation* 1971;44:523–33.
11. Kvasnicka J, Liander B, Broman H, et al. Quantitative evaluation of postectopic beats in the normal and failing human heart using indices derived from catheter-tip manometer readings. *Cardiovasc Res* 1975;9:336–41.
12. Merillon JP, Motte G, Aumont MC, et al. Post-extrasystolic left ventricular peak pressure with and without left ventricular failure. *Cardiovasc Res* 1979;13:338–44.
13. Seed WA, Noble MI, Walker JM, et al. Relationships between beat-to-beat interval and the strength of contraction in the healthy and diseased human heart. Circulation 1984;70:799–805.
14. Sinnecker D, Dirschinger RJ, Barthel P, et al. Postextrasystolic blood pressure potentiation predicts poor outcome of cardiac patients. *J Am Hear Assoc* 2014;3:e000857.
15. Sinnecker D, Barthel P, Huster KM, et al. Force-interval relationship predicts mortality in survivors of myocardial infarction with atrial fibrillation. *Int J Cardiol* 2015;182:315–20.
16. Bers DM. Cardiac excitation-contraction coupling. Nature 2002;415:198–205.
17. Barry WH, Bridge JH. Intracellular calcium homeostasis in cardiac myocytes. *Circulation* 1993;87:1806–15.
18. Mattiazzi A, Bassani RA, Escobar AL, et al. Chasing cardiac physiology and pathology down the CaMKII cascade. *Am J Physiol Heart Circ Physiol* 2015;308:H1177-91.
19. Wang SQ, Song LS, Lakatta EG, et al. Ca^{2+} signalling between single L-type Ca^{2+} channels and ryanodine receptors in heart cells. *Nature* 2001;410:592–6.
20. Bers DM. Altered cardiac myocyte Ca regulation in heart failure. *Physiology (Bethesda)* 2006;21:380–7.

21. Hasenfuss G, Pieske B. Calcium cycling in congestive heart failure. *J Mol Cell Cardiol* 2002;34:951–69.

22. Zima A V., Bovo E, Mazurek SR, et al. Ca handling during excitation–contraction coupling in heart failure. Pflügers Arch - *Eur J Physiol* 2014;466:1129–37.

23. Lompre A-M, Hajjar RJ, Harding SE, et al. Ca^{2+} Cycling and New Therapeutic Approaches for Heart Failure. *Circulation* 2010;121:822–30.

24. Hasenfuss G, Reinecke H, Studer R, et al. Relation between myocardial function and expression of sarcoplasmic reticulum Ca(2+)-ATPase in failing and nonfailing human myocardium. *Circ Res* 1994;75:434–42.

25. Armoundas AA, Rose J, Aggarwal R, et al. Cellular and molecular determinants of altered Ca^{2+} handling in the failing rabbit heart: primary defects in SR Ca^{2+} uptake and release mechanisms. *AJP Hear Circ Physiol* 2006;292:H1607–18.

26. Jiang MT, Lokuta AJ, Farrell EF, et al. Abnormal Ca^{2+} release, but normal ryanodine receptors, in canine and human heart failure. *Circ Res* 2002;91:1015–22.

27. Currie S, Smith GL. Enhanced phosphorylation of phospholamban and downregulation of sarco/endoplasmic reticulum Ca^{2+} ATPase type 2 (SERCA 2) in cardiac sarcoplasmic reticulum from rabbits with heart failure. *Cardiovasc Res* 1999;41:135–46.

28. Studer R, Reinecke H, Bilger J, et al. Gene expression of the cardiac Na(+)-Ca^{2+} exchanger in end-stage human heart failure. *Circ Res* 1994;75:443–53.

29. Pogwizd SM, Schlotthauer K, Li L, et al. Arrhythmogenesis and contractile dysfunction in heart failure: Roles of sodium-calcium exchange, inward rectifier potassium current, and residual beta-adrenergic responsiveness. Circ Res 2001;88:1159–67.

30. Lehnart SE, Wehrens XHT, Kushnir A, et al. Cardiac ryanodine receptor function and regulation in heart disease. *Ann N Y Acad Sci* 2004;1015:144–59.

31. Györke S, Terentyev D. Modulation of ryanodine receptor by luminal calcium and accessory proteins in health and cardiac disease. Cardiovasc Res 2008;77:245–55.

32. Zhou P, Zhao Y-T, Guo Y-B, et al. -Adrenergic signaling accelerates and synchronizes cardiac ryanodine receptor response to a single L-type Ca^{2+} channel. *Proc Natl Acad Sci* 2009;106:18028–33.

33. Kubalova Z, Terentyev D, Viatchenko-Karpinski S, et al. Abnormal intrastore calcium signaling in chronic heart failure. *Proc Natl Acad Sci* 2005;102:14104–9.

34. Schwinger RH, Böhm M, Koch A, et al. Force-frequency-relation in human atrial and ventricular myocardium. *Mol Cell Biochem* 1993;119:73–8.

35. Bowditch HP. Über die Eigentümlichkeiten der Reizbarkeit welche die Muskelfasern des Herzens zeigen. *Ber Verh Saechs Akad Wiss* 1871;23:652–89.

36. Freeman GL, Little WC, O'Rourke RA. Influence of heart rate on left ventricular performance

in conscious dogs. *Circ Res* 1987;61:455–64.

37. Miura T, Miyazaki S, Guth BD, et al. Influence of the force-frequency relation on left ventricular function during exercise in conscious dogs. *Circulation* 1992;86:563–71.

38. Palomeque J, Vila Petroff MG, Mattiazzi A. Pacing Staircase Phenomenon in the Heart: From Bodwitch to the XXI Century. *Hear Lung Circ* 2004;13:410–20.

39. Endoh M. Force–frequency relationship in intact mammalian ventricular myocardium: physiological and pathophysiological relevance. *Eur J Pharmacol* 2004;500:73–86.

40. Müller-Ehmsen J, Brixius K, Schulze C, et al. Na^+ channel modulation and force-frequency relationship in human myocardium. Naunyn Schmiedebergs Arch Pharmacol 1997;355:727–32.

41. Pieske B, Maier LS, Bers DM, et al. Ca^{2+} handling and sarcoplasmic reticulum Ca^{2+} content in isolated failing and nonfailing human myocardium. *Circ Res* 1999;85:38–46.

42. Ahlberg SE, Hamlen RC, Ewert DL, et al. Novel means to monitor cardiac performance: the impact of the force-frequency and force-interval relationships on recirculation fraction and potentiation ratio. *Cardiovasc Eng* 2007;7:32–8.

43. Mulieri LA, Hasenfuss G, Leavitt B, et al. Altered myocardial force-frequency relation in human heart failure. *Circulation* 1992;85:1743–50.

44. Hasenfuss G, Holubarsch C, Hermann HP, et al. Influence of the force-frequency relationship on haemodynamics and left ventricular function in patients with non-failing hearts and in patients with dilated cardiomyopathy. *Eur Heart J* 1994;15:164–70.

45. Crozatier B. Force-frequency relations in nonfailing and failing animal myocardium. *Basic Res Cardiol* 1998;93 Suppl 1:46–50.

46. Pieske B, Kretschmann B, Meyer M, et al. Alterations in intracellular calcium handling associated with the inverse force-frequency relation in human dilated cardiomyopathy. *Circulation* 1995;92:1169–78.

47. Bers DM. Excitation-Contraction Coupling and Cardiac Contractile Force. *Kluwer Academic Publishers*; 2001.

48. Prabhu SD, Freeman GL. Effect of tachycardia heart failure on the restitution of left ventricular function in closed-chest dogs. *Circulation* 1995;91:176–85.

49. Fabiato A. Time and calcium dependence of activation and inactivation of calcium-induced release of calcium from the sarcoplasmic reticulum of a skinned canine cardiac Purkinje cell. *J Gen Physiol* 1985;85:247–89.

50. Hoit BD, Tramuta DA, Kadambi VJ, et al. Influence of Transgenic Overexpression of Phospholamban on Postextrasystolic Potentiation. *J Mol Cell Cardiol* 1999;31:2007–15.

51. Hoit BD, Kadambi VJ, Tramuta DA, et al. Influence of sarcoplasmic reticulum calcium loading on mechanical and relaxation restitution. Am J Physiol Heart Circ Physiol 2000;278:H958-

63.

52. Rice JJ, Jafri MS, Winslow RL. Modeling short-term interval-force relations in cardiac muscle. *Am J Physiol Heart Circ Physiol* 2000;278:H913-31.

53. Prabhu SD, Freeman GL. Postextrasystolic Mechanical Restitution in Closed-Chest Dogs : Effect of Heart Failure. *Circulation* 1995;92:2652–9.

54. Scognamiglio R, Negut C, Palisi M. Spontaneous recovery of myocardial asynergic segments following acute myocardial infarction. The role of post-extrasystolic potentiation echocardiography in the predischarge evaluation. *Eur J Echocardiogr* 2003;4:135–40.

55. Hodgson JM, O'Neill WW, Laufer N, et al. Assessment of potentially salvageable myocardium during acute myocardial infarction: use of postextrasystolic potentiation. *Am J Cardiol* 1984;54:1237–44.

56. Diamond GA, Forrester JS, deLuz PL, et al. Post-extrasystolic potentiation of ischemic myocardium by atrial stimulation. *Am Heart J* 1978;95:204–9.

57. Cooper MW, Lutherer LO, Lust RM. Postextrasystolic potentiation and echocardiography: the effect of varying basic heart rate, extrasystolic coupling interval and postextrasystolic interval. *Circulation* 1982;66:771–6.

58. Lust RM, Lutherer LO, Gardner ME, et al. Postextrasystolic potentiation and contractile reserve: requirements and restrictions. *Am J Physiol* 1982;243:H990-7.

59. Braunwald E, Ross Jr. J, Frommer PL, et al. Clinical observations on paired electrical stimulation of the heart: Effects on ventricular performance and heart rate. Am J Med 1964;37:700–11.

60. Frommer P. Studies on coupled pacing techniques and some comments on paired electrical stimulation. *Bull N Y Acad Med* 1965;41:670–80.

61. Frommer PL, Robinson BF, Braunwald E. Paired electrical stimulation. A comparison of the effects on performance of the failing and nonfailing heart. *Am J Cardiol* 1966;18:738–44.

62. Chevalier-Cholat AM, Torresani J, Saadjian A, et al. Post extra-systolic potentiation during coupled stimulation of the heart. *J Electrocardiol* 1971;4:341–6.

63. Hoffman B, Bartelstone H, Scherlag B, et al. Effects of postextrasystolic potentiation on normal and failing hearts. E. *Bull N Y Acad Med* 1965;41:498–534.

64. Lieberman RA, Yee R, Shorofsky S, et al. Acute Hemodynamic Response to Dual Chamber Coupled Pacing in Heart Failure Patients – Impact of LV vs RV Stimulation. *J Card Fail* 2008;14:S58.

65. Freudenberger R, Aaron M, Krueger S, et al. Acute Electromechanical Effects of Atrioventricular Coupled Pacing in Patients With Heart Failure. *J Card Fail* 2008;14:35–40.

66. Stegemann B, Mihalcz A, Földesi C, et al. Extrasystolic stimulation with bi-ventricular pacing: an acute haemodynamic evaluation. *Europace* 2011;13:1591–6.

67. Brémont C, Lim P, Elbaz N, et al. Cardiac resynchronization therapy plus coupled pacing improves acutely myocardial function in heart failure patients. *Pacing Clin Electrophysiol* 2014;37:803–9.

68. Lyon AR, Samara MA, Feldman DS. Cardiac contractility modulation therapy in advanced systolic heart failure. *Nat Rev Cardiol* 2013;10:584–98.

69. Winter J, Brack KE, Ng GA. Cardiac contractility modulation in the treatment of heart failure: initial results and unanswered questions. *Eur J Heart Fail* 2011;13:700–10.

70. Kuck K-H, Bordachar P, Borggrefe M, et al. New devices in heart failure: an European Heart Rhythm Association report: developed by the European Heart Rhythm Association; endorsed by the Heart Failure Association. *Europace* 2014;16:109–28.

71. Brunckhorst CB, Shemer I, Mika Y, et al. Cardiac contractility modulation by non-excitatory currents: studies in isolated cardiac muscle. Eur J Heart Fail 2006;8:7–15.

72. Mohri S, He K-L, Dickstein M, et al. Cardiac contractility modulation by electric currents applied during the refractory period. *Am J Physiol Heart Circ Physiol* 2002;282:H1642-7.

73. Sabbah HN, Haddad W, Mika Y, et al. Cardiac contractility modulation with the impulse dynamics signal: studies in dogs with chronic heart failure. *Heart Fail Rev* 2001;6:45–53.

74. Pappone C, Rosanio S, Burkhoff D, et al. Cardiac contractility modulation by electric currents applied during the refractory period in patients with heart failure secondary to ischemic or idiopathic dilated cardiomyopathy. *Am J Cardiol* 2002;90:1307–13.

75. Imai M, Rastogi S, Gupta RC, et al. Therapy with cardiac contractility modulation electrical signals improves left ventricular function and remodeling in dogs with chronic heart failure. *J Am Coll Cardiol* 2007;49:2120–8.

76. Gupta RC, Mishra S, Wang M, et al. Cardiac contractility modulation electrical signals normalize activity, expression, and phosphorylation of the Na^{+}-Ca^{2+} exchanger in heart failure. *J Card Fail* 2009;15:48–56.

77. Borggrefe MM, Lawo T, Butter C, et al. Randomized, double blind study of non-excitatory, cardiac contractility modulation electrical impulses for symptomatic heart failure. *Eur Heart J* 2008;29:1019–28.

78. Kadish A, Nademanee K, Volosin K, et al. A randomized controlled trial evaluating the safety and efficacy of cardiac contractility modulation in advanced heart failure. *Am Heart J* 2011;161:329-337-2.

79. Abraham WT, Burkhoff D, Nademanee K, et al. A randomized controlled trial to evaluate the safety and efficacy of cardiac contractility modulation in patients with systolic heart failure: rationale, design, and baseline patient characteristics. *Am Heart J* 2008;156:641–648.e1.

80. Cooper MW. Postextrasystolic potentiation. Do we really know what it means and how to use it? *Circulation* 1993;88:2962–71.

Chapter 3

An augmented negative force-frequency relationship and slowed mechanical restitution are associated with increased susceptibility to drug-induced Torsades de Pointes arrhythmias in the chronic atrioventricular block dog

David J. Sprenkeler, Alexandre Bossu, Jet D.M. Beekman, Marieke Schoenmakers, Marc A. Vos

Department of Medical Physiology, University Medical Center Utrecht, Utrecht, the Netherlands

Front Physiol. 2018 Aug 8;9:1086

Abstract

Background: In the chronic AV-block (CAVB) dog model, structural, contractile and electrical remodeling occur, which predispose the heart to dofetilide-induced Torsades de Pointes (TdP) arrhythmias. Previous studies found a relation between electrical remodeling and inducibility of TdP, while structural remodeling is not a prerequisite for arrhythmogenesis. In this study, we prospectively assessed the relation between *in vivo* markers of contractile remodeling and TdP inducibility.

Methods: In 18 anesthetized dogs, the maximal first derivative of left ventricular pressure (LV dP/dt_{max}) was assessed at acute AV-block (AAVB) and after two weeks of chronic AV-block (CAVB2). Using pacing protocols, three markers of contractile remodeling, i.e. force-frequency relationship (FFR), mechanical restitution (MR) and post-extrasystolic potentiation (PESP) were determined. Infusion of dofetilide (0.025 mg/kg in 5 minutes) was used to test for TdP inducibility.

Results: After infusion of dofetilide, 1/18 dogs and 12/18 were susceptible to TdP arrhythmias at AAVB and CAVB2, respectively ($p = 0.001$). The inducible dogs at CAVB2 showed augmented contractility at a CL of 1200 ms (2354 ± 168 mmHg/s in inducible dogs versus 1091 ± 59 mmHg/s in non-inducible dogs, $p < 0.001$) with a negative FFR, while the non-inducible dogs retained their positive FFR. The time constant of the MR curve was significantly higher in the inducible dogs (158 ±7 ms vs 97±8 ms, $p < 0.001$). Furthermore, a linear correlation was found between a weighted score of the number and severity of arrhythmias and contractile parameters, i.e. contractility at CL of 1200 ms ($r = 0.73$, $p = 0.002$), the slope of the FFR ($r = -0.58$, $p = 0.01$) and the time constant of MR ($r= 0.66$, $p = 0.003$). Thus, more severe arrhythmias were seen in the dogs with the most pronounced contractile remodeling.

Conclusion: Contractile remodeling is concomitantly observed with susceptibility to dofetilide-induced TdP arrhythmias. The inducible dogs show augmented contractile remodeling compared to non-inducible dogs, as seen by a negative FFR, higher maximal response of MR and PESP and slowed MR kinetics. These altered contractility parameters may reflect disrupted Ca^{2+} handling and Ca^{2+} overload, which predispose the heart to delayed- and early afterdepolarizations that could trigger TdP arrhythmias.

Introduction

Despite advances in treatment and prevention strategies, sudden cardiac death due to ventricular arrhythmias remains a common cause of death in patients with heart failure or compensated hypertrophy.[1] In response to certain stressors, these patients exhibit ventricular remodeling, an adaptive process that initially helps to maintain normal cardiac function, but eventually becomes maladaptive, causing electrical instability and an increased risk of life-threatening ventricular arrhythmias.[2]

The chronic complete AV-block (CAVB) dog model is a widely used animal model to study ventricular remodeling and its relation with ventricular arrhythmias.[3–5] In this model, creation of third degree AV-block results in bradycardia and volume overload. To compensate for the resulting drop in cardiac output, ventricular remodeling occurs.[6,7] This remodeling process reduces the so called 'repolarization reserve', the ability of the heart to cope with stressors on repolarization.[8] When repolarization is then further challenged by anesthesia and administration of a pro-arrhythmic drug such as the I_{Kr}-blocker dofetilide, early afterdepolarizations (EADs), ectopic beats and Torsades de Pointes (TdP) arrhythmias start to occur.[9]

Ventricular remodeling is a complex process and can be divided into multiple components, such as structural, electrical and contractile remodeling. However, the contribution of each of the three different components to arrhythmogenesis is not fully elucidated. Previous studies have shown that electrical remodeling is an important contributor to the susceptibility of TdP,[6] while structural remodeling is not a prerequisite.[10] Electrical remodeling, which is reflected by prolongation of the action potential duration (APD) and increased spatial and temporal dispersion of repolarization,[11–14] develops in synchrony with TdP inducibility: both are present after 2 weeks of CAVB.[6,10] Structural remodeling, on the other hand, follows a much slower path and is fully present after 16 weeks of CAVB.[10,15,16]

Yet, the time course of contractile remodeling and its relation to TdP inducibility is less well described. Contractile adaptations, as a result of changes in Ca^{2+} handling, can be measured *in vivo* by three physiological mechanisms of the heart: force-frequency relationship (FFR), mechanical restitution (MR) and post-extrasystolic potentiation (PESP). The FFR accounts for potentiation of contractility when heart rate is increased. MR and PESP relate to changes in contractility of the extrasystolic beat and post-extrasystolic beat, respectively, when a basic stimulation train is interrupted with extrastimuli. MR represents the restoration of contractility of the extrasystolic beat when the coupling interval (CI) of the extrastimulus is lengthened. PESP displays the opposite behavior: when CI is shortened, the contractility of the post-extrasystolic beat is enhanced. Thus, the earlier an extrasystole occurs, the lower the contractility of the extrasystolic beat and the higher the contractility of the post-extrasystolic beat.

De Groot et al. showed that FFR and PESP are altered in the CAVB dogs after 6 weeks of remodeling and that these contractile parameters are associated with delayed afterdepolarizations *in vivo*.[17] Furthermore, in isolated cardiomyocytes from CAVB dogs, Ca^{2+} overload of the sarcoplasmic reticulum (SR) can result in spontaneous Ca^{2+} release, which triggers early and delayed afterdepolarizations (EAD/DADs).[18] However, it is unknown whether these macroscopic measures of Ca^{2+} handling (FFR, MR, PESP) reflect the propensity for sustained TdP arrhythmias. If contractility and arrhythmogenesis are intertwined, contractile parameters could function as markers of pro-arrhythmia and might eventually help to identify the patient at risk of life-threatening arrhythmias. Therefore, we aimed to investigate the relation between *in vivo* contractility measures and susceptibility to TdP arrhythmias in the CAVB dog. We assessed these measures after 2 weeks of remodeling, since CAVB dogs are susceptible to TdP arrhythmias from that moment onwards.

Materials & methods

Animal handling was in accordance with the 'Directive 2010/63/EU of the European Parliament and of the Council of 22 September 2010 on the protection of animals used for scientific purposes' and the Dutch law, laid down in the Experiments on Animals Act. All experiments were performed with approval of the Central Authority for Scientific Procedures on Animals (CCD).

Animal preparation

Eighteen adult purpose-bred mongrel dogs of either sex (Marshal, USA; 5 females, 13 males; bodyweight 26 ± 0.63 kg) were included. Experiments were performed under general anesthesia with mechanical ventilation at 12 breaths/min. The dogs were premedicated with a mixture of 0.5 mg/kg methadone, 0.5 mg/kg acepromazine and 0.02 mg/kg atropine i.m.. General anesthesia was induced with 25 mg/kg pentobarbital i.v. and maintained by isoflurane 1.5% in a mixture of O_2 and N_2O (1:2). Periprocedurally antibiotics (ampicillin 1000 mg i.v. preoperatively and ampicillin 1000 mg i.m. postoperatively) and analgesics (metacam 0.2 mg/kg s.c. preoperatively and buprenorphine 0.3 mg i.m. postoperatively) were administered.

Ten surface-ECG leads (six limb leads, four precordial leads) were recorded throughout the experiment and stored on hard disk. Under aseptic conditions, the femoral artery and vein and carotid artery were dissected and sheaths were placed by Seldinger technique. Right and left ventricular monophasic action potential (RV & LV MAP) catheters (Hugo Sachs Elektronik GmbH, March, Germany) and a left ventricular

7F pressure catheter (CD Leycom Inc., Zoetermeer, Netherlands) were positioned under fluoroscopic guidance.

Experimental protocol

Two serial experiments were performed. In the first experiment, baseline surface ECG, LV and RV MAP duration (MAPD) and left ventricular pressure during sinus rhythm were recorded. Subsequently, His bundle ablation was done as described previously.[10] When the idioventricular rhythm (IVR) was too low, a pacemaker was implanted subcutaneously with a transvenous lead in the RV apex. At acute AV-block (AAVB), a pacing protocol (see below) was performed and the effects on LV pressure were recorded. Next, susceptibility to Torsades de Pointes arrhythmias (TdP) was tested by a pro-arrhythmic challenge with the I_{Kr} blocker dofetilide (0.025 mg/kg i.v, infused during 5 minutes or until the first TdP occurred). TdP was defined as a run of 5 or more ectopic beats, with twisting morphology of the QRS complexes. When ≥3 TdP occurred in the first ten minutes after start of dofetilide administration, the dog was considered inducible.

During the second experiment, after two weeks of remodeling at chronic AV-block (CAVB2), baseline ECG, LV and RV MAPD and left ventricular pressure were recorded and the pacing protocol and susceptibility test with dofetilide were repeated.

Pacing protocol

FFR, MR and PESP were measured during a pacing protocol from the LV MAP catheter. The FFR protocol consisted of 3 minutes of steady-state pacing at three different cycle lengths (CL) of 300 ms, 750 ms and 1200 ms. For the MR and PESP protocol, the LV was paced with a basic CL of 600 ms, which was interrupted every 20th beat by an extrastimulus with an incremental coupling interval (CI) ranging from 250 ms up to 800 ms, with steps of 50 ms.

Data analysis

Contractility measures

As a measure of contractility, the maximal slope of left ventricular pressure rise (LV dP/dt_{max}) was calculated offline with computer software (Conduct NT, CD Leycom). For the FFR, the mean LV dP/dt_{max} of five consecutive beats was used at the three stimulation frequencies. A straight line was fitted through these points and its slope was calculated to quantify the orientation of the FFR. MR and PESP were defined as the LV dP/dt_{max} of the extrasystolic and post-extrasystolic beat, respectively (Figure

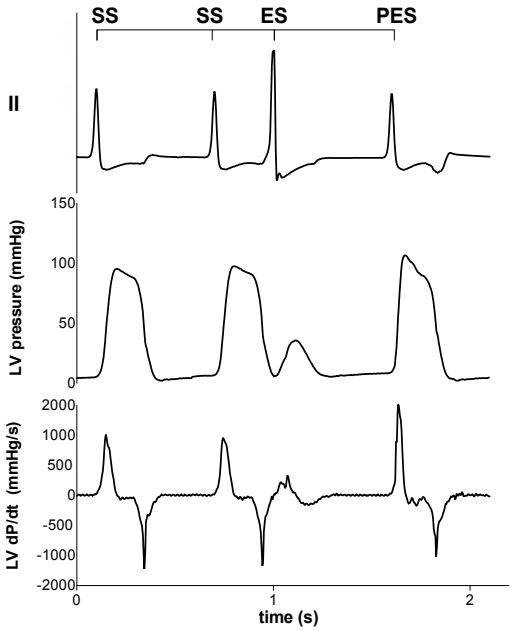

Figure 1. Representative tracing of LV pressure and LV dP/dt of the extrasystolic and post-extrasystolic beat.

A steady state stimulation train (SS) is interrupted with an extrasystolic beat (ES) at different coupling interval (CI), followed by a post-extrasystolic beat (PES) at a fixed CI. With decremental CI of the ES, the LV dP/dt_{max} of the ES decreases, while the the LV dP/dt_{max} of the PES increases.

1). In addition, normalized MR and PESP were calculated by taking the ratio of LV dP/dt_{max} of the extrasystolic and post-extrasystolic beat, respectively, to the mean LV dP/dt_{max} of the five beats immediately preceding the extrasystole. Both MR and PESP were fitted to monoexponential functions using non-linear least squares regression, with the equation: $y = a - b * e^{-\frac{x}{TC}}$ for MR and $y = a + b * e^{-\frac{x}{TC}}$ for PESP to calculate the time constant (TC) of MR and PESP.

Electrophysiological measures

Measurement of RR interval and QT interval was performed with calipers on lead II of the ECG by use of a software program (EPTracer, Cardiotek, Heilbronn). QT interval was corrected for heart rate (QTc) with the van der Water formula[19], which gives a better estimate than Bazett formula in anesthetized dogs. LV and RV MAPD were measured from the initial peak to 80% of repolarization in a custom-made Matlab software program. We defined interventricular dispersion (ΔMAPD) as the difference between LV MAPD and RV MAPD. Short-term variability of LV MAPD (STV) was calculated over 31 consecutive beats using the formula: $STV = \sum|D_{n+1} - D_n|/30 \times \sqrt{2}$, where D represents LV MAPD. STV after dofetilide challenge was measured just prior to the first ectopic beat.

Statistical analysis

Data are expressed as mean ± standard error of the mean (SEM). Serial data were analyzed with a paired Student's *t*-test or a repeated measure analysis of variance

(ANOVA) with post hoc Bonferroni correction. Group analysis was performed with an unpaired Student's *t*-test. Correlation analysis was done with Pearson's correlation coefficient. All statistical analyses were performed with Prism 6.0 (GraphPad Software Inc., La Jolla, CA, USA). A p-value < 0.05 was considered as statistically significant.

Results

Contractile remodeling

Contractile parameters at AAVB and CAVB are shown in Figure 2. Contractile remodeling was present after two weeks of CAVB, as seen by a significant increase in LV dP/dt_{max} during IVR compared to AAVB (Figure 2A). At AAVB, a positive force-frequency relationship was observed with augmentation of LV dP/dt_{max} at higher frequencies (Figure 2B). This relationship was blunted at CAVB2. At AAVB, the MR curve demonstrated a monoexponential rise in LV dP/dt_{max} towards a plateau with lengthening of the CI. The PESP curve displayed the opposite behavior (Figure 2C & 2D). Both these parameters were increased at CAVB2.

Electrical remodeling

The course of electrical remodeling is depicted in Table 1. At AAVB, all electrophysiological parameters have adapted to the sudden drop in heart rate. When challenged with dofetilide, a further significant increase was seen in QT, LV & RV MAPD and STV. After two weeks of CAVB, electrical remodeling was present, as seen by a significant increase in QT, QTc, and LV MAPD under baseline conditions compared to AAVB. RV MAPD did not increase to the same extent as LV MAPD, thus creating a high interventricular dispersion (ΔMAPD). Finally, also STV showed a significant increase, which was further augmented after infusion of dofetilide.

Parameters of remodeling and susceptibility to TdP arrhythmias

Of the 18 dogs tested, one was susceptible to dofetilide-induced TdP at AAVB. After 2 weeks of CAVB, 12/18 dogs (67%, p = 0.002 compared to AAVB) were inducible after dofetilide infusion. Separate measurement of contractile parameters of the inducible and non-inducible dogs are depicted in Figure 3. At AAVB, no differences were found in contractile measures between the two groups. However, at CAVB2, the inducible dogs demonstrated a completely different pattern of contractile remodeling compared to the non-inducible dogs. At low stimulation frequency with a CL of 1200 ms, the inducible

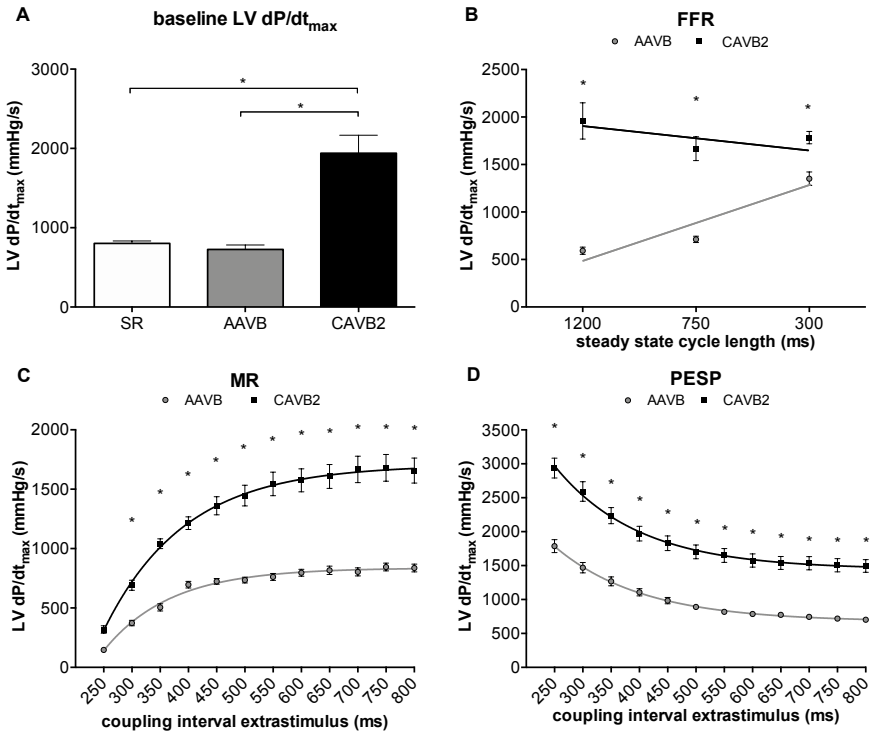

Figure 2. Contractile parameters at AAVB and CAVB2

A) LV dP/dt_{max} at baseline. B) Force-frequency relationship (FFR). C) Mechanical restitution (MR). D) Post-extrasystolic potentiation (PESP). * p< 0.05 compared to AAVB.

Table 1. Electrophysiological parameters

* p< 0.05 versus SR. † p< 0.05 versus AAVB. § p< 0.05 versus CAVB2.

	SR	AAVB	AAVB + dof	CAVB2	CAVB2 + dof
RR (ms)	571 ± 11	1048 ± 72*	1229 ± 75	1262 ± 47†	1452 ± 62§
QT (ms)	261 ± 4	327 ± 9*	552 ± 22†	421 ± 16†	593 ± 19§
QTc (ms)	298 ± 3	319 ± 9*	543 ± 30†	398 ± 14†	553 ± 19§
LV MAPD (ms)	193 ± 3	240 ± 6*	454 ± 23†	302 ± 12†	470 ± 30§
RV MAPD (ms)	190 ± 14	216 ± 6*	345 ± 10†	245 ± 6	341 ± 22§
ΔMAPD (ms)	9 ± 2	24 ± 5*	138 ± 24†	56 ± 8†	130 ± 25§
STV (ms)	0.36 ± 0.02	0.72 ± 0.10*	1.91 ± 0.22†	1.51 ± 0.31†	2.66 ± 0.34§

subjects had augmentation of contractility compared to the non-inducible dogs (2354 ± 168 mmHg/s versus 1091 ± 59 mmHg/s, $p < 0.001$; Figure 3A). Furthermore, the slope of the FFR-curve was inverted in the inducible dogs, while the non-inducible dogs retained their positively-oriented FFR (slope of -0.51 ± 0.19 in inducible dogs versus 0.89 ± 0.06 in non-inducible dogs, $p < 0.001$). As seen from Supplemental table 1, these differences in LV dP/dt_{max} between inducible and non-inducible dogs are not the result of differences in preload, since end-diastolic pressures are similar.

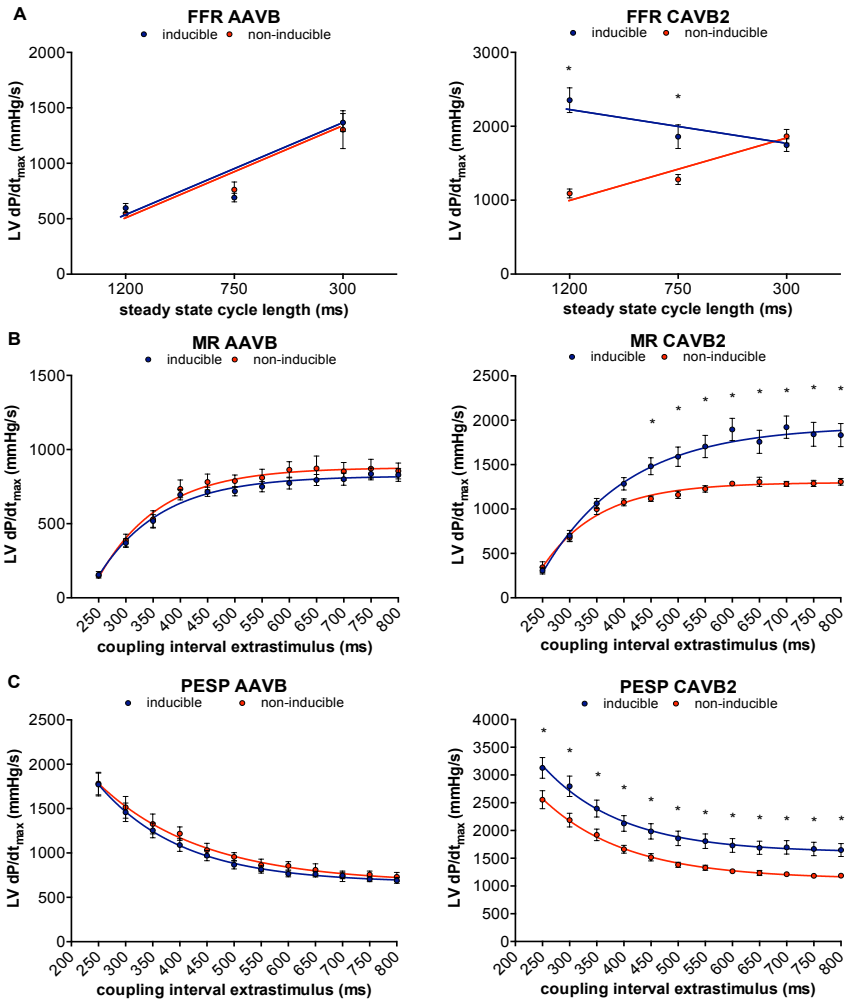

Figure 3. Relation between contractile remodeling and susceptibility to TdP arrhythmias.

FFR (A), MR (B) and PESP (C) of inducible dogs (blue line) and non-inducible dogs (red line) at AAVB (left) and CAVB2 (right). * $p < 0.05$ inducible versus non-inducible

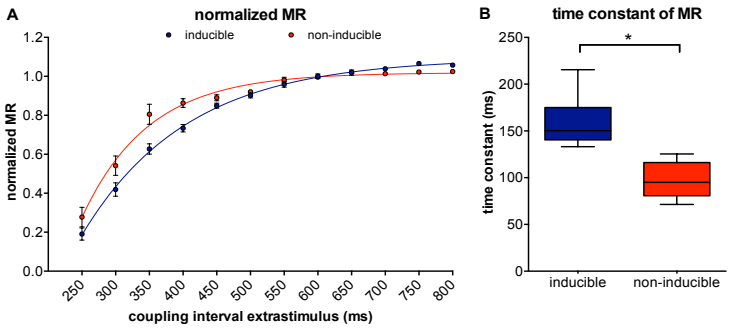

Figure 4. Normalized MR curves of inducible and non-inducible dogs.

The inducible dogs show slower restitution compared to the non-inducible dogs (A) with significantly higher time constants (B). * p< 0.05

At small coupling intervals, MR was similar in both groups, but diverged when the CI of the extrasystole rised above 450 ms, after which the susceptible dogs showed a significantly higher LV dP/dt_{max} (1483 ± 96 mmHg/s versus 1117 ± 31 mmHg/s, p =0.01, Figure 3B). PESP, on the other hand, was increased in the inducible dogs at a whole range of coupling intervals (Figure 3C). When MR was normalized to the LV dP/dt_{max} of the preceding beats, the TC of MR appeared significantly higher in the inducible dogs (TC = 158 ± 7 ms versus TC = 97 ± 8 ms in non-inducible dogs, p < 0.001, Figure 4). Normalized PESP was similar between the groups and had equal TC (143 ± 9 ms versus 153 ± 4 ms, p =0.46, not shown).

Electrically, no differences were found between the two groups at AAVB. At CAVB, the RR interval, QT- and QTc interval, LV MAPD, RV MAPD and ΔMAPD were similar between the inducible and non-inducible dogs (Table 2). Only STV could distinguish between inducible and non-inducible dogs both at baseline and when challenged with dofetilide. Dogs that were inducible to drug-induced TdP had significantly higher STV at baseline (1.98 ± 0.41 ms versus 0.61 ± 0.08 ms, p = 0.009) which increased even more when challenged with dofetilide (3.18 ± 0.36 ms versus 1.35 ± 0.08 ms, p = 0.001).

Table 2. Electrophysiological parameters of non-inducible and inducible dogs

* p < 0.05 versus non-inducible in baseline. † p < 0.05 versus non-inducible during dofetilide infusion.

	baseline		dofetilide	
	non-inducible	inducible	non-inducible	inducible
RR (ms)	1272 ± 33	1257 ± 69	1507 ± 107	1373 ± 72
QT (ms)	383 ± 19	439 ± 20	596 ± 50	587 ± 25
LV MAPD (ms)	292 ± 23	308 ± 14	494 ± 48	460 ± 39
RV MAPD (ms)	236 ± 9	249 ± 8	378 ± 53	328 ± 23
ΔMAPD (ms)	57 ± 10	56 ± 9	116 ± 14	135 ± 35
STV (ms)	0.61 ± 0.08	1.98 ± 0.41*	1.35 ± 0.08	3.18 ± 0.36†

Table 3. Custom-made weighted score of the number and severity of arrhythmias
Score is the total number of points during 10 minutes after start of dofetilide infusion

arrhythmia	points
single ectopic beat	1
double ectopic beats	2
triple ectopic beats	3
four ectopic beats	4
nsTdP (<50 complexes)	10
sustained TdP (>50 complexes) or defibrillation	100
> 1 consecutive defibrillation	200

Relation of contractile and electrical remodeling with severity of arrhythmias

In order to quantify the severity of arrhythmias, we developed a new weighted scoring system, which takes into account both the number of arrhythmias in 10 minutes and whether the arrhythmias were sustained or defibrillations were needed (Table 3). This weighted score was correlated with both contractile and electrical remodeling. As depicted in Figure 5, a linear correlation was found between this weighted score and LV dP/dt_{max} at CL of 1200 ms ($r = 0.71$, $p = 0.002$), the slope of FFR ($r = -0.58$, $p = 0.01$) and time constant of MR ($r= 0.66$, $p = 0.003$). Of the electrical parameters, STV at baseline was also correlated with the weighted score of arrhythmic severity ($r= 0.74$, $p = 0.0006$).

The effect of ouabain on contractility and TdP inducibility

As a proof of principle of the importance of contractile remodeling and Ca^{2+} overload for the inducibility of TdP arrhythmias in the CAVB dog model, we attempted to pharmacologically increase Ca^{2+} load to alter FFR and potentially convert an initial non-inducible dog into an inducible one. Four non-inducible dogs were given a single dose of the cardiac glycoside ouabain (0.045 mg/kg i.v. in 1 minute) prior to administration of dofetilide. In Figure 6, the effects of ouabain administration on FFR are depicted. In all dogs, ouabain resulted in a rise in contractility. Ouabain itself did not induce any arrhythmias. Unfortunately, in 3 out of 4 dogs, contractility at a CL of 1200 ms could not reach a level comparable to that of the inducible dogs and these dogs retained a positive FFR. As expected, these three dogs remained non-inducible after additional dofetilide infusion. Nevertheless, in one dog, contractility after ouabain administration increased to a level similar to that of the inducible dogs, with a more blunted force-frequency relationship. Interestingly, this dog did become inducible to TdP arrhythmias after infusion of dofetilide (Figure 7).

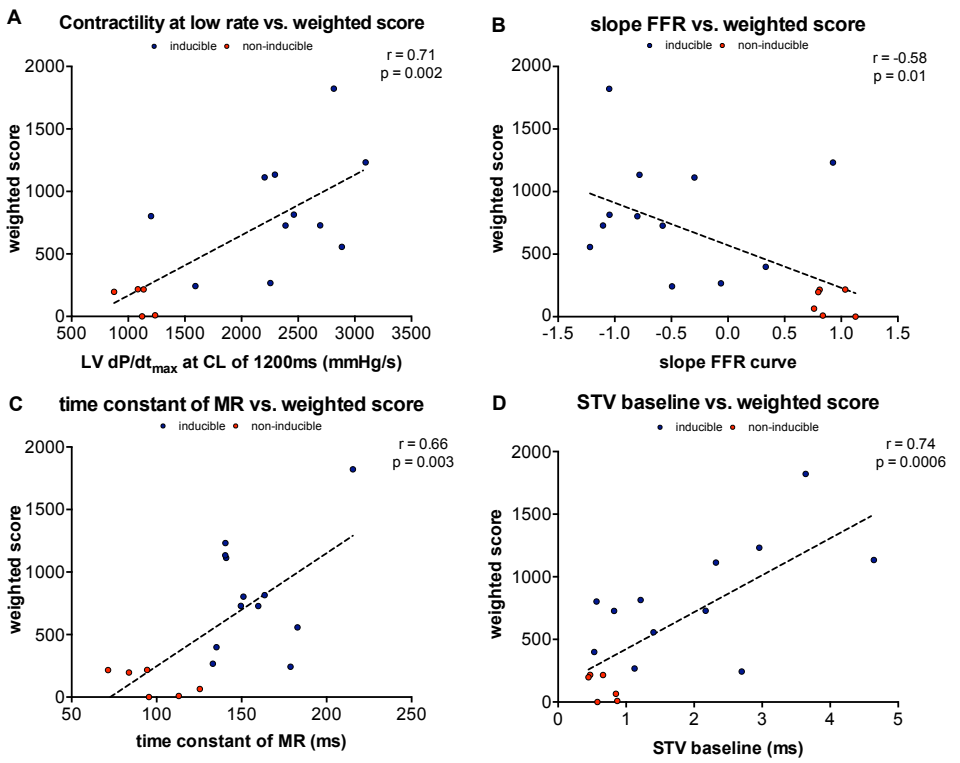

Figure 5. Linear correlations between weighted arrhythmia score and parameters of contractile and electrical remodeling

Linear correlation between weighted arrhythmia score and A) contractility at 1200ms, B) slope of FFR, C) time constant of MR and D) STV at baseline.

Discussion

The results of this study demonstrate that contractile remodeling is already present after two weeks of CAVB and that this remodeling process differs substantially between TdP susceptible and TdP resistant dogs. Moreover, the more contractile or electrical remodeling have occurred, the higher the number and severity of arrhythmias after dofetilide challenge. Alterations in Ca^{2+} homeostasis may be the common denominator that explains the observed relation between contractile remodeling and arrhythmogenesis in the CAVB dog model.

Ca^{2+} overload, DADs & EADs in the CAVB dog

The present study is, to our knowledge, the first to show a direct relation

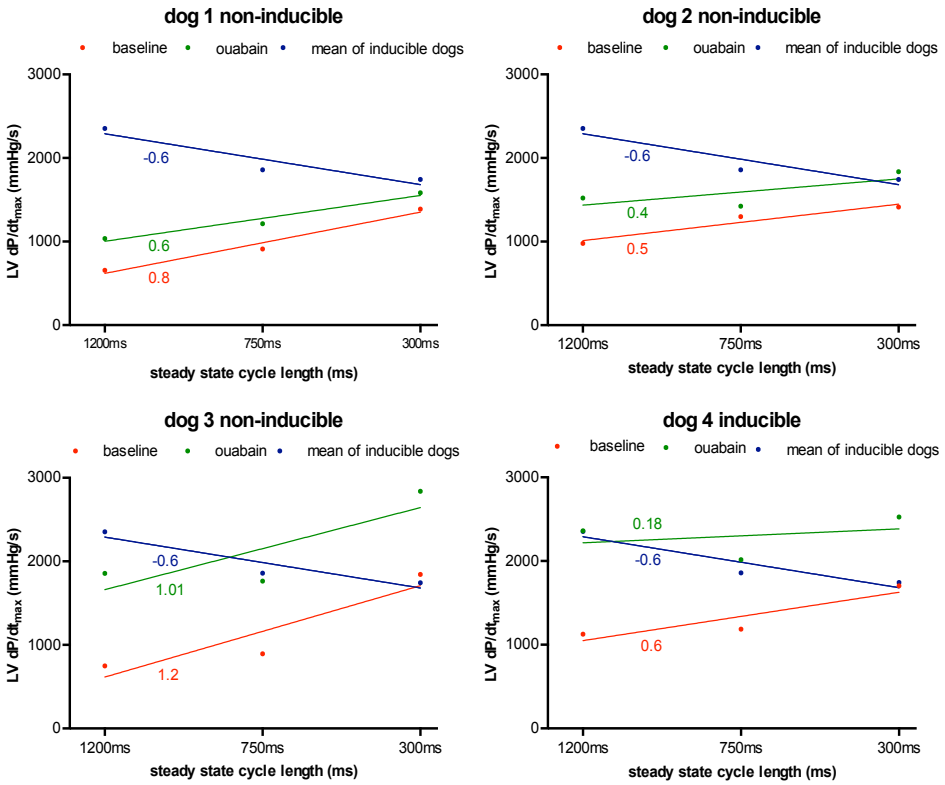

Figure 6. Effect of ouabain on force-frequency relationship in non-inducible subjects (n = 4)

Contractility at CL of 1200ms, 750ms and 300ms at baseline (red line) and after ouabain (green line) in four non-inducible dogs. As comparison, the mean of the inducible dogs is shown (blue line). Only dog 4 became inducible after ouabain in combination with dofetilide. Time constants of the different curves are given.

between *in vivo* measurements of contractility and inducibility of TdP arrhythmias. Nevertheless, on a cellular level the relation between disturbances of Ca^{2+} homeostasis and arrhythmogenesis is well established. Previous *in vitro* studies have demonstrated altered Ca^{2+} handling in isolated cardiomyocytes of CAVB dogs with increased amplitude and duration of Ca^{2+} transients along with a higher Ca^{2+} content of the SR.[20] Furthermore, NCX is upregulated, which contributes to further loading of the SR via 'reverse mode' Ca^{2+} influx.[21] The resulting SR Ca^{2+} overload is associated with spontaneous Ca^{2+} release, which can generate a DAD via 'forward mode' function of NCX (exchange of 1 Ca^{2+} ion for 3 Na^{+} ions, creating an inward current).[22] Furthermore, it has become more and more evident that altered Ca^{2+} handling and upregulation of NCX also play a role in the formation of EADs, which have been regarded as the most important triggers of TdP arrhythmias.[23–25]

Our results are consistent with the study by de Groot et al. which showed that

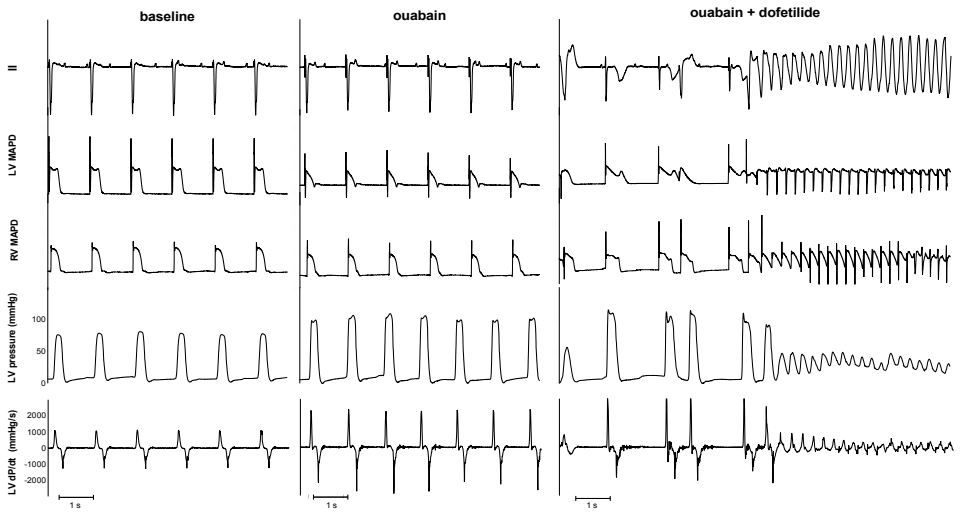

Figure 7. ECG, LV MAP, RV MAP, LV pressure and LV dP/dt of dog 4

Administration of ouabain did not cause any arrhythmias. However, the combination of ouabain and dofetilide resulted in Torsades de Pointes arrhythmias.

the highest LV dP/dt_{max} postpacing (which reflects an increased SR Ca^{2+} load) was associated with the occurrence of DADs on MAP recordings.[17] Since DADs and EADs share a common molecular mechanism, we expected to find the same relation between enhanced contractility and susceptibility of TdP arrhythmias.

Force-frequency relationship and TdP arrhythmias

A blunted or inverted FFR has been observed in isolated muscle preparations of failing myocardium[26–28] as well as in animal models[29,30] or patients with cardiac dysfunction[31–33]. In the CAVB dog, FFR is also inverted, but with increased contractility at low heart rates.[16,17]

In the present study we observed the inverted FFR only in the inducible dogs, while the FFR of the non-inducible dogs remained positive. There is strong evidence that increased $[Na]_i$ during diastole plays a central role in the inversion of the FFR.[34,35] A study on rabbit papillary muscle strips examined the effect of increased $[Na^+]_i$ on FFR and showed that treatment with the Na^+ ionophore monensin, which increases diastolic $[Na^+]_i$, could convert a positive FFR into a negative FFR, mainly by increasing contractility at lower heart rates.[35] The high diastolic $[Na^+]_i$ will favor Ca^{2+} influx via NCX and since the ratio of diastole to systole is highest at low heart rates, Ca^{2+} loading of the SR will be enhanced, resulting in increased contractility. Dogs with chronic AV-block have approximately 4 mM higher $[Na^+]_i$ compared to controls, probably due to reduced

$[Na^+]_i$-affinity of the Na^+-K^+-ATPase and increased Na^+-influx via the Na^+-H^+-exchanger type 1 (NHE-1).[36,37] However, in these studies, no dofetilide challenge was performed, therefore it is unknown whether the $[Na^+]_i$ is higher in inducible dogs compared to non-inducible dogs.

Nevertheless, we could hypothesize that in the inducible dogs a high $[Na^+]_i$ in combination with enhanced NCX activity results in Ca^{2+} overload, spontaneous Ca^{2+} release, and subsequent EADs and TdP arrhythmias. Supporting this hypothesis, it has been shown that lowering $[Na^+]_i$ by administration of the selective late Na^+ current blocker ranolazine could reduce the number of EADs *in vitro* and TdP arrhythmias *in vivo*.[38] In addition, blockade of NCX by SEA-0400 is effective in prevention of TdP arrhythmias in the CAVB dog.[39] As a proof of concept, we tried to increase $[Na^+]_i$ in the non-inducible dogs by blockade of the Na^+-K^+-ATPase with ouabain. In contrast to the cardiac glycoside digitalis, ouabain has a fast onset of action, reaching its maximum after 5 minutes of administration.[40] The increased $[Na^+]_i$ caused by inhibition of the Na^+-K^+-ATPase will be exchanged for Ca^{2+}, causing Ca^{2+} overload of the cardiomyocyte that is responsible for both the inotropic and potential arrhythmogenic effects. As we have shown, only the dog that reached the contractility level of the inducible dogs and developed a more blunted FFR, became susceptible to dofetilide-induced TdP, which further illustrates the importance of $[Na^+]_i$ and $[Ca^{2+}]_i$ for the initiation of TdP arrhythmias.

Mechanical restitution/post-extrasystolic potentiation and TdP arrhythmias

We have demonstrated that inducible dogs have a higher MR and PESP and slower MR kinetics compared to the non-inducible dogs. In previous studies altered MR and PESP have been found in patients with hypertrophy and heart failure.[41–44] Both phenomena are explained by time-dependent availability of releasable Ca^{2+} due to recovery from inactivation of the SR Ca^{2+} release channel, the ryanodine receptor 2 (RyR2).

Discussion on the mechanism of slower MR in the CAVB dog remains speculative, since the kinetics of RyR2 have never been investigated. Furthermore, the precise molecular mechanism behind inactivation and recovery of RyR2 remains controversial.[45] First, it can be hypothesized that the intrinsic gating properties of the RyR2 have been altered by the remodeling process. Secondly, changes in cytosolic $[Ca^{2+}]$ have been proposed to influence the inactivation of RyR2, referred to as Ca^{2+}-dependent inactivation. It is hypothesized that increased dyadic $[Ca^{2+}]_i$, which is responsible for RyR2 activation, might also play a role in RyR2 inactivation.[46] Thirdly, RyR refractoriness might be caused by 'functional depletion' of Ca^{2+} of the SR after global Ca^{2+} release.

Refilling of the SR during Ca^{2+}-reuptake increases the sensitivity of RyR2 to cytosolic Ca^{2+} and accelerates recovery from inactivation.[47] Since Ca^{2+} homeostasis is an interplay between RyR2, SERCA2a and NCX, we can assume that alterations in expression and function of one of these proteins, will subsequently affect normal function of the others. Increased NCX function could result in 'relatively' diminished activity of SERCA2a, by changing the ratio of Ca^{2+} extrusion versus reuptake. In this regard, a study in a transgenic mouse model showed that overexpression of phospholambam, the main inhibitor of SERCA2a, caused a reduced reuptake of Ca^{2+} in the SR, but also resulted in a higher time constant of MR and increased PESP compared to control, just as we found in the inducible dogs.[48,49] Furthermore, in isolated cardiomyocytes, inhibition of SERCA2a could significantly slow down recovery from inactivation of RyR2.[47] Thus, increased NCX function, which contributes to susceptibility to triggered arrhythmias in the CAVB dog, might indirectly influence SERCA2a and RyR2 function, and thus alter MR and PESP *in vivo*.

Electrical remodeling and TdP arrhythmias

Electrically, we found that only STV can distinguish between inducible and non-inducible subjects. This is in line with previous studies on STV in the chronic AV-block dog model, which show that STV both at baseline and after dofetilide infusion is a more powerful predictor of drug-induced TdP arrhythmias compared to the QT interval or LV MAPD itself.[13,14,50] The molecular basis of STV is not fully elucidated, but has been attributed to alterations in Ca^{2+} handling. In isolated cardiomyocytes, β-adrenergic stimulation during reduced repolarization reserve (blockade of the repolarization current I_{Ks}) resulted in increased cellular Ca^{2+} load and spontaneous Ca^{2+} release, which was associated with increased STV and the occurrence of DADs and EADs.[51,52] Buffering of Ca^{2+} by BAPTA-AM, blockade of SR Ca^{2+} release with ryanodine or inhibition of NCX by SEA0400 led to a drastic reduction of STV and eliminated all DADs and EADs.[51,52] A study by Antoons et al. showed that STV is highly dependent on SR Ca^{2+} release, which can modulate Ca^{2+}-dependent currents making the heart more prone to EADs.[53] These data support the hypothesis that increased STV reflects disrupted Ca^{2+} homeostasis as the underlying mechanism of EADs and TdP arrhythmias in the CAVB dog.

Clinical implications

Since the chronic-AV-block dog model is a specific model of compensated hypertrophy caused by volume overload, extrapolation to a population of patients with heart failure with reduced ejection fraction should be done with caution. Nevertheless, since contractile remodeling and arrhythmogenesis are related, contractile parameters

might be used for risk stratification of ventricular arrhythmias and sudden cardiac death. Recently, a study of a non-invasive measurement of PESP of blood pressure, measured via a photoplethysmographic device, showed that higher PESP was correlated with increased mortality in myocardial infarction survivors.[54] The cause of death was not stratified in this study, however increased PESP may be associated with increased arrhythmic risk. The currently ongoing '*EUropean Comparative Effectiveness Research to assess the use of primary prophylacTic Implantable Cardioverter Defibrillators' (EU-CERT-ICD)* study evaluates the relationship between non-invasive measured PESP and the incidence of ICD shocks in a primary prevention ICD-population. This study will give further insight if non-invasive measures of contractility could function as predictors of life-threatening arrhythmias.

Limitations

No direct measurements of Ca^{2+} transients or SR function have been done, therefore hypotheses on the mechanisms of contractile remodeling and the relation with TdP arrhythmias are based on assumptions derived from previous molecular work. Explanations other than related to Ca^{2+} handling may also be possible, such as mechano-electrical feedback, i.e. direct effects of altered loading conditions on repolarization. Secondly, LV dP/dt_{max} has important limitations as a measure of contractility, since it is also dependent on ventricular loading. While we did not measure ventricular volumes, we have shown that end-diastolic pressures are not different between inducible and non-inducible dogs. Therefore, we can assume the differences found in LV dP/dt_{max} are predominantly caused by changes in contractility. Finally, the relation between contractile remodeling and TdP arrhythmias was only measured at CAVB2, therefore no conclusion can be made on this association later in the remodeling process.

Conclusion

In the CAVB dog model, contractile and electrical remodeling are already present after two weeks of AV-block and develop concomitantly with susceptibility to dofetilide-induced TdP arrhythmias. Furthermore, contractile parameters are altered to a far larger extent in inducible dogs, as seen by development of an augmented negative FFR, higher maximal response of MR and PESP and slowed MR kinetics.

Acknowledgements

The research leading to these results has received funding from the European Community's Seventh Framework Programme FP7/2007-2013 under grant agreement

no. 602299, EU-CERT-ICD. The results have been presented as an abstract at the European Heart Rhythm Asssociation (EHRA) congress 2018 and Heart Rhythm annual scientific sessions 2018.

References

1. Tomaselli GF, Zipes DP. What causes sudden death in heart failure? *Circ Res* 2004;95:754–63.
2. Konstam MA, Kramer DG. Left ventricular remodeling in heart failure: current concepts in clinical significance and assessment. *JACC Cardiovasc Imaging* 2011;4:98–108.
3. Oros A, Beekman JDM, Vos MA. The canine model with chronic, complete atrio-ventricular block. *Pharmacol Ther* 2008;119:168–78.
4. Wada T, Ohara H, Nakamura Y, et al. Impacts of Surgically Performed Renal Denervation on the Cardiovascular and Electrophysiological Variables in the Chronic Atrioventricular Block Dogs – Comparison With Those of Amiodarone Treatment –. *Circ J* 2016;80:1556–63.
5. Zhou S, Jung B-C, Tan AY, et al. Spontaneous stellate ganglion nerve activity and ventricular arrhythmia in a canine model of sudden death. *Heart Rhythm* 2008;5:131–9.
6. Vos MA, de Groot SH, Verduyn SC, et al. Enhanced susceptibility for acquired Torsades de pointes arrhythmias in the dog with chronic, complete AV block is related to cardiac hypertrophy and electrical remodeling. *Circulation* 1998;98:1125–35.
7. Volders PG, Sipido KR, Vos MA, et al. Cellular basis of biventricular hypertrophy and arrhythmogenesis in dogs with chronic complete atrioventricular block and acquired Torsades de pointes. *Circulation* 1998;98:1136–47.
8. Roden DM. Taking the “idio” out of “idiosyncratic”: predicting torsades de pointes. *Pacing Clin Electrophysiol* 1998;21:1029–34.
9. Dunnink A, Sharif S, Oosterhoff P, et al. Anesthesia and Arrhythmogenesis in the Chronic Atrioventricular Block Dog Model. *J Cardiovasc Pharmacol* 2010;55:601–8.
10. Schoenmakers M, Ramakers C, van Opstal JM, et al. Asynchronous development of electrical remodeling and cardiac hypertrophy in the complete AV block dog. *Cardiovasc Res* 2003;59:351–9.
11. Verduyn SC, Vos MA, van der Zande J, et al. Further observations to elucidate the role of interventricular dispersion of repolarization and early afterdepolarizations in the genesis of acquired Torsades de pointes arrhythmias: a comparison between almokalant and d-sotalol using the dog as its own co. *J Am Coll Cardiol* 1997;30:1575–84.
12. Verduyn SC, Vos MA, van der Zande J, et al. Role of interventricular dispersion of repolarization in acquired Torsades-de-pointes arrhythmias: reversal by magnesium. *Cardiovasc Res* 1997;34:453–63.

13. Thomsen MB, Volders PGA, Beekman JDM, et al. Beat-to-Beat Variability of Repolarization Determines Proarrhythmic Outcome in Dogs Susceptible to Drug-Induced Torsades de Pointes. *J Am Coll Cardiol* 2006;48:1268–76.

14. Thomsen M, Oros A, Schoenmakers M, et al. Proarrhythmic electrical remodelling is associated with increased beat-to-beat variability of repolarisation. *Cardiovasc Res* 2007;73:521–30.

15. Donker DW, Volders PGA, Arts T, et al. End-diastolic myofiber stress and ejection strain increase with ventricular volume overload--Serial in-vivo analyses in dogs with complete atrioventricular block. *Basic Res Cardiol* 2005;100:372–82.

16. Peschar M, Vernooy K, Cornelussen RN, et al. Structural, electrical and mechanical remodeling of the canine heart in AV-block and LBBB. *Eur Hear J* Suppl 2004;6:D61–5.

17. de Groot SH, Schoenmakers M, Molenschot MM, et al. Contractile adaptations preserving cardiac output predispose the hypertrophied canine heart to delayed afterdepolarization-dependent ventricular arrhythmias. *Circulation* 2000;102:2145–51.

18. Sipido KR. Calcium overload, spontaneous calcium release, and ventricular arrhythmias. *Heart Rhythm* 2006;3:977–9.

19. Van de Water A, Verheyen J, Xhonneux R, et al. An improved method to correct the QT interval of the electrocardiogram for changes in heart rate. *J Pharmacol Methods* 1989;22:207–17.

20. Sipido KR, Volders PGA, Schoenmakers M, et al. Role of the Na/Ca exchanger in arrhythmias in compensated hypertrophy. *Ann N Y Acad Sci* 2002;976:438–45.

21. Sipido KR, Volders PG, de Groot SH, et al. Enhanced Ca(2+) release and Na/Ca exchange activity in hypertrophied canine ventricular myocytes: potential link between contractile adaptation and arrhythmogenesis. *Circulation* 2000;102:2137–44.

22. Pogwizd SM, Bers DM. Calcium cycling in heart failure: the arrhythmia connection. *J Cardiovasc Electrophysiol* 2002;13:88–91.

23. Volders PG, Vos MA, Szabo B, et al. Progress in the understanding of cardiac early afterdepolarizations and torsades de pointes: time to revise current concepts. *Cardiovasc Res* 2000;46:376–92.

24. Němec J, Kim JJ, Gabris B, et al. Calcium oscillations and T wave lability precede ventricular arrhythmias in acquired long QT type 2. *Heart Rhythm* 2010;7:1686–94.

25. Horváth B, Hegyi B, Kistamás K, et al. Cytosolic calcium changes affect the incidence of early afterdepolarizations in canine ventricular myocytes 1. *Can J Physiol Pharmacol* 2015;93:527–34.

26. Pieske B, Kretschmann B, Meyer M, et al. Alterations in intracellular calcium handling associated with the inverse force-frequency relation in human dilated cardiomyopathy. *Circulation* 1995;92:1169–78.

27. Pieske B, Maier LS, Piacentino V, et al. Rate dependence of $[Na^+]i$ and contractility in

nonfailing and failing human myocardium. *Circulation* 2002;106:447–53.

28. Pieske B, Maier LS, Bers DM, et al. Ca^{2+} handling and sarcoplasmic reticulum Ca^{2+} content in isolated failing and nonfailing human myocardium. *Circ Res* 1999;85:38–46.
29. Eising GP, Hammond HK, Helmer GA, et al. Force-frequency relations during heart failure in pigs. *Am J Physiol* 1994;267:H2516-22.
30. Neumann T, Ravens U, Heusch G. Characterization of excitation-contraction coupling in conscious dogs with pacing-induced heart failure. *Cardiovasc Res* 1998;37:456–66.
31. Feldman MD, Alderman JD, Aroesty JM, et al. Depression of systolic and diastolic myocardial reserve during atrial pacing tachycardia in patients with dilated cardiomyopathy. *J Clin Invest* 1988;82:1661–9.
32. Hasenfuss G, Holubarsch C, Hermann HP, et al. Influence of the force-frequency relationship on haemodynamics and left ventricular function in patients with non-failing hearts and in patients with dilated cardiomyopathy. *Eur Heart J* 1994;15:164–70.
33. Schotten U, Voss S, Wiederin TB, et al. Altered force-frequency relation in hypertrophic obstructive cardiomyopathy. *Basic Res Cardiol* 1999;94:120–7.
34. Mills GD, Harris DM, Chen X, et al. Intracellular sodium determines frequency-dependent alterations in contractility in hypertrophied feline ventricular myocytes. *Am J Physiol Heart Circ Physiol* 2007;292:H1129-38.
35. Mubagwa K, Lin W, Sipido K, et al. Monensin-induced Reversal of Positive Force–Frequency Relationship in Cardiac Muscle: Role of Intracellular Sodium in Rest-dependent Potentiation of Contraction. *J Mol Cell Cardiol* 1997;29:977–89.
36. Verdonck F, Volders PGA, Vos MA, et al. Increased Na^+ concentration and altered Na/K pump activity in hypertrophied canine ventricular cells. *Cardiovasc Res* 2003;57:1035–43.
37. van Borren MMGJ, Vos MA, Houtman MJC, et al. Increased sarcolemmal Na^+/H+ exchange activity in hypertrophied myocytes from dogs with chronic atrioventricular block. *Front Physiol* 2013;4:322.
38. Antoons G, Oros A, Beekman JDM, et al. Late Na^+ Current Inhibition by Ranolazine Reduces Torsades de Pointes in the Chronic Atrioventricular Block Dog Model. *J Am Coll Cardiol* 2010;55:801–9.
39. Bourgonje VJA, Vos MA, Ozdemir S, et al. Combined Na^+/Ca^{2+} Exchanger and L-Type Calcium Channel Block as a Potential Strategy to Suppress Arrhythmias and Maintain Ventricular Function. *Circ Arrhythmia Electrophysiol* 2013;6:371–9.
40. Fuerstenwerth H. On the Differences Between Ouabain and Digitalis Glycosides. *Am J Ther* 2014;21:35–42.
41. Prabhu SD, Freeman GL. Effect of tachycardia heart failure on the restitution of left ventricular function in closed-chest dogs. *Circulation* 1995;91:176–85.

42. Seed WA, Noble MI, Walker JM, et al. Relationships between beat-to-beat interval and the strength of contraction in the healthy and diseased human heart. *Circulation* 1984;70:799–805.

43. Merillon JP, Motte G, Aumont MC, et al. Post-extrasystolic left ventricular peak pressure with and without left ventricular failure. *Cardiovasc Res* 1979;13:338–44.

44. Beck W, Chesler E, Schrire V. Postextrasystolic ventricular pressure responses. *Circulation* 1971;44:523–33.

45. Bers DM. Calcium Cycling and Signaling in Cardiac Myocytes. Annu Rev Physiol 2008;70:23–49.

46. Laver DR. Coupled calcium release channels and their regulation by luminal and cytosolic ions. *Eur Biophys J* 2005;34:359–68.

47. Szentesi P, Pignier C, Egger M, et al. Sarcoplasmic reticulum Ca^{2+} refilling controls recovery from Ca^{2+}-induced Ca^{2+} release refractoriness in heart muscle. *Circ Res* 2004;95:807–13.

48. Hoit BD, Kadambi VJ, Tramuta DA, et al. Influence of sarcoplasmic reticulum calcium loading on mechanical and relaxation restitution. *Am J Physiol Heart Circ Physiol* 2000;278:H958-63.

49. Hoit BD, Tramuta DA, Kadambi VJ, et al. Influence of Transgenic Overexpression of Phospholamban on Postextrasystolic Potentiation. *J Mol Cell Cardiol* 1999;31:2007–15.

50. Thomsen MB, Verduyn SC, Stengl M, et al. Increased short-term variability of repolarization predicts d-sotalol-induced torsades de pointes in dogs. *Circulation* 2004;110:2453–9.

51. Johnson DM, Heijman J, Pollard CE, et al. IKs restricts excessive beat-to-beat variability of repolarization during beta-adrenergic receptor stimulation. *J Mol Cell Cardiol* 2010;48:122–30.

52. Johnson DM, Heijman J, Bode EF, et al. Diastolic spontaneous calcium release from the sarcoplasmic reticulum increases beat-to-beat variability of repolarization in canine ventricular myocytes after β-adrenergic stimulation. *Circ Res* 2013;112:246–56.

53. Antoons G, Johnson DM, Dries E, et al. Calcium release near L-type calcium channels promotes beat-to-beat variability in ventricular myocytes from the chronic AV block dog. *J Mol Cell Cardiol* 2015;89:326–34.

54. Sinnecker D, Dirschinger RJ, Barthel P, et al. Postextrasystolic blood pressure potentiation predicts poor outcome of cardiac patients. *J Am Hear Assoc* 2014;3:e000857.

Supplemental Material

Supplemental table 1. hemodynamic parameters of non-inducible and inducible dogs

* p < 0.05 versus non-inducible. LV EDP = left ventricular end-diastolic pressure; LV ESP = left ventricular end-systolic pressure; LV dP/dt_{max} = left ventricular maximal pressure rise.

		AAVB		**CAVB**	
		non-inducible	*inducible*	*non-inducible*	*inducible*
LV EDP (mmHg)	*CL 1200 ms*	14 ± 2	16 ± 1	12 ± 2	11 ± 1
	CL 750 ms	14 ± 2	16 ± 1	10 ± 2	10 ± 1
	CL 300 ms	14 ± 1	15 ± 1	11 ± 3	9 ± 1
LV ESP (mmHg)	*CL 1200 ms*	60 ± 4	55 ± 4	73 ± 3	88 ± 2*
	CL 750 ms	63 ± 9	62 ± 2	85 ± 3	85 ± 3
	CL 300 ms	69 ± 9	69 ± 4	87 ± 6	77 ± 4
LV dP/dt_{max} (mmHg/s)	*CL 1200 ms*	547 ± 10	597 ± 42	1091 ± 59	2354 ± 168*
	CL 750 ms	763 ± 69	692 ± 39	1280 ± 68	1860 ± 160*
	CL 300 ms	1304 ± 170	1368 ± 81	1865 ± 94	1745 ±86

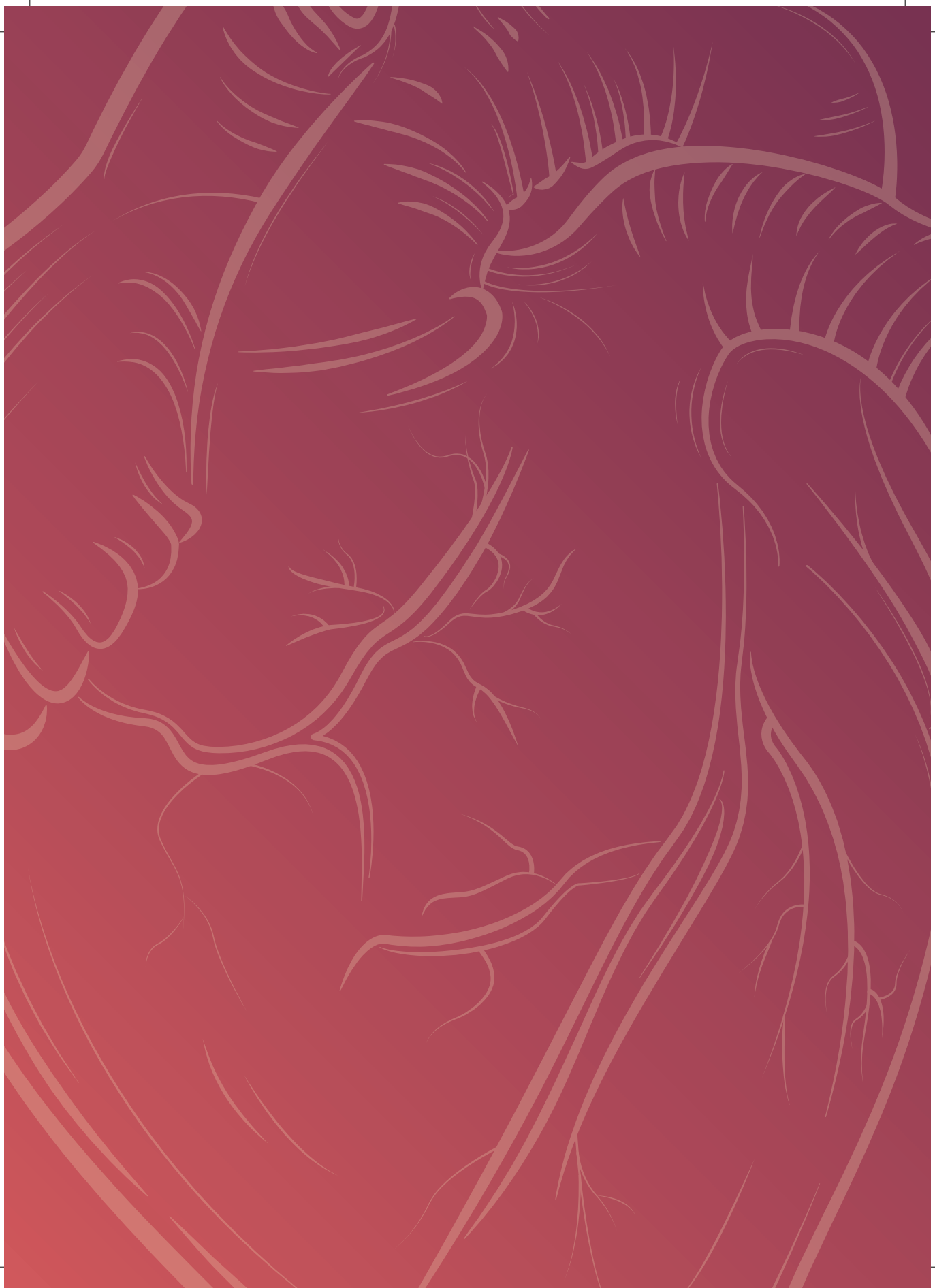

PART II

PARAMETERS OF ELECTRICAL REMODELING FOR RISK PREDICTION & MONITORING

Chapter 4

Differential multivariable risk prediction of appropriate shock versus competing mortality – A prospective cohort study to estimate benefits from ICD therapy

Leonard Bergau[1], Rik Willems[2], David J. Sprenkeler[3], Thomas H. Fischer[1], Panayota Flevari[4], Gerd Hasenfuß[1], Dimitrios Katsaras[4], Aleksandra Kirova[1], Stephan E. Lehnart[1], Lars Lüthje[1], Christian Röver[5], Joachim Seegers[1], Samuel Sossalla[1], Albert Dunnink[3], Rajevaa Sritharan[1], Anton E. Tuinenburg[6], Bert Vandenberk[2], Marc A. Vos[3], Sofieke C. Wijers[3], Tim Friede[5], Markus Zabel[1]

[1] Department of Cardiology and Pneumology, University Medical Center Göttingen, Göttingen, Germany
[2] Department of Cardiology, University hospitals Leuven, Leuven, Belgium
[3] Department of Medical Physiology, University Medical Center Utrecht, Utrecht, The Netherlands
[4] Department of Cardiology, Attikon University Hospital, Athens, Greece
[5] Department of Medical Statistics, University Medical Center Göttingen, Göttingen, Germany
[6] Department of Cardiology, University Medical Center Utrecht, Utrecht, The Netherlands

Int J Cardiol. 2018 Jun;

Abstract

Objective: We prospectively investigated combinations of risk stratifiers including multiple EP diagnostics in a cohort study of ICD patients.

Methods: For 672 enrolled patients, we collected history, LVEF, EP study and T wave alternans testing, 24-h Holter, NT-proBNP, and the eGFR. All-cause mortality and first appropriate ICD shock were predefined endpoints.

Results: The 635 patients included in the final analyses were 63 ± 13 years old, 81% were male, LVEF averaged 40 ± 14%, 20% were inducible at EP study, 63% had a primary prophylactic ICD. During follow-up over 4.3 ± 1.5 years, 108 patients died (4.0% per year), and appropriate shock therapy occurred in n = 96 (3.9% per year). In multivariate regression, age ($p < 0.001$), LVEF ($p < 0.001$), NYHA functional class ($p = 0.007$), eGFR ($p = 0.024$), a history of atrial fibrillation ($p = 0.011$), and NT-pro-BNP ($p = 0.002$) were predictors of mortality. LVEF ($p = 0.002$), inducibility at EP study ($p = 0.007$), and secondary prophylaxis ($p = 0.002$) were identified as independent predictors of appropriate shocks. A high annualized risk of shocks of about 10% per year was prevalent in the upper quintile of the shock score. In contrast, a low annual risk of shocks (1.8% per year) was found in the lower two quintiles of the shock score. The lower two quintiles of the mortality score featured an annual mortality < 0.6%.

Conclusion: In a prospective ICD patient cohort, a very good approximation of mortality versus arrhythmic risk was possible using a multivariable diagnostic strategy. EP stimulation is the best test to assess the risk of arrhythmias resulting in ICD shocks.

Introduction

More than a decade ago, the Implantable Cardioverter-Defibrillator (ICD) has been shown to improve survival in patients at risk of sudden cardiac death (SCD).[1–3] However, a large number of ICD patients never receive appropriate shocks or die prior to appropriate ICD therapy.[4] The DANISH trial revealed that ICD therapy does not reduce mortality in patients with non-ischemic cardiomyopathy.[5] As an explanation it was suggested that improvements in interventional and pharmacological therapies have led to steep reductions of mortality over the past decades.[6,7] In the aftermath, American ACC/AHA/HRS guidelines for ICD treatment were renewed unchanged in 2017, while ESC guidelines have not been updated. ESC and EHRA have, however, proposed the randomized RESET-SCD trial to reassess the effects of primary prophylactic ICD therapy in ischemic cardiomyopathy.[8] Conceptually, any form of ICD therapy can only prevent sudden and tachy-arrhythmic mortality, not that from heart failure or non-cardiac causes.[9] As found in the recently presented VEST trial, a scarcity of life-threatening arrhythmias coincides with lack of an effect of the defibrillator on a primary endpoint of SCD and appropriate shocks. Identification of patient subgroups with significant mortality benefit from ICD therapy remains critical[10,11] and additional risk stratifiers beyond LVEF need to be implemented clinically.[12–14] To date, few studies investigated risk markers of ICD shocks. Most were focused on microvolt T wave alternans (MTWA) and had equivocal results.[15–18] A substantial number of potentially useful parameters of risk stratification, for instance electrophysiological and electrocardiographic markers, parameters from cardiovascular history, biomarkers, and possible combinations thereof have been underused.[12–14] We set out to conduct a large prospective cohort study to test different combinations of these risk factors to predict the risk of ICD shocks versus the competing risk of mortality.

Materials & methods

Study design and baseline testing

A prospective international clinical study was initiated as part of the European Union Seventh Framework funded large-scale cooperative project EUTrigTreat. The rationale, objectives and design of the study including statistical plan and sample size calculations have been published previously.[19] In brief, the study enrolled a contemporary ICD cohort to test multiple carefully selected risk markers of clinical relevance for prediction of mortality and arrhythmias. In order to represent a large range from lower to higher risks of appropriate ICD shocks, the inclusion criteria featured ICD patients with primary or secondary prophylactic guideline indications and age ≥ 18 years. The study

was registered (NCT01209494) and approved by all participating local ethics boards. Baseline assessments included medical and cardiovascular history, measurement of LVEF, non-invasive or invasive programmed ventricular stimulation (PVS), exercise and atrial paced microvolt T wave alternans (MTWA) testing, recording of a 12-lead standard ECG and 24-h Holter (for analysis of heart rate variability, heart rate turbulence, number of premature ventricular complexes and non-sustained runs of ventricular tachycardia), and serum biomarkers (high-sensitivity C-reactive protein [hs-CRP], N-terminal-pro B-type-natriuretic protein [NT-proBNP], and serum creatinine). Expecting a wide range of indications and clinical characteristics, ICD programming recommendations were agreed between sites, but final programming was left to the discretion of the treating physician.

Programmed ventricular stimulation

The large majority of patients (91%) underwent non-invasive PVS via their implanted ICDs. In case of first ICD implantation, an EP study was done invasively in 60 (9%) patients. A validated abbreviated stimulation protocol with three extrastimuli was used.[20] Inducibility of sustained ventricular arrhythmia was defined as induction of a single monomorphic VT lasting for 30 s or two polymorphic VT/VF episodes requiring cardioversion.

MTWA testing

MTWA exercise testing (Cambridge Heart, Tewksbury/MA, USA) was performed if patients were in sinus rhythm. When the patient was unable to exercise, atrial pacing was used to increase the heart rate. MTWA tests were graded according to A and B rules[21] by two blinded investigators each from the enrolling and core centers. In case of disagreement, the enrolling center decided the final grade. For analysis, positive and indeterminate results were grouped as non-negative.

Holter monitoring

A 24 hour Holter monitoring was performed using standard devices (Delmar Reynolds Pathfinder, Spacelabs Healthcare, Snoqualmie, WA; Spiderview, Sorin Group, Paris, France; GE Mars, GE Healthcare, Milwaukee/WI, USA). In case of sinus rhythm and < 15% ventricular or atrial pacing, heart rate variability was analyzed using the respective Holter software submodules. Heart rate turbulence and deceleration capacity were calculated using dedicated software (Librasch Calc, V1.02, Schneider R & Schmidt G, TU Munich, Germany).

Outcomes: all-cause mortality and first appropriate ICD shock

The primary endpoint was all-cause mortality. First appropriate ICD shock was selected as a key secondary endpoint. This endpoint did not include anti-tachycardia pacing. Patients were followed every 3 to 6 months. If ICD shocks occurred, EGM data were forwarded to the endpoint committee (A.T., R.W., M.Z.) for adjudication.

Statistical analysis

Cox regression analysis was implemented as described.[19] Death was considered a censoring event using competing risk adjustments.[22] Risk models for shock and mortality were developed using forward selection among a set of known potential risk factors. Adjusting for these, factors were identified that indicated an incremental risk in univariate analyses ($p < 0.05$). Models were then determined through an exhaustive search through combinations of identified risk factors by minimization of the Bayesian Information Criterion.[23] Using score values, patients were subdivided into three groups at low (lowest two quintiles), intermediate (intermediate two quintiles) and high risk (upper quintile). In 148 patients, NT-proBNP was extrapolated from BNP measurements.[24] Discriminatory power of scores was evaluated using area under the ROC curve (AUC) at a prediction horizon of 2 and 6 years.[25] Bootstrapping (generating 1000 samples) was used to estimate the bias introduced by validating the model from the same data used to develop the score.[26] Kaplan-Meier probabilities were compared using the log-rank test. Correlations are evaluated using Pearson's correlation coefficient. All computations were performed using the R environment for statistical computing and graphics (http://www.r-project.org). Continuous values are expressed as mean ± standard deviation. All p-values are two-tailed, a level of 5% is considered statistically significant.

Results

Patient characteristics

From January 2010 to April 2014, we enrolled 672 ICD patients in four centers. Of 672 patients enrolled, 635 were finally included in the analysis (see Supplemental figure 1 in Supplemental material). The first ICD was implanted 3.8 ± 3.9 years (median 2.9 years) prior to enrolment, 60 (9%) received their implant at enrolment, 63% (n = 400) had primary prophylactic indications. Mean age was 63 ± 13 years, 81% were male. Mean LVEF was 40 ± 14%. Basic rhythm was sinus rhythm in 510 patients (80%), atrial

Table 1. Clinical baseline characteristics for all patients (n=635), surviving patients (n=527), and deceased patients (n=108)

AAD = antiarrhythmic drug, AF = atrial fibrillation, ARVC = arrhythmogenic right ventricular dysplasia, CM = cardiomyopathy, hs-CRP = high sensitivity C-reactive protein, LVEF = left ventricular ejection fraction, NT-proBNP = n-terminal pro brain natriuretic peptide; NYHA = New York Heart Association, * = statistically significant

	All (n=635)	Alive (n=527)	Deceased (n=108)	p-value
Age (years)	63 ± 13	61 ± 13	71 ± 9	<0.001*
Male sex	513 (81 %)	420 (80%)	93 (86%)	0.141
Body mass index (kg/m²)	28.1 ± 5.3	28.3 ± 5.4	27.2 ± 4.7	0.0740
LVEF (%)	40 ± 14	42 ± 14	33 ± 11	<0.001*
DCM	214 (34%)	164 (31%)	50 (46%)	<0.001*
CAD without STEMI	157 (25%)	119 (23%)	38 (35%)	
CAD with STEMI	107 (17%)	93 (18%)	14 (13%)	
Idiopathic VT/VF	46 (7.2%)	45 (8.5%)	1 (0.9%)	
HCM/HOCM	38 (6.0%)	37 (7.0%)	1 (0.9%)	
Brugada	11 (1.7%)	10 (1.9%)	1 (0.9%)	
LQT	8 (1.3%)	8 (1.5%)	0 (0%)	
ARVC	7 (1.1%)	7 (1.3%)	0 (0%)	
CPVT	2 (0.3%)	2 (0.4%)	0 (0%)	
other	45 (7.1%)	42 (8.0%)	3 (2.8%)	
NYHA class				
I	188 (30%)	179 (34%)	9 (8%)	<0.001*
I-II	83 (13%)	71 (13%)	12 (11%)	
II	182 (29%)	148 (28%)	34 (31%)	
II-III	82 (13%)	59 (11%)	23 (21%)	
III	100 (16%)	70 (13%)	30 (28%)	
NT-proBNP (ng/L)	1361 ± 2203	1051 ± 1787	2562 ± 3094	<0.001*
hs-CRP (mg/L)	3.8 ± 5.2	3.4 ± 5.0	5.4 ± 6.0	<0.001*
AF				
Permanent	80 (13%)	48 (9.2%)	32 (30%)	<0.001*
Paroxysmal	137 (22%)	110 (21%)	27 (26%)	
No history of AF	405 (65%)	359 (69%)	46 (44%)	
Intrinsic QRS width (ms)	129 ± 35	126 ± 34	143 ± 35	<0.001*
β-blockers	470 (85%)	390 (85%)	80 (86%)	0.874
Class I antiarrhythmic drug	11 (2.1%)	10 (2.2%)	1 (1.1%)	1.000
Class III antiarrhythmic drug	153 (28 %)	127 (28%)	26 (30%)	0.795
Digitalis glycosides	81 (15%)	52 (12%)	29 (33%)	<0.001*
Oral anticoagulation	191 (35%)	141 (31%)	50 (56%)	<0.001*

fibrillation (AF) in 76 patients (12%), and pacemaker rhythm or higher degree AV block in 49 patients (8%). Baseline parameters are shown in Table 1. A single-chamber ICD was implanted in 45%, dual-chamber ICD in 34%, and biventricular ICD in 21%. All patients had VT and VF zones programmed, with lower and upper boundaries of 344 ± 40 ms, and 276 ± 40 ms at baseline, respectively. A mean of 5.3 ± 2.2 ATPs were programmed

Table 2: Multivariate hazard ratios for prediction of all-cause mortality and appropriate shock
open field = not selected as model variable; AF = atrial fibrillation; eGFR = estimated glomerular filtration rate; EP = electrophysiological; LVEF = left ventricular ejection fraction; NT-proBNP = n-terminal pro brain natriuretic peptide, NYHA = New York Heart Association, * = statistically significant

	Hazard ratio		95 % confidence interval		p-value	
n=635	Mortality	Shock	Mortality	Shock	Mortality	Shock
Age (per 10 yrs)	1.73		1.37 - 2.19		<0.0001*	
LVEF (per 5%)	0.80	0.92	0.73 - 0.87	0.80 - 0.95	<0.0001*	0.0018*
History of AF	1.69		1.13 - 2.54		0.0110*	
NT-pro-BNP (100ng/L)	1.46		1.15 - 1.84		0.0017*	
NYHA functional class (>II)	1.73		1.16 - 2.58		0.0072*	
eGFR (per 30 mL/min)	0.70	0.77	0.52 - 0.95	0.58 - 1.02	0.0236*	0.0700
Secondary prophylaxis		1.98		1.29 - 3.04		0.0017*
EP inducibility		1.86		1.19 - 1.90		0.0067*

before a shock in the VT zone. ATP before shock was programmed in the VF zone in 298 patients (48%).

ECG and Holter parameters

An intrinsic QRS complex was recorded in 535 patients, an RV paced rhythm in 40, a biventricular paced rhythm in 57, in 3 patients QRS classification was not possible. Mean QRS duration of intrinsic complexes was 129 ± 35 ms, mean QT and QTc were 449 ± 52 ms and 459 ± 47 ms, respectively. Mean heart rate on Holter was 67 ± 10 bpm. The number of premature ventricular complexes averaged 2361 ± 5885 per 24 h. The number of non-sustained VT episodes averaged 2 ± 15 per 24 h, and 146 patients (23%) had at least one salvo of non-sustained VT. Not all patients in sinus rhythm (n = 510) were analyzable for heart rate variability and HRT. Absence of the necessary PVCs for HRT analysis occurred in 55 cases. Additional reasons for inability to analyze were > 15% atrial pacing, <66% analysability for heart rate variability, other technical difficulties, or implausible data. The mean standard deviation of normal-to-normal intervals (SDNN) was 113 ± 43 ms; mean square root of mean of squared differences between normal-to-normal RR intervals (RMSSD) was 31 ± 27 ms; mean heart rate turbulence onset was −0.13 ± 2.12%, heart rate turbulence slope was 5.50 ± 5.09 ms/R-R interval, and deceleration capacity (DC) was 2.12 ± 6.58 ms, respectively.

EP study and MTWA

An EP study including programmed stimulation was done in 617 patients (97%). Sustained VT/VF was induced in 124 (20%) patients. Monomorphic VT was induced in 81%, polymorphic VT in 11%, and VF in 8%, respectively. Mean cycle length of induced

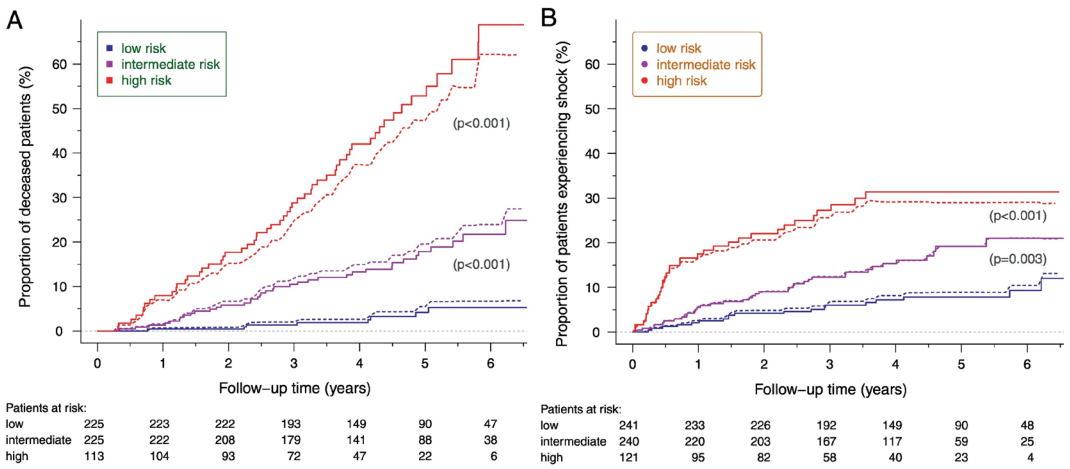

Figure 1. Cumulative event-probability curves for mortality (A) and appropriate shock (B).

For each risk, the cohort is divided into three risk groups (low: two quintiles, intermediate: two quintiles, high: one quintile), the calculation is provided by separate risk scores for all-cause mortality and appropriate shock. The dashed lines indicate the cumulative event-probabilities after bootstrap bias correction.

Panel A: The mortality risk score provides excellent separation of low, intermediate, and high mortality risks. The low risk mortality group (two quintiles) shows an annualized risk of 0.5%. In contrast, the high risk mortality group (one quintile) features an annual risk of 11%. Within the latter patients, it can be expected that non-sudden cardiac deaths or non-cardiac deaths compete with the occurrence of ventricular arrhythmias. In particular, patients with a low predicted shock risk may not improve their prognosis wearing an ICD.

Panel B: The appropriate shock risk score provides good separation of low, intermediate, and high shock risks. The low risk shock group, a large group covering two quintiles and a number of 241 patients, has an average annual risk of 1.8%. Since a first appropriate shock does not always correspond with SCD (if the patient had not had an ICD) but only in 30–50%, this number corresponds to an SCD rate < 1%/yr. In patients with an estimated SCD rate < 1% annually, depending on age and other mortality factors independent of arrhythmias, omission of an ICD may be discussed. In contrast, the high risk group for shock (one quintile) features an average annual risk of ~8.5%, well qualifying the patient for an ICD with high survival benefit. In the intermediate risk of shock group (two quintiles), the risk is still ~4% annually, corresponding to maybe a 2% annual SCD rate. Therefore, patients in the intermediate risk group for shock, should probably also obtain an ICD as they derive ICD benefit, unless a very high competing risk of non-arrhythmic mortality can be seen from the mortality score.

VT/VF was 277 ± 55 ms. MTWA gradings were available for final analysis in 493 patients (97%) with sinus rhythm. Of these, 347 (70%) were performed under exercise, another 146 (30%) via atrial or biventricular stimulation. According to A rules, 28% (n = 140) were graded positive, 51% (n = 249) negative, and 21% (n = 104) indeterminate, respectively. Following B rules, 28% (n = 138) were positive, 57% (n = 282) negative, and 15% (n = 73) indeterminate, respectively.

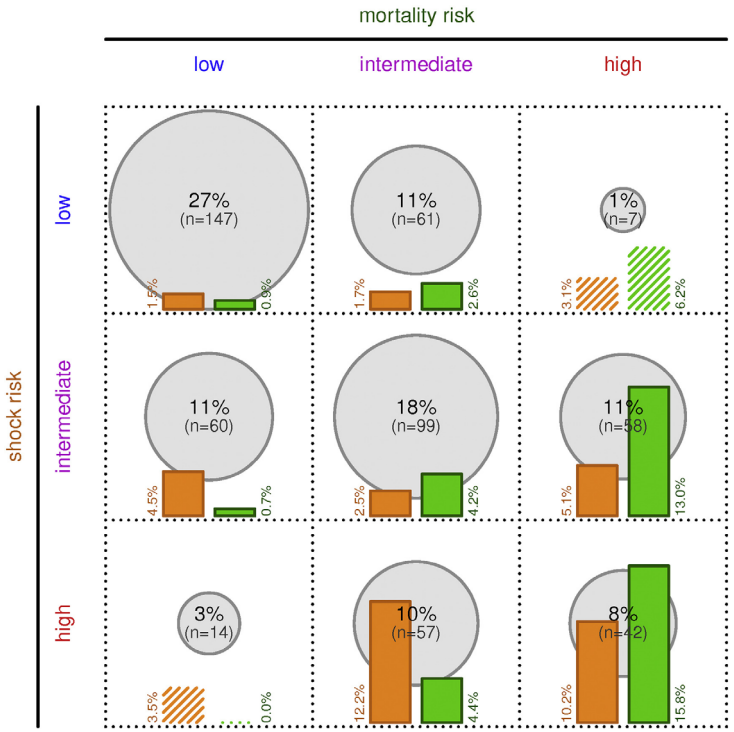

Figure. 2. Distribution of patients to combinations of risk categories (low, intermediate, high) and their associated annualized mortality and shock risk.

Grey circles denote the frequencies of patients in the various categories. The orange and green bars denote the actual annualized shock and mortality risks in a category, respectively. For each risk, the cohort is divided into three risk groups (low: two quintiles, intermediate: two quintiles, high: one quintile), resulting in nine subgroups, of which seven have significant size. Annualized shock risk is found to be >10% per year in the highest quintile of the shock score and can coincide with both an intermediate (4.4% per year) and a high (10.2% per year) mortality. Annualized mortality risk is found to be >10% per year in the highest quintile of the mortality score and can coincide with both an intermediate (5.1% per year) and a high risk of appropriate shock.

Occurrence of endpoints

Over a follow-up of 4.3 ± 1.5 years, 96 (15.1%) patients received a first appropriate shock (annualized rate 3.9% per year). The cycle length of the primary arrhythmia leading to appropriate shock in a VT/VF episode was 255 ± 48 ms (minimum 170 ms, maximum 650 ms), 47% (n = 45) were delivered in the VF zone. Overall mortality was 17.0% (n = 108, annualized rate 4.0% per year), and adjudicated as cardiac in n = 30 (58%), n = 17 (32%) deaths were classified as non-cardiac. Classification of the mode of death was not possible in 5 cases.

Risk prediction for mortality and appropriate shock and associated risk scores

Univariate predictors of mortality

Univariate Cox regression revealed age, LVEF, estimated glomerular filtration rate (eGFR), NYHA functional class, history of AF, ischemic heart disease, COPD, NT-pro-BNP, hs-CRP, non-negative MTWA, deceleration capacity (DC) and several parameters of HRT as strong clinical predictors of mortality (see Supplemental table 1 in Supplemental material). Strong predictors of mortality from Holter monitoring were deceleration capacity (DC), heart rate turbulence category, turbulence onset (TO), and turbulence slope (TS). From the 12-lead ECG, QRS width and QTc predicted mortality.

Univariate predictors of appropriate shock

Univariate clinical predictors of appropriate shock were LVEF, eGFR, COPD, NT-pro-BNP, intrinsic QRS, intrinsic QTc, and secondary prophylactic indication (see Supplemental table 2 in Supplemental material). Non-negative MTWA was a univariate predictor of appropriate shocks, the hazard ratio was 1.85 (CI 1.18–2.92, p = 0.007) for A rules, and 1.73 (CI 1.11–2.69, p = 0.015) for B rules, respectively. None of the Holter parameters were predictive of shock. In general, there were less significant predictors for shock as compared to mortality, and p-values were less significant.

Inducibility at EP study: univariate prediction

Inducibility at EP study was a significant predictor for appropriate shocks but not for mortality. Inducibility at EP study predicted appropriate shock similarly in patients with ischemic (HR 2.13, CI 1.15–3.92, p = 0.0155) or non-ischemic cardiomyopathies (HR 2.03, CI 1.10–3.76, p = 0.0233), primary (HR 2.25, CI 1.24–4.09, p = 0.0080), or secondary prophylactic indication (HR 1.98, CI 1.07–3.68, p = 0.0294), respectively.

Multivariate risk models and risk score

The final mortality model (Table 2) involved 563 patients and 102 deaths, with 8% (n = 53) missing values for NT-pro-BNP and 25% (n = 148) imputed values based on BNP.[24] Missing values for all other parameters were below 3% with the exception of hs-CRP (25%). The final appropriate shock model was based on 602 patients (Table 2). The respective risk scores are shown in Supplemental figure 2 in Supplemental material. Multivariate predictors of mortality were age, LVEF, NYHA functional class, eGFR, history of AF, and NTpro-BNP. Multivariate predictors of appropriate shock were LVEF, secondary prophylaxis, and inducibility at EP study. MTWA A rules missed inclusion in the multivariate shock model (p = 0.058), eGFR was only of borderline significance in

the final model (p = 0.070). The risk score for prediction of all-cause mortality featured a c-index of 0.811 (CI 0.757, 0.866) at 2 years, and 0.865 (CI 0.764, 0.966) at 6 years. The c-index for prediction of shock using the Fine and Gray model was 0.725 (CI 0.634, 0.815) at 2 years of FU, and 0.691 (CI 0.612, 0.771) at 6 years, respectively. In a subgroup of primary prophylactic patients, statistically significant predictors identified in multivariate analyses including all patients for mortality (age, LVEF, NYHA) and shock (LVEF, inducibility) were very similar and had similar HR.

Individualization of risks: cumulative incidence curves by quintiles

In general, risk separation was excellent, as shown in Figure 1. A wide and very individual risk continuum was found for both risks. For instance, the lowest mortality quintile showed zero mortality and the lower two mortality quintiles a combined annual risk of <0.6% (Figure 1A). In the overall cohort, the lower two quintiles of patients (40%) of each respective risk exhibited very low risks (Figure 1A and B).

Correlation between risk scores

The risk of appropriate shock did not match well with the risk of all-cause mortality, as the sub-classification of low, intermediate, and high risk groups for each endpoint shows (Figure 2). Accordingly, the correlation between mortality score and shock score was only moderate (see Supplemental figure 3 in Supplemental material) with an r^2 of 0.31 (r = 0.56, p < 0.001), i.e. 69% of their variation explained by other factors.

Discussion

Main findings

This prospective study in a large ICD patient cohort with guideline-based indications for ICDs in primary and secondary prevention of SCD aimed to identify a differential multivariate risk stratification strategy targeted at predicting either mortality or ICD shocks. To our knowledge, this is the first head-to-head comparison of multiple diagnostic risk factors for this particular aim of predicting ICD shocks in comparison to all-cause mortality. We showed that a very good approximation of the risk of ICD shocks versus total mortality was possible after development of differential risk scores. For the prediction of all-cause mortality, a typical selection of parameters showed high accuracy. For prediction of ICD shocks, inducibility at EP study was an excellent, specific and independent clinical test in addition to LVEF, it was not associated with all-cause mortality. For individual patients, higher mortality risk did not necessarily represent

higher appropriate shock risk, and vice versa. Different combinations of mortality and shock risk suggest different ICD survival benefit, which could be assessed when the implantation of an ICD is considered.

Predictors of outcomes including shocks in ICD patients

In univariate analysis, we confirmed typical risk factors for mortality in our ICD cohort of 635 patients (and with an excellent c-index). The only multivariate factor predicting both shock and mortality was LVEF. Risk factors for mortality have been described in very large ICD registries[27,28] as well as heart failure registries,[29,30] and were fully confirmed in our study. Only few studies have reported predictors of ICD shock, but rather predictors of presumed arrhythmic mortality or SCD. Our data demonstrates that risks of mortality and shock have to be considered separately in ICD recipients. Lee et al.[31] recently reported simultaneous shock and mortality predictors from baseline variables, however, they did not perform additional diagnostic testing and the number of identified patients with a presumed low ICD benefit was <10% of patients. We found similar hazard ratios regarding prediction of appropriate shock, for instance for eGFR as the best clinical baseline shock predictor in our study. Adding specific EP diagnostic tests, we showed that EP stimulation and MTWA outperformed the baseline parameters, and the group of patients that could be defined to have marginal ICD benefits as well as a clearly high benefit was considerably larger than in the paper by Lee et al.[31] The value of Holter parameters to predict appropriate shock was clearly disappointing. We identified a group of 40% of our patients (two quintiles) characterized by a low annual appropriate shock rate of ≈1.8%. This shock rate can be translated to a risk of SCD <1.0% per year had the patient not been implanted an ICD.[32] We also identified a large group of ≈20% of all patients who had a predicted ≈11% annual shock rate associated with low to intermediate mortalities of ≈3–9%, likely resulting in a very high ICD benefit. In between these two well defined groups with low (≈40% of patients) or high (≈20% of patients) shock risk, there is still a large number of patients with intermediate combinations of the two risks calling for individualization of risk versus benefit of the ICD in a given patient. On this part, our study is hypothesis-generating and needs confirmation. As expected, secondary prophylaxis was identified as an independent predictor of shocks, underscoring the good indication of ICD therapy in these patients. As MTWA and heart rate turbulence cannot be assessed in AF, we derived additional models applicable only to patients in sinus rhythm. In the respective model for appropriate shock, MTWA closely missed the final model ($p = 0.058$). Thus, it was possible to calculate a final shock model with variables that were available in all patients. Similarly, for mortality, there was also one final model for all patients, as there was no independent parameter measurable only in sinus rhythm.

Predictive value of EP study versus MTWA in ICD patients

We showed that EP and MTWA testing do have value for the identification of arrhythmic risk in an individual patient. Indeed, upon univariate analysis, we found both tests to be good predictors of appropriate shock with HR of 2.15 for inducibility at EP study ($p = 0.0009$) and 1.85 for MTWA ($p = 0.007$). In general, predictors for shock were less common as compared to predictors of mortality. In the multivariate model for shock, inducibility at EP study had a HR of 1.86 ($p = 0.007$) and was the only diagnostic test specific for the prediction of appropriate shock. In comparison, MTWA ($p = 0.058$) missed inclusion in the multivariate model. Our results are in line with the ABCD trial[18] where EP study and MTWA were directly compared. From our data, PVS is clearly recommended over MTWA when estimating the risk of appropriate shock in an ICD patient. EP stimulation has been historically recommended to assess the risk of malignant ventricular arrhythmias[33,34] in case of the need for risk stratification. It has been involved in the first evidence-based indications for prophylactic ICD therapy,[35–37] EP stimulation was by far the best diagnostic test for shock prediction in our study. This is in line with its proven value in assessing risk of SCD in patients after myocardial infarction and with ischemic cardiomyopathy[37–39] as well as other guideline indications. Its value was similarly high in non-ischemic cardiomyopathy patients. MTWA as a non-invasive test failed to be considered for the final multivariate model.

Future outlook

After publication of the DANISH study, European ICD guideline indications require an update including this landmark trial.[5] Meanwhile, ESC and EHRA have proposed the RESET-SCD trial, a randomized trial reassessing the benefit of primary prophylactic ICD therapy in ischemic cardiomyopathy, without additional risk stratification.[8] We are convinced that the overall group of ischemic cardiomyopathy patients may contain patients that derive clear benefit from the ICD, as identified by subgroups of significant size in the current study. New randomized studies should therefore enroll patients with presumed borderline survival benefit from ICD therapy. For identification, risk markers such as those from our current study could be utilized. The data of large observational ICD studies such as the prospective EU-CERT-ICD-study (NCT 02064192) and the Dutch DO-IT study[40] will become available in the second half of 2018 and can also influence the design of future randomized trials.

Limitations

There are several limitations of our study. We included patients with primary

or secondary prophylactic indications and not necessarily undergoing de novo implantation, with the intent that the results apply to all ICD patients, and also late in their follow-up. Inclusion of 672 patients in four centers was consecutive regarding screening from the outpatient clinics. A common reason to opt for non-participation in the study was the EP stimulation with possible induction of arrhythmias. In the majority of patients, EP stimulation was done via ICD and from a single site. Noninvasive EP study has been described in other studies,[41] and the diagnostic yield appears to be very similar to its invasive counterpart. Despite the simplified approach, EP stimulation was clearly the best diagnostic test to predict appropriate shock, and could not be replaced by MTWA or other risk stratifiers. Our predefined endpoint was appropriate ICD shock, it did not include anti-tachycardia pacing. It cannot be ruled out that some anti-tachycardia pacing episodes were clinically useful for the patient. The study group was convinced from the outset that anti-tachycardia pacing episodes would overestimate life-saving effects of the ICD.[42] In the meantime, this was supported by the MADIT-RIT results where the conventional arm was treated with a large number of ATP but outcomes such as shock or mortality were not improved. Finally, we had a recommended, not mandatory ICD programming, which might have potentially biased the number of appropriate shocks.

Conclusion

Prospective and comprehensive risk stratification in a typical cohort of ICD patients achieved very accurate approximation of both mortality and ICD shock risk. Appropriate shock risk and all-cause mortality diverge in large subgroups. Different combinations of multivariate predictors were identified that differentiate the presumed individual ICD benefit. Among the available diagnostic tests, EP stimulation was an excellent predictor of shock risk not relating to all-cause mortality.

Acknowledgements

The research leading to the results has received funding from the European Community's Seventh Framework Programme FP7/2007–2013 under grant agreement No. HEALTH-F2-2009-241526 , EUTrigTreat, and No. HEALTH-F2-2009-602299 EU-CERT-ICD. G.H., T.F. and S.E.L. are principle investigators of the German Center for Cardiovascular Research (DZHK), partner site Göttingen. R.W. is supported as a postdoctoral clinical researcher by the Fund for Scientific Research Flanders (FWO).

References

1. Antiarrhythmics versus Implantable Defibrillators (AVID) Investigators. A comparison of antiarrhythmic-drug therapy with implantable defibrillators in patients resuscitated from near-fatal ventricular arrhythmias. *N Engl J Med* 1997;337:1576–83.
2. Moss AJ, Zareba W, Hall WJ, et al. Prophylactic implantation of a defibrillator in patients with myocardial infarction and reduced ejection fraction. *N Engl J Med* 2002;346:877–83.
3. Bardy GH, Lee KL, Mark DB, et al. Amiodarone or an implantable cardioverter-defibrillator for congestive heart failure. *N Engl J Med* 2005;352:225–37.
4. Koller MT, Schaer B, Wolbers M, et al. Death without prior appropriate implantable cardioverter-defibrillator therapy: a competing risk study. *Circulation* 2008;117:1918–26.
5. Køber L, Thune JJ, Nielsen JC, et al. Defibrillator Implantation in Patients with Nonischemic Systolic Heart Failure. *N Engl J Med* 2016;375:1221–30.
6. McMurray JJ V. The ICD in Heart Failure - Time for a Rethink? *N Engl J Med* 2016;375:1283–4.
7. Schmidt M, Ulrichsen SP, Pedersen L, et al. Thirty-year trends in heart failure hospitalization and mortality rates and the prognostic impact of co-morbidity: a Danish nationwide cohort study. *Eur J Heart Fail* 2016;18:490–9.
8. Dagres N, Hindricks G. Devices for management of sudden cardiac death: Successes, challenges and perspectives. Int J Cardiol 2017;237:34–7.
9. Packer DL, Prutkin JM, Hellkamp AS, et al. Impact of Implantable Cardioverter-Defibrillator, Amiodarone, and Placebo on the Mode of Death in Stable Patients With Heart Failure: Analysis From the Sudden Cardiac Death in Heart Failure Trial. *Circulation* 2009;120:2170–6.
10. Barsheshet A, Moss AJ, Huang DT, et al. Applicability of a risk score for prediction of the long-term (8-year) benefit of the implantable cardioverter-defibrillator. *J Am Coll Cardiol* 2012;59:2075–9.
11. Goldberger JJ, Buxton AE. Personalized medicine vs guideline-based medicine. *JAMA* 2013;309:2559–60.
12. Huikuri H V, Mäkikallio TH, Raatikainen MJP, et al. Prediction of sudden cardiac death: appraisal of the studies and methods assessing the risk of sudden arrhythmic death. *Circulation* 2003;108:110–5.
13. Wellens HJJ, Schwartz PJ, Lindemans FW, et al. Risk stratification for sudden cardiac death: current status and challenges for the future. *Eur Heart J* 2014;35:1642–51.
14. Goldberger JJ. Evidence-based analysis of risk factors for sudden cardiac death. *Heart Rhythm* 2009;6:S2-7.
15. Chow T, Kereiakes DJ, Bartone C, et al. Microvolt T wave alternans identifies patients with ischemic cardiomyopathy who benefit from implantable cardioverter-defibrillator therapy. *J Am Coll Cardiol* 2007;49:50–8.

16. Chow T, Kereiakes DJ, Onufer J, et al. Does Microvolt T wave Alternans Testing Predict Ventricular Tachyarrhythmias in Patients With Ischemic Cardiomyopathy and Prophylactic Defibrillators? *J Am Coll Cardiol* 2008;52:1607–15.

17. Gold MR, Ip JH, Costantini O, et al. Role of Microvolt T wave Alternans in Assessment of Arrhythmia Vulnerability Among Patients With Heart Failure and Systolic Dysfunction: Primary Results From the T wave Alternans Sudden Cardiac Death in Heart Failure Trial Substudy. *Circulation* 2008;118:2022–8.

18. Costantini O, Hohnloser SH, Kirk MM, et al. The ABCD (Alternans Before Cardioverter Defibrillator) Trial: strategies using T wave alternans to improve efficiency of sudden cardiac death prevention. *J Am Coll Cardiol* 2009;53:471–9.

19. Seegers J, Vos MA, Flevari P, et al. Rationale, objectives, and design of the EUTrigTreat clinical study: a prospective observational study for arrhythmia risk stratification and assessment of interrelationships among repolarization markers and genotype. *Europace* 2012;14:416–22.

20. Hummel JD, Strickberger SA, Daoud E, et al. Results and efficiency of programmed ventricular stimulation with four extrastimuli compared with one, two, and three extrastimuli. *Circulation* 1994;90:2827–32.

21. Bloomfield DM, Hohnloser SH, Cohen RJ. Interpretation and classification of microvolt T wave alternans tests. *J Cardiovasc Electrophysiol* 2002;13:502–12.

22. Fine JP, Gray RJ. A Proportional Hazards Model for the Subdistribution of a Competing Risk. J Am Stat Assoc 1999;94:496–509.

23. Volinsky CT, Raftery AE. Bayesian information criterion for censored survival models. *Biometrics* 2000;56:256–62.

24. Mair J, Gerda F, Renate H, et al. Head-to-head comparison of B-type natriuretic peptide (BNP) and NT-proBNP in daily clinical practice. *Int J Cardiol* 2008;124:244–6.

25. Blanche P, Proust-Lima C, Loubère L, et al. Quantifying and comparing dynamic predictive accuracy of joint models for longitudinal marker and time-to-event in presence of censoring and competing risks. *Biometrics* 2015;71:102–13.

26. Steyerberg EW. Clinical prediction models : a practical approach to development, validation, and updating. *Springer*; 2009.

27. Kramer DB, Friedman PA, Kallinen LM, et al. Development and validation of a risk score to predict early mortality in recipients of implantable cardioverter-defibrillators. *Heart Rhythm* 2012;9:42–6.

28. Bilchick KC, Stukenborg GJ, Kamath S, et al. Prediction of Mortality in Clinical Practice for Medicare Patients Undergoing Defibrillator Implantation for Primary Prevention of Sudden Cardiac Death. *J Am Coll Cardiol* 2012;60:1647–55.

29. Levy WC, Lee KL, Hellkamp AS, et al. Maximizing survival benefit with primary prevention

implantable cardioverter-defibrillator therapy in a heart failure population. *Circulation* 2009;120:835–42.

30. Pocock SJ, Ariti CA, McMurray JJ V, et al. Predicting survival in heart failure: a risk score based on 39 372 patients from 30 studies. *Eur Heart J* 2013;34:1404–13.
31. Lee DS, Hardy J, Yee R, et al. Clinical Risk Stratification for Primary Prevention Implantable Cardioverter Defibrillators. *Circ Hear Fail* 2015;8:927–37.
32. Ellenbogen KA, Levine JH, Berger RD, et al. Are implantable cardioverter defibrillator shocks a surrogate for sudden cardiac death in patients with nonischemic cardiomyopathy? *Circulation* 2006;113:776–82.
33. Al-Khatib SM, Stevenson WG, Ackerman MJ, et al. 2017 AHA/ACC/HRS Guideline for Management of Patients With Ventricular Arrhythmias and the Prevention of Sudden Cardiac Death: Executive Summary. *Heart Rhythm* 2017;
34. Priori SG, Blomström-Lundqvist C, Mazzanti A, et al. 2015 ESC Guidelines for the management of patients with ventricular arrhythmias and the prevention of sudden cardiac death. *Eur Heart J* 2015;36:2793–867.
35. Moss AJ, Hall WJ, Cannom DS, et al. Improved survival with an implanted defibrillator in patients with coronary disease at high risk of ventricular arrhythmia. Multicenter Automatic Defibrillator Implantation Trial Investigators. *N Engl J Med* 1996;335:1933–40.
36. Buxton AE, Lee KL, Fisher JD, et al. A randomized study of the prevention of sudden death in patients with coronary artery disease. Multicenter Unsustained Tachycardia Trial Investigators. *N Engl J Med* 1999;341:1882–90.
37. Buxton AE, Lee KL, DiCarlo L, et al. Electrophysiologic testing to identify patients with coronary artery disease who are at risk of sudden death. Multicenter Unsustained Tachycardia Trial Investigators. *N Engl J Med* 2000;342:1937–45.
38. Zaman S, Sivagangabalan G, Narayan A, et al. Outcomes of Early Risk Stratification and Targeted Implantable Cardioverter-Defibrillator Implantation After ST-Elevation Myocardial Infarction Treated With Primary Percutaneous Coronary Intervention. *Circulation* 2009;120:194–200.
39. Zaman S, Narayan A, Thiagalingam A, et al. Long-Term Arrhythmia-Free Survival in Patients With Severe Left Ventricular Dysfunction and No Inducible Ventricular Tachycardia After Myocardial Infarction. *Circulation* 2014;129:848–54.
40. van Barreveld M, Dijkgraaf MGW, Hulleman M, et al. Dutch outcome in implantable cardioverter-defibrillator therapy (DO-IT): registry design and baseline characteristics of a prospective observational cohort study to predict appropriate indication for implantable cardioverter-defibrillator. *Neth Heart J* 2017;25:574–80.
41. Frankel DS, Mountantonakis SE, Zado ES, et al. Noninvasive programmed ventricular stimulation early after ventricular tachycardia ablation to predict risk of late recurrence. *J*

Am Coll Cardiol 2012;59:1529–35.

42. Connolly SJ. Use and misuse of surrogate outcomes in arrhythmia trials. *Circulation* 2006;113:764–6.

43. Moss AJ, Schuger C, Beck CA, et al. Reduction in Inappropriate Therapy and Mortality through ICD Programming. *N Engl J Med* 2012;367:2275–83.

Supplemental material

Supplemental figure 1. CONSORT graph for patient enrolment, patients not considered for final analysis and clinical endpoints

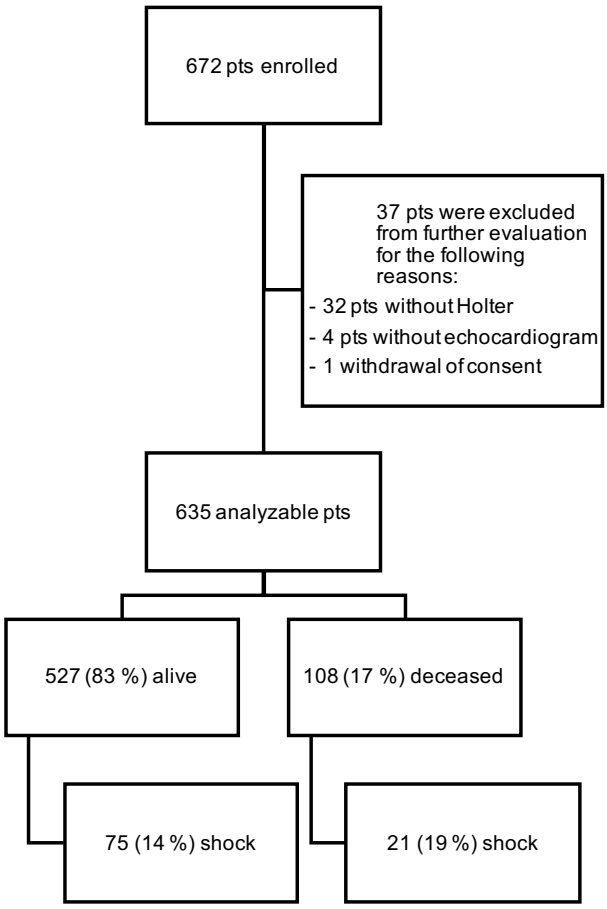

Supplemental table 1. Univariate Cox regression for prediction of mortality (unadjusted and adjusted for base model)

AF = atrial fibrillation, CI = confidence interval, COPD = chronic obstructive pulmonary disease, eGFR = estimated glomerular filtration rate, DC = deceleration capacity, HR = hazard ratio, HRT = heart rate turbulence, hs-CRP = high-sensitivity C-reactive protein, ICD = implantable cardioverter defibrillator, EP = electrophysiological, LVEF = left ventricular ejection fraction, MTWA = microvolt T wave alternans, PVC = premature ventricular contraction, nsVT = non-sustained ventricular tachycardia, NT-pro-BNP = n-terminal-pro-brain natriuretic peptide, NYHA = New York Heart Association functional class, SDNN = standard deviation of RR intervals, RMSSD = mean square root of mean of squared differences between normal-to-normal RR intervals.

		unadjusted			adjusted		
Variable	**n**	**p-value**	**HR**	**CI**	**p-value**	**HR**	**CI**
Age (per 10 years)	635	<0.0001	2.20	1.79-1.2,71			
LVEF (per 5%)	635	<0.0001	0.74	0.68-0.81			
NYHA >2	635	<0.0001	2.65	1.82-3.86			
eGFR (per 30 ml/min)	623	<0.0001	0.45	0.35-0.58			
Male gender	635	0.0749	1.60	0.93-2.76			
Ischemic vs. non-ischemic	634	0.0330	1.73	1.04-2.22			
Secondary prevention	634	0.0211	0.61	0.40-0.94			
History of AF	622	<0.0001	4.02	2.56-6.31			
COPD	635	0.0001	2.78	1.75-4.55			
NTproBNP/BNP (per 100 ng/l)	582	0.0016	1.46	1.23-1.73	0.0155	1.46	1.16-1.84
hs-CRP (per 10 mg/dl)	477	0.0013	1.62	1.29-2.05			
ICD chambers (dual vs. CRT; single vs. others)	635	<0.0001	0.62; 1.99	0.37-1.02; 1.30-3.05	0.0346	0.55; 1.00	0.32-0.91; 0.64-1.56
Intrinsic QRS (per 10 ms)	535	0.0007	1.13	1.05-1.20	0.3650	1.04	0.96-1.12
Intrinsic QT interval (per 10 ms)	535	0.433	1.02	0.98-1.06	0.3960	0.98	0.94-1.03
Intrinsic QTc interval (per 10 ms)	535	0.0362	1.05	1.005-1.10	0.9000	1.00	0.95-1.05
Inducibility on EP testing	616	0.4280	1.21	0.76-1.93	0.9900	1.00	0.61-1.63
MTWA (A rules)	493	0.0125	1.82	1.13-2.93	0.9020	1.03	0.63-1.70
MTWA (B rules)	493	0.0113	1.82	1.14-2.90	0.8240	1.06	0.65-1.72
Holter mean heart rate (per 10 bpm)	634	0.1930	1.14	0.94-1.39	0.0780	1.21	0.98-1.49
Holter PVC/24h (per 100 / 24h)	632	0.6580	1.00	1.00-1.00	0.8640	1.00	1.00-1.00
Holter nsVT/24h	632	0.1640	0.98	0.94-1.02	0.3710	0.98	0.95-1.03
Holter SDNN (per 10 ms)	470	0.0075	0.92	0.86-0.98	0.7900	0.99	0.92-1.06
Holter RMSSD (per ms)	473	0.6980	0.83	0.31-2.22	0.7450	0.85	0.31-2.32
Holter DC (per ms)	474	0.0022	0.96	0.94-0.98	0.2450	0.98	0.95-1.01
Holter HRT category (abnormal)	434	<0.0001	3.95	2.06-7.57	0.036	2.05	1.00-4.17
Holter HRT onset (%)	434	0.0012	1.18	1.08-1.28	0.074	1.12	1.00-1.25
Holter HRT slope (ms/RR interval)	434	0.0001	0.88	0.81-0.95	0.282	0.96	0.90-1.04

Supplemental table 2. Univariate Cox regression for prediction of appropriate shock (unadjusted and adjusted for base model)

AF = atrial fibrillation, CI = confidence interval, COPD = chronic obstructive pulmonary disease, eGFR = estimated glomerular filtration rate, DC = deceleration capacity, HR = hazard ratio, HRT = heart rate turbulence, hs-CRP = high-sensitivity C-reactive protein, ICD = implantable cardioverter defibrillator, EP = electrophysiological, LVEF = left ventricular ejection fraction, MTWA = microvolt T wave alternans, PVC = premature ventricular contraction, nsVT = non-sustained ventricular tachycardia, NT-pro-BNP = n-terminal-pro-brain natriuretic peptide, NYHA = New York Heart Association functional class, SDNN = standard deviation of RR intervals, RMSSD = mean square root of mean of squared differences between normal-to-normal RR intervals

		unadjusted			adjusted		
Variable	**n**	**p-value**	**HR**	**CI**	**p-value**	**HR**	**CI**
Age (per 10 years)	635	0.6970	0.97	0.98-1.01			
LVEF (per 5 %)	635	0.0004	0.87	0.80-0.94			
NYHA >2	635	0.5060	0.86	0.54-1.36			
eGFR (per 30 ml/min)	623	0.0110	0.72	0.55-0.93			
Male gender	635	0.4140	1.24	0.73-2.12			
Secondary prevention	634	0.0051	1.78	1.19-2.66			
Ischemic vs. non-ischemic	633	0.2040	1.30	0.87-1.95			
COPD	635	0.0130	2.29	1.26-4.16			
History of AF	622	0.7640	1.23	0.68-1.82	0.487	1.17	0.75-1.83
NTproBNP/BNP (per 100 ng/l)	582	0.3350	1.20	0.88-1.63	0.895	1.03	0.65-1.64
hs-CRP (per 10 mg/dl)	477	0.6710	0.90	0.53-1.51			
ICD chambers (dual vs. CRT, single vs. other)	635	0.8880	1.12; 1.03	0.71-1.75; 0.60-1.78	0.7590	1.17; 1.17	0.74-1.86; 0.66-2.11
Intrinsic QRS (per 10 ms)	535	0.0306	1.08	1.01-1.15	0.1140	1.06	0.99-1.14
Intrinsic QT (per 10 ms)	535	0.0736	1.04	1.00-1.08	0.1110	1.04	0.99-1.14
Intrinsic QTc (per 10 ms)	535	0.0208	1.06	1.00-1.11	0.0886	1.05	0.99-1.10
EP inducibility	616	0.0009	2.15	1.40-3.30	0.0101	1.84	1.18-2.89
MTWA (A rules)	493	0.0068	1.85	1.18-2.92	0.0592	1.58	0.98-2.56
MTWA (B rules)	493	0.0152	1.73	1.11-2.69	0.1100	1.46	0.92-2.32
Holter mean heart rate (per 10 bpm)	634	0.1990	0.87	0.70-1.08	0.1580	0.85	0.68-1.07
Holter PVCs/24h (per 100 / 24h)	635	0.2880	1.00	1.00-1.00	0.281	1.00	1.00-1.00
Holter nsVT/24h	635	0.9870	1.00	0.99-1.01	0.9120	1.00	0.98-1.01
Holter SDNN (per 10 ms)	470	0.6850	1.01	0.96-1.07	0.4310	1.03	0.96-1.09
Holter RMSSD (per ms)	473	0.9110	1.00	0.99-1.01	0.9240	1.00	0.99-1.01
Holter DC (per ms)	474	0.0896	0.97	0.95-1.00	0.2140	0.98	0.95-1.01
Holter HRT category (TO or TS abnormal, TO/TS abnormal)	434	0.2610	1.52; 1.49	0.87-2.64; 0.78-2.85	0.2580	1.60; 1.60	0.87-2.93; 0.78-3.30
Holter HRT onset (%)	434	0.4470	1.04	0.94-1.16	0.7230	1.02	0.91-1.15
Holter HRT slope (ms/RR interval)	434	0.2640	0.97	0.92-1.02	0.3790	0.97	0.91-1.04

Supplemental figure 2. Risk scores for risk of all-cause mortality and risk of appropriate ICD shock

Mortality score:

0.0547 x age -0.0452 x lvef + 0.548*nyha – 0.0117*egfr + 0.527 x afib + 0.0000376 x ntprobnp

Shock score:

-0.0268 x lvef - 0.00883 x egfr + 0.684 x prevention + 0.619 x inducibility

risk score value for mortality (r=0.56, p<0.001)

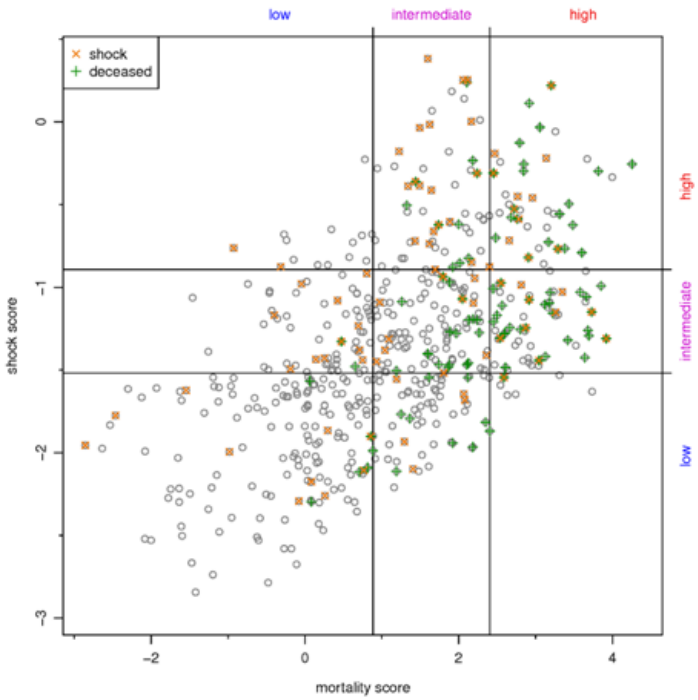

Supplemental figure 3. Correlation scatter plot for calculated risk score values of appropriate shock vs. calculated

Horizontal and vertical lines depict the low, intermediate, and high risk values of each score. The Figure shows that the correlation is at best moderate despite mathematical significance. Thus, all-cause mortality risk does not coincide well with appropriate shock risk. Individually, a low risk of appropriate shock does occur with a high competing risk of death limiting the effectiveness of ICD therapy in a given patient (lower right quadrant). Vice versa, individual patients can be identified with fairly high risks of appropriate shock and concomitant moderate risks of death (upper left quadrant). These individuals are expected to have a higher life-prolonging effect of their ICD therapy, i.e. higher ICD benefit

Chapter 5

Editorial: Do women have less repolarization reserve compared to men?

David J. Sprenkeler, Mathilde Rivaud, Marc A. Vos

Department of Medical Physiology, University Medical Center Utrecht, Utrecht, the Netherlands

Heart Rhythm. 2017 Jan;14(1):96-97.

Do women have less repolarization reserve compared to men?

Female sex is a well-known risk factor for long QT syndrome, as has been demonstrated for congenital[1], drug-[2], and acquired AV block–induced[3] long QT syndrome. In this issue of Heart Rhythm, Chorin et al.[4] question the original explanation that this finding is attributable to longer QTc in women, both at baseline and/or after a proarrhythmic challenge.

Before debating these enlightening findings, we consider it important to explain the existing paradigm for the occurrence of Torsades de Pointes (TdP) arrhythmias (Figure 1). These polymorphic ventricular tachycardias can surface due to an underlying ion channelopathy that renders the heart more susceptible to repolarization-dependent tachyarrhythmias. Ion channelopathies can arise from either inherited or acquired conditions leading to a decrease in the existing repolarization reserve. Sex differences are known to influence this reserve. When challenged with one or more hits, the repolarization reserve may no longer be sufficient and the heart must allow (triggered) beats, possibly leading to TdP arrhythmias. This paradigm is also followed by Chorin et al.[4] : their final hit is the sudden occurrence of AV block leading to severe bradycardia setting the stage for TdP, which occurred more often in women (30% vs 8.5%*).

Chorin et al. should be complimented for their detailed examination of the collected data from 250 persons acutely experiencing AV block. Two questions emerge after careful assessment of the article: 1. how can repolarization reserve be determined; and 2. at what age do patients (specifically women) suffer from these arrhythmias?

Repolarization reserve is currently measured/estimated using the QTc time at baseline or in the period of the final hit before TdP. QT interval is indeed related to arrhythmogenicity but unfortunately lacks sensitivity and specificity. In this study, both

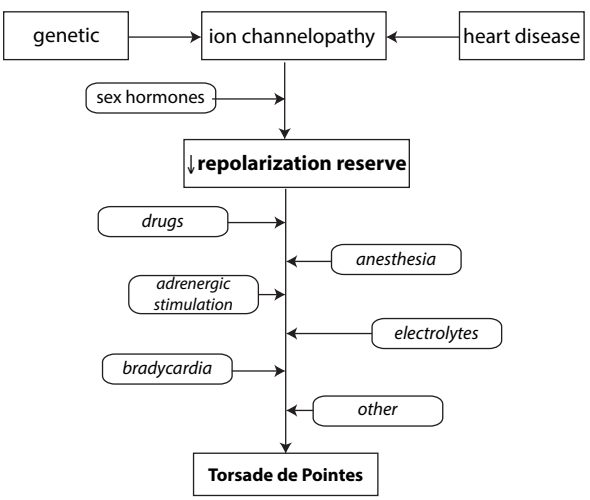

Figure 1. The pathogenesis of TdP
Repolarization reserve describes the redundancy in currents to maintain normal repolarization. A reduction of repolarizing currents, either due to genetic or acquired disease, creates an ion-channelopathy. In combination with sex hormones (estrogen), repolarization reserve is reduced, making the heart vulnerable to arrhythmogenic challenges. Factors such as certain drugs, adrenergic stimulation, anesthesia, electrolyte disturbances or bradycardia, will act as the final 'hit' on repolarization, resulting in TdP.

parameters are determined, and Chorin et al. showed that women have longer QTc at baseline (462 ± 89 ms vs 437 ± 82ms*) but not during bradycardia (the final hit) (553 ± 82 ms vs 602 ± 69 ms).

Therefore, other electrophysiological parameters, such as the QT variability index (QTVI) and short-term variability of repolarization (STV_{QT}), have been suggested to better predict arrhythmia occurrence.

In the past, we manually determined baseline STV_{QT} in 2 groups of long QT patients. Both in inherited long QT (6.4 ± 3.2 ms vs 4.1 ±1.6 ms* with the largest values in the group with the highest risk [9 ± 4 ms])[5] and in drug-induced long QT (8.1 ± 3.7 ms vs 3.6 ± 1.3* ms)[6], we showed that STV_{QT} baseline was increased. In the EUTrigTreat study, we determined STV_{QT} at baseline in patients receiving an Implantable Cardioverter–Defibrillator (ICD) and related the values to sudden cardiac death or (appropriate) ICD shock.[7] STV_{QT} was higher in women compared to men (1.13 ± 0.06 ms vs 1.02 ± 0.03 ms*), indicating, but not proving, that women have less repolarization reserve.

Modulation of cardiac ion channels by sex hormones has been shown to be one of the main causes of sex differences in long QT–induced TdP. Observations in animal models demonstrated that estradiol prolongs the action potential by inhibiting I_{Kr} and stimulating $I_{Ca\text{-}L}$.[8,9] On the other hand, progesterone and testosterone exert an antiarrhythmic effect by increasing the repolarization currents I_{Ks} and I_{K1}. After menopause, both progesterone and estradiol levels decline, but, although progesterone decreases to unmeasurable levels, a small estradiol concentration persists due to extraglandular estrogen production by adipose tissue. This new (im)balance influences repolarization reserve. In patients with long QT syndrome type 2 (in which I_{Kr} is reduced), an increase in arrhythmic events was seen after the onset of menopause.[10] The already diminished repolarization reserve was further reduced by the I_{Kr} blocking effect of estradiol without the protective effects of progesterone, resulting in TdP. In the study by Chorin et al., the age that AV block (and TdP) occurred was 75 years, which implies a high percentage of postmenopausal women with already reduced I_{Kr}. It has also been shown that K_{ATP} channel expression is reduced in aging women, but not in men, thereby participating in reducing repolarization reserve.[11] Bradycardia is the final hit on repolarization, resulting in TdP. However, that is not the “take home message” of this article. It is clear that in cases of acquired AV-block, the QT interval (at bradycardia) should not be the only parameter guiding temporary pacemaker therapy in women. The risk of TdP becomes unacceptably high at much shorter QT intervals in women than (first) anticipated.

* $p < 0.05$

References

1. Migdalovich D, Moss AJ, Lopes CM, et al. Mutation and gender-specific risk in type 2 long QT syndrome: implications for risk stratification for life-threatening cardiac events in patients with long QT syndrome. *Heart Rhythm* 2011;8:1537–43.
2. Makkar RR, Fromm BS, Steinman RT, et al. Female gender as a risk factor for torsades de pointes associated with cardiovascular drugs. *JAMA* 1993;270:2590–7.
3. Kawasaki R, Machado C, Reinoehl J, et al. Increased propensity of women to develop torsades de pointes during complete heart block. J Cardiovasc Electrophysiol 1995;6:1032–8.
4. Chorin E, Hochstadt A, Viskin S, et al. Female gender as independent risk factor of torsades de pointes during acquired atrioventricular block. *Heart Rhythm* 2017;14:90–5.
5. Hinterseer M, Beckmann B-M, Thomsen MB, et al. Relation of increased short-term variability of QT interval to congenital long-QT syndrome. *Am J Cardiol* 2009;103:1244–8.
6. Hinterseer M, Thomsen MB, Beckmann B-M, et al. Beat-to-beat variability of QT intervals is increased in patients with drug-induced long-QT syndrome: a case control pilot study. *Eur Heart J* 2008;29:185–90.
7. Seegers J, Vos MA, Flevari P, et al. Rationale, objectives, and design of the EUTrigTreat clinical study: a prospective observational study for arrhythmia risk stratification and assessment of interrelationships among repolarization markers and genotype. *Europace* 2012;14:416–22.
8. Kurokawa J, Tamagawa M, Harada N, et al. Acute effects of oestrogen on the guinea pig and human IKrchannels and drug-induced prolongation of cardiac repolarization. *J Physiol* 2008;586:2961–73.
9. Odening KE, Choi B-R, Liu GX, et al. Estradiol promotes sudden cardiac death in transgenic long QT type 2 rabbits while progesterone is protective. *Heart Rhythm* 2012;9:823–32.
10. Buber J, Mathew J, Moss AJ, et al. Risk of Recurrent Cardiac Events After Onset of Menopause in Women With Congenital Long-QT Syndrome Types 1 and 2. *Circulation* 2011;123:2784–91.
11. Ranki HJ, Crawford RM, Budas GR, et al. Ageing is associated with a decrease in the number of sarcolemmal ATP-sensitive K^+ channels in a gender-dependent manner. *Mech Ageing Dev* 2002;123:695–705.

Chapter 6

Circadian pattern of short-term variability of the QT interval in primary prevention ICD patients - EU-CERT-ICD methodological pilot study

David J. Sprenkeler[1], Anton E. Tuinenburg[2], Henk J. Ritsema van Eck[3], Marek Malik[4], Markus Zabel[5], Marc A. Vos[1]

[1] Department of Medical Physiology, University Medical Center Utrecht, Utrecht, The Netherlands
[2] Department of Cardiology, University Medical Center Utrecht, Utrecht, The Netherlands
[3] Department of Medical Informatics, Erasmus University Medical Center, Rotterdam, The Netherlands
[4] National Heart & Lung Institute, Imperial College London, London, United Kingdom
[5] Department of Cardiology and Pneumology, University Medical Center Göttingen, Göttingen, Germany

PLOS ONE. 2017 Aug 21;12(8)

Abstract

Objective: Short-term variability of the QT interval (STV_{QT}) is associated with an increased risk of ventricular arrhythmias. We aimed at investigating (a) whether STV_{QT} exhibits a circadian pattern, and (b) whether such pattern differs between patients with high and low arrhythmia risk.

Methods: As part of the ongoing EU-CERT-ICD study, 24h high resolution digital ambulatory 12-lead Holter recordings are collected prior to ICD implantation for primary prophylactic indication. Presently available patients were categorized based on their arrhythmia score (AS), a custom-made weighted score of the number of arrhythmic events on the recording. STV_{QT} was calculated every hour in 30 patients of which 15 and 15 patients had a high and a low AS, respectively.

Results: The overall dynamicity of STV_{QT} showed high intra- and inter-individual variability with different circadian patterns associated with low and high AS. High AS patients showed a prominent peak both at 08:00 and 18:00. At these times, STV_{QT} was significantly higher in the high AS patients compared to the low AS patients (1.22 ± 0.55 ms versus 0.60 ± 0.24 ms at 08:00 and 1.12 ± 0.39 ms versus 0.64 ± 0.29 ms at 18:00, both $p < 0.01$).

Conclusion: In patients with high AS, STV_{QT} peaks in the early morning and late afternoon. This potentially reflects increased arrhythmia risk at these times. Prospective STV_{QT} determination at these times might thus be more sensitive to identify patients at high risk of ventricular arrhythmias.

Introduction

Sudden cardiac death (SCD) due to ventricular arrhythmias remains an important health problem, accounting for approximately 50% of total cardiovascular mortality.[1] Prophylactic implantation of Implantable Cardioverter-Defibrillators (ICD) has shown to reduce mortality in patients with a reduced left ventricular ejection fraction (LVEF).[2,3] LVEF reduction is presently used in international guidelines as a class I indication for ICD implantation in patients with left ventricular dysfunction.[4] However, LVEF lacks sensitivity and specificity of patients stratification, since a large proportion of patients suffering from sudden cardiac arrest have a LVEF above the 35% cut-off.[5] Furthermore, in recent registries of ICD recipients, the incidence of appropriate shock [6,7] was found substantially lower than that reported in the original MADIT II and SCD-HeFT trials,[2,3] possibly explained by improved pharmacological heart failure treatment and ICD-programming algorithms. Consequently, up to two thirds of ICD recipients will never receive an appropriate ICD shock during their lives,[8] indicating that more accurate characterization of a patient at high SCD risk is urgently needed. In the search for better risk assessment, ECG-derived risk parameters are continuously investigated since the ECG is an inexpensive, easy to use, and widely accessible non-invasive tool.

Short-term variability of the QT interval (STV_{QT}) is a relatively new ECG-based parameter that captures repolarization instability in 30 consecutive beats.[9] An increased STV_{QT} was shown in patients with drug-induced and congenital long QT syndrome and in patients with non-ischemic heart failure with a history of ventricular arrhythmias.[10–12] Presently, the predictive value of STV_{QT} is further evaluated in the primary prevention ICD population as part of the *EUropean Comparative Effectiveness Research to assess the use of primary prophylacTic Implantable Cardioverter Defibrillators (EU-CERT-ICD)* study. In contrast to previous studies in which STV_{QT} was measured in 2-minute 12-lead ECG recordings, the EU-CERT-ICD study uses high resolution 24-hour Holter recordings for STV_{QT} analysis. The use of long-term recordings leads to the question of when to take a 30-beat sample during the 24 hours of the recording.

Yet, little is known about the STV_{QT} changes during the day and/or whether the circadian pattern of STV_{QT} is different in patients at low and high SCD risk. If such a difference exists, calculation of STV_{QT} at a certain time of the day might increase the sensitivity and specificity of this parameter in identifying the patients at risk. Therefore, as a methodological pilot study of EU-CERT-ICD, we aimed at investigating (a) whether STV_{QT} exhibits a circadian pattern and (b) whether this pattern differs between high and low risk patients.

Materials & methods

Study design

The EU-CERT-ICD study is a currently enrolling prospective, multicenter, observational study (NCT 02064192) that aims to assess electrocardiographic parameters for prediction of all-cause mortality and appropriate ICD shocks. The study plans to recruit 2500 patients with ischemic and non-ischemic cardiomyopathy fulfilling the international treatment guidelines criteria for primary prophylactic ICD implantation.[13] Patients who are candidate for cardiac resynchronization therapy (CRT) or secondary prophylactic ICD are excluded. The protocol was approved by the institutional review board or ethics committee at each participating hospital and was in compliance with the Declaration of Helsinki. All patients provided written informed consent.

Clinical characteristics including age, sex, race, NYHA class, comorbidities and cardiovascular drug treatment are collected at baseline. Prior to ICD implantation, all patients also undergo a 24-hour 12-lead digital Holter recording using the SEER 12 recorder programmed at 1024 Hz sampling frequency (Getemed, Teltow, Germany). In addition to STV_{QT}, other ECG-derived parameters, including microvolt T wave alternans, heart rate variability, heart rate turbulence, and T wave morphology will be prospectively assessed for the risk stratification purposes. In the current methodological pilot study, STV_{QT} of 30 cardiac cycles was determined at the beginning of every hour during the 24h recording in a subpopulation of already enrolled patients.

Measurement of STV_{QT}

STV_{QT} was determined in lead V2 and was calculated using the method of fiducial segment averaging (FSA).[14] First, each QRS complex was aligned around a trigger point (usually the R peak) by cross correlating each individual complex with the average of the other complexes and then shifted until maximal correlation was achieved. Next, the different fiducial points, i.e. the QRS onset and the end of T wave, were aligned separately by the same technique using a segment of 30 samples around the fiducial point. Correct alignment was checked visually by one of the authors (D.S.) and manually adjusted where necessary. The advantage of our custom-made software is that the program preserves the amount of shifting for each individual beat and thus the QT interval of each beat can be derived from the individual fiducial point estimates.

Using Poincaré plots, the QT interval of each complex was plotted against the former. STV_{QT} was defined (as proposed by Thomson et al.[15]) as the mean orthogonal distance of the points to the line of identity, calculated by the formula

$STV = \sum|D_{n+1} - D_n|/30 \times \sqrt{2}$, where D represents the QT interval. Ventricular and atrial premature complexes together with the following post-extrasystolic beat were excluded from the analysis. In addition to STV_{QT}, both the RR interval and QT interval of the 30 beats were measured automatically.

Endpoints

No definite endpoints, e.g. all-cause mortality or appropriate ICD shocks, are presently known. Nevertheless, previous studies have shown that the presence of non-sustained ventricular tachycardia (nsVT) and/or a high frequency of premature ventricular complexes (PVC) are independent predictors of SCD and/or appropriate ICD shocks.[16,17] Therefore, to differentiate between high and low risk patients, the number of arrhythmic events on the Holter recording was used as a surrogate endpoint. A custom-made arrhythmia score (AS) was designed for this purpose and described in Table 1. Arbitrarily and solely for the purposes of this methodological pilot study, patients were classified based on their AS into three groups: low AS (< 100 points/24h), moderate AS (between 100 and 1000 points/24h) and high AS (>1000 points/24h). Only low AS and high AS patients were included in the present methodological study in order to differentiate clearly between low and high arrhythmia risk.

Statistical analysis

Data are expressed as mean ± standard error of the mean (SEM). Repeated analysis of variance (ANOVA) with Bonferroni correction for multiple comparisons was used for within group analysis. Between-group analysis was performed using a two-tailed Student's *t*-test assuming different variances. Pearson's correlation coefficients were used for correlation analyses. Calculations were performed using SPSS (version 23, IBM). A p-value < 0.05 was considered as statistically significant.

Table 1. Arrhythmia score (AS)

AS is defined as the sum of the points per 24 hours

Arrhythmic event	points
Single PVC	1
Couplet	2
Triplet	3
Bigeminy	4
Non-sustained VT (> 3 complexes)	5

Table 2. Baseline characteristics of study cohort (n = 30)

Mean ± SEM or N (%) * p < 0.05 high AS vs low AS. AS = arrhythmia score; DCM = dilated cardiomyopathy; ICM = ischemic cardiomyopathy; NYHA = New York Heart Association; ACEi = ACE-inhibitor; ARB = angiotensin II receptor blocker; MRA = mineralocorticoid receptor antagonist.

	low AS (n =15)	high AS (n = 15)	Total (n = 30)
Age, years	55.8 ± 3.4	64.3 ± 2.4	60.1 ± 2.2
Sex			
Female	3 (20%)	2 (13.3%)	5 (17%)
Male	12 (80%)	13 (86.7%)	25 (83)
Leading cardiac disease			
DCM	7 (46.7%)	6 (40%)	13 (43%)
ICM	8 (53.3%)	9 (60%)	17 (57%)
LVEF, percentage	26.8 ± 1.7	27.0 ± 1.7	26.9 ± 1.2
NYHA			
I or II	11 (73%)	9 (60%)	20 (67%)
III	4 (27%)	6 (40%)	10 (33%)
Smoking	11 (73.7%)	10 (66.7%)	21 (70%)
Diabetes mellitus	5 (33.3%)	7 (46.7%)	12 (40%)
hypertension	4 (26.7%)	13 (86.7%)*	17 (57%)
Beta-blocker	14 (93.3%)	14 (93.3%)	28 (93%)
ACEi/ARB	15 (100%)	13 (86.7%)	28 (93%)
MRA	12 (80%)	15 (100%)	27 (90%)
statin	12 (80%)	11 (73.3%)	23 (77%)
Class I or III antiarrhythmic drugs	1 (6.7%)	2 (13.3%)	3 (10%)

Results

Out of the EU-CERT-ICD Holter database, AS was assessed for already enrolled patients. Patients with atrial fibrillation, less then 23 hours of noise-free recording or flat T waves in the precordial leads were excluded. A total of 30 patients were selected based on their AS, of which 15 and 15 patients had a high and low AS, respectively.

Baseline criteria

Table 2 shows baseline characteristics of the patients included in the analysis. The mean age was 60 ± 2 years and 80% were men. Patients with high AS appeared to be slightly but not significantly older compared to the low AS patients (p = 0.06). A slight majority of patients had ischemic cardiomyopathy (53%) with a mean left ventricular ejection fraction of 27% ± 1%. Significantly more patients in the high AS group had hypertension. The use of heart failure medications was not different between the two groups.

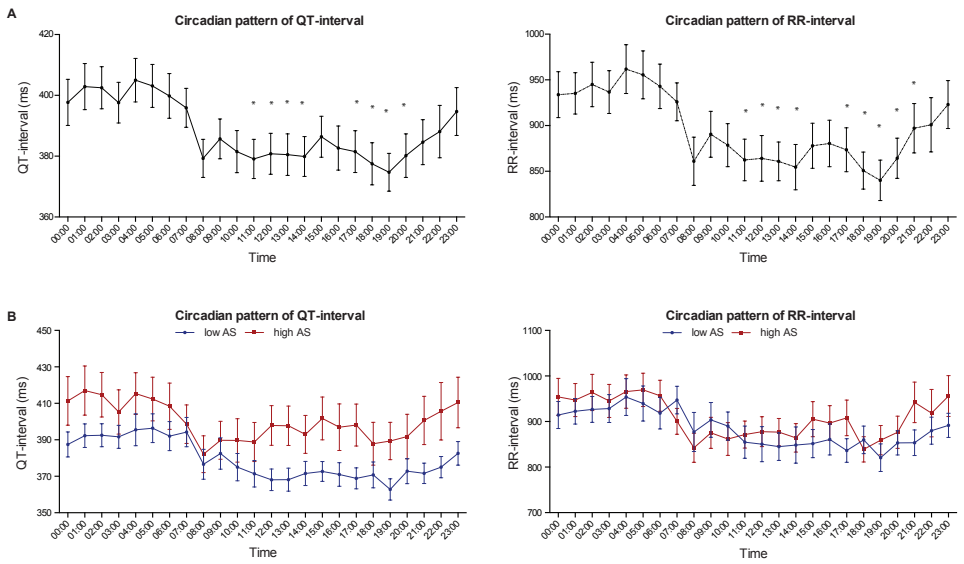

Figure 1. Circadian pattern of RR- and QT interval.

A) mean ± SEM at beginning of every hour of total cohort (n = 30). Significant higher values are seen at night compared to during the day. * = p< 0.05 compared to 0:00. B) Mean ± SEM at beginning of every hour of low AS-group (blue line, n = 15) and high AS group (red line, n = 15). No significant differences are found in the circadian pattern of RR interval or QT interval between low and high AS group.

Circadian pattern of RR and QT

The circadian profile of RR- and QT-intervals is shown in Figure 1. As expected, both show higher values at night with a peak at 04:00, a clear drop in the morning and significantly lower values during the day. No significant differences were found in RR interval between the low AS and high AS group (Figure 1B). The QT interval of the high AS appeared to be slightly but not significantly longer than that of the low AS group during the day.

Circadian pattern of STV_{QT}

No clear circadian pattern of STV_{QT} was found in the total cohort. Nevertheless, two small non-significant peaks are visible at 08:00 and 18:00 (Figure 2). A high intra- and inter-individual variability of STV_{QT} was seen, mainly in the high AS group (Figure 3). A different hour-by-hour behavior of STV_{QT} was seen in the low AS-group and high AS-group (Figure 4). While the low AS patients showed a more-or-less stable STV_{QT} during the day with low variability, high AS patients showed significant STV_{QT} peaks ($p < 0.05$) at 08:00 and 18:00. At these time points, STV_{QT} was significantly higher in high

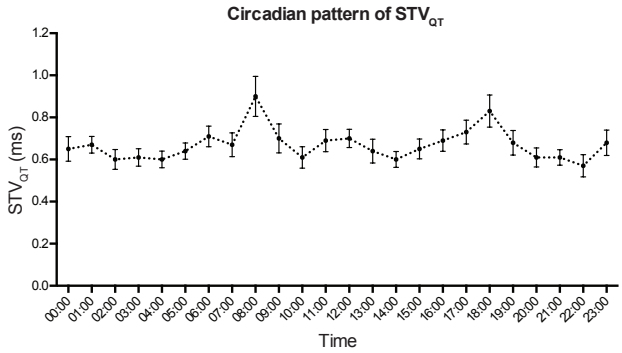

Figure 2. Circadian pattern of STV$_{QT}$. Mean± SEM at beginning of every hour of total cohort (n = 30). No clear circadian pattern is found, however, two non-significant peaks at 08:00 and 18:00 can be discerned.

AS patients compared to low AS patients (1.22 ms ± 0.55 ms versus 0.60 ms ± 0.24 ms at 08:00 and 1.12 ms ± 0.39 ms versus 0.64 ms ± 0.29 ms at 18:00, both $p < 0.01$). At other time points, 07:00, 12:00 and 16:00, STV$_{QT}$ was also increased in the high AS group, but the differences were less expressed. At several time points, especially during the night, STV$_{QT}$ did not differ between the low and high AS groups.

Discussion

The presented results show (a) intra- and interindividual variability of STV$_{QT}$, and (b) distinct STV$_{QT}$ peaks in the early morning and late afternoon that are not seen in the low AS patients. Interestingly, at both of these time points the QT interval was the shortest. In previous animal studies, a positive relation was found between STV and action potential duration (APD) with higher STV at longer APD.[18] This can be explained by the absolute increase in APD variation at longer APD and does not reflect higher repolarization instability. Nevertheless, the opposite was found in the high AS patients in the current study: the highest STV$_{QT}$ was seen when QT interval was the shortest. This implies that an independent pro-arrhythmic component might be partly responsible for this STV$_{QT}$ increase.

In previous clinical studies on STV$_{QT}$, a 2-minute ECG was taken at arbitrary during day-time hours. Nevertheless, as we have shown, the discriminative power of STV$_{QT}$ varies substantially between 8.00 and 17:00. For instance, in the data of this patient subpopulation, samples taken around 14:00 or 15:00 would be less useful for the distinction between the low and high AS groups. It seems plausible to propose that sampling at the time points of 8:00 or 18:00 might increase the predictive capabilities of STV$_{QT}$.

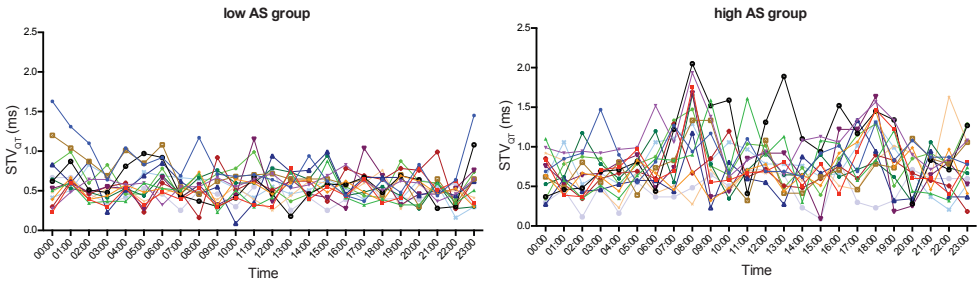

Figure 3. Circadian pattern of STV_{QT} in individual patients.

Individual patients in low AS group (left) and high AS group (right). High inter- and intraindividual variability can be seen, which is more pronounced in the high AS group.

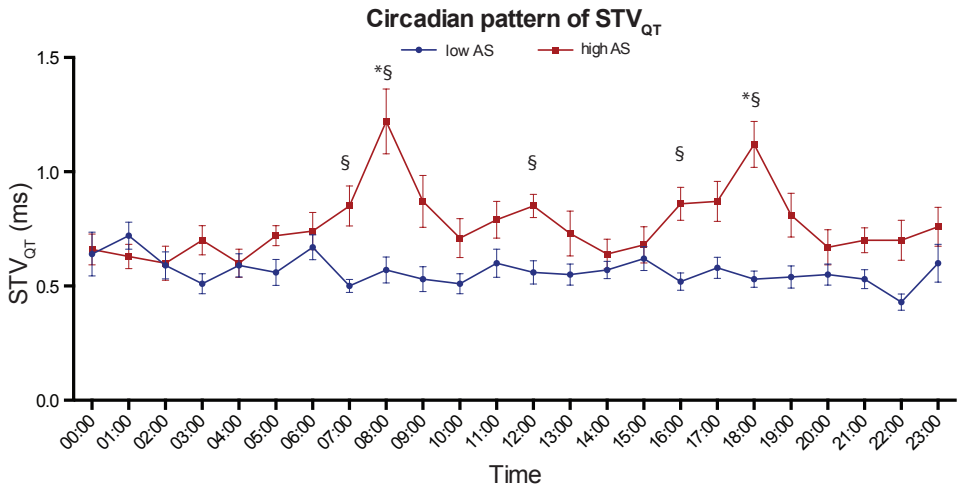

Figure 4. Circadian pattern of STV_{QT} in AS subgroups.

Mean ± SEM at beginning of every hour in low AS (blue line, n = 15) and patients with high AS (red line, n = 15). * p < 0.05 compared to 0:00; § p <0.05 compared to low AS. STV_{QT} peaks at 08:00 and 18:00 in high AS patients, but is stable during the day in low AS patients.

STV_{QT} as a marker of arrhythmic risk

Finding a highly sensitive and specific ECG-derived parameter predictive for sudden cardiac death remains the holy grail in the field of electrocardiology. In particular, a risk stratification technique that identifies arrhythmic rather than overall mortality risk is urgently needed. The most promising ECG-based risk parameters, such as microvolt T wave alternans [19] or QT-variability index (QTVI)[20] are markers of abnormal repolarization and reflect the electrical substrate that predisposes to ventricular arrhythmias. However, none of these parameters have yet been incorporated into

clinical practice. STV_{QT} has the advantage to reflect instability of repolarization on a consecutive basis and can be measured on 30 complexes instead of 256 complexes that are required to calculate QTVI. The method of fiducial segment averaging eliminates the problem of identification of the end of the T wave of every complex separately, therefore diminishes measurement error.[14] STV_{QT} has been investigated in a number of retrospective studies with a wide variety of populations that are at risk of SCD and shows potential for arrhythmic risk prediction. As part of the EU-CERT-ICD study this parameter will be evaluated prospectively in a large cohort of primary prophylactic ICD patients to further establish its role in risk stratification.

Circadian pattern of STV_{QT} resembles circadian profile of sudden cardiac death

Interestingly, the distinct peaks of STV_{QT} in the early morning and late afternoon in the high AS patients resemble the circadian distribution of sudden cardiac death found in large population-based studies.[21,22] These large studies found a peak between 6:00 and noon and a secondary lower peak between 17:00 and 18:00. The same diurnal distribution was found in studies investigating the circadian variation of appropriate ICD shocks.[23,24] The increased incidence of SCD in the morning may be linked to arousal-related increase of sympathetic tone, which might increase myocardial electrical instability and therefore decreases the threshold for ventricular fibrillation. In experimental studies, left stellate ganglion nerve activity (SGNA), which reflects discharge of the sympathetic nervous system, was reported to show similar circadian profile with a high peak in the early morning in dogs with pacing induced heart failure or experimentally induced myocardial infarction.[25–27] SGNA increase was also shown to precede the occurrence of ventricular arrhythmia.[28]

QT variability and the autonomic nervous system

A relation between autonomic tone and higher beat-to-beat QT variability has previously been reported. Yeragani et al investigated the effect of posture and isoproterenol infusion on QT variability and described significantly higher QT variability in standing position and after the infusion of isoproterenol.[29] Recently, a significant correlation was shown between elevated STV_{QT} and parameters of sympathetic predominance in patients with impaired glucose tolerance.[30] A study by Piccirillo et al. found a positive relation between the level of anxiety and a high QTVI.[31] On the other hand, QT variability was significantly reduced after administration of metoprolol or carvedilol compared to placebo in patients with ischemic cardiomyopathy.[32] Also, in a SGNA activity study, the dogs with high sympathetic activity showed significantly higher

QT variability index compared to dogs with low sympathetic activity.[33] Noteworthy, this difference was only seen in the dogs with pacing-induced heart failure. Although all these studies used other QT variability expressions, it seems reasonable to expect the same differences for STV_{QT}.

The increased beat-to-beat repolarization variability during high adrenergic drive might be caused by the autonomic nervous system effects during reduced repolarization reserve. In cellular experiments under baseline conditions, selective I_{Ks} blockade does neither increase repolarization variability nor result in arrhythmias because of compensatory effects of other repolarizing currents[34]. However, when β-adrenergic stimulation is added to I_{Ks} blockade, repolarization variability increases significantly and early and delayed afterdepolarizations start to occur. In our study population, i.e. patients with left ventricular dysfunction, a reduced repolarization reserve is likely, caused by downregulation of repolarizing currents.[35] Sympathetic activity during arousal might thus exhaust the repolarization reserve explaining the STV_{QT} rise. The reasons for the second peak in the late afternoon are more speculative. It might be related to periprandial changes in the autonomic modulation.

Limitations

The present study has important limitations. First, since it is a methodological pilot study, the sample size is small. Second, we used a custom-made score of the number of arrhythmic events on the Holter recording to categorize patients into high and low arrhythmic risk. Whilst this might reasonably correspond to some previous publications, we have no data on actual arrhythmic risk in these patients. A recent study by Seegers et al[16] found a high number of premature ventricular complexes predicting appropriate ICD shocks but not all-cause mortality. Nevertheless, in a substudy of the Prospective Randomized Milrinone Survival Evaluation (PROMISE) trial, high burden of ventricular ectopy on Holter recordings predicted SCD.[17] Finally, no continuous measurement of STV_{QT} during the 24 hours was performed. The current method of FSA is semi-automatically which requires manual identification of fiducial points. Currently, a fully automatic version is being developed and the first results show accurate STV_{QT} measurements in simulated data.[36]

Conclusion

STV_{QT} shows high intra- and interindividual 24-hour variability with peaks in the early morning and late afternoon in high AS patients. Studies on the circadian variation of SCD show a similar circadian profile. Determination of STV_{QT} at these time point might be more sensitive in identifying the patient at risk. It is therefore plausible to propose

that the evaluation of the predictive power of STV_{QT} in the EU-CERT-ICD study should concentrate primarily on these time points.

Acknowledgements

EU-CERT-ICD has received funding from the European Community's Seventh Framework Programme FP7/2007-2013 under grant agreement no. 602299,

References

1. Adabag AS, Luepker R V, Roger VL, et al. Sudden cardiac death: epidemiology and risk factors. *Nat Rev Cardiol* 2010;7:216–25.
2. Moss AJ, Zareba W, Hall WJ, et al. Prophylactic implantation of a defibrillator in patients with myocardial infarction and reduced ejection fraction. *N Engl J Med* 2002;346:877–83.
3. Bardy GH, Lee KL, Mark DB, et al. Amiodarone or an implantable cardioverter-defibrillator for congestive heart failure. *N Engl J Med* 2005;352:225–37.
4. Epstein AE, Dimarco JP, Ellenbogen KA, et al. ACC/AHA/HRS 2008 Guidelines for device-based therapy of cardiac rhythm abnormalities. *Heart Rhythm* 2008;5:e1-62.
5. Stecker EC, Vickers C, Waltz J, et al. Population-based analysis of sudden cardiac death with and without left ventricular systolic dysfunction: two-year findings from the Oregon Sudden Unexpected Death Study. *J Am Coll Cardiol* 2006;47:1161–6.
6. Sabbag A, Suleiman M, Laish-Farkash A, et al. Contemporary rates of appropriate shock therapy in patients who receive implantable device therapy in a real-world setting: From the Israeli ICD Registry. *Heart Rhythm* 2015;12:2426–33.
7. Vandenberk B, Garweg C, Voros G, et al. Changes in Implantation Patterns and Therapy Rates of Implantable Cardioverter Defibrillators over Time in Ischemic and Dilated Cardiomyopathy Patients. *Pacing Clin Electrophysiol* 2016;39:848–57.
8. van Welsenes GH, van Rees JB V, Thijssen J, et al. Primary Prevention Implantable Cardioverter Defibrillator Recipients: The Need for Defibrillator Back-Up After an Event-Free First Battery Service-Life. *J Cardiovasc Electrophysiol* 2011;22:1346–50.
9. Baumert M, Porta A, Vos MA, et al. QT interval variability in body surface ECG: measurement, physiological basis, and clinical value: position statement and consensus guidance endorsed by the European Heart Rhythm Association jointly with the ESC Working Group on Cardiac Cellular Electroph. *Europace* 2016;18:925–44.
10. Hinterseer M, Beckmann B-M, Thomsen MB, et al. Relation of increased short-term variability of QT interval to congenital long-QT syndrome. *Am J Cardiol* 2009;103:1244–8.
11. Hinterseer M, Thomsen MB, Beckmann B-M, et al. Beat-to-beat variability of QT intervals is

increased in patients with drug-induced long-QT syndrome: a case control pilot study. *Eur Heart J* 2008;29:185–90.

12. Hinterseer M, Beckmann B-M, Thomsen MB, et al. Usefulness of short-term variability of QT intervals as a predictor for electrical remodeling and proarrhythmia in patients with nonischemic heart failure. *Am J Cardiol* 2010;106:216–20.
13. McMurray JJV, Adamopoulos S, Anker SD, et al. ESC Guidelines for the diagnosis and treatment of acute and chronic heart failure 2012. *Eur J Heart Fail* 2012;14:803–69.
14. Ritsema van Eck HJ. Fiducial segment averaging to improve cardiac time interval estimates. *J Electrocardiol* 2002;35 Suppl:89–93.
15. Thomsen MB, Verduyn SC, Stengl M, et al. Increased short-term variability of repolarization predicts d-sotalol-induced torsades de pointes in dogs. *Circulation* 2004;110:2453–9.
16. Seegers J, Bergau L, Expósito PM, et al. Prediction of Appropriate Shocks Using 24-Hour Holter Variables and T wave Alternans After First Implantable Cardioverter-Defibrillator Implantation in Patients With Ischemic or Nonischemic Cardiomyopathy. *Am J Cardiol* 2016;118:86–94.
17. Teerlink JR, Jalaluddin M, Anderson S, et al. Ambulatory ventricular arrhythmias in patients with heart failure do not specifically predict an increased risk of sudden death. PROMISE (Prospective Randomized Milrinone Survival Evaluation) Investigators. *Circulation* 101:40–6.
18. Varkevisser R, Wijers SC, van der Heyden MAG, et al. Beat-to-beat variability of repolarization as a new biomarker for proarrhythmia in vivo. *Heart Rhythm* 2012;9:1718–26.
19. Verrier RL, Klingenheben T, Malik M, et al. Microvolt T wave alternans physiological basis, methods of measurement, and clinical utility--consensus guideline by International Society for Holter and Noninvasive Electrocardiology. *J Am Coll Cardiol* 2011;58:1309–24.
20. Berger RD, Kasper EK, Baughman KL, et al. Beat-to-beat QT interval variability: novel evidence for repolarization lability in ischemic and nonischemic dilated cardiomyopathy. *Circulation* 1997;96:1557–65.
21. Muller JE, Ludmer PL, Willich SN, et al. Circadian variation in the frequency of sudden cardiac death. *Circulation* 1987;75:131–8.
22. Willich SN, Levy D, Rocco MB, et al. Circadian variation in the incidence of sudden cardiac death in the Framingham Heart Study population. *Am J Cardiol* 1987;60:801–6.
23. Tofler GH, Gebara OC, Mittleman MA, et al. Morning peak in ventricular tachyarrhythmias detected by time of implantable cardioverter/defibrillator therapy. The CPI Investigators. *Circulation* 1995;92:1203–8.
24. Behrens S, Galecka M, Brüggemann T, et al. Circadian variation of sustained ventricular tachyarrhythmias terminated by appropriate shocks in patients with an implantable cardioverter defibrillator. *Am Heart J* 1995;130:79–84.

25. Ogawa M, Zhou S, Tan AY, et al. Left stellate ganglion and vagal nerve activity and cardiac arrhythmias in ambulatory dogs with pacing-induced congestive heart failure. *J Am Coll Cardiol* 2007;50:335–43.

26. Piccirillo G, Moscucci F, D'Alessandro G, et al. Myocardial repolarization dispersion and autonomic nerve activity in a canine experimental acute myocardial infarction model. *Heart Rhythm* 2014;11:110–8.

27. Han S, Kobayashi K, Joung B, et al. Electroanatomic remodeling of the left stellate ganglion after myocardial infarction. *J Am Coll Cardiol* 2012;59:954–61.

28. Zhou S, Jung B-C, Tan AY, et al. Spontaneous stellate ganglion nerve activity and ventricular arrhythmia in a canine model of sudden death. *Heart Rhythm* 2008;5:131–9.

29. Yeragani VK, Pohl R, Jampala VC, et al. Effect of posture and isoproterenol on beat-to-beat heart rate and QT variability. *Neuropsychobiology* 2000;41:113–23.

30. Orosz A, Baczkó I, Nyiraty S, et al. Increased Short-Term Beat-to-Beat QT Interval Variability in Patients with Impaired Glucose Tolerance. *Front Endocrinol (Lausanne)* 2017;8.

31. Piccirillo G, Cacciafesta M, Lionetti M, et al. Influence of age, the autonomic nervous system and anxiety on QT interval variability. *Clin Sci (Lond)* 2001;101:429–38.

32. Piccirillo G, Quaglione R, Nocco M, et al. Effects of long-term beta-blocker (metoprolol or carvedilol) therapy on QT variability in subjects with chronic heart failure secondary to ischemic cardiomyopathy. *Am J Cardiol* 2002;90:1113–7.

33. Piccirillo G, Magrì D, Ogawa M, et al. Autonomic nervous system activity measured directly and QT interval variability in normal and pacing-induced tachycardia heart failure dogs. *J Am Coll Cardiol* 2009;54:840–50.

34. Johnson DM, Heijman J, Pollard CE, et al. IKs restricts excessive beat-to-beat variability of repolarization during beta-adrenergic receptor stimulation. *J Mol Cell Cardiol* 2010;48:122–30.

35. Nattel S, Maguy A, Le Bouter S, et al. Arrhythmogenic Ion-Channel Remodeling in the Heart: Heart Failure, Myocardial Infarction, and Atrial Fibrillation. *Physiol Rev* 2007;87:425–56.

36. Rijnbeek PR, van den Berg ME, van Herpen G, et al. Validation of automatic measurement of QT interval variability. *PLoS One* 2017;12:e0175087.

Chapter 7

Beat-to-beat variations in activation recovery interval derived from the right ventricular electrogram can monitor arrhythmic risk under anesthetic and awake conditions in the canine chronic atrioventricular block model

Sofieke C. Wijers[1], David J. Sprenkeler[1], Alexandre Bossu[1] , Albert Dunnink[1] , Jet D.M. Beekman[1], Rosanne Varkevisser[1] , Alfonso Aranda Hernández[3], Mathias Meine[2], Marc A. Vos[1]

[1] Department of Medical Physiology, University Medical Center Utrecht, Utrecht, The Netherlands
[2] Department of Cardiology, University Medical Center Utrecht, Utrecht, The Netherlands
[3] Medtronic Bakken Research Center, Maastricht, The Netherlands

Heart Rhythm. 2018 Mar;15(3):442-448.

Abstract

Background: In the chronic atrioventricular block (CAVB) dog model, beat-to-beat variation of repolarization in the left ventricle (LV) quantified as short-term variability of the left monophasic action potential duration (STV_{LVMAPD}) increases abruptly upon challenge with a pro-arrhythmic drug. This increase occurs before the first ectopic beat (EB), specifically in subjects that demonstrate subsequent repetitive Torsades de Pointes arrhythmias (TdP).

Objective: to demonstrate that STV is feasible for monitoring arrhythmic risk through the use of the intracardiac electrogram (EGM) derived from the right ventricular (RV) lead from pacemakers or Implantable Cardioverter-Defibrillators (ICD).

Methods: 1) In 30 anesthetized, inducible (≥3TdP) CAVB dogs, STV of left and right ventricular monophasic action potential duration (STV_{LVMAPD} and STV_{RVMAPD}) were compared. 2) In prospectively enrolled CAVB dogs, STV of the activation recovery interval (ARI) derived from the RV EGM (STV_{RVARI}) was measured before and after a challenge with dofetilide under anesthesia (2a, n=10) and cisapride under awake conditions (2b, n=8).

Results: 1) Both STV_{LVMAPD} and STV_{RVMAPD} increased before the first EB (1.29 ± 0.58 ms to 3.05 ± 1.70 ms and 1.11 ± 0.53 ms to 2.18 ± 1.43 ms, respectively (p=0.001). 2a) STV_{RVARI} increased from 2.82 ± 0.33 ms to 3.77 ± 0.69 ms (p=0.001). 2b) Inducible subjects (4/8) showed an increase in STV_{RVARI} from 2.65 ± 0.55 ms to 3.45 ± 0.33 ms (in the first hour, p=0.02) and 4.20 ± 1.33 ms (before the first EB, p=0.04)

Conclusion: Behavior of STV from the right and the left ventricle is comparable. STV_{RVARI} increases significantly before the occurrence of an arrhythmia, in awake and anesthetized conditions. This can be integrated in devices to monitor arrhythmic risk.

Introduction

Aside from Implantable Cardioverter-Defibrillators (ICDs) to terminate ventricular arrhythmias, additional pharmacological and electrophysiological treatments are still necessary to prevent arrhythmias and avoid (recurrent) ICD shocks. The question arises whether the ICD can also be used to monitor the risk of ventricular arrhythmias and to enable preventive strategies to intervene.

The canine chronic atrioventricular block (CAVB) model, a model made sensitive to Torsades de Pointes arrhythmias (TdP) by inducing bradycardia and subsequent ventricular remodeling, is used to test antiarrhythmic drugs but also to gain a better insight in the (cellular) mechanisms of TdP. Comprehensive studies in the canine CAVB model showed that beat-to-beat variation in repolarization quantified as short-term variability of the left ventricular monophasic action potential duration (STV_{LVMAPD}) is increasing abruptly before the occurrence of the first short coupled ectopic beat (EB), specifically in subjects that demonstrate subsequent multiple EBs and repetitive TdP.[1] Therefore this parameter may be feasible 1) to monitor arrhythmic risk continuously when integrated in devices and 2) to initiate preventive strategies when necessary. For example, pacing at higher rates is applied in patients with long QT syndrome and incorporated in the guidelines for device-based therapy of cardiac rhythm abnormalities.[2–6] In the canine CAVB dog model, temporary accelerated pacing (TAP) is very effective in suppressing TdP, even when started at the moment of the first EB.[7] Therefore STV could be used to guide TAP and prevent chronic pacing at higher rates, which can be detrimental for cardiac function.[8] For this to be feasible in clinical practice, we would like to use the intracardiac electrogram (EGM) derived from the right ventricular (RV) lead to monitor STV, preferably on a 24/7 basis. To investigate if STV of the activation recovery interval (ARI) derived from the RV EGM accurately reflects arrhythmic risk, we performed: 1) A retrospective analysis to evaluate whether STV of the RV MAPD is comparable to the STV of the LV MAPD. 2) A prospective analysis to investigate the value of the STV_{RVARI} derived from the RV EGM in anesthetic (2a) and awake (2b) conditions.

Materials & methods

Animal handling was in accordance with the Dutch law on animal experiments and the 'Directive 2010/63/EU of the European Parliament and of the Council of 22 September 2010 on the protection of animals used for scientific purposes' . The Animal Experiment Committee of the University of Utrecht approved all experiments. For the retrospective study (part 1), we collected recently performed experiments in 30

subjects from our database. For the prospective study (part 2) under anesthetic and awake conditions, 10 purpose-bred mongrel dogs of either sex (body weight 24 ± 3 kg, Marshall, New York) were instrumented and investigated.

Experiments

Anesthesia and creation of AV-block (part 1 and 2a)

Premedication consisted of methadone 0.5 mg/kg, acepromazine 0.5 mg/kg and atropine 0.02 mg/kg i.m. After 30 minutes, complete anesthesia was induced with pentobarbital sodium 25 mg/kg i.v. and maintained by isoflurane 1.5% in O_2 and N_2O, 1:2. MAP catheters (Hugo Sachs Elektronik, March, Germany) were introduced via the femoral vein and artery to measure monophasic action potentials of the free wall of both left and right ventricle (LV MAP and RV MAP, respectively). In the initial experiment, complete atrioventricular (AV) nodal block was created by radiofrequency ablation of the proximal His bundle. The dogs were then let to remodel for at least 2 weeks on idioventricular rhythm (IVR).

Implantation of an ICD (part 2)

In the prospective study, after creation of AV-block a pacemaker or ICD was implanted with one lead in the RV, which was turned off during remodeling.

Inducibility challenge (part 1 and 2a)

During chronic AV-block, inducibility of TdP arrhythmias was tested by infusion of the I_{Kr} (the rapid component of the delayed rectifier potassium current) blocker dofetilide (0.025 mg/kg infused over 5 minutes). TdP was defined as a run of 5 or more short-coupled (occurring before the end of the T wave) ectopic beats, with polymorphic twisting of the QRS axis. The dog was considered inducible, when ≥3 TdP occurred in the first ten minutes after the start of infusion.

Part 1- comparison of electrophysiology in left and right ventricle

For this retrospective analysis, we used the ECG and MAP recordings of 30 subjects (12 male, 18 female) inducible after dofetilide challenge. In 16 subjects, experiments were performed during IVR and in 14 subjects during RV pacing at 60bpm (VVI60). Measurements were done before (baseline) and after administration of dofetilide (before the 1st EB).

Part 2a – the RV EGM for monitoring of arrhythmic risk under anesthetic conditions

Ten CAVB dogs (3 male, 7 female) were included in this prospective analysis. Measurements were done at baseline and before the 1st EB after administration of dofetilide. During the experiments, the subjects were paced from the RV at a rate of 60bpm (VVI60) to stabilize focus and prevent severe bradycardia with concomitant blood pressure drop during anesthesia.

We calculated the correlations between baseline and dofetilide measurements of the RV MAPD and RV ARI and STV_{RVMAPD} and STV_{RVARI}. Subsequently we measured the increase of both RV ARI and STV_{RVARI} after administration of dofetilide, before the 1st EB, to assess the capacity of the RV EGM to monitor arrhythmic risk under anesthetic conditions.

Part 2b– the RV EGM to monitor arrhythmic risk under awake conditions

After a baseline measurement, eight subjects (1 male, 7 female), inducible with dofetilide under anesthesia, received 10-20 mg/kg cisapride (AST farma b.v, Oudewater, The Netherlands) orally in awake conditions. The EGM was recorded until 24 hours after administration of cisapride. In addition, 2-minute 6-lead ECGs were recorded every hour for the first ten hours. The ICD was programmed at ventricular fibrillation (VF) zone > 200 bpm with a VF detection window of 30/40 and a maximum of 3 shocks. During the experiments, all subjects had IVR. In case of an arrhythmia that needed ICD intervention, pacing at higher rates was initiated at VVI80 and gradually increased until VVI100. Additionally, flunarizine 2 mg/kg in 2 minutes was administered intravenously.

Measurements

ECG intervals (RR, QRS, QT and Tpeak-Tend (TpTe)) and MAP signals were recorded with EP Tracer (Cardiotek, Maastricht, The Netherlands) with a sampling frequency of 1 kHz. ECG intervals were calculated from an average of 5 consecutive beats. The MAPs were analyzed in a semi-automatic manner with the AutoMAPD software in which the MAPD was determined using a user-defined template to assess the relevant fiducial points. The LV and RV MAPD were measured from the peak of the MAP until 80% repolarization. The unipolar EGM (sampling frequency of 250 Hz, band pass filter 0.5-50 Hz) was derived from the RV lead between can and tip, resampled to 400 Hz and analyzed offline with custom-made MATLAB software (Medtronic Bakken Research Center, Maastricht, The Netherlands and Mathworks, Natick, USA). This software uses

an overlay plot to discard deviating waveforms and aligns all complexes separately around the ARI onset and offset using the fiducial segment averaging method.[9] The ARI was measured from the minimum dV/dt of the QRS complex to the maximum dV/dt of the T wave. The STV of both MAPD and RV ARI over 31 beats were calculated using the following formula: $STV = \sum|D_{n+1} - D_n|/30 \times \sqrt{2}$ where D represents the determinant of repolarization (in this case the MAPD and ARI, respectively). Inducibility was defined as ≥ 3 TdP and/or one or more non self-limiting TdP that needed to be treated with defibrillation in a set timeframe after administration of the drug. An EB was considered short coupled when the coupling interval was <500 ms.

Statistical analysis

Pooled data are expressed as mean ± standard deviation (SD). All comparisons of electrophysiological data were compared with a paired Student's *t*-test. Correlation coefficients were calculated to measure the association between both baseline and the values prior to the first EB after administration of dofetilide. Pearson's correlation coefficients were calculated for normally distributed variables and Spearman's rank correlation coefficients for non-normally distributed variables. A p-value < 0.05 was considered as statistically significant. SPSS (version 23, IBM) was used for the statistical analysis.

Results

Part 1: Comparison of the electrophysiology of the left and right ventricle

In the 30 inducible CAVB dogs, LV and RV MAPD at baseline were 282 ± 52 ms and 252 ± 38 ms respectively. After administration of dofetilide these values increased to 416 ± 107 ms and 337 ± 83 ms (p<0.001). STV_{LVMAPD} increased from 1.29 ± 0.58 to 3.05 ± 1.70ms and STV_{RVMAPD} from 1.11 ± 0.53 ms to 2.18 ± 1.43 ms (p=0.001). In Figure 1 (panel A), significant correlations between the MAPs (left panel: Pearson's r^2 = 0,79 (p<0.001) and the STVs of the MAPD (right panel: Spearman's r^2 = 0,62 (p <0.01) in the left and right ventricle are shown.

Part 2a: ARI derived from RV EGM compared to RV MAP

In each of the ten included subjects two experiments under anesthesia were performed. Of these 20 experiments, 13 could be used for this analysis. Experiments

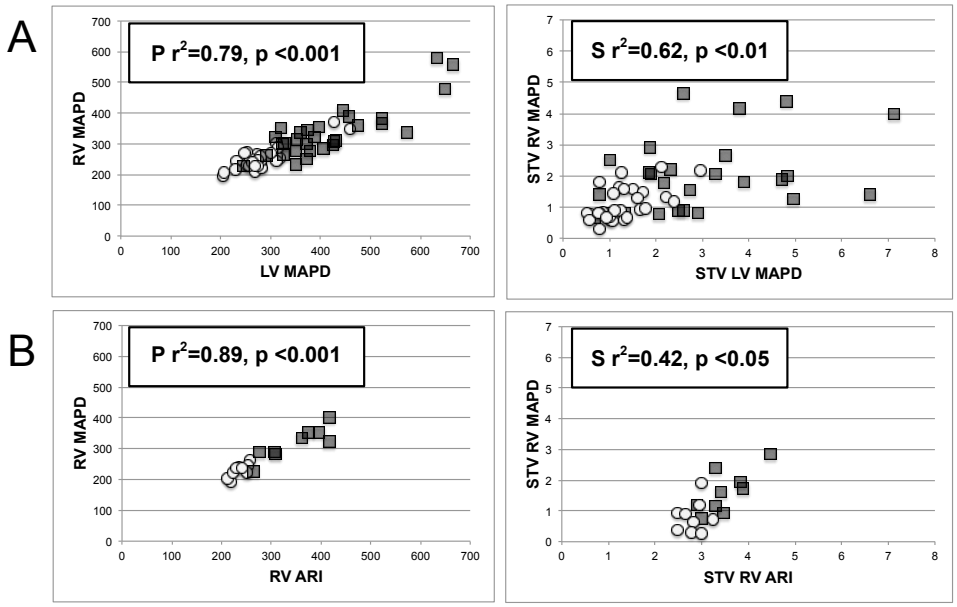

Figure 1. Correlation between left and right ventricular monophasic action potential duration (MAPD) and between MAPD and activation recovery interval (ARI).

A) Correlations between MAP in the left ventricle (LV) and right ventricle (RV). In the left panel, RV MAP is plotted against LV MAP. In the right panel beat-to-beat variations in RV MAP and LV MAP quantified as short-term variability (STV), are plotted. B) Correlations between measurements from the MAP and EGM in the RV. In the left panel RV MAP is plotted against activation recovery interval (ARI) in the RV. In the right panel STV_{RVMAPD} and STV_{RVARI} are plotted. Correlation coefficients are shown in the left upper corner; P r^2 = Pearson's correlation coefficient, S r^2 = Spearman's correlation coefficient. Grey circles = baseline, black squares = before the 1st EB after administration of dofetilide.

were excluded because RV ARI was not recorded (n=6) and RV MAP analysis (n=1) was not possible. For all 13 experiments one baseline and one dofetilide (before the first EB) measurement were done for RV MAPD and RV ARI at the same time.

After administration of dofetilide, RV MAPD increased from 231 ± 22 ms to 309 ± 51 ms (p<0.001) and STV_{RVMAPD} from 0.85 ± 0.49 ms to 1.47 ± 0.65 ms (p=0.01). RV ARI increased from 237 ± 18 ms at baseline to 341 ± 56 ms (p<0.001) and STV_{RVARI} increased from 2.82 ± 0.33 ms to 3.77 ± 0.69 ms (p=0.001).

The correlation coefficient between the RV MAPD and RV ARI was 0.89 (Pearson's r^2,p<0.001) and for STV_{RVMAPD} and STV_{RVARI} 0.42 (Spearman's r^2,p=0.05) (Figure 1, panel B)

Part 2b: Awake

In total 4/8 subjects were inducible with cisapride (10-20 mg/kg). First EB occurred 1.15 ± 0.63 hours after administration of cisapride, the first TdP occurred after

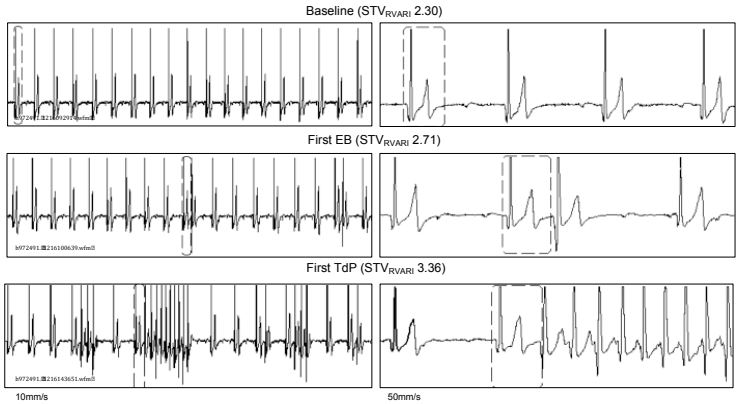

Figure 2. Representative intracardiac electrogram tracings and short-term variability values at different time points.

Representative intracardiac electrogram (EGM) tracings of one subject on baseline and after administration of cisapride before the first ectopic beat (EB) and before the first Torsade de Pointes arrhythmia (TdP). Values of short-term variability (STV) of the right ventricular (RV) activation recovery interval (ARI) of that subject at those time points.

3.57 ± 1.84 hours. Figure 2 shows a representative impression of the EGM tracings with STV_{RVARI} values at baseline (top panel), before the first EB (middle panel) and first TdP (lower panel).

In Table 1, an overview of electrophysiological parameters after administration of cisapride is given. Panel A shows that cisapride caused an increase in repolarization duration (QT) and spatial dispersion (TpTe) in all subjects after one hour of administration of cisapride. Only in the inducible subjects, STV_{RVARI} increased significantly in the first hour after administration of cisapride and before the first EB (Table 1 (panel C), and Figure 3 and 4). The ARI remained similar 213 ± 34 ms and 207 ± 29 ms (p=0.315).

Discussion

Previous studies already showed the capability of the intracardiac EGM to reflect repolarization instability.[10–12] Nevertheless, its application is not further elaborated. In this study, it is shown that 1) measurement of repolarization instability quantified as STV is comparable in the left and right ventricle, and 2) STV_{RVARI} derived from the intracardiac EGM increases upon a pro-arrhythmic challenge in anesthetized and awake conditions. Since the RV EGM is a stable and continuous available signal, it is a particular suitable tool to use for monitoring arrhythmic risk. This gives us the opportunity to act upon a detected increased susceptibility with appropriate antiarrhythmic therapy, for example TAP.

Table 1. Electrophysiological measurements after administration of cisapride in awake conditions.
Mean ± SD. In Table A) all 8 subjects are included. In Table B) only the 4 non-inducible subjects are included and in Table C) the 4 inducible subjects. Measurements were done at baseline and after the first hour in all subjects and also before the first ectopic beat and first TdP in de inducible subjects. $^{\dagger}p \leq 0.05$. versus baseline. NI = non-inducible; I = inducible; ARI = activation recovery interval; EB = ectopic beat; RV = right ventricle; STV = short –term variability; TdP = Torsade de Pointes arrhythmia; Tpe = T peak – T end.

A) total	Baseline	First hour
RR (ms)	1543 ± 345	1523 ± 354
QRS (ms)	105 ± 22	111 ± 18
QT (ms)	333 ± 32	362 ± 37†
TpTe (ms)	69 ± 22	83 ± 27†
RV ARI (ms)	211 ± 26	208 ± 39
STV_{RVARI} (ms)	2.63 ± 0.41	2.98 ± 0.56

B) NI	Baseline	First hour
RR (ms)	1487 ± 260	1353 ± 286
QRS (ms)	112 ± 23	116 ± 15
QT (ms)	324 ± 7	351 ± 15
TpTe (ms)	62 ± 9	70 ± 13
RV ARI (ms)	208 ± 20	208 ± 53
STV_{RVARI} (ms)	2.61 ± 0.30	2.50 ± 0.21

C) I	Baseline	First hour	First EB	First TdP
RR (ms)	1599 ± 449	1694 ± 365	-	-
QRS (ms)	98 ± 22	105 ± 21	-	-
QT (ms)	343 ± 46	373 ± 52†	-	-
TpTe (ms)	77 ± 29	97 ± 33†	-	-
RV ARI (ms)	213 ± 34	207 ± 29	204 ± 34	219 ± 82
STV_{RVARI} (ms)	2.65 ± 0.55	3.45 ± 0.33†	4.20 ± 1.33†	5.10 ± 2.46

Electrophysiology in the left and right ventricle: relevance of location

Our first step to translate the use of STV_{RVARI} for monitoring arrhythmic risk to clinical practice was to show that beat-to-beat variations in repolarization are comparable between the LV and RV. In the retrospective analysis of the 30 subjects that were inducible after a dofetilide challenge, we showed that not only STV_{LVMAPD} but also STV_{RVMAPD} increases before the occurrence of TdP. Although the increase in the RV is less pronounced, it is significant. This does not mean that the electrophysiological adaptations in the left and right ventricle are similar; they're only comparable. In the CAVB dog, it is known that the RV MAPD is shorter than the LV MAPD, which causes the interventricular difference (Δ MAPD). This can be explained by a difference in distribution

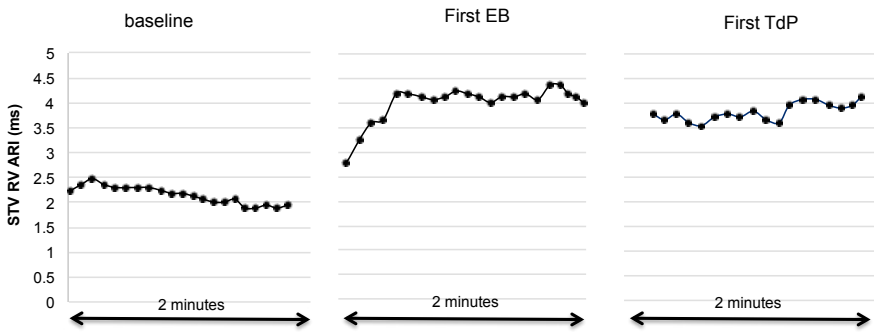

Figure 3. Short-term variability of the right ventricle activation recovery interval in the 4 inducible subjects.

Short-term variability (STV) of the right ventricle (RV) activation recovery interval (ARI) on different time points in an inducible subject. Consecutive STV_{RVARI} values over 2 minutes are plotted on before (baseline) and after cisapride (before the first (short-coupled) ectopic beat (First EB) and before the first Torsade de Pointes arrhythmia (First TdP).

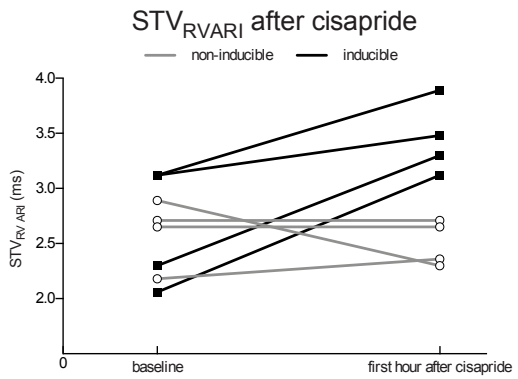

Figure 4. STV_{RVARI} in inducible and non-inducible dogs at baseline and in the first hour after oral cisapride.

STV_{RVARI} increased significantly in the inducible subjects (black lines), but did not change in the non-inducible subjects (gray lines).

of repolarizing ion channels; in the RV there is more I_{Ks} and I_{to}. Nevertheless, they both seem capable to detect increased arrhythmic risk. Although all dogs remodeled at IVR, some of them were paced during the experiments at VVI60. This was done 1) to be able to completely control ventricular focus and 2) prevent severe bradycardia with concomitant blood pressure drop upon induction of anesthesia. Dunnink et al. showed that, although baseline repolarization measures were lower in the subjects paced at VVI60 during the experiments, a similar increase in electrophysiological values and similar TdP inducibility was seen (thesis A. Dunnink, unpublished).

Monitoring of arrhythmic risk using the RV EGM

For calculation of STV, different measures of repolarization can be used. In the canine CAVB model, MAPD has been used as measure of ventricular repolarization. Nevertheless, this determinant of repolarization is not suitable for clinical practice, because of the invasive nature of this measurement and the difficulty to acquire signals of sufficient quality in humans. An attractive alternative is the intracardiac EGM quantified by the ARI. This measurement can be done easily in patients with a pacemaker and/or ICD via the RV lead. Compared to the MAPD, the EGM has the advantage to acquire recordings from the same location (the lead is fixed in the myocardium) and continuously (24/7). Since no transvenous catheter placement is needed, recordings during awake conditions can be easily performed.

Oosterhoff et al. showed that measurements of the MAPD and ARI in the LV are comparable in the canine CAVB model.[13] For better clinical applicability, we used the EGM of the RV and also found a positive correlation between the STV_{RVARI} and STV_{RVMAPD} (Figure 1B, right panel).

That the correlation is not very strong can be explained by the fact that the unipolar EGM reflects a larger region in the heart than the MAPD, which is a bipolar measurement representing only the cells around the MAP catheter tip. Several studies compared the unipolar derived ARI with the MAPD, and suggested that the highest correlation is achieved when Q onset of the ARI is measured as minimum dV/dt and the end of the T wave is measured at the maximum dV/dt.[14,15] With the latter, it is tried to exclude remote repolarization, but still the unipolar EGM is influenced by more distant events in the myocardium.[16] This does not automatically mean that the potential to detect repolarization instability is less, as represented by the significant increase in STV_{RVARI} before the 1st EB upon a challenge with dofetilide (2.82 ± 0.33 ms tot 3.77 ± 0.69 ms, p=0.001). Furthermore, differences in absolute value of STV can be explained by difference in method of analyzing and sampling frequency between the MAP recording (1000 Hz) and the EGM recording (250 Hz, resampled to 400 Hz).

Susceptibility to TdP in awake conditions

We also challenged the subjects under awake conditions to determine the potential of STV_{RVARI} for monitoring electrical instability, since anesthesia has major effect on repolarization and on the sensitivity to TdP.[17] Dunnink et al. serially investigated the effect of anesthesia in different regiments in the CAVB dog model. Under awake conditions, inducibility with dofetilide was absent (0/10), while 7/10 dogs showed reproducible TdP under anesthetic conditions. Furthermore, they showed a significant difference in QT duration between the anesthetized and awake experiments

(281 ± 31 ms and 390 ± 71 ms, p<0.05). The increase of QT duration after administration of dofetilide was only significant under anesthetic conditions (+48 ± 52 ms, ns and +190 ± 71 ms, p<0.05).[17]

We made use of the gastroprokinetic drug cisapride, a selective sertonine 5-HT_4 receptor agonist that also acts indirectly as a parasympathomimetic. It was developed by Janssen Pharmaceutica in the 1980's and withdrawn in most countries in 2000, because of QT prolonging side effects and ventricular arrhythmias. We chose to use cisapride because it has shown to be a potent I_{Kr} blocker.[18]

The previous studies investigating cisapride in the canine CAVB model tell us that 1) remodeling is a prerequisite for susceptibility,[19] 2) absence of anesthesia reduces total incidence of TdP (Winckels et al. 2007, not published), 3) different routes of administration cause different timing of TdP corresponding with the maximum plasma concentration,[20,21] and 4) there is a difference in susceptibility between species. In Supplemental table 1 you can find a schematic overview of these studies.

Electrophysiological changes preceding awake induced TdP

In our study, a significant increase in QT in all subjects is seen after administration of cisapride. Only in the 4 inducible subjects this is accompanied by a significant increase in STV_{RVARI}, reflecting increased instability of repolarization. This significant increase is seen in the first hour and before the occurrence of the first EB, minutes to hours before occurrence of the first TdP. Because in awake conditions more compensation mechanisms are still in place to strengthen repolarization reserve, this situation (an increase in STV) can occur when instability of repolarization is present minutes to hours before the actual occurrence of TdP. This gives a large window of opportunity to interfere.

24/7 monitoring of arrhythmic risk

To be able to monitor repolarization instability continuously automated analysis of the ARI is necessary. We therefore created a software algorithm especially for this purpose in cooperation with Medtronic using MATLAB. To exclude artifacts and deviating waveforms (such as ectopic activity) an overlay plot was applied which was also used to align the QRS onset and end of the T wave separately with the fiducial segment averaging method.[9] This method provides an accurate measurement of beat-to-beat changes since determination of the fiducial point only has to be performed once for all waveforms. This prevents measurement error from beat to beat, which is especially relevant in measuring beat-to-beat changes in repolarization intervals since the end of the T wave is often difficult to determine.

Clinical implications and future directions

Several studies have shown that the RV EGM can be used to predict risk of ventricular arrhythmias in patients.[11,12,22] Also Oosterhoff et al. showed that a high STV 'QT' derived from the intracardiac bipolar EGM and corrected for heart rate (STV ratio) can identify patients at risk of ventricular arrhythmias.[10] We now show that in this experimental set-up, STV increases before the occurrence of an arrhythmia and can be monitored by the EGM derived from the RV lead of a pacemaker and/or ICD, both in anesthetized as in awake conditions. STV_{RVARI} could be used to monitor arrhythmic risk and initiate preventive strategies such as TAP. The next step for translation into clinical practice should be fully automated analysis of STV from (pre-arrhythmia) intracardiac EGMs.

Limitations

The canine CAVB model is a model made sensitive for TdP; results therefore cannot be directly extrapolated to other types of arrhythmias.

Using the unipolar EGM, interference of P waves could not be prevented. This is particular the case in the canine CAVB model and is not to be expected in humans (without AV-block).

The sampling frequency of 250 Hz (resampled at 400 Hz) is relatively low, which could reduce the accuracy of the STV_{RVARI} analysis. Nevertheless, while this would reduce the sensitivity, it will not influence the specificity of the measurement, thus a high STV_{RVARI} still predicts for the occurrence of TdP arrhythmias.

Conclusion

In the canine CAVB model, behavior of STV derived from the RV is comparable to the LV. STV_{RVARI} increases significantly when instability of repolarization becomes present, before the occurrence of TdP, in awake and anesthetized conditions. Continuous measurement of STV_{RVARI} could be integrated in devices to monitor arrhythmic (in) stability continuously and guide antiarrhythmic therapies.

Acknowledgements

The authors would like to thank the Julius Center for the statistical support and Medtronic for providing the defibrillators and leads and the development of the analysis software. This research was performed within the framework of CTMM, the Center for Translational Molecular Medicine (www.ctmm.nl), project Congestive Heart Failure and

Arrhythmogenesis (COHFAR). All authors have read the journal's authorship agreement and policy on disclosure of potential conflicts of interest. No potential conflicts of interests were reported.

References

1. Varkevisser R, Wijers SC, van der Heyden MAG, et al. Beat-to-beat variability of repolarization as a new biomarker for proarrhythmia in vivo. *Heart Rhythm* 2012;9:1718–26.
2. Dorostkar PC, Eldar M, Belhassen B, et al. Long-Term Follow-Up of Patients With Long-QT Syndrome Treated With -Blockers and Continuous Pacing. *Circulation* 1999;100:2431–6.
3. Eldar M, Griffin JC, Abbott JA, et al. Permanent cardiac pacing in patients with the long QT syndrome. *J Am Coll Cardiol* 1987;10:600–7.
4. Eldar M, Griffin JC, Van Hare GF, et al. Combined use of beta-adrenergic blocking agents and long-term cardiac pacing for patients with the long QT syndrome. *J Am Coll Cardiol* 1992;20:830–7.
5. Moss AJ, Liu JE, Gottlieb S, et al. Efficacy of permanent pacing in the management of high-risk patients with long QT syndrome. *Circulation* 1991;84:1524–9.
6. Brignole M, Auricchio A, Baron-Esquivias G, et al. 2013 ESC Guidelines on cardiac pacing and cardiac resynchronization therapy. *Eur Heart J* 2013;34:2281–329.
7. Wijers SC, Bossu A, Dunnink A, et al. Electrophysiological measurements that can explain and guide temporary accelerated pacing to avert (re)occurrence of Torsades de pointes arrhythmias in the canine chronic atrioventricular block model. *Heart Rhythm* 2017;14:749–56.
8. Thambo J-B, Bordachar P, Garrigue S, et al. Detrimental Ventricular Remodeling in Patients With Congenital Complete Heart Block and Chronic Right Ventricular Apical Pacing. *Circulation* 2004;110:3766–72.
9. Ritsema van Eck HJ. Fiducial segment averaging to improve cardiac time interval estimates. *J Electrocardiol* 2002;35 Suppl:89–93.
10. Oosterhoff P, Tereshchenko LG, van der Heyden MAG, et al. Short-term variability of repolarization predicts ventricular tachycardia and sudden cardiac death in patients with structural heart disease: A comparison with QT variability index. *Heart Rhythm* 2011;8:1584–90.
11. Tereshchenko LG, Fetics BJ, Domitrovich PP, et al. Prediction of ventricular tachyarrhythmias by intracardiac repolarization variability analysis. *Circ Arrhythm Electrophysiol* 2009;2:276–84.
12. Paz O, Zhou X, Gillberg J, et al. Detection of T wave alternans using an implantable

cardioverter-defibrillator. *Heart Rhythm* 2006;3:791–7.

13. Oosterhoff P, Thomsen MB, Maas JN, et al. High-rate pacing reduces variability of repolarization and prevents repolarization-dependent arrhythmias in dogs with chronic AV block. *J Cardiovasc Electrophysiol* 2010;21:1384–91.
14. Coronel R, de Bakker JMT, Wilms-Schopman FJG, et al. Monophasic action potentials and activation recovery intervals as measures of ventricular action potential duration: experimental evidence to resolve some controversies. *Heart Rhythm* 2006;3:1043–50.
15. Haws CW, Lux RL. Correlation between *in vivo* transmembrane action potential durations and activation recovery intervals from electrograms. Effects of interventions that alter repolarization time. *Circulation* 1990;81:281–8.
16. Steinhaus BM. Estimating cardiac transmembrane activation and recovery times from unipolar and bipolar extracellular electrograms: a simulation study. *Circ Res* 1989;64:449–62.
17. Dunnink A, Sharif S, Oosterhoff P, et al. Anesthesia and Arrhythmogenesis in the Chronic Atrioventricular Block Dog Model. *J Cardiovasc Pharmacol* 2010;55:601–8.
18. Drolet B, Khalifa M, Daleau P, et al. Block of the Rapid Component of the Delayed Rectifier Potassium Current by the Prokinetic Agent Cisapride Underlies Drug-Related Lengthening of the QT Interval.
19. Sugiyama A, Hashimoto K. Effects of gastrointestinal prokinetic agents, TKS159 and cisapride, on the in situ canine heart assessed by cardiohemodynamic and electrophysiological monitoring. *Toxicol Appl Pharmacol* 1998;152:261–9.
20. Michiels M, Monbaliu J, Hendriks R, et al. Pharmacokinetics and tissue distribution of the new gastrokinetic agent cisapride in rat, rabbit and dog. *Arzneimittelforschung* 1987;37:1159–67.
21. Sugiyam A, Ishida Y, Satoh Y, et al. Electrophysiological, anatomical and histological remodeling of the heart to AV block enhances susceptibility to arrhythmogenic effects of QT-prolonging drugs. *Jpn J Pharmacol* 2002;88:341–50.
22. Sandhu RK, Costantini O, Cummings JE, et al. Intracardiac alternans compared to surface T wave alternans as a predictor of ventricular arrhythmias in humans. *Heart Rhythm* 2008;5:1003–8.

Supplemental material

Supplemental table 1. Cisapride administered in the CAVB dog model under various conditions.

This Table shows electrophysiological effects (heart rate (HR) and QT interval) and inducibility of Torsades the Pointes arrhythmias (TdP, inducible subjects/total subjects) in studied in different species, awake and anesthetized and by different routes of administration (route) at baseline (bl) and after cisapride (cis). C max = maximum plasma concentration of cisapride; I = Isoflorane; H = Halothane; T = thiopental. # A dose of 1.25mg/kg resulted in a Cmax of 1.0 µ/ml in Beagle dogs, Michiels 1987. # # A dose of 10mg oral resulted in a C max of 4.6 microgram/ml in Beagle dogs, Michiels 1987. * = $p<0.05$.

	Species	anesthesia	bradycardia	remodeling	route	Dose	C_{max} (µ/ml)	HR (bl)	HR (cis)	QTc (bl)	QTc (cis)	TdP
Winckels 2007	Mongrel	+ (T+I)	+	+	i.v	1	0.69	63±1	58 ± 3*	470 ± 8	520 ± 14*	5/6
Sugiyama 1998	Beagle	+ (T+H)	-	-	i.v	0.01, 0.1 & 1.0	2.5	128 ± 7	95*	360 ± 11	445*	0/6
Sugiyama 2002	Beagle	-	+	+	Oral	1	≈ 1.0#	33 ± 2	35	208 ± 5	208	1/6
Sugiyama 2002	Beagle	-	+	+	Oral	10	≈ 4.6# #	30 ± 1	35*	224 ± 7	275*	6/6
Current study	Mongrel	-	+	+	Oral	10-20	≈ 4.6# #	39 ± 7	39±7	271 ± 27	296 ± 29*	4/8

Chapter 8

Evaluation of a fully automatic measurement of short-term variability of repolarization on intracardiac electrograms in the chronic atrioventricular block dog

David J. Sprenkeler[1], Alfonso Aranda Hernandez[2], Agnieszka Smoczynska[1], Jet D.M. Beekman[1], Alexandre Bossu[1], Albert Dunnink[1], Sofieke C. Wijers[1], Berthold Stegemann[2], Marc .A. Vos[1]

[1] Department of Medical Physiology, University Medical Center Utrecht, Utrecht, The Netherlands

[2] Medtronic Bakken Research Center, Maastricht, The Netherlands

In preparation

Abstract

Background: Short-term variability of repolarization (STV) of the monophasic action potential duration (MAPD) or activation recovery interval (ARI) on the intracardiac electrogram (EGM) increases abruptly prior to the occurrence of ventricular arrhythmias in the chronic AV-block (CAVB) dog model. Therefore, this parameter might be suitable for continuous monitoring of imminent arrhythmias using the EGM stored on an implanted device. However, 24/7 monitoring would require automatic STV_{ARI} measurement by the device.

Objective: To evaluate a newly developed automatic measurement of STV_{ARI} for prediction of dofetilide-induced Torsades de Pointes (TdP) arrhythmias in the CAVB dog.

Methods: Two retrospective analyses were done on data from recently performed dog experiments. 1.) In 7 anesthetised CAVB dogs, the new automatic STV_{ARI} method was compared with the gold standard STV_{MAPD} at baseline and after dofetilide administration (0.025 mg/kg in 5 minutes). 2.) The predictive value of the automatic method was compared to currently used STV_{ARI} methods, i.e. slope method and fiducial segment averaging (FSA) method, in 11 inducible (≥3 TdP arrhythmias) and 10 non-inducible CAVB-dogs.

Results: 1.) The automatic measurement of STV_{ARI} is strongly correlated with STV_{MAPD} ($r^2 = 0.97$; $p<0.001$). Bland-Altman analysis showed a small bias of 0.4 ms with limits of agreement between -0.4 ms and 1.22 ms. 2.) STV_{ARI} of all three methods was significantly different between inducible and non-inducible dogs after dofetilide. The automatic method showed the highest predictive performance with an area under the ROC-curve of 0.92, compared to 0.85 and 0.87 of the slope and FSA method, respectively. With a threshold of STV set at 1.23 ms, STV_{ARI} measured with the automatic method had a sensitivity of 0.91 and specificity of 0.90 in differentiating inducible from non-inducible subjects.

Conclusion: We developed a fully-automatic method for measurement of STV_{ARI} on the intracardiac EGM that can accurately predict the occurrence of ventricular arrhythmias in the CAVB dog. Future integration of this method into implantable devices could provide the opportunity for 24/7 monitoring of arrhythmic risk.

Introduction

Sudden cardiac arrest due to ventricular tachyarrhythmias, such as ventricular tachycardia (VT) or ventricular fibrillation (VF), is an important cause of death in patients with structural heart disease, accounting for approximately 50% of all cardiovascular deaths.[1] Despite the widespread availability of Automatic External Defibrillators (AEDs), the prognosis after an out-of-hospital cardiac arrest remains poor, with an estimated survival rate around 10%.[2] Therefore, focus has shifted towards preventive strategies in patients at high risk of sudden cardiac death (SCD).

Multiple randomized controlled trials have shown a survival benefit of the Implantable Cardioverter-Defibrillator (ICD) in the prevention of SCD in patients with ischemic or non-ischemic cardiomyopathy and a reduced left ventricular ejection fraction (LVEF) below 35%.[3,4] Since the publication of these landmark trials, both European and American guidelines recommend ICD implantation as a class I indication for these patients.[1,5] Nevertheless, while the ICD is highly effective in the prevention of SCD by termination of sustained ventricular tachyarrhythmias, the device does not prevent the arrhythmia itself from occurring. Despite being potentially life-saving, ICD discharges have also shown to cause severe psychological distress, depression and anxiety and can reduce the quality of life in ICD recipients.[6,7] Moreover, recurrent ICD shocks increase the number of hospital admissions and reduce the lifespan of the generator. Therefore, adjunctive therapy such as radiofrequency ablation of the arrhythmogenic substrate or administration of antiarrhythmic drugs is often necessary to reduce the shock burden.[8,9] However, both these treatment modalities expose the patient to potential adverse effects. In an ideal situation, the implanted device would not only terminate an arrhythmia that is already occurring, but can also monitor if an arrhythmia is imminent and initiate preventive therapy (e.g. temporarily altering pacing rate) before the arrhythmia starts. However, the question remains how the device could predict if an arrhythmia is upcoming.

The chronic complete AV-block (CAVB) dog model is an arrhythmogenic animal model that is often used to evaluate new antiarrhythmic agents or to study the mechanisms of ventricular tachyarrhythmias, mainly Torsades de Pointes (TdP) arrhythmias, in the remodeled heart. In this model, it has been shown that beat-to-beat variation of the monophasic action potential duration (MAPD), quantified as short-term variability (STV), increases abruptly a couple of minutes prior to the occurrence of TdP, after these animals are challenged with a pro-arrhythmic drug.[10] Interestingly, the increase in STV was not seen in dogs that did not develop TdP after the same pro-arrhythmic challenge. While STV seems a promising parameter in predicting upcoming arrhythmic events, the use of monophasic action potential (MAP) catheters is not feasible for 24/7 monitoring in a clinical setting. Recently, it has been shown that STV

of the activation recovery interval (STV_{ARI}) of the electrogram (EGM) derived from the right ventricular ICD lead can be used as surrogate for the MAPD and accurately reflects arrhythmic risk in the CAVB dog under both anesthetized and awake conditions.[11] This would imply that the electrograms stored on the device can be used for the prediction of upcoming arrhythmic events. In the aforementioned study, however, the measurement of STV_{ARI} was done offline by use of semi-automatic custom-made software. In order to integrate continuous STV_{ARI} calculation in an implantable device, development of an automatic measurement, that determines STV_{ARI} precisely and consistently without manual correction, is required.

In the present study, we describe a new automatic method for measuring STV_{ARI} and compare this method with the current methodologies used to measure STV. In addition, we evaluate the potential of this automatic method in identifying imminent TdP arrhythmias in the CAVB dog model.

Materials & methods

Animal handling was in accordance with the 'Directive 2010/63/EU of the European Parliament and of the Council of 22 September 2010 on the protection of animals used for scientific purposes' and the Dutch law, laid down in the Experiments on Animals Act. The Animal Experiment Committee of the University of Utrecht approved all experiments.

The current study is a retrospective analysis of data obtained during animal experiments performed in our laboratory between 2014 and 2017 and can be divided into two parts. In part 1, three different methods of STV_{ARI} measurement, including the newly developed automatic method, are compared to the gold standard STV_{MAPD}. In part 2, the predictive value of the automatic method in identifying dogs inducible to TdP arrhythmias is evaluated and compared to the methods of STV_{ARI} measurement currently used in our department.

Animal experiments

The standard experimental procedures have been described in detail previously.[12,13] In summary, after premedication with methadone 0.5 mg/kg, acepromazine 0.5 mg/kg and atropine 0.02 mg/kg i.m., general anesthesia was induced via pentobarbital sodium 25 mg/kg i.v. and maintained by isoflurane 1.5% in O_2 and N_2O. During the experiments, ten surface ECG leads were recorded. Under aseptic conditions, the femoral artery and vein were dissected and sheaths were inserted. In the initial experiment, complete AV-block was created by radiofrequency ablation of

the proximal His bundle. In the dogs included in part 1, a screw-in lead was placed in the right ventricular apex (RVA) via the jugular vein and connected to an internal pacemaker (Medtronic, Maastricht, The Netherlands), which was implanted subcutaneously. Subsequently, these dogs were left to remodel for at least 3 weeks during RVA pacing at the lowest captured rate. In contrast, the dogs selected for part 2 remodeled for at least 3 weeks on idioventricular rhythm (IVR).

At chronic AV-block, a second experiment was performed to test for TdP susceptibility. Under general anesthesia, left and right ventricular (LV & RV) MAP catheters (Hugo Sachs Elektronik, March, Germany) and/or a duo-decapolar EGM catheter (St. Jude Medical, St. Paul, MN, USA) were inserted and advanced to the apex to record LV & RV MAPD and/or unipolar EGMs. A reference electrode was inserted in a superficial vein of the right hind leg. The I_{Kr} blocker dofetilide (0.025 mg/kg i.v. in 5 minutes or before the first TdP) was administered to test for inducibility of TdP arrhythmias. TdP was defined as a run of 5 or more short-coupled (occurring before the end of the T wave) ectopic beats, with polymorphic twisting of the QRS axis. If a TdP did not terminate by itself, the dog was defibrillated with 100J by use of an external defibrillator. When ≥3 TdP's occurred in the first 10 minutes after the start of infusion, the dog was considered inducible. During baseline and dofetilide challenge, dogs had either IVR or were paced from the RVA by the RV MAP catheter with a cycle length of 1000ms.

Part 1 – comparison of STV_{ARI} with STV_{MAPD}

For part 1, adult mongrel dogs were selected that had both a LV EGM catheter and a LV MAP catheter in place during the experiment and were challenged for TdP inducibility with dofetilide. Since the simultaneous use of both LV EGM and LV MAP catheters is not common practice in our laboratory, only 7 dogs (weight 27 ± 3 kg, all females) were included. All these dogs remodeled during RVA pacing at the lowest captured rate and were tested for inducibility at VVI60.

Part 2 – predictive value of STV_{ARI} measurements

For part 2, dogs were selected that had remodeled on IVR, had an LV EGM catheter inserted and were challenged for TdP inducibility with dofetilide. Of a total of 33 dogs in our database, 12 were excluded for various reasons (Figure 1). The 21 included dogs (weight 24.5 ± 3.2 kg, 7 males, 14 females) consisted of 11 inducible (5 tested at IVR, 6 at VVI60) and 10 non-inducible dogs (2 tested at IVR, 8 at VVI60).

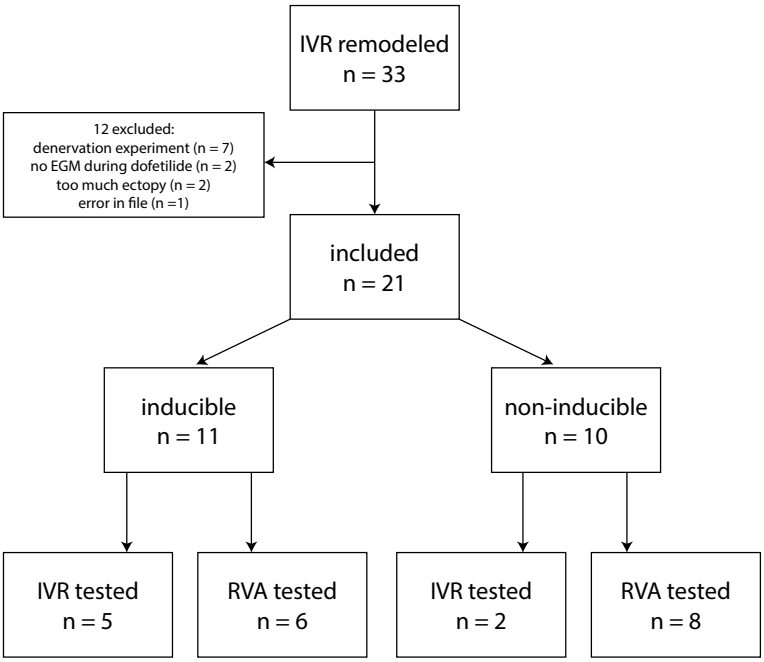

Figure 1. Flowchart of dogs included in part 2

Data analysis

Both the surface ECG, LV MAP and LV unipolar EGM were recorded with EP Tracer (Cardiotek, Maastricht, The Netherlands) at a sampling frequency of 1000Hz. The RR interval and QT interval were measured offline with calipers on lead II. QT interval was corrected for heart rate (QTc) with the van der Water formula.[14] LV MAPD was measured semi-automatically from the initial peak until 80% of repolarization using custom-made software (AutoMAPD, MATLAB, MathWorks, Natick, MA, USA). For comparison of STV_{MAPD} and STV_{ARI}, we chose the EGM electrode that was located most closely to the MAP catheter. For calculation of STV_{ARI}, the ARI of consecutive beats was determined by use of three different methods:

1. Slope method: ARI of every beat was measured from the minimum dV/dt of the QRS complex to the maximum dV/dt of the T wave, irrespectively of the morphology of the T wave (either positive, negative or biphasic).

2. Fiducial Segment Averaging (FSA) method: First, two fiducial points were defined, i.e. the minimum dV/dt of the QRS complex as the ARI onset and the

maximum dV/dt of the T wave as the ARI offset. Using the method of Fiducial Segment Averaging[15], all complexes were aligned separately around the ARI onset and ARI offset by cross-correlating the individual complex to the average of the other complexes until maximal correlation is achieved. The ARI of every single beat was then defined as the interval between the two fiducial points, taking the amount of shifting into account.

3. Automatic method: First, the EGM signal was filtered with a bandpass filter between 1 and 10 Hz. After that, the QRS complex was blanked to avoid interference in the T wave end detection. Once the QRS complex was blanked, the gradient of the resultant signal is calculated over time to detect changes in the slope. The gradient signal is then squared in order to make all data points positive and to emphasize slope changes in the signal. Finally, the T wave end is defined as the point at 60% of the area under the curve of the resultant signal. The ARI is defined from the minimum dV/dt of the QRS complex to the T wave end, derived with this method.

Short-term variability of MAPD or ARI was calculated over 31 consecutive beats using the formula: $STV = \sum|D_{n+1} - D_n|/30 \times \sqrt{2}$, where D represents MAPD or ARI. All measurements were performed both at baseline and after administration of dofetilide. After dofetilide, parameters were determined just prior to the first ectopic beat. In the non-inducible dogs that did not show any ectopic beats after dofetilide infusion, all parameters were assessed at that time, where, on average, the first ectopic occurred in the inducible subjects.

Statistical analysis

Numerical values are expressed as mean ± standard deviation (SD). Comparison of serial data was performed with a paired Student's *t*-test. Group comparison was done with an unpaired Student's *t*-test. Group comparison with both a within-subject variable and a between-subject variable was performed with a mixed analysis of variance (ANOVA) with Sidak's correction for multiple comparisons. The relation between the different STV modalities was analyzed by use of simple linear regression. In addition, Bland-Altman analysis was done to assess for systematic bias and limits of agreements. The area under the Receiver Operator Characteristics (ROC) curve was used to evaluate the predictive power of the different STV_{ARI} methods. All statistical analyses were performed with Prism 6.0 (GraphPad Software Inc., La Jolla, CA, USA). A p-value < 0.05 was considered as statistically significant.

Results

Part 1 – Comparison of STV_{ARI} with STV_{MAPD}

Electrophysiological parameters at baseline and after dofetilide of the 7 included animals are summarized in Table 1. As expected, dofetilide induced an increase in all repolarization parameters compared to baseline, including STV by all four different methods. MAPD and ARI were comparable at baseline (251 ± 18 ms and 263 ± 21 ms, respectively, p = 0.26), and showed a similar increase after dofetilide (395 ± 53 ms and 396 ± 53 ms, respectively, p = 0.98). The highest values of STV, both at baseline and after dofetilide, were found when using the slope method (0.85 ± 0.39 and 3.68 ± 1.62 ms respectively). The automatic method derived the lowest values of STV (0.36 ± 0.21 ms at baseline and 1.77 ±.94 ms after dofetilide). However, this method showed the biggest relative increase compared to baseline.

Figure 2 shows the regression analysis and Bland-Altman plots of the three different STV_{ARI} methods compared to the gold standard STV_{MAPD}. The slope method had a moderate correlation with STV_{MAPD} (r^2 of 0.68, $p < 0.001$). A systematic bias was found of -0.79ms with increasing differences between the two methods at higher values. The limits of agreement of the Bland-Altman plot were -2.8 and 1.29 ms. The FSA method had a better correlation with an r^2 of 0.79 ($p < 0.001$). No systematic bias was found with limits of agreement between -1.23 to 1.15 ms. The new automatic method showed a very good correlation with STV_{MAPD} with an r^2 of 0.97 ($p < 0.001$). A small systematic bias was seen of 0.40 ms. The automatic measurement gave systematically lower STV values, especially at higher mean values. The bandwidth of agreement was small, between -0.41 to 1.21 ms.

Table 1. Electrophysiological parameters of animals of part 1 (n = 7)

mean ± SD. MAPD = monophasic action potential duration; ARI = activation recovery interval; FSA fiducial segment averaging. * $p < 0.05$ vs. baseline

	baseline	dofetilide
RR (ms)	1000	1000
QT (ms)	350 ± 20	499 ± 57*
QTc (ms)	350 ± 20	499 ± 57*
$MAPD_{80}$ (ms)	251 ± 18	395 ± 53*
ARI (ms)	263 ± 21	396 ± 53*
STV_{MAPD} (ms)	0.55 ± 0.27	2.44 ± 1.30*
STV_{ARI} slope (ms)	0.85 ± 0.39	3.68 ± 1.62*
STV_{ARI} FSA (ms)	0.61 ± 0.21	2.42 ± 1.09*
STV_{ARI} automatic (ms)	0.36 ± 0.21	1.77 ± 0.94*

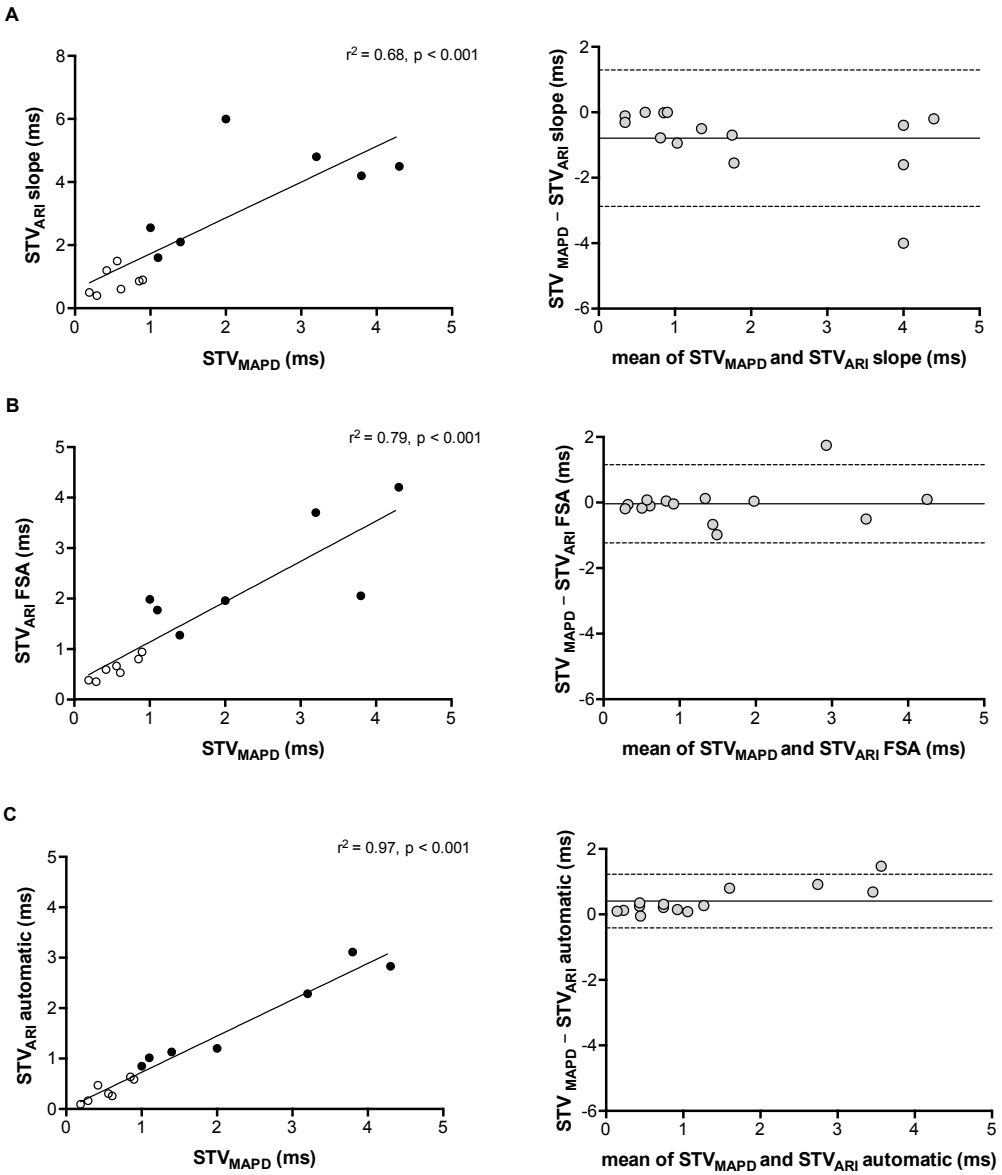

Figure 2. linear regression (left) and Bland-Altman analysis (right) of STV_{MAPD} compared to STV_{ARI}.
A) STV_{MAPD} versus STV_{ARI} measured with the slope method. B) STV_{MAPD} versus STV_{ARI} measured with the Fiducial Segment Averaging (FSA) method. C) STV_{MAPD} versus STV_{ARI} measured with the new automatic method.

Table 2. Electrophysiological parameters of animals of part 2 (n = 21)

mean ± SD. MAPD = monophasic action potential duration; ARI = activation recovery interval; FSA = fiducial segment averaging. * $p < 0.05$ vs. baseline. § $p < 0.05$ vs. inducible

	Baseline			dofetilide		
	total	**I**	**NI**	**total**	**I**	**NI**
RR (ms)	1186 ± 255	1263 ± 229	1102 ± 267	1197 ± 257	1274 ± 219	1111 ± 266
QT (ms)	395 ± 57	403 ± 59	387 ± 56	569 ± 72*	578 ± 76*	560 ± 75*
QTc (ms)	379 ± 59	380 ± 61	378 ± 59	522 ± 70*	554 ± 70*	550 ± 71*
ARI (ms)	296 ± 49	309 ± 52	282 ± 44	411 ± 88*	443 ± 85*	375 ± 80 *
STV_{ARI} slope (ms)	1.44 ± 1.04	1.69 ± 1.33	1.15 ± 0.49	3.62 ± 2.72*	5.09 ± 3.07*	2.00 ± 0.65§
STV_{ARI} FSA (ms)	1.14 ± 0.68	1.20 ± 0.88	1.08 ± 0.42	2.40 ± 1.26*	3.11 ± 1.30*	1.62 ± 0.58§
STV_{ARI} automatic (ms)	0.42 ± 0.59	0.54 ± 0.36	0.30 ± 0.24	1.39 ± 0.79*	1.91 ± 0.76*	0.82 ± 0.27*§

Part 2 – predictive value of STV_{ARI} measurements

In Table 2 the electrophysiological parameters at baseline and after dofetilide of the 21 included dogs are shown, separately analyzed for inducible and non-inducible dogs. No differences were found in RR interval, QT interval, QTc interval or ARI between inducible and non-inducible dogs, both at baseline and after administration of dofetilide. In addition, at baseline STV_{ARI} was similar for inducible and non-inducible dogs. Administration of dofetilide significantly increased baseline levels of STV_{ARI} in inducible dogs. Levels of STV_{ARI} after dofetilide were significantly higher in inducible dogs compared to non-inducible subjects. In the non-inducible dogs, only the automatic method demonstrated a statistically significant increase in STV_{ARI} after dofetilide, while the other methods showed a trend. Figure 3 shows an example of the effect of dofetilide infusion on the three different methods of STV_{ARI} in both an inducible and non-inducible dog. While the non-inducible dog shows only a mild increase of STV_{ARI}, a prominent rise in STV is observed in the inducible dog prior to the occurrence of TdP arrhythmias.

The predictive performance of the three methods was evaluated, i.e. to what extend the different methods of STV_{ARI} were able to distinguish between dogs that were inducible versus those that were not inducible to drug-induced TdP arrhythmias. In Figure 4, the STV_{ARI} of the three methods is presented separately for inducible and non-inducible dogs, both at baseline and dofetilide. One can clearly see that, whilst STV_{ARI} measured with the slope and FSA method partly overlap for some inducible and non-inducible subjects after dofetilide, an almost total separation in STV_{ARI} between the two groups can be found with the new automatic measurement. This is further illustrated in the ROC-curves of the different methods. The automatic method results in the highest AUC of 0.92, compared to an AUC of 0.85 and 0.87 of the slope method and FSA method, respectively. With a threshold set at 1.23 ms, the automatic method yields a sensitivity of 0.91 (95% CI 0.58 – 0.99) and a specificity of 0.90 (95% CI 0.55 – 0.99).

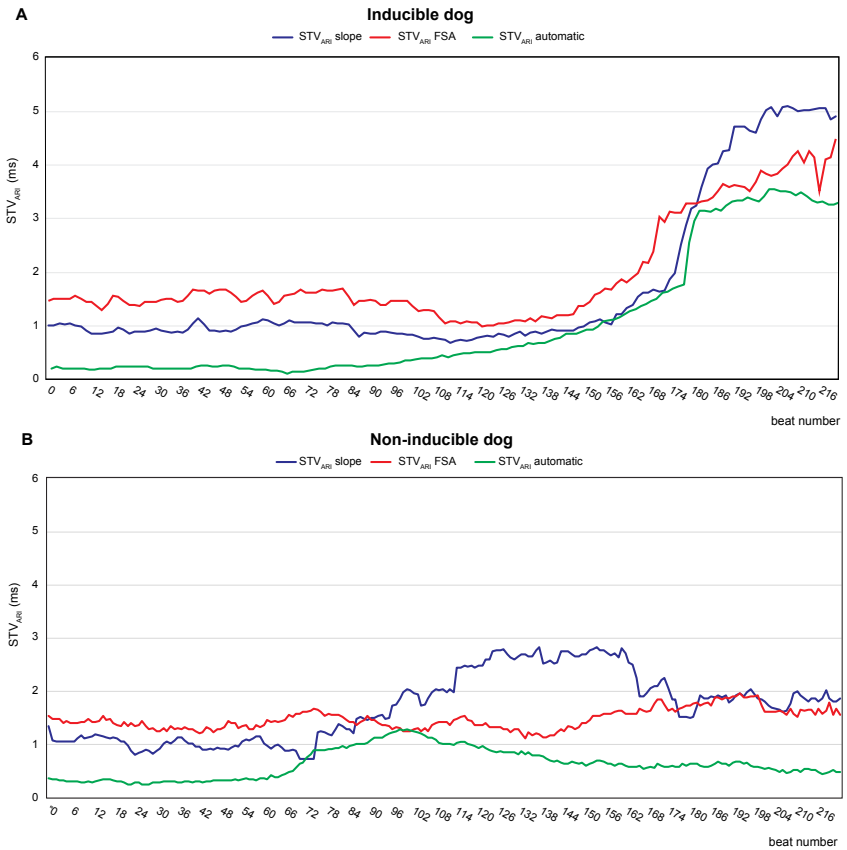

Figure 3. example of STV_{ARI} in inducible (A) and non-inducible dog (B) after dofetilide

STV_{ARI} measured with the slope method (blue line), fiducial segment averaging (FSA) method (red line) and automatic method (green line).

Discussion

In the present study, we evaluated a fully automatic method of STV_{ARI} measurement in the chronic AV-block dog model and compared this new method with the current gold standard STV_{MAPD} and two other methods used in our laboratory to derive STV_{ARI} from the intracardiac EGM. The results show that 1.) STV_{ARI} determined with the automatic method is highly comparable to STV_{MAPD} both under baseline conditions and after dofetilide, 2.) the automatically determined STV_{ARI} performs better in predicting imminent TdP arrhythmias after dofetilide administration compared to the current STV_{ARI} methods.

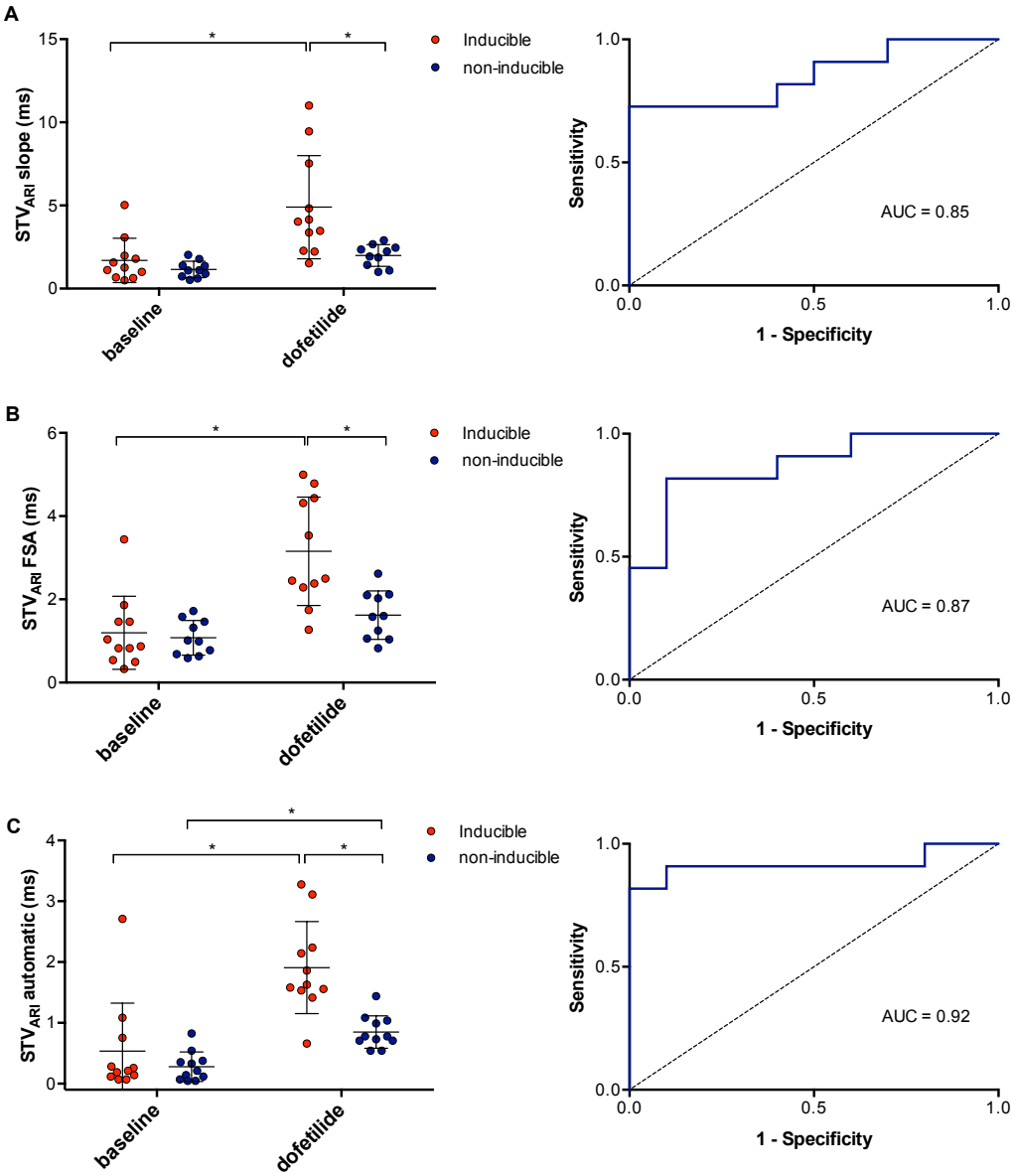

Figure 4. Predictive value of different methods of STV_{ARI}

STV_{ARI} at baseline and after dofetilide in inducible (red) and non-inducible dogs (blue) measured with the slope method (A), FSA method (B) and automatic method (C) with the corresponding Receiver Operating Characteristics (ROC) curves. AUC = area under the curve. * $p < 0.05$

STV as a marker of arrhythmic risk

As expected, of all electrophysiological parameters, only STV could distinguish between inducible and non-inducible subjects after dofetilide administration (Table 2). Previous studies in the CAVB dog model have well established STV as a better marker of reduced repolarization reserve and arrhythmic risk compared to parameters of repolarization duration (QT, MAPD or ARI) alone.[16,17] In pro-arrhythmic drug testing, STV was able to identify safe from unsafe drugs, despite similar QT prolongation.[18,19] In addition, reduction of STV is highly related to efficacy of antiarrhythmic agents.[20] Furthermore, Thomsen et al. observed that after infusion of dofetilide, STV of LV MAPD shows a steep increase just prior to the occurrence of TdP arrhythmias, which was not present in the non-inducible dogs.[10] Therefore, STV dynamics could provide important information about impending arrhythmic events. Since MAP catheters are rarely used outside the experimental laboratory, recent interest shifted towards measurement of STV on the EGM of chronically implanted ICD leads.[11,21,22] These leads have the advantage of recording electrograms 24/7 from a fixed position on the myocardium.

Different methods of STV_{ARI} compared to STV_{MAPD}

We demonstrated a moderate to good correlation between STV_{ARI} of the LV EGM with STV of the LV MAPD, with an r^2 ranging from 0.68 to 0.97 for the different methodologies (Figure 2). This finding is in line with results of previous studies. Oosterhoff et al. compared STV_{LVMAPD} and STV_{LVARI} measured epicardially via a screw electrode with a slightly lower sampling rate of 800 Hz.[21] Despite the methodological differences, a similar correlation between STV_{ARI} and STV_{MAPD} was found with an r^2 of 0.71. Recently, Wijers et al. observed a positive correlation between STV_{MAPD} and STV_{ARI} from the RV EGM.[11] Yet, the correlation was less strong ($r^2 = 0.41$), possibly due to differences in sampling frequency between the MAP and EGM recording (1000Hz for the MAP and 250 Hz, resampled to 400 Hz, for the EGM).

When comparing the three methods of STV_{ARI}, important differences in correlation with STV_{MAPD} are found. The slope method had the weakest correlation with an r^2 of 0.68. This method incorporates the widely used definition of ARI as proposed by Wyatt et al.[23], who showed that the interval from the minimum dV/dt of the QRS complex to the maximum dV/dt of the T wave of the unipolar electrogram correlates highly with action potential duration. While there is general consensus on the use of the minimum dV/dt as local depolarization time, a debate exists on whether the maximum or minimum dV/dt of the T wave should be used as index of local repolarization time, especially when the T wave is positive or biphasic. However, recent computer simulation and experimental studies have demonstrated that, irrespective of T wave morphology, the upstroke of

the T wave coincides with repolarization on the MAP and that the minimum dV/dt of a positive T wave represents remote repolarization.[24,25] Therefore, we have chosen to use maximal upstroke as index of local repolarization for all T wave morphologies (negative, positive or biphasic). Nevertheless, most of the EGMs used for the analysis had negative upsloping T waves, possibly due to their location in the apex of the heart. Therefore, the definition of ARI offset does not seem the reason for the weak correlation of the slope method with MAPD. While at baseline STV_{ARI} by the slope method is more or less similar to STV_{MAPD}, the discrepancy between the two methods starts to arise after dofetilide (Figure 2). This is further illustrated by the Bland-Altman plot, which shows that the systematic bias of the slope method increases at higher average values. The explanation for this bias is probably related to the inaccuracy of determining maximal dV/dt of the T wave at longer ARIs. After infusion of dofetilide, the ARI prolongs and the T wave widens. Hence, the upstroke of the T wave the becomes less steep, making it difficult to determine the exact point of maximal dV/dt for every beat, thereby introducing measurement error. Since the STV formula uses absolute differences between consecutive ARI, there is no cancellation of measurement error, resulting in a higher STV.

STV_{ARI} measured with the FSA method shows better correlation with STV_{MAPD} and has no clear systematic bias on the Bland-Altman plot. FSA has been developed for accurate determination of intervals between certain fiducial points and thus prevents the aforementioned problem of summation of measurement error that is caused by determining ARI for every single beat separately. FSA determines the fiducial points (i.e. ARI onset and the ARI offset) for all complexes at once. After alignment of the complexes around these fiducial points, the individual shifts between the fiducial points are used to calculate the individual ARIs. Therefore, the beat-to-beat variations in ARI are preserved, without introducing repeated measurement error. However, while this method shows improved accuracy in measurement of STV compared to the slope method, the use of FSA for continuous monitoring in an implanted device is problematic, because it requires a lot of data storage for the calculation. Therefore, we tried to develop a new method that is easy to calculate, requires less storage and does not drain the battery of the device, even when used continuously.

The automatic method of STV_{ARI} shows an excellent correlation with STV_{MAPD} with an r^2 of 0.97. Interestingly, this method calculates overall lower values of STV compared to LV MAPD (Table 1 and Figure 4). The underestimation of STV is particularly present after dofetilide. The cause of the low absolute values of STV lies in the fact that the actual STV value is an average between the measure STV and the prior STV. By doing so, noise in STV values is removed and trends are smoothed. Therefore, it performs similar to STV_{MAPD}, which is also resistant to noise because of direct contact with the myocardium and its bipolar configuration.

The performance of STV_{ARI} in prediction of TdP arrhythmia

In part 2 of the study, the three different methods were evaluated on their ability to identify a change in STV_{ARI} prior to the occurrence of TdP arrhythmias in the inducible dogs. At baseline, all electrophysiological parameters including STV_{ARI} were similar for inducible and non-inducible dogs (Table 2). This is contrast to the study by Thomsen et al. which already found a difference in STV_{MAPD} at baseline between inducible and non-inducible subjects. However, since the values of STV at baseline are very low with a substantial SD, it is imaginable that you do not find a statistically significant difference. Nonetheless, after infusion of dofetilide, all three STV methods showed a significant higher STV_{ARI} in the inducible dogs prior to the occurrence of the first ectopic beat compared to a similar timepoint in the non-inducible dogs. While the slope method derived the largest absolute difference of STV_{ARI} between inducible and non-inducible dogs (5.09 ms vs. 2.0 ms), there was also a high variability, with some dogs showing a very large increase in STV, while others had STV values comparable to the non-inducible subjects. This has resulted in a lower predictive capability as seen by a lower AUC of the ROC curve. The same applies for the FSA method. On the other hand, the new automatic method could almost completely separate inducible from non-inducible dogs, resulting in a very high specificity and sensitivity. This would make it possible to define a specific threshold, above which STV_{ARI} predicts, with high accuracy, the occurrence of upcoming arrhythmic events.

Interestingly, the automatic method also found a statistically significant increase in STV_{ARI} after dofetilide in the non-inducible dogs (Figure 4), while this increase was not significant by the other methods. It is known that the rise in STV has both a pro-arrhythmic component and an APD-dependent component[18]; STV increases at longer APD, which is unrelated to pro-arrhythmic lability of repolarization. For example, pacing at lower stimulation rate, results in APD prolongation and a subsequent increase in STV. This increase does not represent increased arrhythmic risk. The significant increase in STV_{ARI} detected by the automatic method in the non-inducible dogs can therefore be explained by the positive APD-STV relationship. The reason this significant increase is not found by the other two methods further supports the superior accuracy of the automatic method in measurement of very subtle STV_{ARI} differences.

Clinical utility of the intracardiac EGM

A number of clinical studies have evaluated the use of intracardiac EGMs for the prediction of ventricular tachyarrhythmias. Tereschenko et al. analyzed the predictive value of QT variability index (QTVI) on intracardiac EGMs in 298 ICD patients.[26] The highest quartile of QTVI was an independent predictor of VT/VF and appropriate ICD therapy at

a mean follow-up of 16 months. In addition, Sandhu et al. analyzed intracardiac T wave alternans on the EGM during an electrophysiological study in 78 patients and found a positive predictive value of only 14%, but a high negative predictive value of 95% at 1 year.[27] However, both these studies investigated the use of intracardiac EGM parameters for prediction of sustained arrhythmias during long-term follow-up. Swerdlow et al. did a prospective multicentre study in 68 ICD patients and evaluated T wave alternans and non-alternans T wave variability (TWA/V) on EGMs preceding spontaneous ventricular tachyarrhythmias.[28] They observed a significantly higher TWA/V immediately before the occurrence of arrhythmias compared to four control recordings. In line with our findings, this study demonstrates that the intracardiac EGM can provide valuable information for the prediction of imminent life-threatening arrhythmias in a clinical setting. However, this information would only be useful if appropriate treatment, such as alternative pacing algorithms, can be initiated in time to prevent the arrhythmia from occurring. Recently, Wijers et al. demonstrated that temporary accelerated pacing (TAP) initiated just after the first ectopic beat can prevent TdP arrhythmias in the CAVB dog.[29] This is in agreement with clinical studies that show that rate-smoothing pacing algorithms can reduce the number of sustained ventricular tachyarrhythmias in ICD recipients and patients with long QT syndrome.[30,31] Therefore, by use of 24/7 automatic measurement of STV_{ARI}, the device does not have to wait for an ectopic beat to initiate pacing therapy, but can already start with treatment when STV rises above a certain threshold value, thereby preventing the arrhythmia and subsequent ICD shock.

Limitations

Certain limitations of the current study must be addressed. First, this study had a retrospective study design, therefore not all variables could be controlled. This resulted in important differences between the dogs used for the analyses of part 1 and part 2. For the comparison of STV_{MAPD} and STV_{ARI} in part 1, we were limited in the number of animals, because the combined use of an LV MAP and LV EGM catheter has only been used in a few experiments, in which dogs remodeled at low rate RVA pacing. It is known from previous (unpublished) data from our laboratory that control of the activation pattern by pacing can influence the course of electrical remodeling and the arrhythmic susceptibility compared to dogs that remodeled on their own IVR. Therefore, for part 2, in which no additional MAP catheter was required, we selected only IVR remodeled dogs to maintain a more homogeneous population. It should also be noted that we included both dogs that had IVR or were RVA paced at VVI60 during the experiment. Since the IVR can be lower than 60/min, these dogs could have had longer APD and thus higher STV, which may act as a possible confounder in the differences of STV between inducible and non-inducible dogs. Finally, we should acknowledge that the CAVB

dog is a specific animal model sensitive to triggered-activity based TdP arrhythmias. Therefore, extrapolation of the predictive value of STV to other types of ventricular tachyarrhythmias should be done with caution.

Future directions

The development of a reliable and accurate automatic method of STV measurement on intracardiac EGMs is an important step towards clinical implementation of STV for continuous monitoring. Prospective observational studies in ICD patients should evaluate if the same increase in STV_{ARI} prior to the occurrence ventricular arrhythmias is observed in a clinical setting.

Furthermore, in future studies, the detection mode of predicting imminent arrhythmias should be coupled to a fully automatic algorithm for the initiation of preventive pacing therapy, such as TAP. When a sudden increase of STV above a certain threshold value is detected, the device could then automatically start a pacing algorithm, thereby preventing the arrhythmia from occurring.

Conclusion

In conclusion, we have developed a new fully-automatic method for measuring STV_{ARI} on the intracardiac EGM in the chronic AV-block dog model. This method is highly correlated to the gold standard STV_{MAPD} and can accurately identify a pro-arrhythmic rise in STV_{ARI} prior to the occurrence of dofetilide-induced TdP arrhythmias. This technique could be integrated in implantable devices for prediction of imminent ventricular tachyarrhythmias and initiation of preventive pacing therapy.

References

1. Al-Khatib SM, Stevenson WG, Ackerman MJ, et al. 2017 AHA/ACC/HRS Guideline for Management of Patients With Ventricular Arrhythmias and the Prevention of Sudden Cardiac Death. *Heart Rhythm* 2017;
2. Benjamin EJ, Blaha MJ, Chiuve SE, et al. Heart Disease and Stroke Statistics—2017 Update: A Report From the American Heart Association. *Circulation* 2017;135:e146–603.
3. Moss AJ, Zareba W, Hall WJ, et al. Prophylactic implantation of a defibrillator in patients with myocardial infarction and reduced ejection fraction. *N Engl J Med* 2002;346:877–83.
4. Bardy GH, Lee KL, Mark DB, et al. Amiodarone or an implantable cardioverter-defibrillator for congestive heart failure. *N Engl J Med* 2005;352:225–37.
5. Priori SG, Blomström-Lundqvist C, Mazzanti A, et al. 2015 ESC Guidelines for the

management of patients with ventricular arrhythmias and the prevention of sudden cardiac death: The Task Force for the Management of Patients with Ventricular Arrhythmias and the Prevention of Sudden Cardiac Death of the Europe. *Eur Heart J* 2015;36:2793–867.

6. Bostwick JM, Sola CL. An Updated Review of Implantable Cardioverter/Defibrillators, Induced Anxiety, and Quality of Life. *Heart Fail Clin* 2011;7:101–8.
7. Schron EB, Exner D V, Yao Q, et al. Quality of life in the antiarrhythmics versus implantable defibrillators trial: impact of therapy and influence of adverse symptoms and defibrillator shocks. *Circulation* 2002;105:589–94.
8. Van Herendael H, Pinter A, Ahmad K, et al. Role of antiarrhythmic drugs in patients with implantable cardioverter defibrillators. *Europace* 2010;12:618–25.
9. Reddy VY, Reynolds MR, Neuzil P, et al. Prophylactic Catheter Ablation for the Prevention of Defibrillator Therapy. *N Engl J Med* 2007;357:2657–65.
10. Thomsen M, Oros A, Schoenmakers M, et al. Proarrhythmic electrical remodelling is associated with increased beat-to-beat variability of repolarisation. *Cardiovasc Res* 2007;73:521–30.
11. Wijers SC, Sprenkeler DJ, Bossu A, et al. Beat-to-beat variations in activation recovery interval derived from the right ventricular electrogram can monitor arrhythmic risk under anesthetic and awake conditions in the canine chronic atrioventricular block model. *Heart Rhythm* 2017;
12. Dunnink A, Sharif S, Oosterhoff P, et al. Anesthesia and Arrhythmogenesis in the Chronic Atrioventricular Block Dog Model. *J Cardiovasc Pharmacol* 2010;55:601–8.
13. Dunnink A, van Opstal JM, Oosterhoff P, et al. Ventricular remodelling is a prerequisite for the induction of dofetilide-induced Torsades de pointes arrhythmias in the anaesthetized, complete atrio-ventricular-block dog. *Europace* 2012;14:431–6.
14. Van de Water A, Verheyen J, Xhonneux R, et al. An improved method to correct the QT interval of the electrocardiogram for changes in heart rate. J Pharmacol Methods 1989;22:207–17.
15. Ritsema van Eck HJ. Fiducial segment averaging to improve cardiac time interval estimates. *J Electrocardiol* 2002;35 Suppl:89–93.
16. Thomsen MB, Verduyn SC, Stengl M, et al. Increased short-term variability of repolarization predicts d-sotalol-induced torsades de pointes in dogs. *Circulation* 2004;110:2453–9.
17. Thomsen MB, Volders PGA, Beekman JDM, et al. Beat-to-Beat Variability of Repolarization Determines Proarrhythmic Outcome in Dogs Susceptible to Drug-Induced Torsades de Pointes. *J Am Coll Cardiol* 2006;48:1268–76.
18. Varkevisser R, Wijers SC, van der Heyden MAG, et al. Beat-to-beat variability of repolarization as a new biomarker for proarrhythmia in vivo. *Heart Rhythm* 2012;9:1718–26.
19. Thomsen MB, Beekman JDM, Attevelt NJM, et al. No proarrhythmic properties of the antibiotics Moxifloxacin or Azithromycin in anaesthetized dogs with chronic-AV block. *Br J*

Pharmacol 2006;149:1039–48.

20. Bossu A, Varkevisser R, Beekman HDM, et al. Short-term Variability of Repolarization Is Superior to Other Repolarization Parameters in the Evaluation of Diverse Antiarrhythmic Interventions in the Chronic Atrioventricular Block Dog. *J Cardiovasc Pharmacol* 2017;69:398–407.
21. Oosterhoff P, Thomsen MB, Maas JN, et al. High-rate pacing reduces variability of repolarization and prevents repolarization-dependent arrhythmias in dogs with chronic AV block. *J Cardiovasc Electrophysiol* 2010;21:1384–91.
22. Oosterhoff P, Tereshchenko LG, van der Heyden MAG, et al. Short-term variability of repolarization predicts ventricular tachycardia and sudden cardiac death in patients with structural heart disease: A comparison with QT variability index. *Heart Rhythm* 2011;8:1584–90.
23. Wyatt R. Comparison of estimates of activation and recovery times from bipolar and unipolar electrograms to *in vivo* transmembrane action potential durations. *Proc IEEE/ Engineering Med Biol Soc* 2nd Annu Conf Washington, DC 1980;22–5.
24. Western D, Hanson B, Taggart P. Measurement bias in activation recovery intervals from unipolar electrograms. *Am J Physiol Heart Circ Physiol* 2015;308:H331-8.
25. Coronel R, de Bakker JMT, Wilms-Schopman FJG, et al. Monophasic action potentials and activation recovery intervals as measures of ventricular action potential duration: experimental evidence to resolve some controversies. *Heart Rhythm* 2006;3:1043–50.
26. Tereshchenko LG, Fetics BJ, Domitrovich PP, et al. Prediction of Ventricular Tachyarrhythmias by Intracardiac Repolarization Variability Analysis. *Circ Arrhythmia Electrophysiol* 2009;2:276–84.
27. Sandhu RK, Costantini O, Cummings JE, et al. Intracardiac alternans compared to surface T wave alternans as a predictor of ventricular arrhythmias in humans. *Heart Rhythm* 2008;5:1003–8.
28. Swerdlow C, Chow T, Das M, et al. Intracardiac electrogram T wave alternans/variability increases before spontaneous ventricular tachyarrhythmias in implantable cardioverter-defibrillator patients: a prospective, multi-center study. *Circulation* 2011;123:1052–60.
29. Wijers SC, Bossu A, Dunnink A, et al. Electrophysiological measurements that can explain and guide temporary accelerated pacing to avert (re)occurrence of Torsades de pointes arrhythmias in the canine chronic atrioventricular block model. *Heart Rhythm* 2017;14:749–56.
30. Wietholt D, Kuehlkamp V, Meisel E, et al. Prevention of sustained ventricular tachyarrhythmias in patients with implantable cardioverter-defibrillators-the PREVENT study. *J Interv Card Electrophysiol* 2003;9:383–9.
31. Viskin S, Glikson M, Fish R, et al. Rate smoothing with cardiac pacing for preventing Torsades de pointes. *Am J Cardiol* 2000;86:111K–115K.

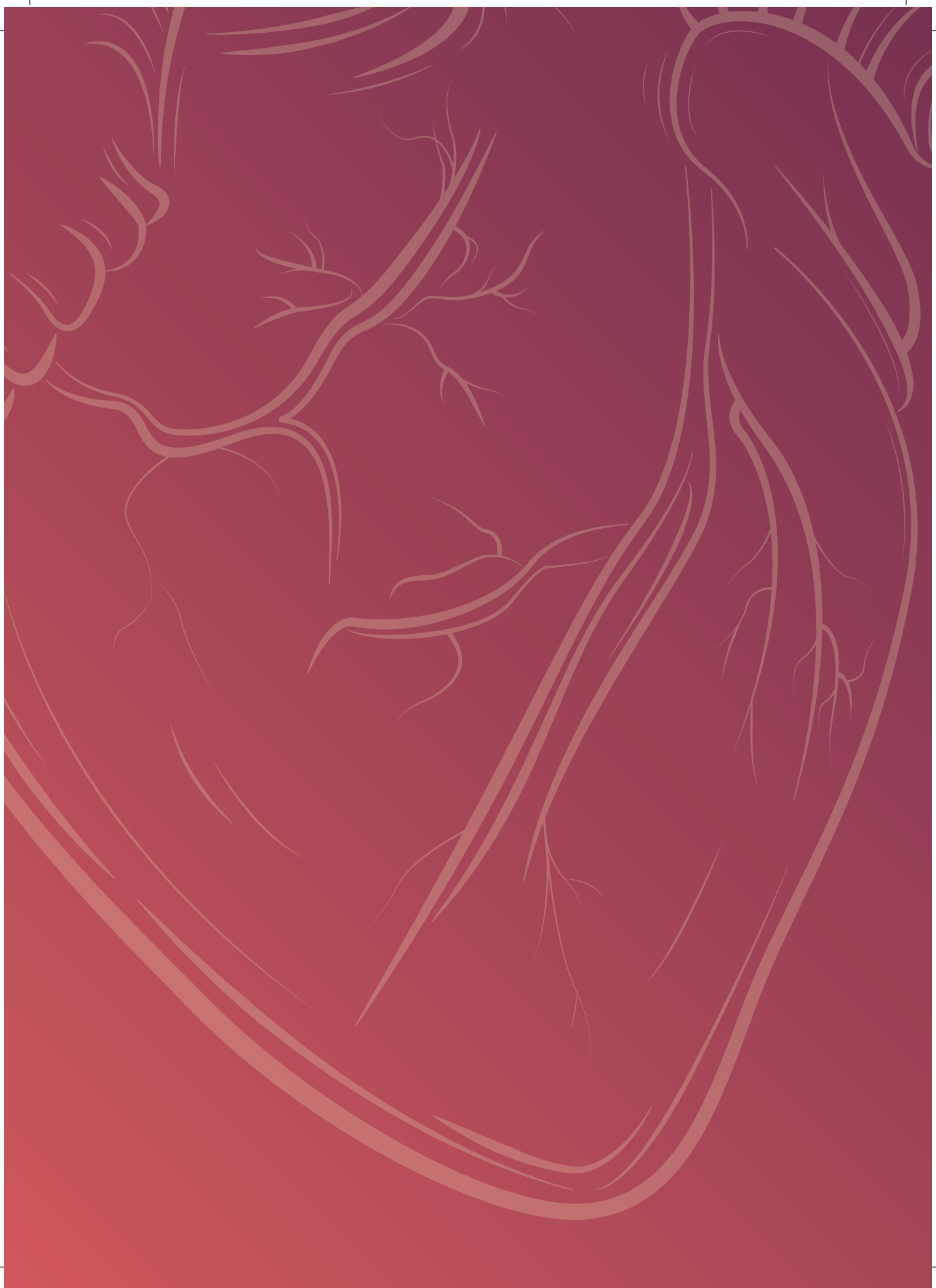

PART III

PARAMETERS OF NEURAL REMODELING FOR RISK PREDICTION

Chapter 9

Pro-arrhythmic ventricular remodeling is associated with increased respiratory and low frequency oscillations of monophasic action potential duration in the chronic atrioventricular block dog

David J. Sprenkeler, Jet D.M. Beekman, Alexandre Bossu, Albert Dunnink, Marc A. Vos

Department of Medical Physiology, University Medical Center Utrecht, Utrecht, the Netherlands

In preparation

Abstract

Background: In the chronic complete AV-block (CAVB) dog model, ventricular remodeling increases repolarization variability, which is associated with susceptibility to ventricular arrhythmias. In addition to beat-to-beat fluctuations, action potential duration (APD) also oscillates at 1.) a respiratory frequency and 2.) a low frequency (< 0.1 Hz), caused by bursts of sympathetic nervous system discharge. This study investigates whether ventricular remodeling also alters these oscillations of APD in the CAVB dog and whether this has consequences for arrhythmogenesis.

Methods: We performed a retrospective analysis of 39 previously performed dog experiments in sinus rhythm (SR), acute AV-block (AAVB) and after at least 2 weeks of chronic AV-block (CAVB). Left ventricular monophasic action potential duration (LV MAPD) was recorded for 5 minutes during acute steady state RVA pacing. Subsequently, dofetilide (0.025mg/kg in 5 minutes) was infused to test for inducibility of Torsades de Pointes (TdP) arrhythmias. Spectral analysis was performed to quantify respiratory frequency (RF) power (0.19 to 0.21 Hz) and low frequency (LF) power (0.04 to 0.15 Hz). For LF power, analysis was done on the MAPD difference between consecutive beats instead of MAPD.

Results: 1.) RF power was significantly increased at CAVB compared to AAVB and SR (log[RF] of -1.13 ± 1.62 at CAVB versus log[RF] of -2.82 ± 1.24 and -3.29 ± 1.29 at SR and AAVB, respectively, $p<0.001$). No significant differences in RF power were seen between inducible and non-inducible subjects. 2.) LF power of MAPD difference was already significantly increased at AAVB and increased even further at CAVB (-3.91 ± 0.70 at SR, versus -2.52 ± 0.85 at AAVB and -1.14 ± 1.62 at CAVB, $p<0.001$). In addition, LF power was significantly larger in inducible CAVB dogs compared to non-inducible CAVB dogs. (log[LF] -0.6 ± 1.54 in inducible dogs vs. -2.56 ± 0.43 in non-inducible dogs, $p < 0.001$).

Conclusion: In the CAVB dog, ventricular remodeling results in augmentation of respiratory and low frequency oscillations of LV MAPD. Furthermore, TdP inducible CAVB dogs show increased LF power compared to their non-inducible counterparts. The latter may reflect increased sympathetic firing that contributes to arrhythmogenesis.

Introduction

Repolarization lability, quantified as beat-to-beat fluctuations in action potential duration (APD), is known to contribute to arrhythmogenesis.[1,2] An increased beat-to-beat repolarization variability has been found in patients with a high risk of ventricular arrhythmias, such as patients with heart failure[3,4], ischemia[5], long QT syndrome[6,7], hypertrophic cardiomyopathy[8] or hypertension with left ventricular hypertrophy[9]. In these patients, adverse ventricular remodeling has caused a heterogeneous downregulation of repolarizing ionic currents and a disruption of normal Ca^{2+} handling.[10] As a result, the so called 'repolarization reserve' is reduced, making the process of repolarization instable and prone to arrhythmogenic challenges.[11]

In addition to beat-to-beat variations in repolarization, the APD also oscillates at a broader range of frequencies. First, APD fluctuates with respiration, which appears to be independent of the respiratory effects on heart rate.[12] Second, APD oscillates at a low frequency of around 0.1 Hz, which has been attributed to low frequency bursts of sympathetic nerve terminals on the ventricular myocardium.[13] While a sympathetically mediated low frequency pattern of arterial blood pressure (known as Mayer waves) has been well described,[14] oscillations at 0.1 Hz have only recently been found in APD as well.[13,15] Moreover, these fluctuations have also been identified on the surface ECG as changes in T wave vector angle between consecutive beats, referred to as 'periodic repolarization dynamics' (PRD).[16]

However, it is unknown whether APD oscillations at these frequency bands (i.e. respiratory and low frequency) reflect normal physiology or whether they are linked to the occurrence of ventricular arrhythmias. In this regard, a computational modeling study showed that during Ca^{2+} overload and reduction of repolarizing currents, APD oscillations could become arrhythmogenic and elicit afterdepolarizations.[17] Furthermore, in clinical studies of post-myocardial infarction patients, PRD appears to be a strong independent predictor of all-cause mortality.[18,19] Therefore, we could hypothesize that these oscillations are altered by ventricular remodeling, thereby further destabilising repolarization and contributing to arrhythmogenesis.

In the present study, we evaluated both respiratory and low frequency oscillations of APD in the chronic complete AV-block dog model. In this arrhythmogenic animal model, creation of complete AV-block results in ventricular remodeling and reduction of repolarization reserve. Administration of anesthesia and a pro-arrhythmic drug, i.e. the I_{Kr} blocker dofetilide, will act as the final 'hit' on repolarization, resulting in electrical storm with multiple episodes of Torsades de Pointes (TdP) arrhythmias in approximately 75% of the dogs.[20] This model has been widely used in our laboratory and by others to investigate the mechanisms of arrhythmogenesis in the remodeled heart.[2,21–23] Therefore, we could use this model to investigate whether ventricular

remodeling alters respiratory and low frequency oscillations of APD.

The current study is a retrospective analysis of previously performed experiments in which we have analyzed respiratory and low frequency oscillations under different conditions of remodeling, i.e. during sinus rhythm (SR), acutely after creation of AV-block (AAVB) and after (at least 2 weeks) of remodeling at chronic AV-block (CAVB). In addition, we compared inducible with non-inducible CAVB dogs, to evaluate the relevance of these oscillations for arrhythmogenesis.

Materials & methods

Animal handling was in accordance with the 'Directive 2010/63/EU of the European Parliament and of the Council of 22 September 2010 on the protection of animals used for scientific purposes' and the Dutch law, laid down in the Experiments on Animals Act. The Animal Experiment Committee of the University of Utrecht approved all experiments.

We did a retrospective analysis on electrophysiological data in our database of dog experiments executed between 2014 and 2017, that were done to study the mechanisms of TdP arrhythmias or to test new antiarrhythmic agents or interventions. In order to maintain a homogenous population, only dogs remodeled on their own idioventricular rhythm (IVR) were included, thereby excluding dogs that were chronically paced from the right ventricular apex (RVA), which has shown to influence the remodeling process. Furthermore, only baseline recordings before the administration of any antiarrhythmic drugs were used for the analysis to exclude the effect of these interventions on the oscillatory pattern of APD. In addition, we excluded experiments that had a baseline recording shorter than 5 minutes or recordings that had too much ectopy or noise.

Animal experiments

Detailed description of the experimental setup has been reported previously.[24,22] In brief, all experiments were performed under general anesthesia with induction via pentobarbital sodium 25 mg/kg i.v. and maintained by isoflurane 1.5% in O_2 and N_2O, 1:2. Animals were ventilated with positive pressure ventilation at a rate of 12 breaths/min. Next, monophasic action potential catheters (Hugo Sachs Elektronik, March, Germany) were introduced via the femoral artery and vein into the heart to measure the left ventricular and right ventricular monophasic action potential duration (LV and RV MAPD). In the initial experiment, complete atrioventricular (AV) block was created by radiofrequency ablation of the proximal His bundle. Subsequently, the dogs remodeled for at least 2 weeks on IVR.

In all experiments, after a baseline measurement of at least 5 minutes, infusion of the I_{Kr} blocker dofetilide (0.025 mg/kg in 5 minutes or before the first TdP) was started to test for inducibility of TdP arrhythmias. TdP was defined as a run of 5 or more short-coupled (occurring before the end of the T wave) ectopic beats, with polymorphic twisting of the QRS axis. When ≥3 TdP arrhythmias occurred in the first ten minutes after the start of infusion, the dog was considered inducible. During baseline and dofetilide challenge, all subjects were paced from the RV-apex at VVI60.

Data analysis

For this retrospective analysis, we used LV MAPD recordings at both SR, AAVB and CAVB conditions. The monophasic action potential was recorded with EP Tracer (Cardiotek, Maastricht, The Netherlands) at a sampling frequency of 1 kHz. LV MAPD was measured offline semi-automatically from the initial peak to 80% of repolarization using custom-made software in MATLAB (MathWorks, Natick, USA). In addition, for analysis of low frequency oscillations, the absolute difference in LV MAPD between two consecutive beats was calculated. Any extrasystolic beats and the subsequent post-extrasystolic beats were removed. The 5-minute time series of MAPD or MAPD difference was detrended and interpolated at 4 Hz via cubic spline interpolation to get evenly spaced samples. Data series were split into epochs of 512 samples with 50% overlap. Spectral analysis was performed in MATLAB with Welch's periodogram and a Hanning window to derive the power spectral density (PSD). The power of the frequency bands was calculated by integrating the area under the PSD plot for bandwidths of different frequencies. For the respiratory frequency (RF), we selected a frequency band between 0.19 Hz and 0.21 Hz, since all dogs were ventilated at 12 breaths per minute (every 5 seconds, 0.2 Hz). For the low frequency (LF) oscillations, we used a frequency band between 0.04 Hz and 0.15 Hz as has been used in previous studies[13,15], since the frequency of sympathetic bursts can differ between individual subjects.

Measurement of RR interval and QT interval was performed in lead II of the surface ECG. QT interval was corrected for heart rate (QTc) with the van der Water formula. Short-term variability (STV) of LV MAPD was calculated over 31 consecutive beats using the formula: $STV = \sum|D_{n+1} - D_n|/30 \times \sqrt{2}$, where D represents LV MAPD.

Statistical analysis

Numerical values are expressed as mean ± standard deviation (SD). Logarithmic transformation of both RF and LF was used to correct for skewness of the data. Normality of the transformed data was checked with the Shapiro-Wilk test. Group comparison was done with an unpaired Student's *t*-test. Group comparison of more than two groups was performed with a one-way analysis of variance (ANOVA) with Tukey's correction for

multiple comparisons. Statistical analysis of serial data was performed with a paired Student's *t*-test. A p-value < 0.05 was considered as statistically significant. Prism 6 (GraphPad Software, Inc., La Jolla, CA, USA) was used for the statistical analysis.

Results

A total of 39 experiments in 29 adult mongrel dogs (13 males, 16 females, weight 25 ± 2.5 kg) were used for the analysis. We included 10 dogs in SR, 10 dogs in AAVB and 19 dogs in CAVB (14 inducible, 5 non-inducible).

Baseline electrophysiological parameters

Baseline electrophysiological data at the three conditions (SR, AAVB, CAVB) are depicted in Table 1. As expected, QT interval increased acutely after creation of AV-block, due to the sudden drop in heart rate. In CAVB, electrical remodeling has occurred as seen by a significant increase in QT, QTc and LV MAPD. Furthermore, STV has significantly increased, reflecting a reduced repolarization reserve. Table 2 shows electrophysiological parameters separately for the non-inducible and inducible CAVB dogs. Of all parameters, only STV is significantly higher in the inducible dogs.

Table 1. electrophysiological parameters at sinus rhythm (SR), acute AV-block (AAVB) and chronic AV-block (CAVB)

* p < 0.05 vs. SR; § p < 0.05 vs. AAVB

	SR (n = 10)	AAVB (n = 10)	CAVB (n = 19)
RR (ms)	557 ± 32	1000*	1000
QT (ms)	267 ± 15	357 ± 19*	407 ± 56§
QTc (ms)	305 ± 15	357 ± 19	407 ± 56§
LV $MAPD_{80}$ (ms)	200 ± 11	243 ± 14*	275 ± 36§
STV LV $MAPD_{80}$ (ms)	0.31 ± 0.06	0.54 ± 0.30	1.20 ± 0.80§

Table 2. electrophysiological parameters of inducible vs. non-inducible CAVB dogs

* p < 0.05 vs. non-inducible

	inducible (n = 14)	non-inducible (n = 5)
RR (ms)	1000	1000
QT (ms)	414 ± 60	388 ± 43
QTc (ms)	414 ± 60	388 ± 43
LV $MAPD_{80}$ (ms)	283 ± 34	260 ± 34
STV LV $MAPD_{80}$ (ms)	1.39 ± 0.83*	0.64 ± 0.40

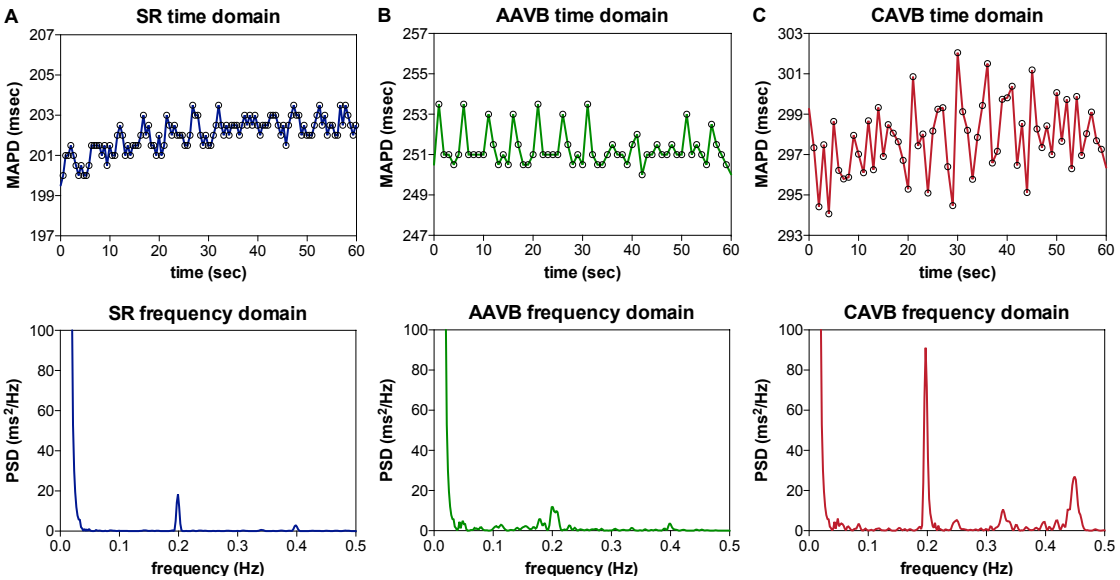

Figure 1. respiratory frequency oscillations in time and frequency domain

Representative examples of oscillations in monophasic action potential duration (MAPD) in the time domain and frequency domain during A) sinus rhythm (SR), B) acutely after creation of AV-block (AAVB) and C) after remodeling at chronic AV-block (CAVB). A clear increase in a 0.2 Hz oscillation is seen at CAVB.

Respiratory oscillations

Figure 1 show an example of the respiratory fluctuations in MAPD of dogs in SR, AAVB and CAVB in both the time domain and frequency domain. At SR and AAVB, low amplitude respiratory oscillations of LV MAPD were present, while at CAVB larger oscillations are seen around the respiratory frequency. Figure 2 displays the quantified logarithmic RF power (log[RF]) of the analysed dogs. The remodeling process (Figure 2A) has led to augmentation of the variability at the respiratory frequency, as seen by a significant increase in a log[RF] of -2.55 ± 1.48 and -2.99 ± 1.20 at SR and AAVB, respectively, to a log[RF] of -0.82 ± 1.53 ($p < 0.001$) at CAVB. When comparing inducible to non-inducible dogs, no significant difference could be found in RF power (Figure 2B).

Low frequency oscillations

Next, we examined low frequency oscillations in MAPD difference in SR, AAVB and CAVB. As depicted in Figure 3A, already a significant rise in LF power can be seen at AAVB compared to SR, which further increased after 2 weeks of remodeling (log[LF] of -3.91 ± 0.70 at SR, versus -2.52 ± 0.85 at AAVB and -1.14 ± 1.62 at CAVB, $p<0.001$). Finally, we looked for differences of these oscillations between inducible and non-inducible

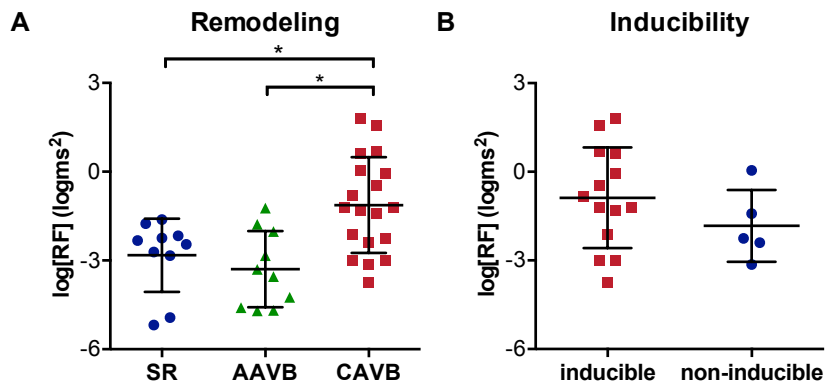

Figure 2. . Respiratory oscillations of monophasic action potential duration

A.) The logarithmic transformed power of respiratory oscillations of APD (log[RF]) at sinus rhythm (SR) acutely after AV-block (AAVB) and at chronic AV-block (CAVB). B.) log[RF] of the inducible versus the non-inducible CAVB dogs. * $p < 0.05$.

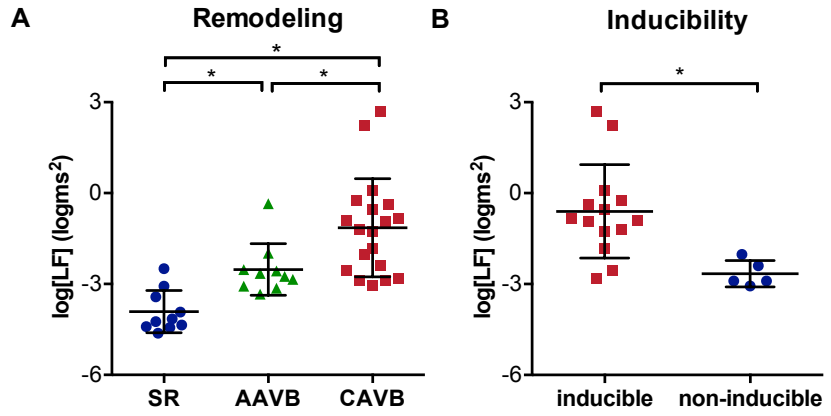

Figure 3. low frequency oscillations of monophasic action potential duration

A.) The logarithmic transformed power of low frequency oscillations of APD (log[LF]) at sinus rhythm (SR) acutely after AV-block (AAVB) and at chronic AV-block (CAVB). B.) log[LF] of the inducible versus the non-inducible CAVB dogs. * $p < 0.05$.

CAVB dogs. A representative example of the MAPD during the 5-minute recording of an inducible and a non-inducible dog is shown in Figure 4A. A clear oscillation can be observed in the inducible subject, with a rhythmic fluctuation in MAPD. This oscillatory behavior of MAPD can be more clearly discerned when the difference between consecutive beats is plotted against time (Figure 4B): approximately every 10-15 seconds, a clear increase in the variability between successive beats is seen. When this MAPD variability is visualized in the frequency domain by spectral analysis (Figure

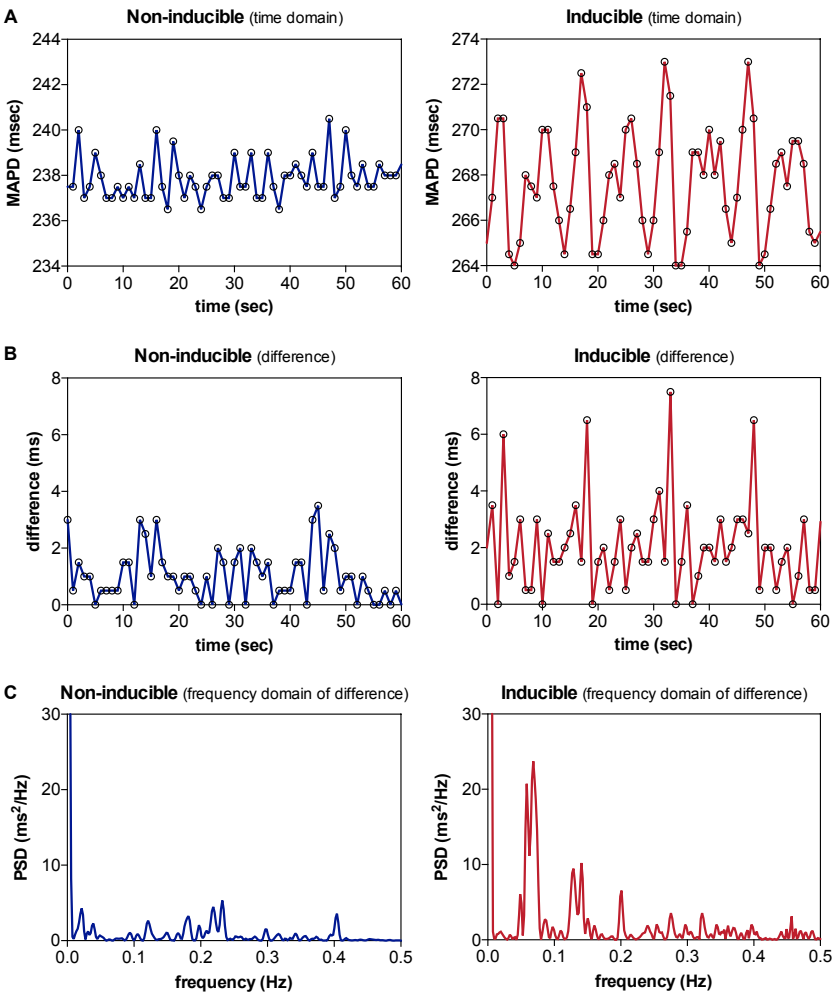

Figure 4. low frequency oscillations in a non-inducible dog versus an inducible dog

A representative example of MAPD (A), MAPD difference in the time domain (B) and MAPD difference in the frequency domain (C) of a non-inducible dog (left) and an inducible dog (right). A clear low frequency pattern in MAPD difference can be discerned in the inducible dog.

4C), a prominent peak appears in the low frequency band (0.04 – 0.15 Hz). As depicted in Figure 3B, the inducible dogs demonstrated a significant higher LF power of MAPD difference when compared to non-inducible dogs (log[LF] -0.6 ± 1.54 vs. -2.56 ± 0.43, $p < 0.001$).

Discussion

In this retrospective analysis of previously performed animal experiments we demonstrated that 1.) respiratory frequency oscillations of MAPD are increased after electrical remodeling, but they do not differentiate between inducible and non-inducible dogs, and 2.) Low frequency oscillations of MAPD difference are already increased at AAVB and rise even further at CAVB. Furthermore, these 0.1 Hz oscillations are more pronounced in CAVB dogs that are susceptible to dofetilide-induced TdP arrhythmias.

The CAVB dog model to study the effects of ventricular remodeling on arrhythmogenesis

A variety of structural heart diseases (e.g. myocardial infarction, pressure overload due to hypertension or aortic stenosis, volume overload as seen in valvular regurgitation) can lead to ventricular remodeling, thereby causing downregulation of potassium currents (I_{to}, I_{Ks}, I_{Kr}, I_{K1})[25], enhanced late Na^+ current ($I_{Na\text{-}L}$)[26] and Ca^{2+} handling abnormalities[27]. As a result, repolarization reserve is reduced, making the heart prone to repolarization-dependent ventricular arrhythmias. The CAVB dog model, as used in this study, is a model of ventricular remodeling and reduced repolarization reserve that reflects the vulnerable patient at risk of these arrhythmias. In this model, it has been shown that beat-to-beat variability of APD, quantified as STV, is a better marker of reduced repolarization reserve and pro-arrhythmia than APD prolongation itself.[1] STV is significantly increased at CAVB compared to AAVB and dogs susceptible to dofetilide-induced TdP arrhythmias show a further rise in STV prior to the occurrence of arrhythmias.[2] The predictive capabilities of STV have also been demonstrated in clinical studies, both in patients with congenital[6] or drug-induced long QT syndrome[7] as well as in patients with non-ischemic heart failure with a history of ventricular arrhythmias.[4]

In the current study, we have shown that not only successive beat-to-beat fluctuations of APD exists in the CAVB dog, but that the APD also oscillates at other frequency bands. This is in line with previous studies that have demonstrated important contributions of variation in heart rate[28], respiration[12] and autonomic nervous system activity[29] on APD variability. Concerning heart rate, a complex and dynamic APD to heart rate relation exists that is highly individual-specific and contains significant hysteresis effects.[30] In this study, we have eliminated important heart rate effects on APD by including only dogs that were paced during the experiments. Therefore, we could focus solely on the respiratory and autonomic influences on APD.

Respiratory oscillations of APD in the CAVB dog

While heart rate is well-known to fluctuate with respiration, it was recently shown by Hanson et al. that APD, measured as activation recovery interval (ARI) from the intracardiac electrogram, also displays rhythmic fluctuations in synchrony with respiration, even when heart rate was controlled by pacing. The authors suggested multiple mechanisms for the respiratory oscillations of APD. One of these, mechano-electrical feedback, relates to the modulation of electrophysiology by changes in ventricular loading conditions. Both in animal models as well as in patient studies, a direct effect of altered mechanical load on APD have been found; increased ventricular load resulted in shortening of the APD, while reduction in load was associated with prolongation of the APD.[31,32] Stress-activated ion-channels or alterations in Ca^{2+} handling have been suggested as the underlying molecular mechanism of load-dependent APD-changes.[33] Stress-activated ion channels are non-specific cation (Na^+, K^+ and Ca^{2+}) channels that open in respond to changes in mechanical stress instead of voltage.[34] In addition, mechanical stretch increases Ca^{2+} release from the sarcoplasmic reticulum, which can alter action potential duration by exchange for Na^+ in a 3:1 ratio via the Na^+-Ca^{2+}-exchanger.[35] One important physiological mechanism that can alter ventricular loading conditions is the change in intrathoracic pressure during respiration. During spontaneous inspiration, intrathoracic pressure drops, causing an increased systemic venous return to the RV, which will shift the interventricular septum into the LV. As a result, left ventricular end-diastolic volume and left ventricular preload will decrease. The opposite will occur during positive pressure ventilation: in that situation an increase in left ventricular preload will be seen during inspiration.[36] Nevertheless, in either case, a respiratory oscillatory behavior of ventricular loading is present, which could therefore alter APD in a cyclical pattern.

In the present study, we showed that the modulating effect of respiration on APD is enhanced after ventricular remodeling. A possible explanation could be that alternating changes in ventricular loading have greater impact on repolarization, when repolarization reserve is reduced. This is consistent with a study by Stams et al. in which the effect of preload changes on beat-to-beat variability of APD were studied in the CAVB dog.[37] The authors used a pacing protocol with either a constant or alternating PQ-interval to artificially control preload conditions. They observed that in AAVB, alternating preload had no effect on APD or STV. In contrast, in CAVB dogs pacing with an alternating PQ resulted in APD variability and a significantly higher STV compared to conditions of constant preload. Furthermore, blockade of stretch-activated ion current (I_{SAC}) by streptomycine prevented the increase of STV_{LVMAPD} during alternating preload. Although streptomycine is not a selective I_{SAC} -blocker and also has affinity for other ion channels that could affect STV (like L-type Ca^{2+} channels), these results suggest

that mechano-electrical feedback via specialized stretch-activated ion channels could have profound influence on repolarization during reduced repolarization reserve. This is further supported by a study of Kamkin et al., which showed that isolated cardiomyocytes from hypertrophied ventricles were more sensitive to stretch than control cardiomyocytes, resulting in changes in APD at smaller mechanical stimuli.[38] Thus, we may hypothesize that after remodeling and downregulation of repolarizing K^+ currents, the relative contribution of I_{SAC} to the repolarization process is increased, resulting in augmentation of APD variability caused by changes in respiration-mediated loading conditions.

Interestingly, we did not find a difference in respiratory oscillations between inducible and non-inducible CAVB dogs. A similar finding was reported by the study of Stams et al.: alternating preload, which led to an increase in APD variability, did not result in more TdP arrhythmias compared to conditions of constant preload. Therefore, we can assume that an additional trigger is required to create the optimal environment for dofetilide-induced TdP arrhythmias.

Low frequency oscillations of APD difference in the CAVB dog

Low frequency oscillations in the range from 0.04 to 0.15 Hz that are unrelated to respiration have long been observed in both heart rate and arterial blood pressure and are referred to as Mayer waves.[39] These oscillations have been linked to rhythmic bursts of sympathetic nervous system activity, however, the precise mechanism remains controversial. Two theories exist: 1.) these oscillations are the effect of a central autonomous oscillator within the central nervous system that fires at a certain frequency, or 2.) they are the result of a time delay in the baroreflex loop, causing resonance in the feedback system.[14] Either way, states of increased sympathetic activation, such as during tilt test or when blood pressure was artificially lowered, resulted in an increase in the magnitude of Mayer waves.[40,41] In addition, blockade of sympathetic drive resulted in a reduction of low frequency components of both RR interval and blood pressure.[41]

In addition to respiratory fluctuations, Hanson et al. showed that APD also displays an oscillatory pattern at Mayer wave frequency.[13] Moreover, these low frequency oscillations increased during autonomic challenge with Valsalva manoeuvre.[15] A similar low frequency oscillatory pattern was found by Rizas et al. in T wave vector changes on the surface ECG, called periodic repolarization dynamics (PRD).[42] These variations in T wave vector could also be increased with exercise and reduced by β-adrenergic blockade, suggesting a role for sympathetic input on the myocardium in the pathogenesis of these oscillations. Furthermore, increased PRD appeared to be a strong predictor of all-cause mortality in a cohort of more than 900 post-MI patients. Combined with a marker of

vagal activity (i.e. deceleration capacity), PRD was able to accurately stratify mortality risk in these patients.[19] Nevertheless, the cause of death, whether arrhythmic or due to pump failure, was not further specified.

In this regard, the findings of the current study could be of great interest. In this study we evaluated the effect of ventricular remodeling on low frequency oscillations, but, more importantly, whether these oscillations were different in dogs susceptible to arrhythmias. For this analysis the MAPD difference between two consecutive beats was used, instead of MAPD itself. The reason for this is that in the previous study by Rizas et al. PRD was also measured on differences in T wave vector between beats. They observed that approximately every 10 seconds, the T wave vector changed markedly, while in the intermittent periods T wave vector remained relatively stable. We hypothesized that 0.1Hz bursts of sympathetic discharge could also result in sudden changes in MAPD, which are more clearly visualized when spectral analysis is done on MAPD difference instead of MAPD.

Consequently, we could show that acutely after creation of AV-block, LF power of MAPD difference is already significantly increased. The sudden drop in cardiac output and blood pressure that occur after creation of AV-block will be sensed by baroreceptors in the aortic arch and carotid sinus, which will increase efferent sympathetic input on the heart, while simultaneously reducing parasympathetic firing. We observed this baroreflex-mediated increase in sympathetic tone by augmentation of low frequency APD oscillations acutely after AV-block. More importantly, ventricular remodeling further increased the low frequency oscillatory behavior of APD difference, but predominantly in CAVB dogs susceptible to drug-induced TdP arrhythmias. From the existing literature it becomes clear that increased sympathetic nervous system activity is an important contributor to repolarization variability and arrhythmogenesis. A study by Johnson et al. in isolated cardiomyocytes showed that the addition of β-adrenergic stimulation to a state of reduced repolarization reserve (by blockade of I_{Ks}) led to a dramatically increase in beat-to-beat variability of repolarization.[43] In addition, sympathetic stimulation promotes Ca^{2+} overload, spontaneous Ca^{2+} release and the formation of early and delayed afterdepolarizations (EADs/DADs).[44] More recently, a simulation study by Pueyo et al. evaluated the effect of phasic β-adrenergic stimulation on APD dynamics.[17] They observed a low frequency oscillatory pattern of APD, which magnitude increased with higher β-adrenergic strength. Interestingly, simulated pathological conditions of Ca^{2+} overload and reduced repolarization reserve (comparable to the CAVB dog model) enhanced the APD oscillations caused by adrenergic stimulation. Therefore, the authors suggested an important role of these oscillations for arrhythmogenesis. In the present study, we could confirm these *in silico* results experimentally in an arrhythmogenic *in vivo* model.

The reason for the clear differences in low frequency oscillations of APD difference

between inducible and non-inducible dogs remains speculative. Two mechanisms can be proposed: either repolarization reserve is even more reduced in the inducible dogs, therefore making the effect of β-adrenergic stimulation on repolarization more prominent and repolarization more vulnerable to arrhythmogenic challenges; however, in that case we would also have found an increased effect of respiration on APD in the inducible dogs. More likely the sympathetic output itself (either systematically or due to increased local density of sympathetic neurons) is further enhanced in the inducible dogs, causing increased repolarization instability, Ca^{2+} overload and triggered activity. Concerning the latter, studies in dogs with chronic AV-block and MI have shown that in addition to electrical remodeling, also neural remodeling takes place, as seen by denervation, hyperinnervation and nerve sprouting.[45,46] Regional hyperinnervation, where some regions are more densely innervated than others, combined with heterogeneous electrical remodeling, further enhances spatial dispersion of repolarization, thereby facilitating the initiation and perpetuation of ventricular arrhythmias.

Implications

In addition to beat-to-beat variation in APD or QT interval, we have shown that fluctuations in other frequency bands are altered in subjects with pro-arrhythmic ventricular remodeling and an increased risk of ventricular arrhythmias. Therefore, these oscillations may eventually be used in risk stratification of patients at high risk of sudden cardiac death, who might benefit from implantation of an Implantable Cardioverter-Defibrillator (ICD). While in the current study MAP catheters were used, Hanson et al. showed that respiratory and low frequency oscillations are also measurable on the ARI of intracardiac EGM, which could be obtained from implantable devices. Furthermore, PRD is a non-invasive parameter that can be measured from a converted 12-lead ECG, which would make it more suitable for risk stratification prior to ICD implantation. In this regard, PRD is currently being studied as a predictive marker in the multicentre, observational *EUropean Comparative Effectiveness Research to assess the use of primary prophylacTic Implantable Cardioverter Defibrillators (EU-CERT-ICD)* study (NCT02064192), which evaluates new risk stratification methods that could identify subgroups of patients with low or high risk of ICD shocks or mortality.

Study limitations

Since the CAVB dog is a specific model of ventricular remodeling caused by volume overload, extrapolation of these results to patients with other causes of remodeling (ischemia, infarction, pressure overload) should be done with caution.

Second, an important limitation of the study is its retrospective nature, which made it impossible to control for all, possibly confounding, variables. By selecting only dogs remodeled on IVR without control of activation pattern we tried to keep the analysed group of dogs as homogeneous as possible. Next, all dogs were mechanically ventilated with positive pressures, which has an opposite effect on loading conditions of the heart compared to spontaneous breathing. Nevertheless, both ventilation techniques result in an oscillatory pattern, albeit with a shift in phase. In addition, no direct measurements of neural activity were done to confirm that the low frequency oscillations of APD we found are caused by sympathetic discharge. Finally, all experiments were done under general anesthesia, which has profound effects on the autonomic nervous system. Yet, we know from other experiments in CAVB dogs that stellectomy results in significant reduction in TdP inducibility, which implies that, even under anesthetic conditions, the sympathetic nervous system contributes to arrhythmogenesis in this model.

Conclusion

In the chronic AV-block dog model, we observed oscillations of LV MAPD at respiratory frequency, which are augmented after remodeling compared to non-remodeled conditions. In addition, low frequency oscillations of MAPD difference were already altered acutely after creation of AV-block and increased even further at chronic AV-block conditions. Furthermore, CAVB dogs, that are susceptible to drug-induced TdP, show increased low frequency oscillations compared to their non-inducible counterparts. Thus, 0.1 Hz sympathetic bursts affect APD variability, which has important consequences for arrhythmogenesis.

References

1. Thomsen MB, Verduyn SC, Stengl M, et al. Increased short-term variability of repolarization predicts d-sotalol-induced torsades de pointes in dogs. *Circulation* 2004;110:2453–9.
2. Thomsen M, Oros A, Schoenmakers M, et al. Proarrhythmic electrical remodelling is associated with increased beat-to-beat variability of repolarisation. *Cardiovasc Res* 2007;73:521–30.
3. Berger RD, Kasper EK, Baughman KL, et al. Beat-to-beat QT interval variability: novel evidence for repolarization lability in ischemic and nonischemic dilated cardiomyopathy. *Circulation* 1997;96:1557–65.
4. Hinterseer M, Beckmann B-M, Thomsen MB, et al. Usefulness of short-term variability of QT intervals as a predictor for electrical remodeling and proarrhythmia in patients with nonischemic heart failure. *Am J Cardiol* 2010;106:216–20.

5. Murabayashi T, Fetics B, Kass D, et al. Beat-to-beat QT interval variability associated with acute myocardial ischemia. *J Electrocardiol* 2002;35:19–25.

6. Hinterseer M, Beckmann B-M, Thomsen MB, et al. Relation of increased short-term variability of QT interval to congenital long-QT syndrome. Am J Cardiol 2009;103:1244–8.

7. Hinterseer M, Thomsen MB, Beckmann B-M, et al. Beat-to-beat variability of QT intervals is increased in patients with drug-induced long-QT syndrome: a case control pilot study. E*ur Heart J* 2008;29:185–90.

8. Atiga WL, Fananapazir L, McAreavey D, et al. Temporal repolarization lability in hypertrophic cardiomyopathy caused by beta-myosin heavy-chain gene mutations. *Circulation* 2000;101:1237–42.

9. Piccirillo G, Germanò G, Quaglione R, et al. QT interval variability and autonomic control in hypertensive subjects with left ventricular hypertrophy. *Clin Sci (Lond)* 2002;102:363–71.

10. Armoundas AA, Wu R, Juang G, et al. Electrical and structural remodeling of the failing ventricle. *Pharmacol Ther* 2001;92:213–30.

11. Roden DM. Taking the “idio” out of “idiosyncratic”: predicting torsades de pointes. *Pacing Clin Electrophysiol* 1998;21:1029–34.

12. Hanson B, Gill J, Western D, et al. Cyclical modulation of human ventricular repolarization by respiration. *Front Physiol* 2012;3:379.

13. Hanson B, Child N, Van Duijvenboden S, et al. Oscillatory behavior of ventricular action potential duration in heart failure patients at respiratory rate and low frequency. *Front Physiol* 2014;5:414.

14. Malpas SC. Neural influences on cardiovascular variability: possibilities and pitfalls. Am J *Physiol Heart Circ Physiol* 2002;282:H6-20.

15. Porter B, van Duijvenboden S, Bishop MJ, et al. Beat-to-Beat Variability of Ventricular Action Potential Duration Oscillates at Low Frequency During Sympathetic Provocation in Humans. *Front Physiol* 2018;9.

16. Rizas KD, Nieminen T, Barthel P, et al. Sympathetic activity–associated periodic repolarization dynamics predict mortality following myocardial infarction. *J Clin Invest* 2014;124:1770–80.

17. Pueyo E, Orini M, Rodríguez JF, et al. Interactive effect of beta-adrenergic stimulation and mechanical stretch on low-frequency oscillations of ventricular action potential duration in humans. *J Mol Cell Cardiol* 2016;97:93–105.

18. Rizas KD, McNitt S, Hamm W, et al. Prediction of sudden and non-sudden cardiac death in post-infarction patients with reduced left ventricular ejection fraction by periodic repolarization dynamics: MADIT-II substudy. *Eur Heart J* 2017;38:2110–8.

19. Hamm W, Stülpnagel L, Vdovin N, et al. Risk prediction in post-infarction patients with moderately reduced left ventricular ejection fraction by combined assessment of the

sympathetic and vagal cardiac autonomic nervous system. *Int J Cardiol* 2017;249:1–5.

20. Oros A, Beekman JDM, Vos MA. The canine model with chronic, complete atrio-ventricular block. *Pharmacol Ther* 2008;119:168–78.
21. Oosterhoff P, Thomsen MB, Maas JN, et al. High-rate pacing reduces variability of repolarization and prevents repolarization-dependent arrhythmias in dogs with chronic AV block. *J Cardiovasc Electrophysiol* 2010;21:1384–91.
22. Dunnink A, van Opstal JM, Oosterhoff P, et al. Ventricular remodelling is a prerequisite for the induction of dofetilide-induced Torsades de pointes arrhythmias in the anaesthetized, complete atrio-ventricular-block dog. *Europace* 2012;14:431–6.
23. Zhou S, Jung B-C, Tan AY, et al. Spontaneous stellate ganglion nerve activity and ventricular arrhythmia in a canine model of sudden death. *Heart Rhythm* 2008;5:131–9.
24. Dunnink A, Sharif S, Oosterhoff P, et al. Anesthesia and Arrhythmogenesis in the Chronic Atrioventricular Block Dog Model. *J Cardiovasc Pharmacol* 2010;55:601–8.
25. Long VP, Bonilla IM, Vargas-Pinto P, et al. Heart failure duration progressively modulates the arrhythmia substrate through structural and electrical remodeling. *Life Sci* 2015;123:61–71.
26. Antzelevitch C, Nesterenko V, Shryock JC, et al. The Role of Late I Na in Development of Cardiac Arrhythmias. 2014. p. 137–68.
27. Sipido KR, Volders PGA, Schoenmakers M, et al. Role of the Na/Ca exchanger in arrhythmias in compensated hypertrophy. *Ann N Y Acad Sci* 2002;976:438–45.
28. Hnatkova K, Kowalski D, Keirns JJ, et al. Relationship of QT interval variability to heart rate and RR interval variability. *J Electrocardiol* 2013;46:591–6.
29. Baumert M, Schlaich MP, Nalivaiko E, et al. Relation between QT interval variability and cardiac sympathetic activity in hypertension. *Am J Physiol Circ Physiol* 2011;300:H1412–7.
30. Malik M, Hnatkova K, Novotny T, et al. Subject-specific profiles of QT/RR hysteresis. *Am J Physiol Circ Physiol* 2008;295:H2356–63.
31. Zabel M, Portnoy S, Franz MR. Effect of sustained load on dispersion of ventricular repolarization and conduction time in the isolated intact rabbit heart. *J Cardiovasc Electrophysiol* 1996;7:9–16.
32. Levine JH, Guarnieri T, Kadish AH, et al. Changes in myocardial repolarization in patients undergoing balloon valvuloplasty for congenital pulmonary stenosis: evidence for contraction-excitation feedback in humans. *Circulation* 1988;77:70–7.
33. Eckardt L, Kirchhof P, Breithardt G, et al. Load-induced changes in repolarization: evidence from experimental and clinical data. *Basic Res Cardiol* 2001;96:369–80.
34. Zeng T, Bett GCL, Sachs F. Stretch-activated whole cell currents in adult rat cardiac myocytes. *Am J Physiol Circ Physiol* 2000;278:H548–57.
35. Iribe G, Ward CW, Camelliti P, et al. Axial stretch of rat single ventricular cardiomyocytes

causes an acute and transient increase in Ca^{2+} spark rate. *Circ Res* 2009;104:787–95.

36. Mitchell JR, Whitelaw WA, Sas R, et al. RV filling modulates LV function by direct ventricular interaction during mechanical ventilation. *Am J Physiol Circ Physiol* 2005;289:H549–57.
37. Stams TR, Oosterhoff P, Heijdel A, et al. Beat-to-Beat Variability in Preload Unmasks Latent Risk of Torsades de Pointes in Anesthetized Chronic Atrioventricular Block Dogs. *Circ J* 2016;80:1336–45.
38. Kamkin A, Kiseleva I, Isenberg G. Stretch-activated currents in ventricular myocytes: amplitude and arrhythmogenic effects increase with hypertrophy. *Cardiovasc Res* 2000;48:409–20.
39. Julien C. The enigma of Mayer waves: Facts and models. Cardiovasc Res 2006;70:12–21.
40. Furlan R, Porta A, Costa F, et al. Oscillatory patterns in sympathetic neural discharge and cardiovascular variables during orthostatic stimulus. *Circulation* 2000;101:886–92.
41. Pagani M, Montano N, Porta A, et al. Relationship between spectral components of cardiovascular variabilities and direct measures of muscle sympathetic nerve activity in humans. *Circulation* 1997;95:1441–8.
42. Rizas KD, Nieminen T, Barthel P, et al. Sympathetic activity–associated periodic repolarization dynamics predict mortality following myocardial infarction. *J Clin Invest* 2014;124:1770–80.
43. Johnson DM, Heijman J, Pollard CE, et al. IKs restricts excessive beat-to-beat variability of repolarization during beta-adrenergic receptor stimulation. *J Mol Cell Cardiol* 2010;48:122–30.
44. Johnson DM, Heijman J, Bode EF, et al. Diastolic spontaneous calcium release from the sarcoplasmic reticulum increases beat-to-beat variability of repolarization in canine ventricular myocytes after β-adrenergic stimulation. *Circ Res* 2013;112:246–56.
45. Cao JM, Fishbein MC, Han JB, et al. Relationship between regional cardiac hyperinnervation and ventricular arrhythmia. *Circulation* 2000;101:1960–9.
46. Cao JM, Chen LS, KenKnight BH, et al. Nerve sprouting and sudden cardiac death. *Circ Res* 2000;86:816–21.

Chapter 10

General discussion

David J. Sprenkeler

General discussion

In the last 50 years, mortality of cardiovascular diseases has shown a steep decline, mainly attributed to improvement in the treatment of coronary artery disease and reduction of major cardiovascular risk factors.[1] Nevertheless, while nowadays most patients survive their acute cardiac event, many of them will go into ventricular remodeling, resulting in compensated hypertrophy and even heart failure. Since the prevention and treatment of hypertrophy and heart failure has shown less success, its prevalence continues to rise, making it a major public health problem worldwide.[2] Moreover, in patients with ventricular remodeling, the occurrence of ventricular tachyarrhythmias is an important and challenging issue, because these arrhythmias often occur without any warning signs and can result in sudden cardiac death (SCD).

Since the beginning of this century, the role of the Implantable Cardioverter-Defibrillator (ICD) for prevention of SCD in patients with left ventricular dysfunction has been well established.[3–5] However, while the ICD is effective in terminating malignant ventricular arrhythmias, important challenges remain in order to maximize the health benefit of ICD therapy.

Two of those challenges have been addressed in this thesis:

1) patient selection, i.e. how can we identify the patient at highest risk of SCD, who will have the most benefit from the ICD?

2) ICD functionality, i.e. how can we improve the functionality of the device in such a way, that it does not only work as 'rescue' treatment, but also prevents ventricular arrhythmias from occurring at all?

A parameter that predicts the occurrence of ventricular arrhythmias, for risk prediction in the long-term and for monitoring in the short-term, is essential to answer these questions. In order to find such a predictive parameter, we have focussed on the underlying process that plays a key role in the pathogenesis of ventricular arrhythmias: ventricular remodeling. Alterations in cardiac structure, Ca^{2+} handling, ion channel expression and autonomic nervous system function create the optimal environment for malignant arrhythmias to initiate and perpetuate. Simple biomarkers that reflect these changes are therefore ideal to function as parameters of increased arrhythmic risk. In this thesis, we have studied parameters of contractile (**part I**), electrical (**part II**) and neural remodeling (**part III)** and evaluated their relation to arrhythmogenesis both in the chronic complete AV-block (CAVB) dog as well as in patients at risk of SCD.

Part I – Parameters of contractile remodeling for risk prediction

Calcium is an essential second messenger in the process of excitation-contraction coupling, which drives contraction and relaxation of the cardiomyocyte.[6]

In normal physiology, modulation of intracellular [Ca^{2+}] enables the heart to alter its contractile performance in order to meet changing demands of the body. However, under pathological conditions, alterations in Ca^{2+} influx or release from the sarcoplasmic reticulum (SR) will have direct influence on cardiac contractility. In addition to contractile dysfunction, Ca^{2+} mishandling has been associated with arrhythmogenesis.[7] Therefore, we hypothesized that contractile parameters can give insight into someone's risk of developing triggered activity-related ventricular arrhythmias.

In **Chapter 2** we have discussed three physiological phenomena that reflect dynamic changes in intracellular Ca^{2+} handling: force-frequency relationship (FFR), mechanical restitution (MR) and post-extrasystolic potentiation (PESP). These parameters are regarded as macroscopic measures of intracellular Ca^{2+} homeostasis and appear to be altered in hypertrophy and heart failure.[8–10] However, data on the relation between these contractility measures and arrhythmogenesis are sparse. A previous study by de Groot et al. studied contractile remodeling in the CAVB dog and its association with triggered activity.[11] They demonstrated that ventricular remodeling resulted in increased contractility with a negative FFR and increased PESP. Furthermore, the dogs with highest inotropy were most susceptible to DADs. In **Chapter 3** we have demonstrated that the same relation can be found between contractile remodeling and Torsades de Pointes (TdP) arrhythmias: dogs inducible to TdP arrhythmias had higher contractility at low heart rate, a negative FFR, higher MR and PESP and slower MR kinetics. The results of this study further aid in our understanding how the different remodeling processes (electrical, structural, contractile) contribute to arrhythmia susceptibility in this animal model. In previous studies it became clear that electrical remodeling is already present after 2 weeks of remodeling, while biventricular hypertrophy develops more slowly, being fully present after 12-16 weeks of AV-block.[12,13] In addition, Peschar et al. have shown that pacing at a physiological rate after 8 weeks of CAVB could reverse structural remodeling, whilst having no effects on electrical remodeling.[14] These data indicate that structural and electrical remodeling are independent processes and that the structural changes are of far less importance for arrhythmogenesis. Regarding contractile remodeling, we have shown that contractile adaptations follow a similar path as electrical remodeling and are also already present at CAVB2. More importantly, the clear differences we found in contractile parameters between inducible and non-inducible dogs suggest an important role of contractile remodeling for arrhythmia susceptibility. While we did not perform any cellular experiments, we hypothesized that these observations are related to disruption of normal Ca^{2+} handling as the underlying mechanism of TdP arrhythmias. Previous *in vitro* studies have shown higher Ca^{2+} content of the SR, enhanced NCX current and increased $[Na^+]_i$ in cardiomyocytes of CAVB dogs.[15–17] The combination of an upregulated NCX and high $[Na^+]_i$ contributes to Ca^{2+} overload of the cardiomyocyte via 'reverse mode' Na^+-Ca^{2+}-exchange. Moreover,

under conditions of reduced repolarization reserve, spontaneous Ca^{2+} release aids in the formation of EADs, which is the main trigger of TdP arrhythmias.[15] We have tested this hypothesis by increasing $[Na^+]_i$ via blockade of Na^+-K^+-ATPase with ouabain, which could convert a non-inducible dog into an inducible one, indicating the importance of high $[Na^+]_i$ and Ca^{2+} overload for the initiation of TdP arrhythmias.

More importantly, we were able to identify the inducible dogs by *in vivo* risk markers with high specificity and sensitivity. Three contractile parameters, i.e. LV dP/dt_{max} at low rate, the slope of the FFR-curve and the time constant of the MR-curve could almost completely separate inducible from non-inducible dogs and were also linearly correlated with the amount and the severity of TdP arrhythmias. This could be explained by the direct relation between these markers and Ca^{2+} handling. Inversion of the FFR reflects enhanced NCX activity, high $[Na^+]_i$ and Ca^{2+} overload and thus an increased risk of triggered arrhythmias.[18] MR is related to the time-dependent availability of releasable Ca^{2+}. Slower MR (i.e. a higher MR time constant) is the result of altered RyR2 function or reduced reuptake of Ca^{2+} into the SR by SERCA2a. While SERCA2a expression has shown to be unchanged in the CAVB dog, a study by Peschar et al. showed that the SERCA2a/NCX ratio is reduced, which could have impact on Ca^{2+} reuptake.[13] Therefore, alterations in NCX activity also affect the time constant of MR. As such, both MR and FFR function as biomarkers of changes in Ca^{2+} cycling of the cardiomyocyte and the associated risk of triggered arrhythmias.

Furthermore, we must address that the most sensitive parameter of electrical remodeling, STV (see below), is also attributed, directly or indirectly, to altered Ca^{2+} handling. We know that buffering of Ca^{2+} with BAPTA-AM, reducing Ca^{2+} overload by flunarizine or blockade of NCX by SEA-4000 all reduce STV and can prevent EADs and TdP arrhythmias.[19–22] Therefore, we may conclude that contractile and electrical remodeling are partially interconnected and together create the trigger of ventricular arrhythmias, as illustrated in Figure 1.

Future directions

A number of questions remain. First of all, new *in vitro* studies are needed to confirm our hypotheses that the differences in contractile parameters between inducible and non-inducible dogs are caused by alterations in Ca^{2+} handling and $[Na^+]_i$.

Second, as depicted in Figure 2 of the Introduction, LV dP/dt_{max} starts to decline again after 6 weeks of remodeling, while TdP inducibility remains relatively stable in time. This would argue against a role of contractile alterations in the generation of TdP arrhythmias. Therefore, we must keep the option open that the correlation we found between contractile remodeling and arrhythmogenesis is not causal. However, limited data is available on the exact course of contractile remodeling at longer durations of CAVB. Moreover, the other contractile parameters (FFR, MR & PESP) have never been

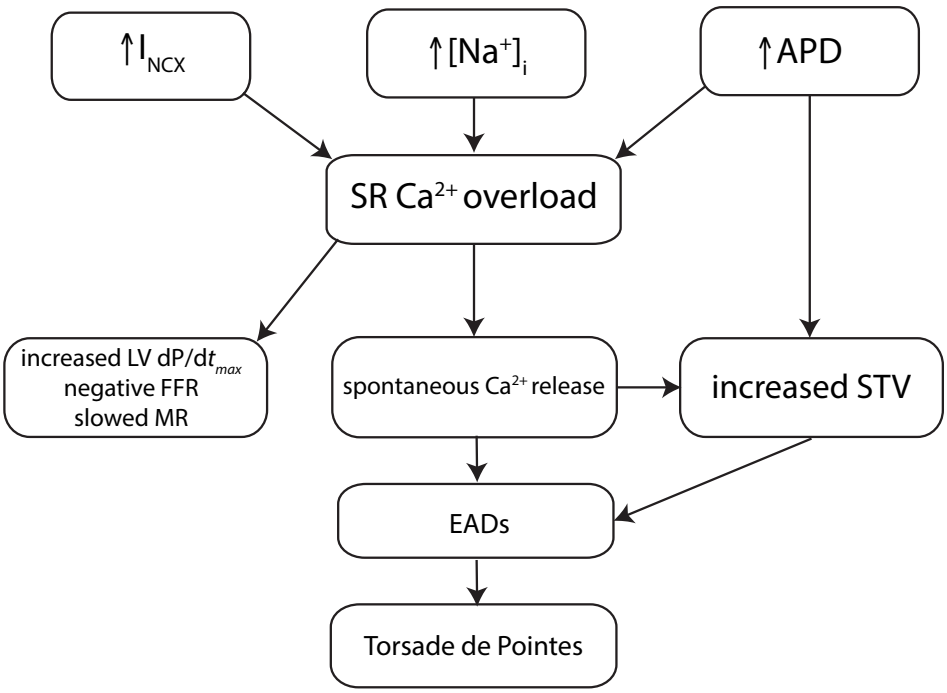

Figure 1. Schematic overview of the relation between contractile remodeling, electrical remodeling and the initiation of TdP arrhythmias.

Contractile remodeling results in SR Ca^{2+} overload, which can be measured *in vivo* by contractility parameters. Spontaneous Ca^{2+} release during Ca^{2+} overload can facilitate the occurrence of EADs and TdP arrhythmias. Spontaneous Ca^{2+} release also contributes to STV.

studied later then CAVB6. Therefore, these parameters might potentially be more sensitive markers of Ca^{2+} handling than LV dP/dt_{max} alone.

Finally, in their current form, these contractile parameters are not suitable for risk prediction on a large scale. They are measured with an intracardiac pressure catheter, which requires an invasive procedure with risk of complications. However, a study by Sinnecker et al. evaluated PESP of arterial blood pressure via a finger photoplethysmographic device.[23] While this requires spontaneous ectopy to occur, of which the coupling intervals cannot be controlled, it has the advantage of being simple to use, non-invasive and repeatable in time. Currently, this method is being studied as a potential predictor of mortality or appropriate ICD shock in the EU-CERT-ICD study.

Part II. Parameters of electrical remodeling for risk prediction & monitoring

Electrophysiological risk predictors, such as markers of altered depolarization or

repolarization, have been studied extensively in clinical studies of risk stratification.[24–27] However, the results have not been unambiguous and none of these risk markers have yet been implemented into clinical practice. Currently, the indication for ICD implantation is solely based on heart failure symptoms (NYHA class) and a mechanical parameter, left ventricular ejection fraction (LVEF), which is known to have limited sensitivity and specificity in identification of the patient at high risk of SCD. This has become even more apparent after publication of the DANISH trial, which failed to show a survival benefit of ICD therapy in patients with non-ischemic cardiomyopathy. These observations highlight the need for selection criteria that are more directly related to the trigger or the substrate of ventricular arrhythmias.

Differentiating arrhythmia and mortality risk

An important problem in risk prediction for ICD therapy is that of a competing risk of non-arrhythmic causes of death, which mainly involves the risk of dying of pump failure due to progression of heart disease. Patients who have progressed into overt heart failure are at increased risk of dying before having a life-saving ICD shock, therefore they will not benefit from ICD implantation, but are still at risk of device-related complications. In contrast, the ideal patient will have a high arrhythmic risk, but a low to moderate risk of death from non-sudden causes (Figure 2). This is supported by the subgroup analysis of the DANISH trial which shows a survival benefit of ICD therapy in younger patients (below 59 years of age) and in patients with a low NT-pro-BNP, thus patients who have a lower risk of dying from progressive heart failure.[28]

The issue of competing risks is addressed in **Chapter 4**, where the results of the EU-TrigTreat clinical study are presented. In this prospective cohort study, a number of demographic and electrical parameters were put into a multivariate prediction model to get an approximation of the risk of appropriate ICD shock, separate from the risk of all-cause mortality. Interesting to notice, LVEF was an independent predictor of both appropriate shock and all-cause mortality, which further emphasizes that LVEF is not the right criterion to select a patient for ICD implantation. Using data from more than 600 patients, two separate risk models for shock and mortality could be constructed with a high degree of accuracy. For appropriate shock risk, programmed electrical stimulation during EP-study was an independent predictor, while microvolt T wave alternans (MTWA) just missed the final model. Interestingly, the predictors of appropriate shock were less significant than predictors of all-cause mortality, stressing the difficulty in identifying the patients at high arrhythmia risk.

What will be the implications if this study for risk stratification in ICD therapy? An important drawback of the study is the mixed bag population of patients with a primary or secondary prevention ICD-indication. There is strong consensus about the validity of ICD implantation for secondary prophylaxis, which is confirmed again in

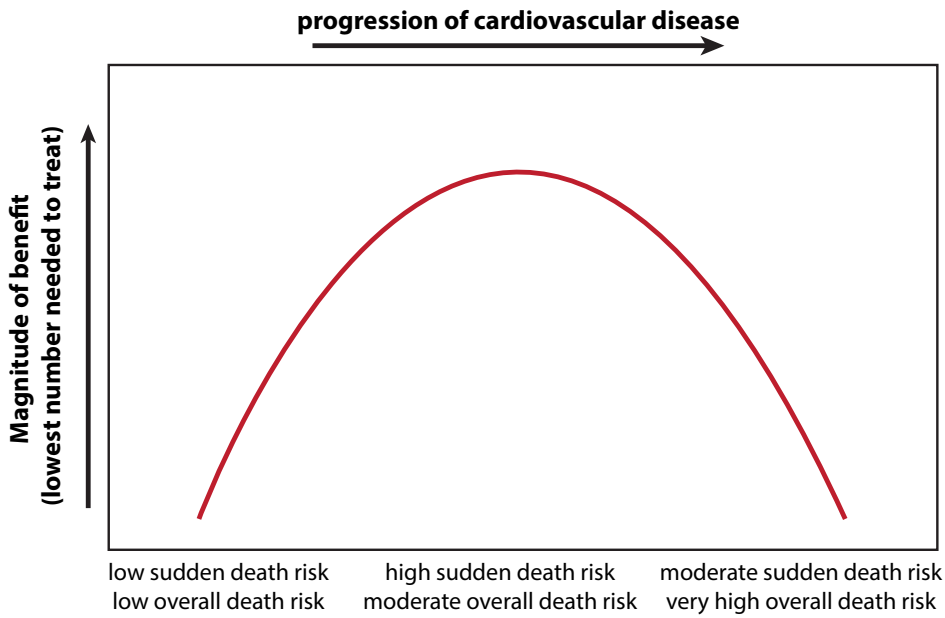

Figure 2. relation between the benefit of ICD implantation and progression of cardiovascular disease. During progression of the disease the risk of competing causes of death increases, thereby reducing the benefit of ICD therapy. Adapted from Dorian P. CMAJ. 2009

this study, since a secondary indication was a strong predictor of appropriate shock. Nonetheless, the current debate mainly concerns the primary prevention indications for ICD implantation. However, applying these risk models, which were studied in a mixed population, on these primary prevention patients only, should be done with caution.

Secondly, the strongest predictor of appropriate shock, programmed electrical stimulation, is not an ideal tool for risk prediction in clinical practice: it requires an invasive procedure and the negative predictive value is poor.[29] MTWA, albeit less invasive, requires exercise testing or pacing, cannot be performed during atrial fibrillation and is often inconclusive.[30] Therefore, it remains to be seen if the results of this study will directly affect current practice. Nevertheless, the EU-TrigTreat clinical study gives a prime example of the complexity of risk prediction in the decision-making of ICD implantation. The currently enrolling EU-CERT-ICD study investigates solely non-invasive risk predictors in a larger cohort of 2200 primary prevention ICD patients and the results are expected in 2019. Hopefully, the outcome of this large observational study will make it possible to construct a simple risk prediction score that can be implemented in the new guidelines.

STV at baseline: a marker of reduced repolarization reserve

The principle of repolarization reserve was introduced in 1997 by Dan Roden

and describes the redundancy in repolarizing currents (I_{Ks}, I_{Kr}, I_{K1}) to ensure normal repolarization, even when one repolarizing current is lost.[31] During ventricular remodeling, downregulation of potassium channels results in a reduction of repolarization reserve, making the heart prone to arrhythmogenic challenges. Short-term variability (STV) is a quantification of beat-to-beat variations in repolarization and can be derived from either the monophasic action potential (STV_{MAPD}), intracardiac EGM (STV_{ARI}) or 12-lead ECG (STV_{QT}). STV has been regarded as a simple measure of repolarization reserve and is superior to repolarization duration alone. Previous studies in the CAVB dog showed that STV_{MAPD} at baseline is increased after remodeling and higher in inducible versus non-inducible dogs.[32] Furthermore, the same was found in STV_{QT} in retrospective cohorts of patients with reduced repolarization reserve, such as patients with congenital or acquired long QT syndrome or non-ischemic heart failure.[33–35] Initially, STV_{QT} was included in the EU-TrigTreat clinical study, but failed to predict shock or mortality during long-term follow-up and was therefore excluded from the final manuscript. One possible explanation for this negative result is addressed in **Chapter 6**. In this chapter, we studied the circadian pattern of STV_{QT} in low and high arrhythmogenic subgroups of ICD patients as a pilot study of the EU-CERT-ICD study. Patients with a high number of arrhythmic events on Holter had two prominent peaks of STV_{QT} around 08:00 and 18:00, while at other time points no significant differences were seen between the two groups. In the EU-TrigTreat clinical study, only a minority of ECGs were made during these two time points, which may have reduced the predictive power of STV_{QT} for shock and all-cause mortality.

The study presented in Chapter 6 also highlights the dynamics of STV_{QT} in time. The peaks in the early morning and late afternoon in the arrhythmogenic group may be caused by a shift in autonomic tone from predominantly vagal to sympathetic activity, which would increase STV_{QT} in patients with reduced repolarization reserve. This is in line with cellular studies, in which additional β-adrenergic stimulation to a reduced repolarization reserve increased beat-to-beat repolarization variability and induced EADs and DADs.[19,20] Furthermore, studies in dogs with pacing-induced heart failure, found an increased QT variability associated with high sympathetic activity.[36] Therefore, STV_{QT} will be a more sensitive marker of increased arrhythmia risk, when measured during moments of high sympathetic tone. In the EU-CERT-ICD study, analysis of STV_{QT} is done at these time points to further explore its potential as risk predictor.

STV prior to arrhythmia: monitoring of arrhythmic risk

In addition to its dynamic behavior over the day, STV has also shown to increase abruptly prior to the occurrence of drug-induced TdP arrhythmias in the CAVB dog.[32] Therefore, STV might not only be suitable for risk stratification, but could also be used for continuous monitoring of imminent arrhythmic risk. In **Chapter 7** we assessed whether

we could use STV_{ARI} derived from the EGM of the ICD lead for prediction of upcoming arrhythmic episodes. We showed that STV_{ARI} of the RV is comparable to STV_{MAPD} of the LV and that STV_{ARI} increases significantly prior to the occurrence of ventricular arrhythmias under both anesthetic and awake conditions. Incorporating STV measurement for monitoring of arrhythmic risk would greatly improve the functionality of implantable devices. Currently, the ICD exerts its therapy in the form of anti-tachycardia pacing (ATP) or shock, only if the presence of a ventricular arrhythmia is sensed by the device. Both appropriate and inappropriate ICD therapy are known to have profound impact on the lives of ICD recipients. Furthermore, because of a time delay between arrhythmia detection and shock delivery, there is a risk of injury. Combining monitoring with a preventive intervention would avoid these negative consequences of ICD therapy.

However, continuous monitoring requires automatic and accurate STV calculation. In cooperation with Medtronic, we have developed a new method for automatic STV measurement by the ICD, which is presented in **Chapter 8**. This method uses the area under the gradient of the T wave signal to determine with great precision the end of the T wave for every single beat. We have shown that the automatic STV_{ARI} calculation is highly correlated with the gold standard STV_{MAPD} and that it has very good sensitivity and specificity in predicting the occurrence of TdP arrhythmias in the CAVB dog. An advantage of the new method is its independence on T wave morphology; current methodologies use the maximal dV/dt of the T wave as T wave end, however, there is still controversy about the validity of this method for positive or biphasic T waves.[37] Furthermore, the new method appears less dependent on sampling frequency compared to previous methods, possibly due to the use of the area of the gradient

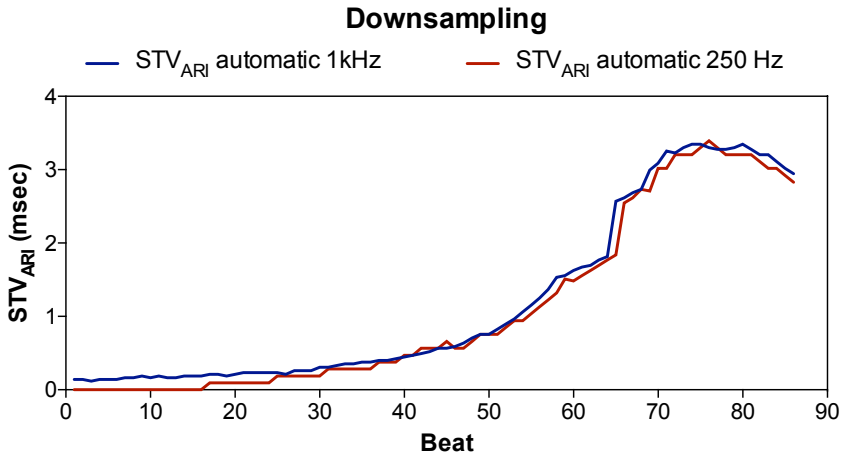

Figure 3. The effect of downsampling of the EGM-signal on STV_{ARI}.
No clear differences are seen between STV_{ARI} measured with the automatic method on a signal sampled with 1 kHz or the same signal downsampled to 250 Hz.

instead of a single time point of the raw signal (see Figure 3). Using a lower sampling rate, premature battery depletion is prevented when this monitoring option is used continuously.

Moreover, monitoring would be pointless, if it does not have any therapeutic consequences. Ideally, the device would start a preventive intervention when it senses that an arrhythmic episode is upcoming. Wijers et al. have demonstrated that temporary accelerated pacing (TAP), initiated just after the first ectopic beat, is highly effective in prevention of TdP arrhythmias in the CAVB dog.[38] Pacing at a higher heart rate shortens action potential duration and thereby strengthens repolarization. In addition, rate smoothing algorithms have shown to prevent ventricular arrhythmias in patients with long QT syndrome.[39] Continuous monitoring by STV_{ARI} would make it possible to anticipate and therefore start these interventions at an earlier moment, well before the occurrence of any ectopic beats.

Future directions

We have shown that short-term variability of repolarization has potential for both long-term risk prediction as well as 24/7 monitoring. However, there are still some challenges to be solved, before STV will be used in clinical practice. Since there is no cancellation of measurement error and the values of STV are in order of milliseconds, precise determination of fiducial points is key to find meaningfull data. The method of fiducial segment averaging, as used in Chapter 6 and 7, greatly improves the accuracy of STV calculation. Nonetheless, even this method is susceptible to noise in the recording. The automatic method, introduced in Chapter 8, is more precise; however, this method is only available for intracardiac EGMs. An accurate automatic method for STV_{QT} is needed when this parameter is used for risk stratification on a large scale. In addition to these methodological problems, STV is also greatly affected by heart rate, because of a complex and highly individual RR/QT-relation; however, the right way to correct for this (if any) is still under investigation. Finally, while we have considerable evidence for the importance of reduced repolarization reserve in patients with congenital or acquired long QT syndrome, it is less clear if STV predicts ventricular arrhythmias in patients with other underlying heart diseases. Along these lines, the abrupt increase in STV prior to ventricular arrhythmias has only been demonstrated in the CAVB dog model. It would be of great interest to see if these results can be confirmed in animal models or patients with other causes of ventricular remodeling. Currently, the automatic STV determination method is being made suitable for download on a device in order to further investigate the combination of continuous monitoring and temporary accelerated pacing for the prevention of ventricular arrhythmias. Furthermore, plans are made for a clinical study to evaluate if this new functionality can reduce the number of ICD shocks.

Part III. Parameters of neural remodeling for risk prediction

In the final part of this thesis we shortly addressed the effects of ventricular remodeling on two oscillatory patterns of APD, other than beat-to-beat variability (see Figure 4). One of these oscillatory patterns is due to respiration. Respiratory oscillations of APD have been demonstrated on intracardiac EGMs of heart failure patients, even when heart rate was controlled by pacing.[40] Recently it was found that APD also oscillates at an even lower frequency, below 0.1Hz.[41] These low frequency fluctuations resemble the so called 'Mayer waves': 0.1 Hz fluctuations in blood pressure, which have been attributed to bursts of sympathetic nervous system activity on the vasculature. In **Chapter 9** we performed spectral analysis of MAP-recordings to visualize oscillations of APD at these different frequency bands in the CAVB dog. In this study, we were able to identify oscillations at both a respiratory frequency as well as a low frequency and we discovered that ventricular remodeling alters the amplitude of both these oscillations. Noteworthy, only the effects on low frequency oscillations were different for inducible and non-inducible dogs.

Regarding the respiratory fluctuations of APD, mechano-electrical feedback has been suggested as one of the mechanisms: variations in intrathoracic pressure alters venous return and end-diastolic wall stress, which is known to have direct effect on repolarization.[42] After ventricular remodeling, the effects of wall stress on APD are amplified. These results are perfectly in line with a study by Stams et al. which showed increased APD fluctuations in the CAVB dog, when preload was varied by pacing with an alternating PQ-interval.[43] Important to notice, this preload-induced APD variability could only be observed under remodeled conditions. Therefore we can hypothesize that under conditions of reduced repolarization reserve, APD is more sensitive to changes in wall stress, possibly due to a greater contribution of stress-activated ion channels on repolarization. However, we did not find differences in respiratory oscillations between inducible and non-inducible dogs. Thus, while an increase in respiratory oscillations at CAVB reflects a reduced repolarization reserve, additional modulating factors are needed to create an environment where arrhythmias can be induced.

The autonomic nervous system may take this role as modifier of arrhythmic susceptibility. We have seen that the low frequency oscillations of APD, which are attributed to sympathetic nervous system firing, are significantly higher in inducible CAVB dogs compared to non-inducible dogs. This may be due to functional or even anatomical alterations of the autonomic nervous system, referred to as neural remodeling. Previous studies in dogs with AV-block and myocardial infarction have shown regional denervation, hyperinnervation and sprouting of cardiac neurons, which led to spontaneous ventricular arrhythmias and SCD.[44,45] Besides direct damage to nerve endings by ischemia, it is also known that chronic exposure to sympathetic

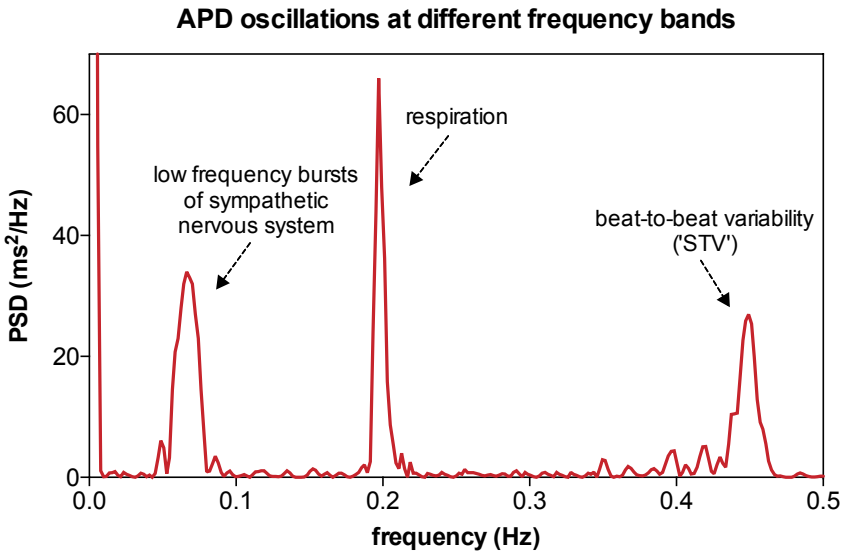

Figure 4. Schematic overview of APD oscillations different frequency bands.

Beat-to-beat variability resides at a high frequency within the frequency spectrum. Respiratory effects on APD has a peak at 0.2 Hz (12 breaths/min). The effect of sympathetic activity is seen in the low frequency range (below 0.1 Hz).

activity, such as during states of pressure or volume overload, can result in sympathetic rejuvenation and hyperinnervation.[46] In the CAVB dog, it has been shown that removing sympathetic input on the ventricular myocardium by bilateral stellectomy resulted in almost complete prevention of dofetilide-induced TdP arrhythmias (thesis A. Bossu, unpublished data). Therefore, autonomic modulation of the arrhythmogenic substrate or trigger seems to be of great importance for arrhythmogenesis.

Future directions

Currently, direct evidence for the presence of neural remodeling in the CAVB dog is lacking. In addition, no direct measurements of sympathetic nerve activity have been performed. Also, the effect of stellectomy on low frequency oscillations of APD needs to be demonstrated. Together this would give more insight into the role of sympathetic remodeling on arrhythmogenesis in this model. More importantly, since low frequency oscillations of APD reflect enhanced sympathetic activity, they can be used for risk stratification. While the use of MAP catheters is cumbersome in clinical practice, a low frequency oscillatory pattern has recently been found in T wave vector angle on the 12-lead surface ECG.[47] This non-invasive parameter, called periodic repolarization dynamics (PRD), appeared to be a strong predictor of mortality in post-MI patients. Currently, PRD is included in the EU-CERT-ICD study to help identify the patient at high risk of SCD.

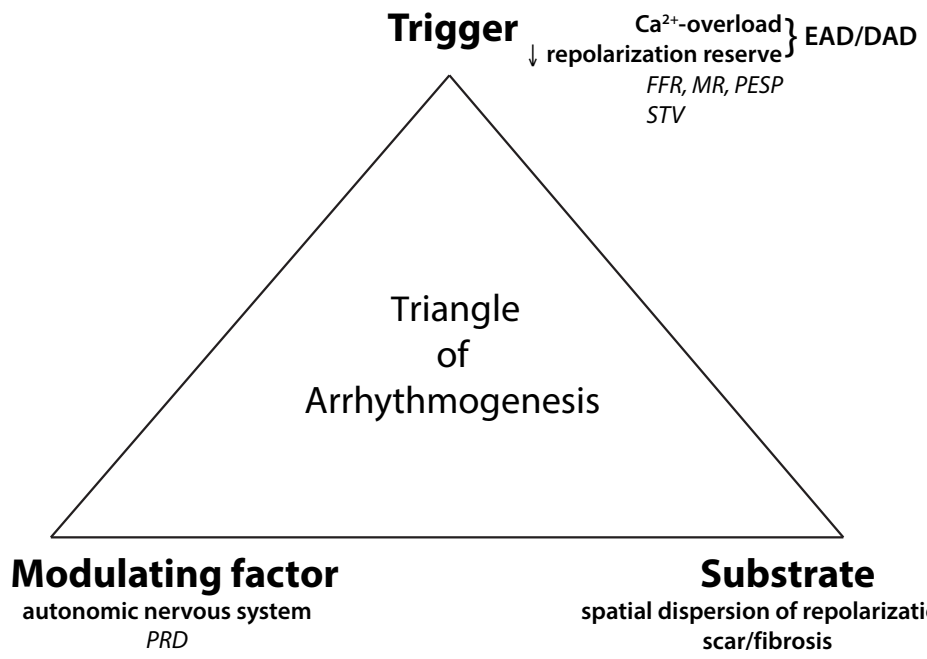

Figure 5. Philippe Coumel's Triangle of Arrhythmogenesis.

A clinical significant arrhythmia requires a trigger, a substrate and a modulating factor. EADs and DADs are triggers of ventricular arrhythmias. In the CAVB dog, spatial dispersion of repolarization enables the arrhythmia to perpetuate. In other forms of remodeling, conduction slowing and fibrosis, e.g. due to scar, form a substrate for reentry. Finally, the autonomic nervous system is a modulating factor, affecting both the trigger (Ca^{2+} overload) as well as the substrate (spatial dispersion).

Conclusion

More than thirty years ago, one of the founding fathers of modern electrophysiology, Philippe Coumel, stated that 'it is not the arrhythmic event that is interesting, but what was before the arrhythmic event', by which he stressed the importance of finding risk markers for ventricular arrhythmias.[48] In this thesis, we have explored markers of different components of ventricular remodeling as possible candidates. We have shown that contractility and arrhythmogenesis are intertwined and that contractile parameters have the potential in defining the patient at risk. We have demonstrated that STV is a highly dynamic marker of repolarization reserve and that it can be used for both long-term risk prediction as well as for continuous monitoring. Finally, we found that the low frequency bursts of sympathetic nervous system activity are related to arrhythmic susceptibility. All these findings can be put together in a concept, founded by Phillipe Coumel, known as the triangle of arrhythmogenesis (Figure 5): a clinical relevant arrhythmia requires both a trigger, an

arrhythmogenic substrate, and a modulating factor. In the CAVB dog, the triggers for arrhythmia are EADs and DADs, caused by Ca^{2+} overload and reduced repolarization reserve. Contractile parameters and STV are risk markers that reflect the propensity of these triggers to occur. Next, a substrate is needed for the triggered arrhythmias to perpetuate. While not addressed in this thesis, it is known that spatial dispersion of repolarization is required for TdP arrhythmias to sustain in the CAVB dog. In other forms of remodeling, for example when healthy myocardium has been replaced by scar tissue, both conduction delay and fibrosis contribute to the substrate. Currently, late gadolinium enhanced MRI (LGE-MRI) is a promising risk marker for visualization of the arrhythmogenic substrate in these patients. Finally, the sympathetic nervous system is the modifying factor, affecting both the trigger as well as the substrate: it contributes to Ca^{2+} overload, it further reduces repolarization reserve and it enhances spatial dispersion of repolarization.

Keeping these three factors in mind, one clearly understands why the individual risk markers alone are limited in predicting arrhythmic risk. However, combining markers of both the trigger (e.g. STV), modulating factor (e.g. PRD) and the substrate (e.g LGE-MRI), would make it possible to define a risk prediction score that is far more accurate. Using this polyparametric approach, we will be able to deliver tailored and personalized medicine by identifying patients who will benefit the most from ICD therapy.

References

1. Atlas Writing Group A, Timmis A, Townsend N, et al. European Society of Cardiology: Cardiovascular Disease Statistics 2017. *Eur Heart J* 2018;39:508–79.
2. Savarese G, Lund LH. Global Public Health Burden of Heart Failure. Card Fail Rev 2017;3:7.
3. Moss AJ, Zareba W, Hall WJ, et al. Prophylactic implantation of a defibrillator in patients with myocardial infarction and reduced ejection fraction. *N Engl J Med* 2002;346:877–83.
4. Bardy GH, Lee KL, Mark DB, et al. Amiodarone or an implantable cardioverter-defibrillator for congestive heart failure. *N Engl J Med* 2005;352:225–37.
5. Kurtz SM, Ochoa JA, Lau E, et al. Implantation trends and patient profiles for pacemakers and implantable cardioverter defibrillators in the United States: 1993-2006. *Pacing Clin Electrophysiol* 2010;33:705–11.
6. Bers DM. Cardiac excitation-contraction coupling. *Nature* 2002;415:198–205.
7. Sipido KR. Calcium overload, spontaneous calcium release, and ventricular arrhythmias. *Heart Rhythm* 2006;3:977–9.

8. Prabhu SD, Freeman GL. Effect of tachycardia heart failure on the restitution of left ventricular function in closed-chest dogs. *Circulation* 1995;91:176–85.

9. Pieske B, Kretschmann B, Meyer M, et al. Alterations in intracellular calcium handling associated with the inverse force-frequency relation in human dilated cardiomyopathy. *Circulation* 1995;92:1169–78.

10. Seed WA, Noble MI, Walker JM, et al. Relationships between beat-to-beat interval and the strength of contraction in the healthy and diseased human heart. *Circulation* 1984;70:799–805.

11. de Groot SH, Schoenmakers M, Molenschot MM, et al. Contractile adaptations preserving cardiac output predispose the hypertrophied canine heart to delayed afterdepolarization-dependent ventricular arrhythmias. *Circulation* 2000;102:2145–51.

12. Donker DW, Volders PGA, Arts T, et al. End-diastolic myofiber stress and ejection strain increase with ventricular volume overload--Serial in-vivo analyses in dogs with complete atrioventricular block. *Basic Res Cardiol* 2005;100:372–82.

13. Peschar M, Vernooy K, Cornelussen RN, et al. Structural, electrical and mechanical remodeling of the canine heart in AV-block and LBBB. *Eur Hear J* Suppl 2004;6:D61–5.

14. Peschar M, Vernooy K, Vanagt WYR, et al. Absence of reverse electrical remodeling during regression of volume overload hypertrophy in canine ventricles. *Cardiovasc Res* 2003;58:510–7.

15. Sipido KR, Volders PGA, Schoenmakers M, et al. Role of the Na/Ca exchanger in arrhythmias in compensated hypertrophy. *Ann N Y Acad Sci* 2002;976:438–45.

16. Verdonck F, Volders PGA, Vos MA, et al. Increased Na^+ concentration and altered Na/K pump activity in hypertrophied canine ventricular cells. *Cardiovasc Res* 2003;57:1035–43.

17. van Borren MMGJ, Vos MA, Houtman MJC, et al. Increased sarcolemmal Na^+/H+ exchange activity in hypertrophied myocytes from dogs with chronic atrioventricular block. *Front Physiol* 2013;4:322.

18. Verdonck F, Volders PGA, Vos MA, et al. Intracellular Na^+ and altered Na^+ transport mechanisms in cardiac hypertrophy and failure. *J Mol Cell Cardiol* 2003;35:5–25.

19. Johnson DM, Heijman J, Pollard CE, et al. IKs restricts excessive beat-to-beat variability of repolarization during beta-adrenergic receptor stimulation. *J Mol Cell Cardiol* 2010;48:122–30.

20. Johnson DM, Heijman J, Bode EF, et al. Diastolic spontaneous calcium release from the sarcoplasmic reticulum increases beat-to-beat variability of repolarization in canine ventricular myocytes after β-adrenergic stimulation. *Circ Res* 2013;112:246–56.

21. Verduyn SC, Vos MA, Gorgels AP, et al. The effect of flunarizine and ryanodine on acquired torsades de pointes arrhythmias in the intact canine heart. J *Cardiovasc Electrophysiol* 1995;6:189–200.

22. Bourgonje VJA, Vos MA, Ozdemir S, et al. Combined Na^+/Ca^{2+} Exchanger and L-Type Calcium Channel Block as a Potential Strategy to Suppress Arrhythmias and Maintain Ventricular Function. *Circ Arrhythmia Electrophysiol* 2013;6:371–9.

23. Sinnecker D, Dirschinger RJ, Barthel P, et al. Postextrasystolic blood pressure potentiation predicts poor outcome of cardiac patients. *J Am Hear Assoc* 2014;3:e000857.

24. Aro AL, Reinier K, Rusinaru C, et al. Electrical risk score beyond the left ventricular ejection fraction: prediction of sudden cardiac death in the Oregon Sudden Unexpected Death Study and the Atherosclerosis Risk in Communities Study. *Eur Heart J* 2017;38:3017–25.

25. Darouian N, Narayanan K, Aro AL, et al. Delayed intrinsicoid deflection of the QRS complex is associated with sudden cardiac arrest. *Heart Rhythm* 2016;13:927–32.

26. DeMazumder D, Limpitikul WB, Dorante M, et al. Entropy of cardiac repolarization predicts ventricular arrhythmias and mortality in patients receiving an implantable cardioverter-defibrillator for primary prevention of sudden death. *Europace* 2016;euv399.

27. Waks JW, Sitlani CM, Soliman EZ, et al. Global Electric Heterogeneity Risk Score for Prediction of Sudden Cardiac Death in the General Population: The Atherosclerosis Risk in Communities (ARIC) and Cardiovascular Health (CHS) Studies. *Circulation* 2016;133:2222–34.

28. Køber L, Thune JJ, Nielsen JC, et al. Defibrillator Implantation in Patients with Nonischemic Systolic Heart Failure. *N Engl J Med* 2016;375:1221–30.

29. Thomas KE, Josephson ME. The Role of Electrophysiology Study in Risk Stratification of Sudden Cardiac Death. *Prog Cardiovasc Dis* 2008;51:97–105.

30. Wijers SC, Vos MA, Meine M. Microvolt T wave alternans in an unselected heart failure population: pros and cons. *Eur J Heart Fail* 2012;14:344–7.

31. Roden DM. Taking the "idio" out of "idiosyncratic": predicting torsades de pointes. *Pacing Clin Electrophysiol* 1998;21:1029–34.

32. Thomsen M, Oros A, Schoenmakers M, et al. Proarrhythmic electrical remodelling is associated with increased beat-to-beat variability of repolarisation. *Cardiovasc Res* 2007;73:521–30.

33. Hinterseer M, Beckmann B-M, Thomsen MB, et al. Relation of increased short-term variability of QT interval to congenital long-QT syndrome. *Am J Cardiol* 2009;103:1244–8.

34. Hinterseer M, Thomsen MB, Beckmann B-M, et al. Beat-to-beat variability of QT intervals is increased in patients with drug-induced long-QT syndrome: a case control pilot study. *Eur Heart J* 2008;29:185–90.

35. Hinterseer M, Beckmann B-M, Thomsen MB, et al. Usefulness of short-term variability of QT intervals as a predictor for electrical remodeling and proarrhythmia in patients with nonischemic heart failure. *Am J Cardiol* 2010;106:216–20.

36. Piccirillo G, Magrì D, Ogawa M, et al. Autonomic nervous system activity measured directly

and QT interval variability in normal and pacing-induced tachycardia heart failure dogs. *J Am Coll Cardiol* 2009;54:840–50.

37. Coronel R, de Bakker JMT, Wilms-Schopman FJG, et al. Monophasic action potentials and activation recovery intervals as measures of ventricular action potential duration: experimental evidence to resolve some controversies. *Heart Rhythm* 2006;3:1043–50.
38. Wijers SC, Bossu A, Dunnink A, et al. Electrophysiological measurements that can explain and guide temporary accelerated pacing to avert (re)occurrence of Torsades de pointes arrhythmias in the canine chronic atrioventricular block model. *Heart Rhythm* 2017;14:749–56.
39. Viskin S, Glikson M, Fish R, et al. Rate smoothing with cardiac pacing for preventing Torsades de pointes. *Am J Cardiol 2000*;86:111K–115K.
40. Hanson B, Gill J, Western D, et al. Cyclical modulation of human ventricular repolarization by respiration. *Front Physiol* 2012;3:379.
41. Hanson B, Child N, Van Duijvenboden S, et al. Oscillatory behavior of ventricular action potential duration in heart failure patients at respiratory rate and low frequency. *Front Physiol* 2014;5:414.
42. Eckardt L, Kirchhof P, Breithardt G, et al. Load-induced changes in repolarization: evidence from experimental and clinical data. *Basic Res Cardiol* 2001;96:369–80.
43. Stams TR, Oosterhoff P, Heijdel A, et al. Beat-to-Beat Variability in Preload Unmasks Latent Risk of Torsades de Pointes in Anesthetized Chronic Atrioventricular Block Dogs. *Circ J* 2016;80:1336–45.
44. Cao JM, Chen LS, KenKnight BH, et al. Nerve sprouting and sudden cardiac death. *Circ Res* 2000;86:816–21.
45. Cao JM, Fishbein MC, Han JB, et al. Relationship between regional cardiac hyperinnervation and ventricular arrhythmia. *Circulation* 2000;101:1960–9.
46. Kimura K, Ieda M, Kanazawa H, et al. Cardiac sympathetic rejuvenation: a link between nerve function and cardiac hypertrophy. *Circ Res* 2007;100:1755–64.
47. Rizas KD, Nieminen T, Barthel P, et al. Sympathetic activity–associated periodic repolarization dynamics predict mortality following myocardial infarction. *J Clin Invest* 2014;124:1770–80.
48. Leenhardt A, Beaufils P, Slama R. Obituary to Philippe Coumel, MD, 1935-2004. *Heart Rhythm* 2004;1:527.

10

English summary

Summary

Sudden cardiac death (SCD) due to a cardiac arrest accounts for up to 50% of total mortality in patients with structural heart disease, such as coronary artery disease, compensated hypertrophy or heart failure. Most cardiac arrests are caused by a ventricular arrhythmia (a fast or chaotic heart rhythm that impedes the heart to circulate blood). Despite resuscitation attempts, overall survival after a cardiac arrest is only 5-10%. Therefore, focus has shifted towards prevention of SCD in high risk subgroups of patients. The Implantable Cardioverter-Defibrillator (ICD) is a device that continuously monitors the rhythm of the heart and can terminate life-threatening arrhythmias by delivery of an electric shock. Large randomized controlled trials have demonstrated a significant survival benefit of ICD therapy in patients with a diminished pump function of the heart as measured by left ventricular ejection fraction (LVEF). Currently, ICD implantation is indicated for all patients with a LVEF below 35%.

However, in recent years it has become clear that LVEF lacks specificity and sensitivity in defining the subgroup at highest risk of malignant ventricular arrhythmias. Currently, more than 2 out 3 ICD recipients will never experience a life-saving ICD shock in their lives. Nonetheless, these patients are at risk of complications, such as lead fractures, infection, battery replacements or inappropriate shocks. Therefore, other, more accurate risk predictors are needed to improve patient selection for ICD therapy. In order to find new risk markers of SCD, one must have insight in the underlying mechanisms responsible for these arrhythmias. In patients with structural heart disease, alterations in cardiac structure, Ca^{2+} handling, ion channel expression and autonomic nervous system function have occurred. This process, called ventricular remodeling, initially helps to maintain normal cardiac performance, but will eventually lead to deterioration of pump function, electrical instability and ventricular arrhythmias.

In this thesis, parameters of contractile (**Part I**), electrical (**Part II**) and neural remodeling (**Part III**) are evaluated in relation to susceptibility of ventricular arrhythmias in order to find new markers of increased arrhythmic risk. To do so, an arrhythmogenic animal model is used: the chronic atrioventricular block (CAVB) dog. In this model, ablation of the AV-node causes a drop in heart rate and thereby volume overload of the left ventricle. In response to a reduced cardiac output, the heart starts to remodel by increasing contractility and growing in size. Moreover, the animals become susceptible to a typical ventricular arrhythmia, Torsades de Pointes (TdP), when they are further challenged with the pro-arrhythmic drug dofetilide. The CAVB dog is thus an ideal model to investigate the relation between ventricular remodeling and arrhythmogenesis.

Part I – parameters of contractile remodeling for risk prediction

Ca^{2+} is an essential ion for normal contractile function of the cardiomyocyte. During ventricular remodeling, the expression of key proteins in Ca^{2+} handling is altered, resulting in Ca^{2+} overload of the cardiomyocyte. The excess Ca^{2+} does not only affect contractility, but can also trigger ventricular arrhythmias. In **Chapter 2** three *in vivo* contractile parameters are discussed that reflect intracellular Ca^{2+} handling: the force-frequency relationship (FFR), mechanical restitution (MR) and post-extrasystolic potentiation (PESP). These parameters describe changes in contractility when heart rate varies or when extrasystolic beats occur. In **Chapter 3**, we assessed whether alterations in FFR, MR and PESP are associated with susceptibility to arrhythmias in the CAVB dog. We showed that inducible CAVB dogs have a higher contractile force at low rate with an inverted FFR, higher MR and PESP and higher time constants of MR. Furthermore, the more these parameters are altered, the more arrhythmias can be induced. Based on these observations, we hypothesized that the inducible dogs have more disturbed Ca^{2+} handling leading to Ca^{2+} overload. These differences in Ca^{2+} handling would then be measurable macroscopically by FFR, MR and PESP. We tested this hypothesis by pharmacologically increasing Ca^{2+} load with the Na^{+}-K^{+}-ATPase blocker ouabain in an attempt to convert a non-inducible dog into an inducible one. While only one out of four dogs reached a contractility level comparable to the inducible subjects, this one dog did become inducible after a combination of ouabain and dofetilide, hereby supporting our hypothesis. While these parameters were measured intracardially in this study, a non-invasive assessment of PESP is currently being investigated in the EU-CERT-ICD study as a potential predictor of SCD risk.

Part II – parameters of electrical remodeling for risk prediction and monitoring

Parameters that reflect changes in electrophysiology are potential markers of arrhythmic risk. In **Chapter 4** we presented the results of the EU-TrigTreat clinical study. This multicenter study investigated demographic and electrocardiographic parameters for risk prediction of appropriate shock and all-cause mortality in more than 600 ICD patients. Two separate risk prediction models were constructed which gave a very good approximation of both arrhythmia risk as well as overall mortality risk. This study highlights the importance of differentiating between these two competing risks, since patients will only benefit from the ICD if the risk of lethal arrhythmias is high, but the risk of dying from other, non-arrhythmic, causes is low. Two parameters, microvolt T wave alternans and programmed electrical stimulation, were predictive for appropriate shock, but not for mortality. LVEF, on the other hand, was predictive for both shock

and mortality, which further stresses the limitations of LVEF as main criterion for ICD implantation.

An important electrical parameter of arrhythmic risk is short-term variability of repolarization (STV), which is studied in depth in Chapter 5, 6, 7 and 8. STV is a quantification of the beat-to-beat variations in repolarization and has been regarded as an accurate measure of so the called 'repolarization reserve', the redundancy in repolarizing currents to maintain normal repolarization. During ventricular remodeling, repolarization reserve is reduced, making the heart vulnerable to arrhythmogenic challenges on repolarization. This reduced repolarization reserve is reflected by an increased STV. In **Chapter 5** we argue that women have less repolarization reserve compared to men, possibly due to the direct effect of sex hormones on repolarizing currents, which would explain why women are more prone to TdP arrhythmias. In **Chapter 6** we evaluated the circadian rhythm of STV of the QT interval (STV_{QT}) in a subpopulation of patients from the EU-CERT-ICD study. We demonstrated that highly arrhythmogenic patients (as defined by the number of arrhythmic events on the Holter recording) have a different circadian pattern of STV_{QT} compared to patients with no arrhythmias. The STV_{QT} in the arrhythmogenic group shows two prominent peaks in the early morning and late afternoon, possibly related to a shift in autonomic tone. Therefore, measurement of STV_{QT} during these two time points would increase the sensitivity in identifying the patient at risk.

Importantly, STV does not only predict the risk of developing life-threatening arrhythmias in the future, but also shows a sudden increase a couple of minutes prior to the occurrence of these arrhythmias. Therefore, STV may be used for continuous monitoring of arrhythmias that are upcoming. These dynamic STV changes are currently measured on the left ventricular monophasic action potential duration (STV_{MAPD}). However, these signals are measured with a catheter that is not commonly used in clinical practice. In **Chapter 7** we assessed whether the local electrogram (EGM) recorded via the right ventricular ICD lead is suitable for measurement of STV. We demonstrated that STV of the activation recovery interval (STV_{ARI}) of the EGM is comparable to STV_{MAPD}, and that STV_{ARI} shows a similar increase prior to TdP arrhythmias in anesthetized and awake CAVB dogs. These findings are of major importance for further development of in-device monitoring. Incorporating 24/7 monitoring into an ICD could significantly improve the functionality of these devices. Currently, the ICD works as 'rescue' therapy by terminating malignant arrhythmias when present. Therefore, patients often require additional treatment with antiarrhythmic drugs or radiofrequency ablation to prevent multiple ICD shocks. However, using continuous STV_{ARI} measurement, the ICD would be able to foresee if arrhythmias are upcoming and possibly initiate therapy to prevent the arrhythmia itself from occurring. Nonetheless, this new treatment modality would require an accurate automatic determination of STV_{ARI} by the device. In **Chapter 8** we

presented a new automatic method of measuring STV_{ARI} which is highly correlated with the gold standard STV_{MAPD} in the CAVB dog. Moreover, this method shows excellent sensitivity and specificity in identifying dogs that will develop TdP arrhythmias. In the near future, this new monitoring modality will be made available for further evaluation of its efficacy in patients.

Part III - parameters of neural remodeling for risk prediction

In addition to beat-to-beat fluctuations, the action potential duration (APD) oscillates at other frequency bands as well. Two of those oscillatory patterns are addressed in the final part of this thesis. In **Chapter 9** we assessed the effects of remodeling on respiratory and low frequency oscillations of APD in the CAVB dog. We observed that APD varies with respiration, even in sinus rhythm or acutely after AV-block. However, at chronic AV-block, respiratory oscillations of APD are significantly augmented. We hypothesized that this is caused by a more pronounced effect of mechano-electrical feedback on APD when repolarization reserve is reduced. However, no differences were found in these oscillations between inducible and non-inducible CAVB dogs. Besides respiratory fluctuations, we also found low frequency oscillations of APD at around 0.1Hz, which have been attributed to bursts of sympathetic nervous system activity on the heart. This oscillatory pattern is also enhanced after remodeling, but to a far greater extend in inducible compared to non-inducible dogs. We argue that this observation is related to neural remodeling, by which alterations in cardiac sympathetic innervation result in differences in low frequency oscillations of APD in inducible versus non-inducible dogs. Altered autonomic modulation is known to increase both temporal and spatial dispersion of repolarization, which facilitates the initiation and perpetuation of ventricular arrhythmias.

Conclusion

Prevention of SCD remains an important challenge in patients with structural heart disease. Ventricular remodeling is responsible for changes in cardiac structure and function that make the heart prone to life-threatening ventricular arrhythmias. We have shown that *in vivo* markers of contractile, electrical or neural remodeling are potential candidates for identifying the subject at risk of developing malignant arrhythmias. In addition, continuous monitoring of imminent arrhythmic risk using these parameters can enhance the functionality of implantable devices. Accurate risk prediction and in-device monitoring help to maximize the benefit of ICD therapy, which will eventually improve the quality of life of ICD recipients.

Nederlandse samenvatting

Samenvatting

Plotse hartdood ten gevolge van een hartstilstand is verantwoordelijk voor 50% van de totale sterfte in patiënten met een structurele hartziekte, zoals coronarialijden, gecompenseerde hypertrofie of hartfalen. In het merendeel van de gevallen wordt de hartstilstand veroorzaakt door een ventriculaire ritmestoornis (een snel of chaotisch hartritme, afkomstig uit de kamers van het hart, waardoor het hart amper bloed rond kan pompen). Reanimatiepogingen ten spijt, is de overleving na een hartstilstand slechts 5-10%. Daarom wordt tegenwoordig de meeste aandacht gericht op het voorkomen van plotse hartdood in patiënten met een hoog risico op ventriculaire ritmestoornissen.

De Implanteerbare Cardioverter-Defibrillator (ICD) is een apparaat dat continu het hartritme kan monitoren en levensbedreigende ritmestoornissen kan beëindigen door middel van een elektrische schok. Grote, gerandomiseerde, klinische studies hebben aangetoond dat ICD therapie de overleving verbetert in patiënten met een verminderde pompfunctie van het hart, gemeten aan de linker ventrikel ejectiefractie (LVEF). Tegenwoordig is implantatie van een ICD geïndiceerd voor alle patiënten met een LVEF onder de 35%.

Echter, in de afgelopen jaren is duidelijk geworden dat de LVEF een te lage sensitiviteit en specificiteit heeft in het identificeren van de groep patiënten met het hoogste risico op plotse hartdood. Momenteel zal 2 van de 3 ICD dragers nooit een levensreddende ICD schok meemaken in zijn of haar leven. Echter, deze patiënten lopen wel risico op het krijgen van complicaties, zoals draadbreuken, infecties, batterijvervangingen of onterechte schokken. Derhalve zijn nieuwe, meer accurate risicovoorspellers nodig om de selectie van patiënten voor ICD therapie te verbeteren. Om deze voorspellers te vinden heeft men inzicht nodig in de onderliggende mechanismen waardoor ritmestoornissen kunnen ontstaan. In patiënten met structurele hartziekten hebben veranderingen plaatsgevonden in de structuur van het hart, de Ca^{2+} huishouding, de expressie van ionkanalen en de functie van het autonome zenuwstelsel. Dit proces, genaamd ventriculaire remodellering, draagt initieel bij aan behoud van een normale werking van het hart, maar kan op den duur resulteren in een verdere verslechtering van de pompfunctie, elektrische instabiliteit en ventriculaire ritmestoornissen.

In dit proefschrift worden parameters van contractiele (**deel I**), elektrische (**deel II**) en neurale remodellering (**deel III**) in relatie tot de gevoeligheid voor ventriculaire ritmestoornissen onderzocht ten doel nieuwe markers van verhoogd aritmisch risico te vinden. Hiervoor wordt gebruik gemaakt van een aritmogeen diermodel: de chronische atrioventriculair blok (CAVB) hond. In dit model veroorzaakt ablatie van de AV-knoop een daling van de hartfrequentie en derhalve volume-overbelasting van het linker ventrikel. Als reactie op de verlaagde cardiac output, remodelleert het hart door verhoging van

de contractiekracht en verdikking van de hartspier. Tevens worden de dieren vatbaar voor een bepaalde ventriculaire ritmestoornis, Torsades de Pointes (TdP), wanneer eveneens het pro-aritmogene medicament dofetilide wordt toegediend. De CAVB-hond is daarom een ideaal model voor het bestuderen van de relatie tussen ventriculaire remodellering en het optreden van ventriculaire ritmestoornissen.

Deel I – parameters van contractiele remodellering voor risicopredictie

Ca^{2+} is een essentieel ion voor normale contractie en relaxatie van de hartspiercel, de cardiomyocyt. Tijdens ventriculaire remodellering verandert de expressie van belangrijke eiwitten in de Ca^{2+} huishouding wat leidt tot een overschot aan Ca^{2+} in de cardiomyocyt. Dit teveel aan Ca^{2+} heeft niet alleen invloed op de contractiliteit, maar kan ook ventriculaire ritmestoornissen opwekken. In **Hoofdstuk 2** worden drie *in vivo* contractiele parameters besproken die een afspiegeling zijn van de intracellulaire Ca^{2+} huishouding: de force-frequency relatie (FFR), mechanische restitutie (MR) en post-extraystolische potentiatie (PESP). Deze parameters beschrijven de veranderingen in contractiliteit wanneer de hartfrequentie varieert of wanneer er zich extraslagen voordoen. In **Hoofdstuk 3** wordt de relatie onderzocht tussen veranderingen in FFR, MR en PESP en de vatbaarheid voor ritmestoornissen in de CAVB-hond. In dit hoofdstuk wordt duidelijk dat induceerbare CAVB-honden een hogere contractiekracht hebben bij een lage hartfrequentie met daarbij een negatieve FFR, een hogere MR en PESP en tevens een hogere tijdsconstante van de MR-curve. Verder blijkt dat hoe meer deze contractiele parameters zijn veranderd, hoe meer ritmestoornissen kunnen worden opgewekt. Op basis van deze observaties, wordt verondersteld dat de induceerbare honden een ernstigere verstoring van hun Ca^{2+} huishouding hebben, die leidt tot Ca^{2+} overschot. Deze verstoring kan macroscopisch worden gemeten middels FFR, MR en PESP. Deze hypothese werd getest door farmacologisch een groter Ca^{2+} overschot te creëren middels de Na^{+}-K^{+}-blokker ouabaïne, om zodoende een niet-induceerbare hond induceerbaar te maken. Hoewel het slechts bij 1 van de 4 honden lukte de contractiekracht naar het niveau van de induceerbare honden te verhogen, bleek deze hond wel induceerbaar bij een combinatie van ouabaïne en dofetilide, wat onze hypothese ondersteunt. Alhoewel de contractiele parameters in deze studie intracardiaal werden gemeten, wordt momenteel in de EU-CERT-ICD studie onderzocht of een niet-invasieve PESP-meting als eventuele risico voorspeller van plotse hartdood kan fungeren.

Deel II – parameters van elektrische remodellering voor risicopredictie en monitoring

Parameters die veranderingen in de elektrofysiologie van het hart weergeven zijn veelbelovende markers van een verhoogd risico op ventriculaire ritmestoornissen. In **Hoofdstuk 4** worden de resultaten van de EU-TrigTreat clinical study gepresenteerd. Deze studie onderzocht verschillende demografische en elektrocardiografische parameters ter risicopredictie van terechte ICD schokken en mortaliteit in meer dan 600 ICD patiënten. Twee verschillende predictiemodellen konden worden opgesteld die beide een zeer goede benadering gaven van het risico op een terechte ICD schok alsmede het mortaliteitsrisico. Deze studie benadrukt hoe belangrijk het is onderscheid te maken tussen deze twee concurrerende risico's, aangezien patiënten enkel profijt hebben van de ICD als het risico op levensbedreigende ritmestoornissen groot is, maar het risico op overlijden aan andere oorzaken klein. Twee parameters, microvolt T wave alternans en geprogrammeerde elektrische stimulatie, waren voorspellend voor terechte ICD schokken, maar niet voor mortaliteit. LVEF, daarentegen, was voorspellend voor beiden. Dit onderstreept wederom de beperkingen van LVEF als belangrijkste criterium voor ICD implantatie.

Een belangrijke elektrische parameter is short-term variability of repolarization (STV), welke onderwerp van discussie is in Hoofdstuk 5, 6, 7 en 8. STV is een kwantificatie van de slag-op-slag variatie in repolarisatie (de herstelfase in de hartcyclus). Deze parameter reflecteert de mate van 'repolarisatie reserve', de overtolligheid in ionstromen verantwoordelijk voor repolarisatie, waardoor een normale repolarisatie kan plaatsvinden zelfs als één van de stromen is geblokkeerd. Echter, ten gevolge van remodellering vermindert de repolarisatie reserve, waardoor het hart kwetsbaar wordt voor aritmogene invloeden op de repolarisatie. De verlaagde repolarisatie reserve wordt weerspiegeld in een hogere STV.

In **Hoofdstuk 5** wordt bediscussieerd of vrouwen minder repolarisatie reserve hebben dan mannen, mogelijk veroorzaakt door het effect van geslachtshormonen op repolariserende ionstromen. Dit zou verklaren waarom vrouwen gevoeliger zijn voor TdP ritmestoornissen. In **Hoofdstuk 6** wordt het circadiane ritme van STV van het QT interval (STV_{QT}) bestudeerd in een subpopulatie van de EU-CERT-ICD studie. Hier wordt aangetoond dat sterk aritmogene patiënten (gebaseerd op het aantal aritmische events op de Holterregistratie) een totaal ander circadiaan patroon van STV_{QT} hebben vergeleken met patiënten zonder ritmestoornissen. De STV_{QT} in de aritmogene groep vertoont twee prominente pieken in de vroege ochtend en late namiddag, mogelijk gerelateerd aan verschuivingen in autonome tonus. Het meten van STV_{QT} gedurende deze tijdspunten zou dus de sensitiviteit kunnen verbeteren in het identificeren van de patiënten met een hoog risico op ventriculaire ritmestoornissen.

STV voorspelt niet alleen het risico op het ontwikkelen van levensbedreigende ritmestoornissen in de toekomst, maar toont ook een acute stijging een paar minuten voor het optreden van deze ritmestoornissen. Daarom zou STV kunnen worden gebruikt voor continue monitoring van ritmestoornissen die aanstaande zijn. Deze dynamische veranderingen in STV vlak voor het ontstaan van de ritmestoornis worden nu gemeten aan de monofasische actiepotentiaalduur (STV_{MAPD}). Echter, deze signalen kunnen enkel worden geregistreerd met een speciale katheter, die zelden wordt gebruikt in de klinische praktijk. In **Hoofdstuk 7** wordt daarom onderzocht of het lokale elektrogram (EGM) van de ICD draad in het rechter ventrikel kan worden gebruikt om STV op te meten. In dit hoofdstuk wordt aangetoond dat STV van het activation recovery interval (STV_{ARI}) van het EGM vergelijkbaar is aan STV_{MAPD} en dat STV_{ARI} een overeenkomstige stijging laat zien vlak voor het ontstaan van TdP ritmestoornissen in de CAVB hond, zowel onder narcose als wakker. Deze bevindingen zijn van groot belang voor de verdere ontwikkeling van in-device monitoring. Het implementeren van 24/7 monitoring in een ICD zou de functionaliteit van het device aanzienlijk kunnen vergroten. Nu werkt de ICD als 'rescue' therapie: het device kan een levensbedreigende ritmestoornis beëindigen wanneer deze aanwezig is. Meestal is aanvullende therapie in de vorm van anti-aritmische medicatie of radiofrequente ablatie noodzakelijk om meerdere ICD schokken te voorkomen. Echter, middels continue STV_{ARI} analyse kan de ICD gevaarlijke ritmestoornissen aan zien komen en eerder ingrijpen om zodoende de ritmestoornis te voorkomen. Het device moet hiervoor wel in staat zijn automatisch STV_{ARI} te bepalen. In **Hoofdstuk 8** wordt een nieuwe geautomatiseerde methode gepresenteerd om STV_{ARI} te meten. Deze methode blijkt sterk gecorreleerd aan de gouden standaard STV_{MAPD} en heeft bovendien een uitstekende sensitiviteit en specificiteit in het aantonen van een stijging van STV vóór het optreden van TdP ritmestoornissen in de induceerbare honden. Momenteel wordt deze nieuwe monitoringsfunctie doorontwikkeld voor verdere evaluatie in patiënten.

Deel III - parameters van neurale remodellering voor risicopredictie

Naast slag-op-slag fluctuaties, oscilleert de actiepotentiaalduur (APD) ook op andere frequenties. Twee van die oscillaties worden onderzocht in het laatste deel van dit proefschrift. In **Hoofdstuk 9** wordt het effect van remodellering op respiratoire en laag frequente oscillaties van APD in de CAVB-hond geëvalueerd. Respiratoire oscillaties van APD kunnen worden geobserveerd in sinusritme en acuut na het maken van AV-blok. Echter, na remodellering zijn deze respiratoire oscillaties aanzienlijk versterkt. Dit kan worden toegeschreven aan een belangrijker effect van mechano-elektrische feedback op de APD wanneer de repolarisatie reserve is verminderd. Echter, er werden geen verschillen gevonden in respiratoire oscillaties tussen induceerbare

en niet-induceerbare CAVB-honden. Naast deze schommelingen veroorzaakt door de ademhaling, wordt ook een laag frequente oscillatie in APD gezien van rond de 0.1 Hz, waarschijnlijk veroorzaakt door het vuren van sympathische neuronen op het ventriculaire myocard. Deze laag frequente oscillatie neemt ook toe na remodellering, echter in een veel grotere mate in de induceerbare honden. Dit verschil is mogelijk gerelateerd aan neurale remodellering, waarbij aanpassingen in sympathische innervatie van het hart kunnen leiden tot verschillen in de laag frequente oscillatie van de APD in induceerbare versus niet induceerbare honden. Bovendien is bekend dat veranderende autonome modulatie zowel spatiele als temporele dispersie in repolarisatie kan vergroten, waardoor ventriculaire ritmestoornissen gemakkelijk kunnen ontstaan en aanhouden.

Conclusie

Preventie van plotse hartdood blijft een belangrijke uitdaging in patiënten met structurele hartziekten. Ventriculaire remodellering is verantwoordelijk voor veranderingen in de structuur en de functie van het hart, waardoor het hart vatbaar wordt voor levensbedreigende ritmestoornissen. In dit proefschrift is aangetoond dat *in vivo* markers van contractiele, elektrische of neurale remodellering potentiele kandidaten zijn om patiënten te identificeren die een hoog risico lopen op het ontwikkelen van deze gevaarlijke ritmestoornissen.

Daarnaast kan continue monitoring van op handen zijnde ritmestoornissen middels deze parameters de functionaliteit van implanteerbare apparaten verhogen. Zowel accurate risicopredictie als in-device monitoring dragen bij aan het vergroten van het profijt van ICD therapie voor de patiënt en zullen daarmee op den duur de kwaliteit van leven van ICD dragers aanzienlijk verbeteren.

Acknowledgements

Acknowledgements

De pen kan neer. Het einde is in zicht. In december 2014 legde ik de eed af en werd ik dokter, straks, in december 2018, leg ik de eed af en word ik doctor. En dan te bedenken dat ik december altijd een verschrikkelijke maand heb gevonden. Dit proefschrift heeft me in de afgelopen drie jaar heel wat grijze haren gekost (voor bewijs kijkt u maar naar mijn baard), maar op het eindresultaat kan ik meer dan trots zijn. Dit alles was echter nooit gelukt zonder de hulp en steun van mijn familie, vrienden, collega's en begeleiders. Op deze laatste (doch meest gelezen) pagina's van het proefschrift wil ik hen dan ook hartelijk bedanken.

Prof. dr. Vos, beste **Marc**, wat een flater sloeg ik, toen ik in 2015 onvoorbereid bij jou op sollicitatiegesprek kwam. 'Hoezo lees je je niet in als je gaat solliciteren voor een promotieplek?', vroeg jij verontwaardigd. 'Weet je eigenlijk wel wat STV is?', ik knikte braaf, maar had werkelijk geen idee. Ik ben je nog steeds dankbaar dat jij mij, ondanks mijn onervarenheid in de wetenschap, deze kans hebt gegeven. In het begin was het behoorlijk wennen, het werk van onderzoeker, maar met de nodige, soms felle, discussies leidde jij mij er goed doorheen. Waar ik met veel plezier op terug zal kijken zijn onze reizen samen. Onder de palmbomen in Georgia, genieten van een grote schaal paella in Barcelona, currywurst en Hefeweizen in Berlijn, maar natuurlijk met stip bovenaan, de oesters in de Union Oyster House in Boston! Marc, je hebt me veel geleerd, niet alleen over onderzoek en fysiologie, maar ook over de organisatie van het ziekenhuis, het samenwerken met een commerciële partner, bier (NOOIT MEER Miller lite, alstublieft), Amerikaanse sporten (sorry, ice hockey/baseball/football, het boeit me allemaal nog steeds niet...) maar met name over het bourgondische leven. Heel, heel veel dank hiervoor!

Dr. Tuinenburg, beste **Anton**, ontzettend bedankt dat jij mij in 2015 in contact hebt gebracht met Sofieke en Marc. Zonder jou was dit promotietraject nooit op mijn pad gekomen. Ik had jou een jaar eerder al leren kennen toen ik op zoek was naar een wetenschapsstage. Alhoewel we de resultaten van die stage nooit hebben kunnen publiceren, werd daar wel mijn interesse voor de elektrofysiologie gewekt. In de afgelopen jaren waren wij samen verantwoordelijk voor de patiënteninclusie van EU-CERT-ICD. Ondanks de trage start, hebben wij, met de hulp van de R&D, toch het beoogd aantal patiënten kunnen includeren! Hopelijk wordt dit succes bekroond met een mooie publicatie volgend jaar. Ook onze reizen samen met Marc zal ik niet snel vergeten. Terwijl wij in Wenckebach met Marc ons bier dronken (wij liepen steeds verder op hem achter, tot we er één oversloegen), genoot ik van de mooie verhalen die jij altijd te vertellen had. Ik hoop dat wij ook in de toekomst blijven samenwerken!

Ik wil de beoordelingscommissie bestaande uit **prof. dr. Sluijter, prof. dr. Chamuleau, prof. dr. van Rijen, dr. van Laake** en **prof. dr. Willems** bedanken voor het kritisch lezen en beoordelen van mijn proefschrift.

Jet, ik wil jou bedanken voor alle ondersteuning die je hebt geboden tijdens de dierexperimenten. Wij als promovendi bij de Medische Fysiologie mogen ons gelukkig prijzen met een technicus zoals jij, want wat ben jij goed in je vak! Afgezien van jouw ongelofelijke handvaardigheid (menig vaatchirurg zou jaloers op je zijn), kennis en ervaring met de honden, was je ook altijd bereid mee te denken over de opzet en de uitvoering van de experimenten. Die lange dagen op de OK waren een feestje dankzij jou (ook al ging het soms niet helemaal zoals gepland, maar ook dat hoort bij onderzoek, zo heb ik de afgelopen jaren geleerd). Jet, je bent een heerlijk mens en ik wens je veel geluk toe in de toekomst.

Dr. Meine, beste **Mathias**, hartelijk dank voor de fijne samenwerking het laatste jaar, met name tijdens de studie met Medtronic. Ondanks je flauwe grappen (waar ik stiekem best vaak om moet lachen), ben je een bewonderenswaardig cardioloog. Jouw onuitputtelijke kennis en kunde, je passie voor onderzoek, maar met name de brug die jij slaat tussen de fysiologie en de kliniek, maken dat jij een groot voorbeeld voor mij bent. Ik hoop de komende jaren nog veel van je te mogen leren (behalve het kunnen herkennen van het type lead op een thoraxfoto, die vaardigheid slaat natuurlijk nergens op).

Dear **Alfonso Aranda Hernandez** and dr. **Berthold Stegemann**, thank you both for the great cooperation between Medtronic and Medical Physiology over the last years. We made great progress with the STV project, especially due to your ingenious T wave end algorithm, Alfonso. I have high hopes that this project will turn out to be a success and I'm looking forward to many great studies together.

Dear **Markus Zabel** and all EU-CERT-ICD collaborators, thank you for the opportunity to be part of this large European study consortium. I learned a lot during our meetings in Budapest, Barcelona, Frankfurt and Berlin. I would also like to thank you, Markus, for all the effort you have put into the long-term follow-up of the EU-TrigTreat clinical study, which is now finally published. Hopefully, the EU-CERT-ICD main paper will have similar success. Of the EU-CERT-ICD colleagues, I would like to thank **Marek Malik** in particular, because of his critical review of the pilot study, which definitely helped getting it published.

Beste **Henk Ritsema van Eck**, ik wil je bedanken voor je hulp in het onder de knie

krijgen van het STV-analyseprogramma. Ik kon altijd bij je terecht als het programma niet deed wat ik wilde. Zonder jouw hulp had ik nooit de STV-analyses kunnen doen die hebben geleid tot de PLOS ONE publicatie.

De Medische Fysiologie is de afgelopen jaren toch een beetje als een tweede familie gaan voelen en dat is voornamelijk te danken aan jou, **Tonny**. Jij bent de moeder van de afdeling, bij jou kan je altijd terecht voor hulp, koekjes of gewoon om even uit te razen als er iets tegenzit. En net als een echte moeder gaf je me ook op mijn donder als ik weer een puinzooi van de keuken had gemaakt. Tonny, wat zal de sfeer op de afdeling veranderen als jij volgend jaar met pensioen gaat. Desalnietemin wens ik jou veel geluk en plezier in de jaren die komen!

Natuurlijk wil ik mijn voorgangers in het STV-onderzoek bedanken. **Sofieke**, jij hebt mij geïntroduceerd bij de Medische Fysiologie en was altijd mijn steun en toeverlaat voor vragen over STV. Onze samenwerking heb ik altijd als zeer prettig ervaren en ik ben dan ook erg trots dat wij de cisapride studie uiteindelijk in Heart Rhythm hebben kunnen wegzetten. Tot slot wil ik je bedanken voor alle tips die je me hebt gegeven voor het sollicitatiegesprek bij de Cardiologie. Ik hoop in de toekomst je collega elektrofysioloog te worden! Beste **Albert**, ik wil jou heel erg bedanken voor alle tijd en moeite die jij hebt gestoken om mij de eerste maanden wegwijs te maken op de afdeling. Ontelbare keren heb ik je moeten storen met vragen over de STV-analyse. In de afgelopen maanden zijn de rollen omgedraaid en heb ik zelf een opvolger die ik de kneepjes van het vak moet bijbrengen. Nu merk ik pas hoeveel ik geleerd heb in de afgelopen jaren, mede dankzij jou. Ik kijk ook met plezier terug naar onze trip naar Budapest, waar we samen met Marc in een donker sportscafe Tom Dumoulin de tijdrit zagen winnen in de Vuelta van 2015. We zullen elkaar in toekomst vast nog tegenkomen!

Over mijn opvolger gesproken, ik wil natuurlijk ook jou bedanken, **Agnieszka**. De afdeling is helemaal opgebloeid sinds jouw komst. Wil je me beloven dat je jouw vrolijkheid, enthousiasme en doorzettingsvermogen niet verliest gedurende je promotietraject? Ik wens je veel succes met het voortzetten van het STV-project. Houd je me af en toe op de hoogte?

Chanti, ik geef me gewonnen, jij hebt meer certificaten aan de muur dan ik, wil je nu eindelijk stoppen met posterprijzen winnen? Geintje natuurlijk, zo'n workaholic als jij laat zich niet temmen, en dat is maar goed ook. Ik vond het geweldig om met zo'n rasechte wetenschapper op de kamer te zitten en om samen met jou Utrecht te vertegenwoordigen bij de Dutch Physiology Days. Ik verwacht wel een uitnodiging voor je oratie als je professor wordt.

Ik zal je sarcasme gaan missen, **Birgit**. Het gezicht dat jij trekt als iemand iets doms zegt, zal voor altijd in mijn geheugen gegrift staan. Succes met het afronden van je promotie, ik ben benieuwd naar de titel van je boekje ('I_{K1}, where art thou?', weet je nog?).

Alexandre, rot op naar je eigen land! No, please don't, it's nice to have you here. Thank you for all your help with experiments, analyses, statistics, InDesign and what not. I really admire your insight and knowledge of electrophysiology, I have learned a lot from you the last few years. Hopefully we'll keep in touch. We should definitely cycle more often together!

Dank aan alle andere promovendi en post-docs die de Medische Fysiologie zo geweldig maken: **Elise**, je bent dan nu officieel geen MedFys'er meer, maar je was wel altijd één van de gangmakers. Ik heb genoten van je enthousiasme en je 'heyhey' als je weer eens onze kamer op kwam. De werkgroepen die we samen gaven waren ook zeer geslaagd! Veel succes bij de Experimentele Cardiologie. **Joanne**, dankjewel voor het leiden van de Marc meetings, sinds jouw komst is er eindelijk weer wat structuur in onze groep. Na al mijn geklaag zal ik mijn uiterste best doen ervoor te zorgen dat mijn promotiefeest niet tegenvalt (neem jij je swiffer en borstel dan mee?), **Muge**, I hope the rest of your PhD will be just a success as the project with LUF7244, good luck!, **Valerie**, bewonderingswaardig hoe jij promotieonderzoek met een fulltime geneeskunde studie kan combineren, **Lotte**, succes met de laatste loodjes, **Alan**, jouw Nederlands is zo veel beter dan mijn Italiaans. Ik ga je tiramisu ook zeker missen! Daarnaast ook veel dank aan alle (oud)studenten. De karaokeavond in Ome Willem was top. **Caroline, Doreth, Meye, Michiel, Clarissa, Willem, Vera** en vele anderen, heel veel succes met het afronden van jullie studie!

Ook wil ik de (semi)stafleden bedanken: **Toon**, je bent een fantastisch fysioloog, ik heb genoten van bier en burgers met jou in Boston, **Marcel**, gezien de moeilijkheidsgraad van jouw tentamenvragen, ben ik blij dat ik geen student meer ben, **Marti, Teun, Sanne, Marien** en natuurlijk **Leonie**, ook al heb ik nog nooit een stap op het lab durven zetten, het was toch altijd heel gezellig met jou op de afdeling!

Tot slot, heel veel dank aan de oud-MedFys'ers: **Bastiaan**, jouw aanstekelijke lach zal ik nooit vergeten. Veel succes met de opleiding Interne Geneeskunde, we zullen elkaar vast nog eens treffen, in of buiten het ziekenhuis, **Iris, Yuan, Mathilde, Magda, Martin** en **Maria**.

Natuurlijk moet ik de collega's van 'de overkant' niet vergeten. Ontelbare keren heb ik het stuk door de parkeergarage naar het UMC moeten afleggen, soms zelfs meerdere keren per dag. Veel dank aan de elektrofysiologen, fellows en PA's van de elektrofysiologie: **Peter Loh, Jeroen van der Heijden, Rutger Hassink, Moniek Cox, Irene Hof, Margot Boogaard, Samir Brka** en **Niels Jongejan**. Dankzij jullie heb ik tijdens het EFO- en ICD-onderwijs, de CRT-meetings en de grote visites op vrijdagochtend mijn klinische kennis bij kunnen spijkeren en is mijn interesse voor de elektrofysiologie alleen maar meer gegroeid. Daarnaast ben ik **Wil Kassenberg** en alle medewerkers van de HCK veel dank verschuldigd voor hun ondersteuning in de klinische STV_{ARI} studie. **Wouter van Everdingen**, ook jij bedankt voor je al je hulp en advies en het mogen lenen van het PV-loop systeem. Mijn collega PhD'ers bij de Elektrofysiologie: **Odette, Lennart, Rob**, veel succes met jullie promotietraject, ik verwacht wel een boekje van jullie!

Heel veel dank gaat natuurlijk uit naar de R&D van de Cardiologie: **Tanja, Karen,** maar in het bijzonder **Manon**, wat had ik zonder jullie hulp gemoeten. De EU-CERT-ICD studie was af en toe een last aan jullie been met al die queries en e-mails vanuit Göttingen, maar we hebben ons er goed door heen geslagen. Ook veel dank voor de ondersteuning die jullie boden bij de inclusie van de patiënten.

Ik wil de dokters van de Vasculaire Geneeskunde en iedereen van de SMART office bedanken voor de leuke 'bijbaan' die ik had tijdens mijn promotietraject. **Lies, Yvonne, Ursula, Yannick, Melvin, Stan** en **Frank**, het was niet alleen heel leerzaam voor mij, maar bovenal ook ontzettend gezellig, dat uurtje met jullie op de dinsdag/woensdagochtend.

Mijn (niet-cardiale) collega dokters, maar bovenal vrienden: **Thomas, Peter, Eric** en **Onno.** Heel veel dank voor alle goede gesprekken over geneeskunde, onzer carrières, de blues, Boh Foi Toch, van Kooten en de Bie en natuurlijk alle spannende avonturen van Lippi in Bielefeld. Ik kijk met weemoed terug naar de twee prachtige weekenden in Bielefeld en Buurse. Hopelijk komt er snel een vervolg.

Leden van de **Gang**, u dacht toch niet dat ik u zou vergeten! 'Oude liefde roest niet', zo luidt het spreekwoord en mijn liefde voor u glanst als nooit tevoren. Van scholier naar student naar onmiskenbaar yup: we hebben het allemaal met elkaar meegemaakt. 2018 gaat de boeken in als een geweldig jaar voor onze groep, met een huwelijk en de aankondiging van de eerste Gang-baby. Laten we dit jaar dan ook feestelijk afsluiten: de tweede doctorstitel is (bijna) binnen. Drs. de Jong, het is nu aan u om het drieluik te voltooien.

Heren der **Collegium Horologium Oscillatorium**, het is mij een groot genoegen u op deze gewijde plek aan te mogen schrijven. Alhier wil ik mijn dankbaarheid uiten voor de onvoorwaardelijke steun die ik van u heb mogen ontvangen de afgelopen drie jaar. In het bijzonder, ben ik veel dank verschuldigd aan **Jens Weidenaar** voor het prachtige voorblad van dit proefschrift. Het doet mij deugd dat het voorbeeld om te gaan promoveren wordt opgevolgd binnen ons dispuut. Meneer Stemerdink, ik wens u al het beste toe de komende jaren. Op de 13e van december zal voor velen van u voor het allereerst het officiële 'hora est' klinken. Bedenkt u dan maar, dat dit niet alleen het eindsignaal is van een belangrijke periode in mijn leven, maar tevens een proost op de prachtige toekomst die ons nog te wachten staat.

Beste **Ruben** en **Kamermans**, men zegt altijd dat je in je studententijd vrienden voor het leven maakt. Nou, ik denk dat dat bij ons wel gelukt is. Het bier zuipen is (gelukkig) wat op de achtergrond geraakt, maar de laatste jaren hebben wij in het wielrennen een gezamenlijke hobby gevonden. Onze fietsvakanties naar de Jura, Provence en Alpen waren in één woord subliem en gaven mij steeds nieuwe energie om door te blijven gaan. Heel veel dank daarvoor. De eerste tien jaar vriendschap zit erop, de volgende tien wordt alleen maar makkelijker, denken jullie niet?

Mijn paranimf, **Helen**. Mijn roomie, mijn festivalmaatje. Ik durfde jou maar niet te vragen, want je had het al zo druk. Maar Helen, ik wist zeker: er is echt niemand anders die mijn paranimf kan zijn dan jij. We begonnen bijna tegelijk bij de Medische Fysiologie en ook bijna tegelijk gaan wij hier weg. We deelden frustraties en publicaties, op ons eigen eiland en later in ons eigen kantoor. We begonnen een eigen filmstudio (MedPhys Productions), zeer professioneel met scripts, een rolling camera en een greenscreen. We keken heel burgerlijk Heel Holland Bakt of dansten tot 8 uur 's ochtends op kneiterharde techno. We konden lachen met elkaar, maar ook snauwen naar elkaar. Helen, je bent een prachtig mens: jouw directheid kleurt je, je loyaliteit die siert je. Ik ben blij dat jij mijn paranimf wilt zijn.

Mijn paranimf, **Astrid**. lieve Assie, mijn BFF, dank voor je steun op al die ontelbare momenten dat ik de wanhoop nabij was en dacht dat ik dit proefschrift nooit af zou krijgen. Jij wist zeker dat het goed zou komen en je hebt natuurlijk weer gelijk gekregen. Al sinds het begin van onze studie delen we lief en leed, maar de afgelopen jaren met name de lol en de vele frustraties van het doktersleven. Assie, ik wil dat je twee dingen niet vergeet: dat je een geweldige dokter bent, maar ook de beste vriendin die ik ooit had kunnen wensen!

Lieve **vader**, heel veel dank voor alle liefde en steun die je mij hebt gegeven in mijn leven. Ook al woon je al een tijd niet meer om de hoek, je bent er altijd voor mij geweest. Ik weet hoe trots je nu op mij bent. Hetzelfde geldt voor jullie, **Frances, Chris, Amy** en natuurlijk **Vincent**. Jullie vormen een warme familie, waar ik altijd met veel plezier naar terugkeer.

Tot slot wil jou bedanken, lieve **moeder**, ima sheli. Jij hebt bij mij van kinds af aan de passie voor de geneeskunde gewekt. Tijdens mijn studie luisterde je vol verwondering naar mijn verhalen over de snijzaal, anamnesetraining met simulatiepatiënten en alle avonturen tijdens de coschappen. Nu, op mijn 28e, is ook het volgende hoofdstuk volbracht. Het doet mij veel verdriet dat je dit niet meer mee kan maken. De laatste tijd denk ik vaak hoe het had kunnen zijn: Jij zou daar zitten, op de eerste rij in de Senaatszaal van het Academiegebouw, waarschijnlijk nog zenuwachtiger dan ik, en vol bewondering naar de verdediging luisteren. Dan, na het hora est en de laudatio, zou ik me omdraaien en zou ik jou zien opspringen uit je stoel, hard applaudisseren, fluiten wellicht, stralend van trots. Helaas heeft het niet zo mogen zijn. Mam, je hebt me zoveel gegeven in mijn leven. Deze is voor jou.

List of publications

List of publications

Sprenkeler DJ, Bossu A, Beekman HDM, Schoenmakers M, Vos MA. An augmented negative force-frequency relationship and slowed mechanical restitution are associated with increased susceptibility to drug-induced Torsades de Pointes arrhythmias in the chronic atrioventricular block dog. *Front Physiol.* 2018 Aug 8;9:1086.

Bergau L, Willems R, **Sprenkeler DJ**, Fischer TH, Flevari P, Hasenfuß G, Katsaras D, Kirova A, Lehnart SE, Lüthje L, Röver C, Seegers J, Sossalla S, Dunnink A, Sritharan R, Tuinenburg AE, Vandenberk B, Vos MA, Wijers SC, Friede T, Zabel M. Differential multivariable risk prediction of appropriate shock versus competing mortality - A prospective cohort study to estimate benefits from ICD therapy. *Int J Cardiol*. 2018 Jun.

Wijers SC, **Sprenkeler DJ**, Bossu A, Dunnink A, Beekman JDM, Varkevisser R, Hernández AA, Meine M, Vos MA. Beat-to-beat variations in activation recovery interval derived from the right ventricular electrogram can monitor arrhythmic risk under anesthetic and awake conditions in the canine chronic atrioventricular block model. *Heart Rhythm*. 2018 Mar;15(3):442-448.

Sprenkeler DJ, Tuinenburg AE, Ritsema van Eck HJ, Malik M, Zabel M, Vos MA. Circadian pattern of short-term variability of the QT interval in primary prevention ICD patients - EU-CERT-ICD methodological pilot study. *PLOS ONE*. 2017 Aug 21;12(8)

Sprenkeler DJ, Rivaud MR, Vos MA. Do women have less repolarization reserve compared to men? *Heart Rhythm*. 2017 Jan;14(1):96-97.

Sprenkeler DJ, Vos MA. Post-extrasystolic Potentiation: Link between Ca^{2+} homeostasis and Heart Failure? *Arrhythm Electrophysiol Rev.* 2016 May;5(1):20-6.

Bennaghmouch N, **Sprenkeler D**, Qaderdan K, ten Berg JM. Optimizing antithrombotic therapy after coronary stent implantation in patients on chronic oral anticoagulation. *J Cardiovasc Transl Res*. 2014 Feb;7(1):64-71.

Curriculum vitae

Curriculum vitae

David Jaap Sprenkeler was born on the 2nd of May, 1990 in Amsterdam, the Netherlands. He attended secondary education at the St. Ignatiusgymnasium in Amsterdam, from which he graduated with honours in 2008. The same year he started his medical training at Utrecht University. He received his Bachelor degree in Medicine in 2011. During the Master program of Medicine, he obtained a specific interest in the field of Cardiology after doing an elective rotation at the Cardiology department of the St. Antonius hospital in Nieuwegein. In his final year of Medicine, he got into contact with dr. Anton Tuinenburg, electrophysiologist of the University Medical Center Utrecht, who became his supervisor during his 3 months research internship. During his final rotation at the Cardiology department of the UMC Utrecht, he discovered his fascination for the field of cardiac arrhythmias and electrophysiology.

After obtaining his Medical degree in 2014, he worked as a resident at the Cardiology department of the Jeroen Bosch hospital in ‘s Hertogenbosch. Here he had his first clinical experience as a medical doctor. In September 2015, he was introduced to prof. dr. Marc Vos, who offered him a translational PhD trajectory at the department of Medical Physiology and Cardiology, of which the results are presented in this thesis. He will defend his thesis entitled ‘*Ventricular arrhythmias in the remodeled heart: focus on risk prediction and monitoring*’ on the 13th of December 2018. In 2019, he will start his training in Cardiology at the UMC Utrecht.